

**Development of Chemoenzymatic Labeling Approaches for the
Detection of Fucosylated Biomarkers**

Thesis by
Jean-Luc Chaubard

In Partial Fulfillment of the Requirements for
the Degree of
Doctor of Philosophy

CALIFORNIA INSTITUTE OF TECHNOLOGY

Pasadena, California

2016

(Defended April 11, 2016)

© 2016
Jean-Luc Chaubard
All Rights Reserved

...in loving memory of my grandparents and aunt Trish...

Acknowledgements

Without the support of so many people, the work in this thesis could not have been possible. I was challenged while at Caltech almost everyday, and my strong network of friends, both scientific and personal, got me through tough the times that I have faced in my time here. For the first time in my life, I have truly learned my limits as a human being. In the later years of my time at Caltech, I truly challenged myself and learned more about myself than I ever knew.

I would first like to thank my advisor, Prof. Linda Hsieh-Wilson, for her advice and guidance during my time here. She taught me how to develop the biggest impact projects possible. I would also like to thank my committee members, Prof. Dave Tirrell, Prof. Jackie Barton, Prof. Henry Lester, and Prof. Jim Heath. They were all instrumental in my success at Caltech and also challenged me to be the best scientist possible. Their motivation, support, and guidance helped me navigate through my graduate career.

I could not have gotten to where I am today if it were not for my undergraduate advisor, Prof. Robert Haltiwanger. He taught me what being a scientist means and showed me how to be an amazing scientist and person. His guidance has strongly impacted my scientific career and I will forever be grateful for all he has done for me. I also am greatly appreciative of Dr. Hideyuki Takeuchi, Dr. Jianguang Du, and Dr. Christina Leonhard-Melief. They were the scientists in the Haltiwanger lab who trained me and taught me how to do science. I will always respect their scientific skills and will never forget the effort they put forth to help me succeed. I need to thank Prof. Liz Boon and Prof. Isaac Carrico. They introduced me to chemical biology and guided me to Caltech. Without their insight and guidance, I would not have been interested in the field I am currently a part of. Finally,

I need to thank the Beckman Foundation. I was part of the Beckman Scholars program at Stony Brook and through this program I was able to learn about the history of Arnold Beckman. His life story of achievement was and still is an inspiration to me every day.

I would also like to thank the people who have enabled me to conduct the scientific studies in this thesis. The external collaborators Prof. David Smith and Prof. Peng George Wang were instrumental in conducting studies that could not have been completed without their help. Here at Caltech, I want to thank Dr. Chithra Krishnamurthy, Dr. Lan Ban, and Prof. Wen Yi. They all helped me complete the studies described in this thesis and without their help, this thesis would be a bit thinner.

The scientific staff here at Caltech is amazing and firstly, I am indebted to the knowledge and help I received from Scott Virgil. He helped me more than once and taught me more about chemistry than anyone at Caltech. I also would like to thank Mona Shahgholi for teaching me so much about mass spectrometry and helping me complete my MS based studies. She was also a friendly ear when things were not going well. Finally, Shelly Diamond was integral to the flow cytometry studies that are presented in this thesis.

I am also very grateful for all the help and support from Agnes Tong. She is truly a special person to have as a resource and friend. Joe Drew helped me out in so many different ways and is an asset to the Caltech community. Silva Virgil was also a great person to speak with and helped me numerous times during my graduate career. Also, Felicia Hunt was a tremendous help and amazing source of support. She helped me through some tough times and was a great person to talk with about life, education, and diversity. Finally, I would like to thank Lucy and Kim from Broad Café. They were so pleasant and

helpful every morning when I would get coffee. They always helped me keep my head on straight and keep my eye on the prize.

I would also like to thank the good friends I have made here at Caltech. Myles Herbert, Andrew Wang, Alexis Komor, JJ Kang, Jeff Holder, and Abby Pulsipher were all great friends and I have learned so much from them. I am thankful for their friendship and support through tough times I encountered during my time at Caltech. Things got a lot tougher in my last two years when they all started moving away. I also need to thank Alex Hansler for being a life-long friend who helped me tremendously in my final year at Caltech, when living apart from my wife. I would also like to thank my Stony Brook friends Matt Almond and Avinash Khanna for getting me interested in and excited about science in the first place. Finally, I need to thank the endless friends I have made in Southern California through hockey. While volunteering my time coaching youth hockey here and playing in adult leagues, I have many friends who have helped me get through some tough times.

I would especially like to thank my family for the strong support they have provided me over the years. Despite some rough patches growing up, they were always there and stuck by my side. I will forever be grateful for all they have done for me over the years. It is my family that is ultimately responsible for my scientific pursuit. After my aunt Trish died of lung cancer while I was in college, I then knew what I was destined to do. This event gave my life direction and I hope one day that my science can prevent other families from the hurt that I witnessed my family suffer during that time.

Finally, I want to thank my person, best friend, and wife, Christina Hagedorn. She is the strongest and most amazing person in my life and has taught me more than anyone

listed above. She challenged me to learn about myself and has taught me how to be a more caring and thoughtful person. Without her loving support I would have struggled greatly to get to this point. She has helped me grow into the man I am today and I cannot imagine a day without her in my life. I am a better person just by having her as my best friend.

Abstract

Protein fucosylation regulates a diverse set of physiological functions such as memory and learning, development, and disease pathogenesis. However, our current understanding of these processes is far behind that of other post-translational modifications, such as phosphorylation. This is, in part, due to the lack of tools available for the study of this important protein modification. To address this need, I have developed novel chemoenzymatic methods that enable the labeling and detection of unique forms of fucosylation, specifically fucose- α (1-2)-galactose (Fuc α (1-2)Gal) and core fucose. Additionally, novel glycosyltransferase assays were developed in-house to aid in the future development of both new and existing chemoenzymatic approaches.

I have demonstrated that the approach to detect Fuc α (1-2)Gal is highly selective for this disaccharide motif, detects a variety of complex glycans and glycoproteins, and can be used to profile the relative abundance of this motif on live cells, discriminating malignant from normal cells. I have also shown that the chemoenzymatic detection of core fucose exhibits superior specificity towards this glycan on a variety of complex *N*-glycans and when compared to current fucose-specific lectins. Further, the approach is amenable to detection of core fucosylated glycans from multiple biological settings, can be exploited as an antibody-conjugation method, and can be integrated into a diagnostic platform for the profiling of protein specific core fucosylation levels. These approaches represent new potential strategies for biomarker identification and expand the technologies available for understanding the role of these important fucosylated glycans in physiology and disease.

Published Content and Contributions

Chapter 2 is published as:

Chaubard, J-L., Krishnamurthy, C., Yi, W., Smith, D. F., and Hsieh-Wilson, L. C., (2012)
Chemoenzymatic Probes for Detecting and Imaging Fucose- α (1-2)-Galactose Glycan
Biomarkers. *J. Am. Chem. Soc.* 134(10): 4489-4492.

DOI: 10.1021/ja211312u

J-L. C. participated in the conception of this project, completed all experiments except the microscopy, flow cytometry and lectin affinity chromatography with synapsin I and participated in the writing of the manuscript.

Table of Contents

Acknowledgements.....	iv
Abstract.....	viii
Published Content and Contributions.....	ix
Table of Contents.....	x
List of Figures and Tables.....	xi
List of Abbreviations.....	xv
Chapter 1: Introduction: Chemical Approaches for the Detection of Fucose and the Biological Significance of Fucose- α (1-2)-Galactose and Core Fucose	1
Chapter 2: Chemoenzymatic Detection of the Fucose- α (1-2)-Galactose Glycan Biomarker.....	16
Chapter 3: Chemoenzymatic Detection of the Cancer-Relevant Core Fucose Biomarker	53
Chapter 4: Antibody-Conjugation using the Core Fucose Chemoenzymatic Approach.....	96
Chapter 5: Glycosyltransferase Assay Development.....	110
Appendix 1: Glycan Array Data Profiling the Acceptor Substrate Specificity of BgtA.....	128

List of Figures

Chapter 1: Chemical Approaches for the Detection of Fucose and the Biological Significance of Fucose- α (1-2)-Galactose and Core Fucose

Figure 1.1	Comparison of metabolic labeling to <i>in situ</i> chemoenzymatic labeling of glycans.....	7
Figure 1.2	The Fucose- α (1-2)-Galactose disaccharide	8
Figure 1.3	The Globo H antigen	9
Figure 1.4	The structure of core fucose	10

Chapter 2: Chemoenzymatic Detection of the Fucose- α (1-2)-Galactose Glycan Biomarker

Figure 2.1	The chemoenzymatic labeling approach for the detection of Fuca(1-2)Gal glycoconjugates.....	19
Figure 2.2	Probes used for detection of Fuca(1-2)Gal glycans	20
Figure 2.3	Synthesis of Fuca(1-2)Gal substrate 1	21
Figure 2.4	Purified BgtA.....	21
Figure 2.5	HPLC-MS analysis of the chemoenzymatic labeling of substrate 1 with UDP-ketoGal.....	22
Figure 2.6	HPLC-MS analysis of the chemoenzymatic labeling of substrate 1 with UDP-GalNAz	23
Figure 2.7	LC-MS/MS analysis of chemoenzymatically labeled Fuca(1-2)Gal substrate 1	24
Figure 2.8	Kinetic analysis of BgtA	25
Figure 2.9	Scheme of the work flow using the glycan microarray	26
Figure 2.10	Time course analysis using the glycan microarray, top 26 structures.....	27
Figure 2.11	Additional Fuca(1-2)Gal structures labeled on the glycan microarray ...	28

Figure 2.12	BgtA labels a variety of glycan structures	29
Figure 2.13	Additional specificity analysis from glycan microarray	30
Figure 2.14	Chemoenzymatic labeling of Fuc α (1,2)Gal glycoproteins.....	31
Figure 2.15	Comparison of UEA1 lectin affinity chromatography to the chemoenzymatic strategy	33
Figure 2.16	Fluorescence detection of Fuc α (1,2)Gal glycans (green) on HeLa cells	34
Figure 2.17	Fluorescence detection of Fuc α (1,2)Gal glycans (green) on live MCF-7 cells	35
Figure 2.18	Flow cytometry analysis of the relative expression levels of Fuc α (1,2)Gal glycans across various cancer cell lines	36
 Chapter 3: Chemoenzymatic Detection of the Cancer-Relevant Core Fucose Biomarker		
Figure 3.1	The chemoenzymatic labeling approach for the detection of core fucosylated glycoproteins.....	56
Figure 3.2	Probes used for detection of core fucose glycans	57
Figure 3.3	MALDI-TOF-MS analysis of GALT-1 donor substrate specificity using a dabsylated glycopeptide acceptor substrate	58
Figure 3.4	Determination of kinetic parameters for GALT-1 towards its substrates.....	59
Figure 3.5	GALT-1 acceptor substrate specificity MALDI-TOF analysis.....	61
Figure 3.6	GALT-1 acceptor substrate specificity quantified.....	62
Figure 3.7	GALT-1 efficiently labels core fucosylated glycoproteins	63
Figure 3.8	GALT-1 enzymatic efficiency comparing natural and non-natural donor substrates	64
Figure 3.9	GALT-1 specifically labels core fucosylated glycoproteins	66

Figure 3.10	Lectin blot analysis of <i>Fut8</i> ^{-/-} and <i>Fut8</i> ^{+/+} mouse brain lysates	67
Figure 3.11	Chemoenzymatic labeling of cell surface core fucose	68
Figure 3.12	GALT-1 efficiently labels samples of comparable protein concentration with differing levels of core fucosylation	70
Figure 3.13	Chemoenzymatic labeling of serum from a healthy donor and an HCC patient	71
Figure 3.14	The chemoenzymatic approach incorporated into a proteomic work flow with the <i>N</i> -glycan cleavable linker	73
Figure 3.15	The chemoenzymatic approach labels the Hepatocellular Carcinoma biomarker, core fucosylated α -fetoprotein	74
Figure 3.16	Integration of the chemoenzymatic approach into an ELISA format for quantification of core fucosylated AFP – AFP capture	75
Figure 3.17	Integration of the chemoenzymatic approach into an ELISA format for quantification of core fucosylated AFP – biotin capture	76
 Chapter 4: Antibody-Conjugation using the Core Fucose Chemoenzymatic Approach		
Figure 4.1	Scheme utilizing the core fucose chemoenzymatic approach for antibody-conjugation	99
Figure 4.2	Optimization of ADIBO-biotin concentration for antibody-conjugation using the chemoenzymatic approach.....	101
Figure 4.3	Antibody-conjugation using anti-CSE antibody.....	102
Figure 4.4	HCD MS ² spectra of the enzymatically labeled anti-CSE glycopeptide.....	104
Figure 4.5	Full MS spectra of the enzymatically labeled anti-CSE glycopeptide.....	105
 Chapter 5: Glycosyltransferase Assay Development		
Figure 5.1	Turn-on fluorescence xanthene-based Zn (II) complex chemosensor for the monitoring of glycosyltransferase reactions	113

Figure 5.2	Use of the fluorescent sensor for development of a chemoenzymatic high-throughput discovery platform (Scheme).....	114
Figure 5.3	Emission profile optimization for the sensor (17-2Zn(II)) in presence of UDP	115
Figure 5.4	Investigating the effects of sensor (17-2Zn(II)) concentration and efficacy in the presence of 5 mM MnCl ₂ and 1% Triton X-100	116
Figure 5.5	MS-based glycosyltransferase assay for GalT, the enzyme used for or the chemoenzymatic labeling of <i>O</i> -GlcNAc	118
Figure 5.6	HPLC-based glycosyltransferase assay for GalT	120
Figure 5.7	Fluorescence-based glycosyltransferase assay for GalT	121
Figure 5.8	Fluorescent glycosyltransferase assay to monitor reaction progress during chemoenzymatic labeling of alpha-crystallin	123

Appendix 1: Glycan Array Data Profiling the Acceptor Substrate Specificity of BgtA

Table 1	Time course analysis of BgtA specificity on the glycan microarray.....	129
----------------	------------------------------------------------------------------------	-----

List of Abbreviations

2-D-Gal	2-deoxy-galactose
AAD	7-amino-actinomycin D
AAL	Aleuria Aurantia Lectin
AcOH	acetic acid
ADC	antibody-drug conjugate
ADCC	antibody-dependent cell-mediated cytotoxicity
ADIBO	azadibenzocyclooctyne
AFP	α -fetoprotein
AOL	Aspergillus Oryzae Lectin
APCI	atmospheric pressure chemical ionization
Asn	asparagine
BCA	bicinchoninic acid
BgtA	bacterial analogue of blood group A transferase
BSA	bovine serum albumin
CaCl ₂	calcium chloride
CCRC	Complex Carbohydrate Research Center
CE	capillary electrophoresis
CFG	consortium for functional glycomics
CHCA	α -Cyano-4-hydroxycinnamic acid
CHCl ₃	chloroform
CSE	chondroitin sulfate-E
CuAAC	Cu(I)-catalyzed azide-alkyne cycloaddition
CuSO ₄	copper sulfate
DAPI	4',6-diamidino-2-phenylindole
DAR	drug-antibody ratio
DHB	2,5-dihydroxybenzoic acid
DMEM	Dulbecco's modified Eagle media
DMSO	dimethyl sulfoxide
DTT	dithiothreitol
EDTA	ethylenediaminetetraacetic acid
EGFR	epidermal growth factor receptor
EGTA	ethylene glycol tetraacetic acid
ELISA	enzyme-linked immunosorbent assay
ESI	electrospray ionization
FBS	fetal bovine serum
FDA	Food and Drug Administration
FITC	fluorescein isothiocyanate
Fuc	fucose
Fuc α (1-2)Gal	fucose- α (1-2)-galactose
Fut 1	fucosyltransferase 1

Fut 2	fucosyltransferase 2
Fut 8	fucosyltransferase 8
Gal	galactose
Gal-6-NH ₂	6-galactosamine
GalNAc	<i>N</i> -Acetylgalactosamine
GalNaz	<i>N</i> -azidoacetylgalactosamine
GalT	bovine β-1,4 galactosyltransferase
GALT-1	<i>C. elegans</i> β-1,4-galactosyltransferase
Galβ(1-4)GlcNAc	galactose-β-1,4- <i>N</i> -Acetylglucosamine
GDP	guanosine diphosphate
GlcNAc	<i>N</i> -Acetylglucosamine
H ₂ O	water
HBSS	Hank's Balanced Salt Solution
HCC	Hepatocellular Carcinoma
HCD	higher-energy collisional dissociation
HCl	hydrochloric acid
HEPES	4-(2-hydroxyethyl)-1-piperazineethanesulfonic acid
HRP	horseradish peroxidase
IDT	Integrated DNA Technologies
IgG	immunoglobulin G
IMAC	immobilized metal affinity chromatography
IPTG	isopropyl-1-thio-β-D-galactopyranoside
kDa	kilodalton
L1CAM	L1 Cell Adhesion Molecule
LacNAc	<i>N</i> -Acetylglucosamine
LB	lysogeny broth
LC-MS	liquid chromatography - mass spectrometry
LCA	Lens Culinaris Agglutinin
LTP	long-term potentiation
LTQ	linear triple quadrupole
MALDI-TOF	matrix assisted laser desorption/ionization - time of flight
MeCN	acetonitrile
MeOH	methanol
MgCl ₂	magnesium chloride
MnCl ₂	manganese chloride
MS	mass spectrometry
MW	molecular weight
MWCO	molecular weight cut-off
Na ₂ HPO ₄	sodium phosphate dibasic
NaCl	sodium chloride
NaCNBH ₃	sodium cyanoborohydride
NaOAc	sodium acetate

NCAM	neural cell adhesion molecule
NDP	nucleotide diphosphate
NH ₄ Cl	ammonium chloride
<i>O</i> -GlcNAc	<i>O</i> -linked- β - <i>N</i> -acetylglucosamine
p44 MAPK	p44 mitogen-associated protein kinase
PBS	phosphate buffer with saline
PCR	polymerase chain reaction
PIC	protease inhibitor cocktails
PNGaseF	Peptide <i>N</i> -glycosidase F
pnp	<i>p</i> -nitrophenol
POFUT1	protein <i>O</i> -fucosyltransferase 1
POFUT2	protein <i>O</i> -fucosyltransferase 2
PSA	prostate-specific antigen
PVDF	polyvinylidene fluoride
RFU	relative fluorescence units
RPMI	Roswell Park Memorial Institute
SAV	streptavidin-conjugated Alexa Fluor 680
SDS	sodium dodecyl-sulfate
SDS-PAGE	sodium dodecyl sulfate polyacrylamide gel electrophoresis
SPAAC	strain-promoted alkyne-azide cycloaddition
SUMO	small ubiquitin-related modifier
TAMRA	tetramethyl-6-carboxy-rhodamine
TBS	tris buffered saline
TBST	tris buffered saline with triton X-100
TFA	trifluoroacetic acid
TGF	transforming growth factor
THTPA	tris(3-hydroxypropyltriazolylmethyl)amine
UDP	uridine diphosphate
UDP-Gal-6-N ₃	6-deoxy-6-azido-galactose
UDP-GalNAz	<i>N</i> -azidoacetylgalactosamine
UDP-ketoGal	2-deoxy-2-(acetyl)- β -D-galactopyranoside
UEA1	Ulex Europaeus Agglutinin
UV	ultra violet
VCAM	vascular cell adhesion protein
ZnCl ₂	zinc chloride

Chapter 1

Introduction:

Chemical Approaches for the Detection of Fucose and
the Biological Significance of Fucose- α (1-2)-Galactose and Core Fucose

INTRODUCTION

Protein glycosylation is an abundant post-translational modification found in all forms of life.¹ However, our understanding of this important protein modification is decades behind that of other post-translational modifications, such as phosphorylation, due to the vast complexity of glycan structure, biosynthesis, and the lack of tools available to effectively study specific types of glycosylation. Protein fucosylation is a specific form of glycosylation that has been shown to regulate a variety of physiological functions such as memory and learning, development, and disease pathogenesis.¹ Multiple forms of fucosylation exist, further complicating our understanding of their individual functions.

CHEMICAL APPROACHES USED FOR THE DETECTION OF FUCOSE

Lectins

Currently, the work directed at characterizing protein fucosylation relies heavily on fucose-specific antibodies or lectins. However, these reagents generally suffer from poor specificity and weak binding affinities. These issues cause lectins and antibodies to display cross-reactivity with multiple different glycan structures.²⁻⁴ For example, the lectin Ulex Europaeus Agglutinin I (UEA1) claims specificity towards the Fucose- α (1-2)-Galactose disaccharide; however it was shown to detect multiple forms of fucosylation, and free fucose itself.³ The recent development and application of glycan microarrays have enabled researchers to carefully characterize the specificity of carbohydrate-specific antibodies and lectins in a high throughput fashion.⁵

Metabolic Labeling

An alternative method for glycan detection, metabolic labeling, provides a powerful approach for the study of glycans.⁶⁻¹⁰ This method requires the uptake of non-natural monosaccharide analogues, bearing bioorthogonal chemical functionality such as an azide or alkyne. This non-natural monosaccharide makes its way through the biosynthetic pathway and ultimately gets incorporated into the cellular glycans that normally contain this monosaccharide (Figure 1.1A). Next, bioorthogonal chemistry is performed on the sample to install a visualization tag (Figure 1.1A). While this method has provided numerous publications and is invaluable to the study of glycans, it suffers from specificity and sensitivity issues as well. First, specific disaccharides or trisaccharides of specific linkage and composition, such as Fucose- α (1-2)-Galactose, cannot be identified. For example, metabolic labeling of cells with a fucose analogue will not enable researchers to distinguish Fucose- α (1-2)-Galactose from *O*-linked fucose or core fucose. Additionally, non-natural sugar analogues will be competing with the endogenous, naturally occurring, monosaccharides. This competition will cause sensitivity issues, as the non-natural analogue will be incorporated in sub-stoichiometric levels.

Unfortunately, these sensitivity and specificity issues are not the only potential problems when utilizing the metabolic labeling approach. The path a non-natural sugar analogue takes from uptake to incorporation into the glycoconjugates is not simple. The non-natural monosaccharides need to be converted into the nucleotide diphosphate-non-natural sugar (NDP-non-natural sugar), pass through transporters from the cytosol into the golgi and/or ER, and be recognized by glycosyltransferases. Any one of these points can create a bottleneck. However, the most pressing issue with this process is that of

glycosyltransferase preference. Since one NDP-sugar donor substrate can be utilized by multiple glycosyltransferases, it is reasonable to assume that some glycosyltransferases utilize particular non-natural substrates better than others. In the case of fucose, over 13 fucosyltransferase are established in mammalian systems; however, they do not utilize 6-alkyne-fucose with the same efficiency.¹¹ It was determined that protein O-fucosyltransferase 1 (POFUT1) and protein O-fucosyltransferase 2 (POFUT2) utilize this non-natural substrate much better than fucosyltransferase 8 (FUT8). The issue here is that in most systems, the metabolic labeling approach will yield biased incorporation stoichiometries among different glycoconjugates of similar monosaccharide composition and this type of information is not currently characterized.

Another potential issue is that large amounts of sugar are being introduced to the cells, potentially perturbing the endogenous cellular metabolism. To date, studies have not been conducted that determine the physiological or metabolic effects of these non-natural sugar analogues. Finally, because this approach requires that the cells or organism be incubated with the non-natural sugar, biological material from human samples cannot be interrogated using this approach. This metabolic approach has been invaluable to the scientific community and has advanced our understanding of glycan function over the recent decade; however, this approach suffers from sensitivity and selectivity issues, among other limitations.

Chemoenzymatic Labeling

Most recently, the chemoenzymatic approach has been utilized to detect specific glycan structures with superior sensitivity and selectivity over the preceding methods. This

approach involves incubating cells or proteins, from any biological source, with an exogenous glycosyltransferase and a non-natural donor substrate (Figure 1.1B). Then, as with the metabolic labeling approach discussed above, bioorthogonal chemistry is performed to install detection tags specifically onto the glycan structure of interest (Figure 1.1B). This approach provides several advantages over the metabolic labeling approach. First, the specificity is dictated by the glycosyltransferase, which installs the non-natural sugar onto very specific glycan structures of defined connectivity and composition. Additionally, because the reaction proceeds in quantitative yield, the sensitivity of detection is much greater than that of the metabolic labeling or lectin based approaches. Because this approach covalently installs detection tags onto the specific glycan structures, it is amenable to direct glycoproteomic profiling and site mapping studies of these unique glycoproteins. Finally, because any biological sample can be interrogated using this approach, the chemoenzymatic labeling strategy is an excellent resource for identification of carbohydrate-based disease biomarkers.

To date, only a handful of these methods exist, with two of them described in this thesis. Developed over a decade ago by the Hsieh-Wilson group, the first chemoenzymatic approach was used to selectively detect *O*-linked- β -*N*-acetylglucosamine (*O*-GlcNAc).¹² This approach exploited the β -1,4 galactosyltransferase, GalT, which was engineered to accept galactose analogs with non-natural functionality installed at the C-2 position. In this initial publication of the method, a ketone-galactose analogue was used with aminoxy-derivatized detection reagents. Years later this approach was updated to include the use of an azido-galactose analogue, GalNAz, and the copper catalyzed azide-alkyne cycloaddition (CuAAC), commonly referred to as “click chemistry”.¹³ Recently, this approach was

modified to determine the stoichiometry of glycosylation on specific proteins.¹⁴ In this approach, the enzymatic labeling step was unchanged; however, instead of installing a detection tag, a 2- or 5- kilodalton mass tag was installed onto the labeled *O*-GlcNAc glycoproteins. The samples were then subjected to SDS-PAGE and resolved by western blot analysis for specific proteins of interest. This enabled visualization of the different glycoforms of a particular glycoprotein and informed the protein specific dynamics of this modification. A tremendous amount of information has been learned with this single chemoenzymatic approach, demonstrating the value of this method.

More recently, Wu and co-workers developed a chemoenzymatic approach for the detection of *N*-acetyllactosamine (LacNAc), a disaccharide of defined compositing and connectivity.¹⁵ This was the first study to utilize the chemoenzymatic approach for the visualization of specific glycan motifs on whole organisms, *C. elegans*, and utilizing a flow cytometry readout, highlighting the versatility of the chemoenzymatic approach.

It was during this time that I was finalizing the second chemoenzymatic approach from the Hsieh-Wilson lab. This approach enabled the detection of the Fucose- α (1-2)-Galactose motif, and with this approach I was able to profile the cell surface expression levels of this disaccharide across various cancer cell lines.¹⁶ Further, I was able to distinguish prostate cancer cells from healthy prostate epithelial cells, demonstrating the diagnostic capacity of the chemoenzymatic approach. This method is described in detail in chapter 2.

Finally, I have recently completed the development of a chemoenzymatic approach for the detection of core fucosylated glycoproteins (in preparation). I was able to integrate this approach into a diagnostic ELISA platform (Chapter 3), develop a biomarker

identification proteomic workflow (Chapter 3), and exploit this approach as an antibody-conjugation method (Chapter 4).

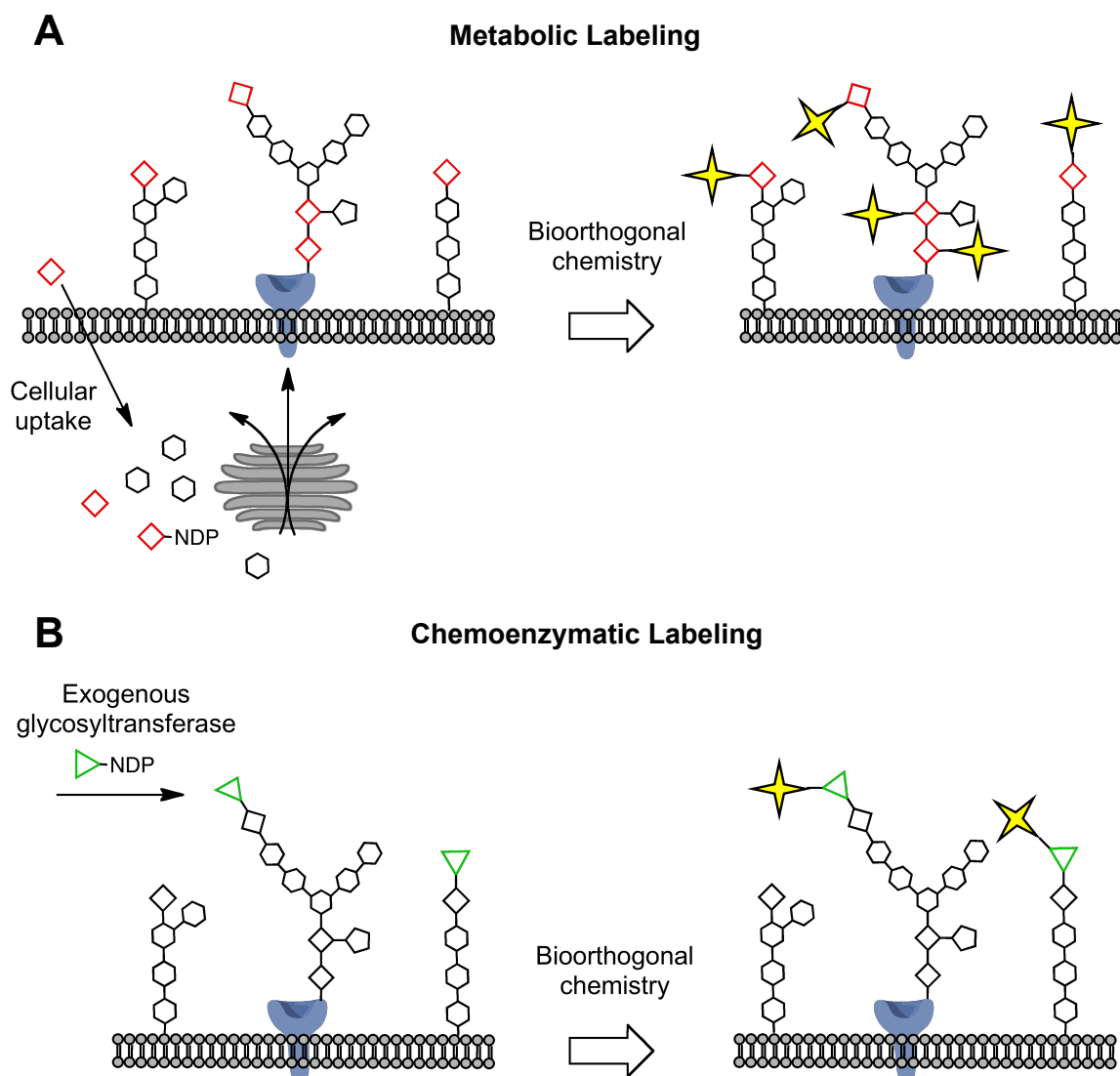


Figure 1.1 Comparison of metabolic labeling to *in situ* chemoenzymatic labeling of glycans. In metabolic labeling, a non-natural sugar (red) containing a bioorthogonal functional group is taken up by the cell and incorporated via the cell's biosynthetic machinery into glycoconjugates. In chemoenzymatic labeling, an exogenous glycosyltransferase enzyme and non-natural nucleotide sugar analog (green) are used to transfer a non-natural sugar containing a bioorthogonal group onto specific glycan structures. Once a bioorthogonal group is installed, both methods use bioorthogonal ligation chemistry to install a detectable probe (yellow) to track the labeled glycans.

BIOLOGICAL SIGNIFICANCE OF FUCOSE- α (1-2)-GALACTOSE AND CORE FUCOSE

Fucose- α (1-2)-Galactose

The Fucose- α (1-2)-Galactose (Fuca(1-2)Gal) disaccharide is produced by the α (1-2) addition of fucose (red) to galactose, catalyzed by either FUT1 or FUT2, which are differentially expressed in a tissue dependent fashion (Figure 1.2). Fuca(1-2)Gal is found on the non-reducing terminus of a many important glycans, including blood group H1 and H2, Globo H, Fuc-GM1, Lewis B, and Lewis Y. These glycans play important roles in processes such as learning and memory and contribute to asthma, inflammation, and tumorigenesis.¹⁷⁻²⁶

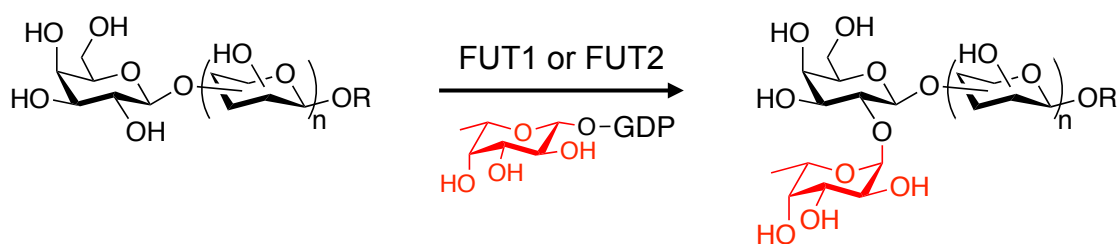
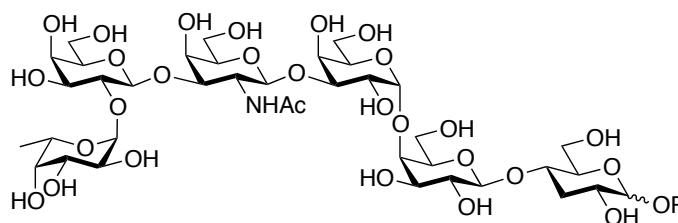


Figure 1.2 The Fucose- α (1-2)-Galactose disaccharide is produced by the α (1-2) addition of fucose (red) to galactose, catalyzed by either FUT1 or FUT2. R can be either protein or lipid and this disaccharide is generally a terminal motif of longer glycan chains.

Interestingly, task-specific learning and long-term potentiation (LTP) induce this glycan in hippocampal neurons.¹⁸ Additionally, the injection of 2-deoxy-galactose (2-D-Gal), an inhibitor of Fuca(1-2)Gal synthesis, causes reversible amnesia in rats and interferes with the maintenance of LTP.²⁷ The Fuca(1-2)Gal glycan also regulates the stability and turnover of synapsin I, a protein important for synapse formation and neurotransmitter release.²⁸

This glycan has also been implicated as a cancer biomarker.²⁹⁻³³ Specifically, the Globo H antigen, a hexasaccharide glycosphingolipid with a terminal Fuca(1-2)Gal

epitope, is overexpressed on a variety of epithelial cell tumors (Figure 1.3).^{21,29,31} Fuc α (1-2)Gal glycan expression was also elevated in prostate cancer tissue and on the tumorigenic prostate-specific antigen (PSA) protein, when compared to normal epithelial tissue or PSA.³²



Globo H Antigen

Figure 1.3 The Globo H antigen is a hexasaccharide glycosphingolipid, terminating with the Fucose- α (1-2)-Galactose disaccharide, and is overexpressed on a variety of epithelial cell tumors.

More recently, it has been determined that this glycan is induced in the small intestine of mice upon bacterial infection and modulates microbe-host interactions.^{33,34} Systemic infection led to increased expression of the Fut2 gene and subsequent cell surface and secreted Fuc α (1-2)Gal glycoproteins. Fucose was cleaved from this disaccharide by bacterial fucosidases and utilized by the microbes in an unknown manner. This process led to a suppression of pathogen virulence, providing a protective role towards the host. This glycan clearly plays roles in many facets of healthy and disease physiology.

Core Fucose

Core fucose is a FUT8 catalyzed α -1,6-fucose attached to the reducing end *N*-Acetylglucosamine (GlcNAc) of *N*-glycans (Figure 1.4).¹ This modification is the most abundant post-translational fucosylation and regulates a variety of important biological processes such as cell signaling,^{35,36} cell adhesion,^{37,38} long-term potentiation,³⁹ and antibody-dependent cellular cytotoxicity⁴⁰ and is upregulated in various cancers.⁴¹⁻⁵⁰ The

recent development of *fut8* knock-out mice has led to numerous discoveries, demonstrating that misregulation of core fucose has broad consequences and implicating this protein modification in physiological, developmental, and immunological disorders.⁵¹

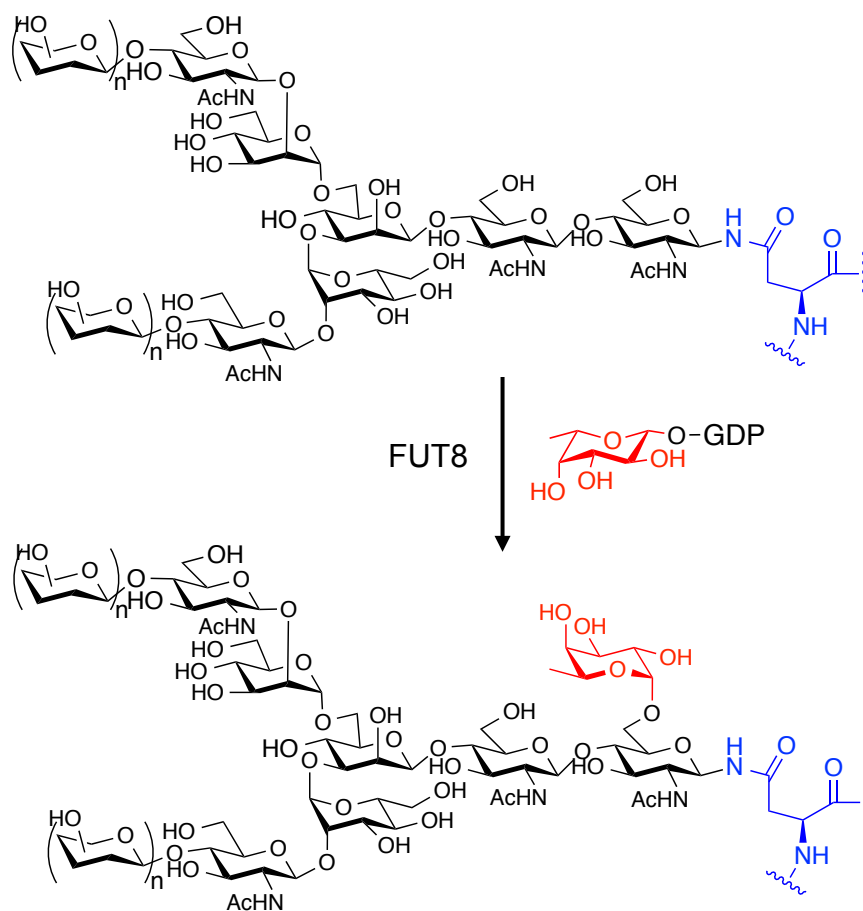


Figure 1.4 Core fucose (red) is an alpha-1,6 fucose attached to the core GlcNAc of *N*-linked glycans and catalyzed by fucosyltransferase 8 (FUT8). The *N*-Glycan is directed attached to asparagine residues (blue).

The *fut8* knock-out mice have been used to show that the loss of core fucose on the TGF- β 1 receptor led to deregulation of this signaling pathway, presenting a emphysema-like phenotype.⁵² Also, loss of core fucose on the EGF-receptor attenuated the EGF signaling pathway³⁵ and downregulated integrin α 4 β 1-mediated cell adhesion.³⁷ Additionally, loss of VCAM-1 core fucosylation led to decreased pre-B cell binding to stromal cells, leading to misregulated B cell development and function.³⁸ Finally, with the

recent use of therapeutic antibodies, work has demonstrated that loss of core fucose on human IgG1 antibodies leads to ~ 100 fold increase in antibody-dependent cellular cytotoxicity (ADCC).⁴⁰

Core fucose has also been implicated in both cancer pathogenesis and as a diagnostic marker.⁴¹⁻⁴⁷ Specifically, increased core fucosylation of serum glycoproteins has been discovered in breast,⁴¹ prostate,⁴² and pancreatic cancers,⁴³ but perhaps best studied in the case of Hepatocellular Carcinoma (HCC) where increased core fucosylation of α -fetoprotein (AFP), among other proteins, has been shown to directly correlate with HCC pathogenesis.⁴⁴⁻⁵⁰ AFP levels are currently used to monitor HCC progression and used as a prognostic marker.⁴⁸ However, AFP levels are also elevated during other liver disorders such as chronic hepatitis (in both HepB and HepC) and cirrhosis.^{49,50} The core fucosylation levels on AFP, regardless of the total AFP levels, have been shown to be the strongest correlate with HCC prognosis. Taken together, these observations clearly demonstrate multiple physiological roles for core fucose, likely influencing protein structure and dynamics, and this glycan can be used in a protein-specific fashion for cancer diagnostics.

REFERENCES

1. Varki, A.; Cummings, R.D.; Esko, J.D.; H Freeze, H.H.; Stanley, P.; Bertozzi, C.R.; Hart, G.W.; Etzler, M.E. *Essential of Glycobiology, 2nd Edition*; Cold Spring Harbor Laboratory Press: Cold Spring Harbor, New York, **2009**.
2. Manimala, J. C.; Roach, T. A.; Li, Z.; Gildersleeve, J. C. *Angewandte Chemie International Edition* **2006**, 45, 3607.
3. Manimala, J. C.; Roach, T. A.; Li, Z.; Gildersleeve, J. C. *Glycobiology* **2007**, 17, 17C.
4. Chang, C.-F.; Pan, J.-F.; Lin, C.-N.; Wu, I.-L.; Wong, C.-H.; Lin, C.-H. *Glycobiology* **2011**, 21, 895.

5. Blixt, O.; Head, S.; Mondala, T.; Scanlan, C.; Huflejt, M. E.; Alvarez, R.; Bryan, M. C.; Fazio, F.; Calarese, D.; Stevens, J.; Razi, N.; Stevens, D. J.; Skehel, J. J.; van Die, I.; Burton, D. R.; Wilson, I. A.; Cummings, R.; Bovin, N.; Wong, C.-H.; Paulson, J. C. *Proceedings of the National Academy of Sciences USA* **2004**, 101, 17033.
6. Laughlin, S. T.; Baskin, J. M.; Amacher, S. L.; Bertozzi, C. R. *Science* **2008**, 320, 664.
7. Laughlin, S.T.; Bertozzi, C.R. *Proceedings of the National Academy of Sciences USA* **2009**, 106, 12.
8. Hanson, S. R.; Hsu, T.-L.; Weerapana, E.; Kishikawa, K.; Simon, G. M.; Cravatt, B. F.; Wong, C.-H. *Journal of the American Chemical Society* **2007**, 129, 7266.
9. Tanaka, Y.; Kohler, J. J. *Journal of the American Chemical Society* **2008**, 130, 3278.
10. Zaro, B. W.; Yang, Y.-Y.; Hang, H. C.; Pratt, M. R. *Proceedings of the National Academy of Sciences USA* **2011**, 108, 8146.
11. Al-Shareffi, E.; Chaubard, J.-L.; Leonhard-Melief, C.; Wang, S.-K.; Wong, C.-H.; Haltiwanger, R. S. *Glycobiology* **2013**, 23, 188.
12. Khidekel, N.; Arndt, S.; Lamarre-Vincent, N.; Lippert, A.; Poulin-Kerstien, K. G.; Ramakrishnan, B.; Qasba, P. K.; Hsieh-Wilson, L. C. *Journal of the American Chemical Society* **2003**, 125, 16162.
13. Clark, P. M.; Dweck, J. F.; Mason, D. E.; Hart, C. R.; Buck, S. B.; Peters, E. C.; Agnew, B. J.; Hsieh-Wilson, L. C. *Journal of the American Chemical Society* **2008**, 130, 11576.
14. Clark, P. M.; Rexach, J. E.; Hsieh-Wilson, L. C. *Current Protocols in Chemical Biology* **2013**, 5, 281-302.
15. Zheng, T.; Jiang, H.; Gros, M.; Soriano del Amo, D.; Sundaram, S.; Lauvau, G.; Marlow, F.; Liu, Y.; Stanley, P.; Wu, P. *Angewandte Chemie International Edition* **2011**, 50, 4113.
16. Chaubard, J.-L.; Krishnamurthy, C.; Yi, W.; Smith, D. F.; Hsieh-Wilson, L. C. *Journal of the American Chemical Society* **2012**, 134, 4489.
17. McCabe, N. R.; Rose, S. P. *Neurochemistry Research* **1985**, 10, 1083.

18. Pohle, W.; Acosta, L.; Ruthrich, H.; Krug, M.; Matthies, H. R. *Brain Research* **1987**, 410, 245.
19. Tiunova, A.A.; Anokhin, K.V.; Rose, S.P. *Learning and Memory* **1998**, 4, 401.
20. Becker, D. J.; Lowe, J. B. *Glycobiology* **2003**, 13, 41R.
21. Chang, W.-W.; Lee, C. H.; Lee, P.; Lin, J.; Hsu, C.-W.; Hung, J.-T.; Lin, J.-J.; Yu, J.-C.; Shao, L.-e.; Yu, J.; Wong, C.-H.; Yu, A. L. *Proceedings of the National Academy of Sciences USA* **2008**, 105, 11667.
22. Menard, S.; Tagliabue, E.; Canevari, S.; Fossati, G.; Colnaghi, M.I. *Cancer Research* **1983**, 43, 1295.
23. Zhang, S.; Zhang, H.S.; Cordon-Cardo, C.; Ragupathi, G.; Livingston, P.O. *Clinical Cancer Research* **1998**, 4, 2669.
24. Miyake, M.; Taki, T.; Hitomi, S.; Hakomori, S.-i. N. *New England Journal of Medicine* **1992**, 327, 14.
25. Colnaghi, M. I.; Da Dalt, M.G.; Agresti, R.; Cattoretti, G.; Andreola, S.; Di Fronzo, G.; Del Vecchio, M.; Verderio, L.; Cascinelli, N.; Rilke, F. In *Immunological Approaches to the Diagnosis and Therapy of Breast Cancer*; Ceriani, R. L., Ed.; *Plenum Publishing: New York*, **1987**, 21.
26. Lee J.S.; Sahin A.A.; Hong, W.K.; Brown, B.W.; Mountain, C.F.; Hittleman, W.N. N. *New England Journal of Medicine* **1991**, 324, 1084.
27. Tiunova A.A.; Anokhin K.V.; Rose S.P. *Learning and Memory* **1998**, 4, 401.
28. Murrey, H.E.; Gama, C.I.; Kalovidouris, S.A.; Luo, W.I.; Driggers, E.M.; Porton, B.; and Hsieh-Wilson, L.C., *Proceedings of the National Academy of Sciences USA* **2006**, 103, 21.
29. Bremer, E.G.; *et al.* *Journal of Biological Chemistry* **1984**, 259, 14773.
30. Mènard, S.; Tagliabue, E.; Canevari, S.; Fossati, G.; Colnaghi, M.I. *Cancer Research* **1983**, 43, 1295.
31. Lee, J.S.; *et al.* *New England Journal of Medicine* **1991**, 324, 1084.
32. Peracaula, R.; Tabarés, G.; Royle, L.; Harvey, D.J.; Dwek, R.A.; Rudd, P.M.; de Llorens, R. *Glycobiology* **2003**, 13, 457.

33. Pickard, J.M.; Maurice, C.F.; Kinnebrew, M.A.; Abt, M.C.; Schenten, D.; Golovkina, T.V.; Bogatyrev, S.R.; Ismagilov, R.F.; Pamer, E.G.; Turnbaugh, P.J.; and Chervonsky, A.V. *Nature* **2014**, 514, 638.
34. Pham, T.A.N.; Clare, S.; Goulding, D.; Arasteh, J.M.; Stares, M.D.; Browne, H.P.; Keane, J.A.; Page, A.J.; Kumasaka, N.; Kane, L.; and Mottram, L. *Cell Host & Microbe* **2014**, 16, 504.
35. Wang, X.; Gu, J.; Ihara, H.; Miyoshi, E.; Honke, K.; Taniguchi, N. *Journal of Biological Chemistry* **2006**, 281, 2572.
36. Shen, N.; Lin, H.; Wu, T.; Wang, D.; Wang, W.; Xie, H.; Zhang, J.; Feng, Z. *Kidney International* **2013**, 84, 64.
37. Zhao, Y.; Itoh, S.; Wang, X.; Isaji, T.; Miyoshi, E.; Kariya, Y.; Miyazaki, K.; Kawasaki, N.; Taniguchi, N.; Gu, J. *Journal of Biological Chemistry* **2006**, 281, 38343.
38. Li, W.; Ishihara, K.; Yokota, T.; Nakagawa, T.; Koyama, N.; Jin, J.; Mizuno-Horikawa, Y.; Wang, X.; Miyoshi, E.; Taniguchi, N. *Glycobiology* **2008**, 18, 114.
39. Gu, W.; Fukuda, T.; Isaji, T.; Hang, Q.; Lee, H.-h.; Sakai, S.; Morise, J.; Mitoma, J.; Higashi, H.; Taniguchi, N. *Journal of Biological Chemistry* **2015**, 290, 17566.
40. Shields, R. L.; Lai, J.; Keck, R.; O'Connell, L. Y.; Hong, K.; Meng, Y. G.; Weikert, S. H.; Presta, L. G. *Journal of Biological Chemistry* **2002**, 277, 26733.
41. Kyselova, Z.; Mechref, Y.; Kang, P.; Goetz, J. A.; Dobrolecki, L. E.; Sledge, G. W.; Schnaper, L.; Hickey, R. J.; Malkas, L. H.; Novotny, M. V. *Clinical Chemistry* **2008**, 54, 1166.
42. Saldova, R.; Fan, Y.; Fitzpatrick, J. M.; Watson, R. W. G.; Rudd, P. M. *Glycobiology* **2011**, 21, 195.
43. Lin, Z.; Simeone, D. M.; Anderson, M. A.; Brand, R. E.; Xie, X.; Shedden, K. A.; Ruffin, M. T.; Lubman, D. M. *Journal of Proteome Research* **2011**, 10, 2602.
44. Comunale, M. A.; Wang, M.; Hafner, J.; Krakover, J.; Rodemich, L.; Kopenhaver, B.; Long, R. E.; Junaidi, O.; Bisceglie, A. M. D.; Block, T. M.; Mehta, A.S. *Journal of Proteome Research* **2009**, 8, 595.
45. Block, T. M.; Comunale, M. A.; Lowman, M.; Steel, L. F.; Romano, P. R.; Fimmel, C.; Tennant, B. C.; London, W. T.; Evans, A. A.; Blumberg, B. S. *Proceedings of the National Academy of Sciences USA* **2005**, 102, 779.

46. Zhu, J.; Lin, Z.; Wu, J.; Yin, H.; Dai, J.; Feng, Z.; Marrero, J.; Lubman, D. M. *Journal of Proteome Research* **2014**, *13*, 2986.
47. Comunale, M. A.; Rodemich-Betesh, L.; Hafner, J.; Wang, M.; Norton, P.; Di Bisceglie, A. M.; Block, T.; Mehta, A. *PloS One* **2010**, *5*, e12419.
48. Yuen, M.-F.; Lai, C.-L. *Best Practice & Research Clinical Gastroenterology* **2005**, *19*, 91.
49. Chen, D.-S.; Sung, J.; Sheu, J.; Lai, M.-Y.; How, S.; Hsu, H.; Lee, C.-S.; Wei, T. *Gastroenterology* **1984**, *86*, 9.
50. Buamah, P. K.; Gibb, I.; Bates, G.; Ward, A. M. *Clinica chimica acta* **1984**, *139*, 313.
51. Gu, W.; Fukuda, T.; Gu, J. *Sugar Chains*, Chapter 17, Springer Japan, **2015**.
52. Wang, X.; Inoue, S.; Gu, J.; Miyoshi, E.; Noda, K.; Li, W.; Mizuno-Horikawa, Y.; Nakano, M.; Asahi, M.; Takahashi, M.; Uozumi, N.; Ihara, S.; Lee, S.H.; Ikeda, Y.; Yamaguchi, Y.; Aze, Y.; Tomiyama, Y.; Fujii, J.; Suzuki, K.; Kondo, A.; Shapiro, S.D.; Lopez-Otin, C.; Kuwaki, T.; Okabe, M.; Honke, K.; Taniguchi, N. *Proceedings of the National Academy of Sciences USA* **2005**, *102*, 15791.

Chapter 2

Chemoenzymatic Detection of the Fucose- α (1-2)-Galactose Glycan Biomarker

This chapter is published as:

Chaubard, J-L., Krishnamurthy, C., Yi, W., Smith, D. F., and Hsieh-Wilson, L. C., (2012)
Chemoenzymatic Probes for Detecting and Imaging Fucose- α (1-2)-Galactose Glycan
Biomarkers. *J. Am. Chem. Soc.* 134(10): 4489-4492.

ABSTRACT

The disaccharide motif fucose- α (1-2)-galactose (Fuc α (1-2)Gal) is involved in many important physiological processes, such as learning and memory, inflammation, asthma, and tumorigenesis. However, the size and structural complexity of Fuc α (1-2)Gal-containing glycans have posed a significant challenge to their detection and study. In this chapter, I report a new chemoenzymatic strategy for the rapid, sensitive detection of Fuc α (1-2)Gal glycans. I have demonstrated that the approach is highly selective for the Fuc α (1-2)Gal motif, detects a variety of complex glycans and glycoproteins, and can be used to profile the relative abundance of the motif on live cells, discriminating malignant from normal cells. This approach represents a new potential strategy for biomarker detection and expands the technologies available for understanding the roles of this important class of carbohydrates in physiology and disease.

INTRODUCTION

Defects in glycosylation are a hallmark of many human diseases, including autoimmune disorders, neurodegenerative diseases, and cancer.¹⁻³ As part of a general interest in understanding the role of protein glycosylation in disease, I investigated the glycan motif fucose- α (1,2)-galactose (Fuc α (1-2)Gal). Fuc α (1-2)Gal is found on the non-reducing terminus of a large family of important glycans, including blood group H1 and H2, Globo H, Fuc-GM1, Lewis B, and Lewis Y. These glycans play important roles in processes such as learning and memory and contribute to asthma, inflammation, and tumorigenesis.⁴⁻¹³ However, the size and structural complexity of Fuc α (1-2)Gal glycans, which range from simple linear to large branched structures, has posed a significant challenge to their detection and study.

Antibodies or lectins are typically used to detect glycans, but these methods often suffer from weak binding affinity and limited specificity, displaying cross-reactivity toward multiple glycan epitopes.¹⁴⁻¹⁶ An alternative method, metabolic labeling, provides a powerful and versatile approach to the detection of glycans.¹⁷⁻²¹ However, as stated in chapter one, metabolic labeling requires the uptake of non-natural monosaccharide analogs into biosynthetic pathways, which allows for their incorporation into numerous glycans. As a consequence, disaccharide or trisaccharide motifs of specific sugar composition and glycosidic linkage, such as Fuc α (1-2)Gal, cannot be uniquely detected. Furthermore, the non-natural sugar must compete with natural sugars and thus is often incorporated sub-stoichiometrically into glycoconjugates, thereby reducing detection sensitivity. Given the diversity of carbohydrate structures at the cell surface, there is an urgent need to develop new technologies for the specific detection of complex glycans.

In this chapter, I report the first strategy for the rapid, sensitive, and selective detection of Fuc α (1-2)Gal glycoconjugates. The approach capitalizes on the substrate tolerance of a bacterial glycosyltransferase to covalently tag specific glycans of interest with a non-natural sugar analog (Figure 2.1). As the reaction proceeds in quantitative yield, stoichiometric addition of the non-natural sugar can be achieved, affording higher detection sensitivity relative to antibodies, lectins, and metabolic labeling. Although chemoenzymatic approaches have been reported for two saccharides, *O*-linked- β -*N*-acetylglucosamine (*O*-GlcNAc)^{22,23} and *N*-acetyllactosamine (LacNAc),²⁴ this study demonstrates the first direct detection of complex oligosaccharides, opening up the potential to track a broad range of physiologically important glycans.

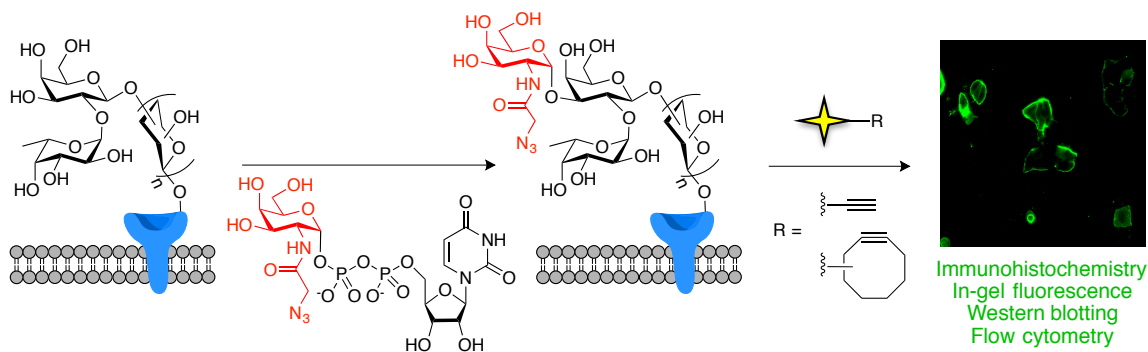


Figure 2.1 The chemoenzymatic labeling approach for the detection of Fuc α (1-2)Gal glycoconjugates.

RESULTS AND DISCUSSION

To develop this approach, I exploited the bacterial homologue of the human blood group A antigen glycosyltransferase (BgtA), which has been shown to transfer *N*-acetylgalactosamine (GalNAc) from UDP-GalNAc onto the C-3 position of Gal in Fuc α (1-2)Gal structures.²⁵ I suspected that BgtA might tolerate substitution at the C-2

position of GalNAc, which would allow for the selective tagging of Fuca(1-2)Gal with an azido or ketone functionality (Figure 2.2).

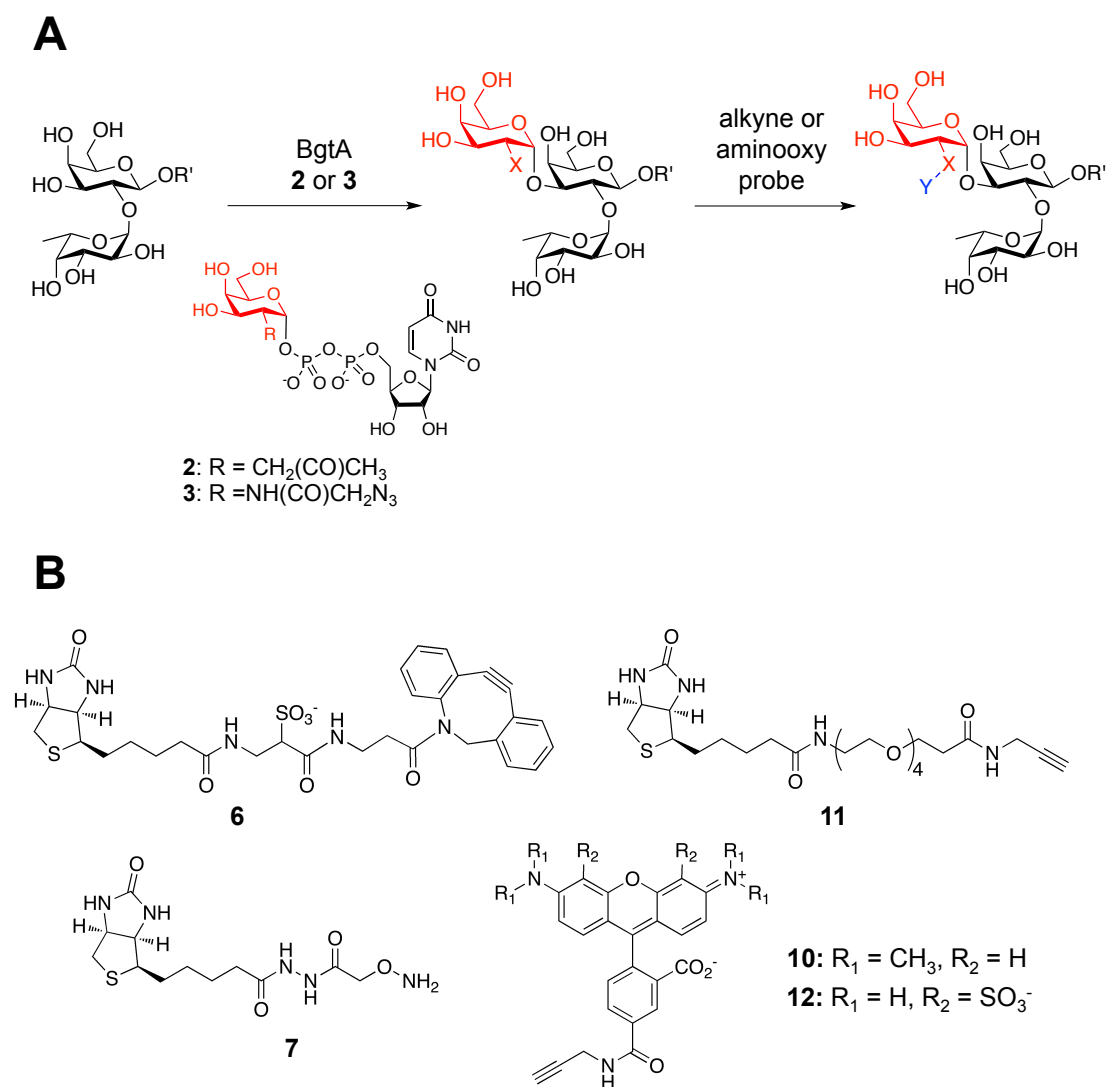


Figure 2.2 (A) Chemoenzymatic strategy for the detection of Fuca(1-2)Gal glycans. (B) Alkyne or aminoxy probes used for detection of glycans.

To test the approach, Fuca(1-2)Gal substrate **1** was synthesized via reductive amination of 2'-fucosyllactose with *p*-nitrobenzylamine and sodium cyanoborohydride (Figure 2.3). Additionally, BgtA was expressed and purified as described (Figure 2.4).²⁵ Indeed, treatment of **1** with BgtA and either UDP-2-deoxy-2-(acetyl)- β -D-galactopyranoside (UDP-ketoGal, **2**) or UDP-*N*-azidoacetylglactosamine (UDP-

GalNAz, **3**) led to complete conversion to the desired products **4** and **5**, respectively, after 12 h at 4 °C, as determined by liquid chromatography-mass spectrometry (LC-MS; Figures 2.5 and 2.6). Subsequent reaction with the aminoxy-biotin derivative **7** (Figure 2.2) or with an aza-dibenzo-cyclooctyne-biotin derivative (ADIBO-biotin, **6**; Figure 2.2), using copper-free click chemistry (3 h, rt), afforded the biotinylated products **8** and **9**, respectively, in quantitative yield (Figures 2.5 and 2.6).

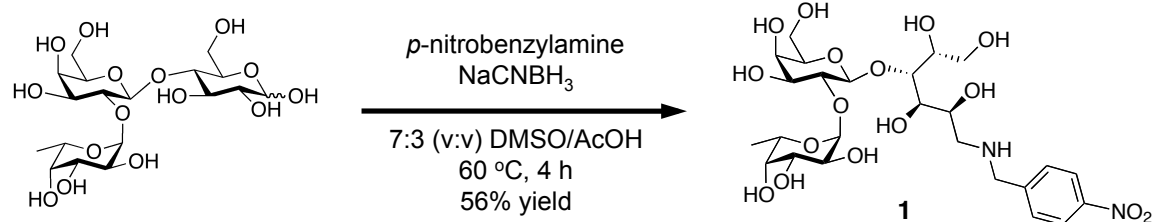


Figure 2.3 Synthesis of Fuca(1-2)Gal substrate **1**.

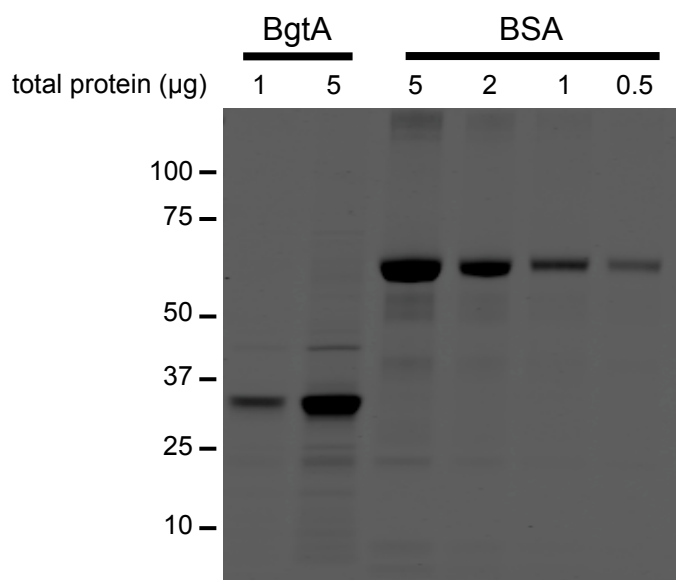


Figure 2.4 Purified BgtA visualized with SDS-PAGE and coomassie stain. Bovine serum albumin (BSA) is also run on the gel as a standard.

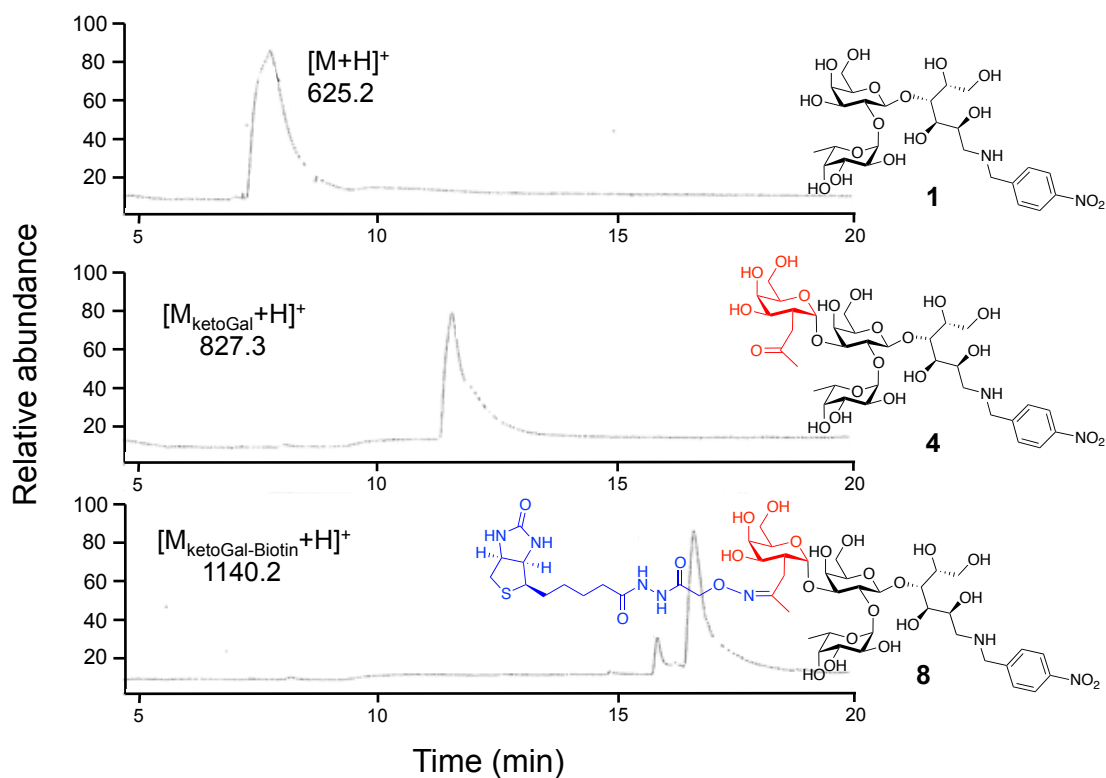


Figure 2.5 (A) Chemoenzymatic labeling of substrate **1** with UDP-ketoGal **2**. HPLC-MS analysis of the reaction progress at time 0 (top), 12 h after the addition of BgtA and **2** (middle), and 24 h after the addition of aminoxy-biotin derivative **7** (bottom). HPLC chromatogram is shown.

Given the repertoire of probes that can react with azides, as well as the high background labeling witnessed using aminoxy probes in protein lysates (data not shown), it was decided that UDP-GalNAz (**3**) would be used moving forward. To more rigorously characterize the products generated after treating **1** with BgtA and UDP-GalNAz (**3**), followed by ADIBO-biotin (**6**), MS/MS spectra were collected and fragmentation ions were characterized (Figure 2.7). The fragmentation of compounds **1**, **5**, and **9** produced b, c, y, and z ions, consistent with the fact that GalNAz is directly modifying the galactose of **1** (Figure 2.7B). Additionally, the MS/MS analysis of **9** demonstrates that ADIBO-biotin (**6**) does not produce non-specific reactions with **1** and

is specific for the azide of GalNAz (Figure 2.7C). These findings provide evidence that BgtA adds GalNAz directly onto the galactose of $\text{Fuca}(1-2)\text{Gal}$ molecules.

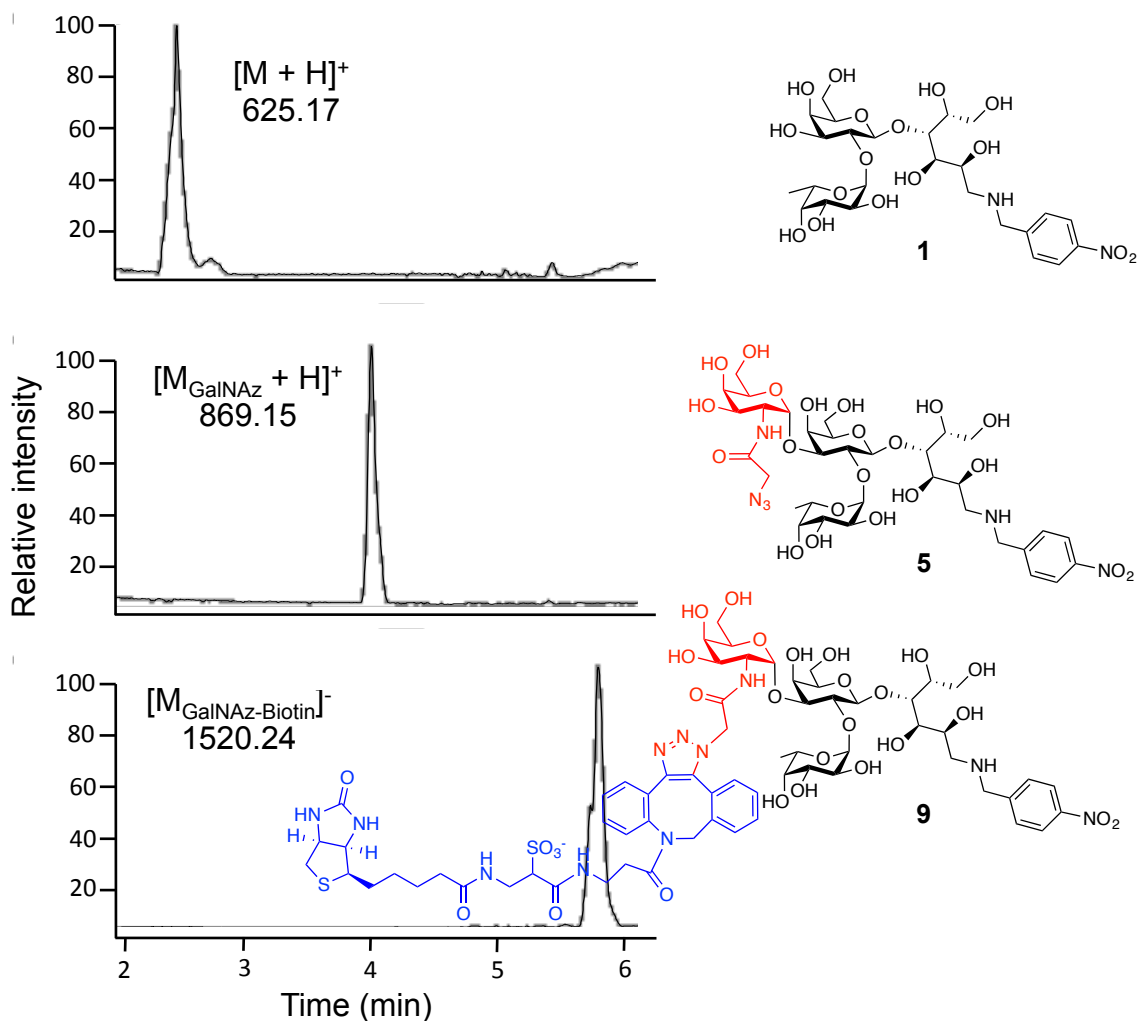


Figure 2.6 Labeling of substrate **1**. LC-MS traces monitoring the reaction progress at time 0 (top), 12 h after the addition of BgtA and **3** (middle), and 3 h after the addition of ADIBO-biotin **6** (bottom). Total ion chromatogram is shown.

Kinetic analysis revealed an apparent k_{cat}/K_m value of $5.7 \text{ nM}^{-1}\text{min}^{-1}$ for UDP-GalNAz, approximately 7-fold lower than the value of $40.4 \text{ nM}^{-1}\text{min}^{-1}$ obtained for the natural UDP-GalNAc substrate (Figure 2.8).²⁵ Additionally, the apparent K_m values were determined to be $127 \pm 36 \text{ }\mu\text{M}$ (UDP-GalNAc) and $168 \pm 55 \text{ }\mu\text{M}$ (UDP-GalNAz).

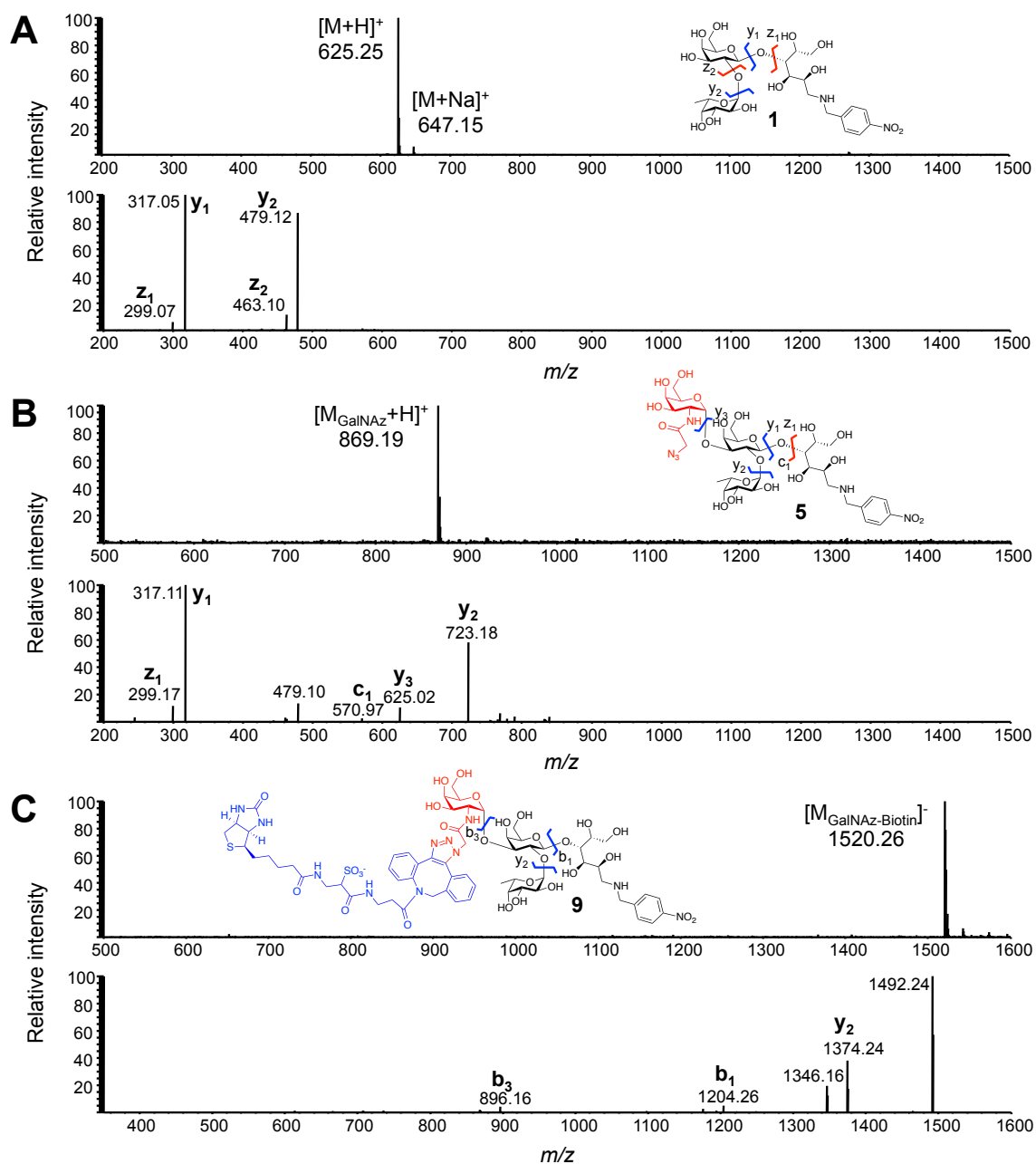


Figure 2.7 LC-MS/MS analysis of **1**, **5**, and **9** during the chemoenzymatic labeling process. (A) Compound **1** at time 0. (B) Compound **5**, 12 h after the addition of BgtA and UDP-GalNAz **3**. (C) Biotinylated glycan **9**, 3 h after reaction with ADIBO-biotin **6**. The MS spectrum for each compound is shown on top; the MS/MS spectrum for the most abundant ion is shown on the bottom. The m/z of peaks found in each MS/MS analysis are shown as either b and y or c and z ions. The corresponding fragmentation products and probable cleavage sites are denoted in the respective structures. **1** and **5** were detected in positive scanning mode; **9** was detected in negative scanning mode.

Finally, the apparent V_{\max} value for UDP-GalNAc ($0.100 \pm 0.010 \text{ nmol}\cdot\text{min}^{-1}$) is approximately 5-fold higher than that of UDP-GalNAz ($0.020 \pm 0.002 \text{ nmol}\cdot\text{min}^{-1}$; Figure 2.8). These parameters suggest that UDP-GalNAc is a preferred substrate for BgtA; however, UDP-GalNAz still exhibits sufficient kinetic parameters to enable efficient chemoenzymatic labeling.

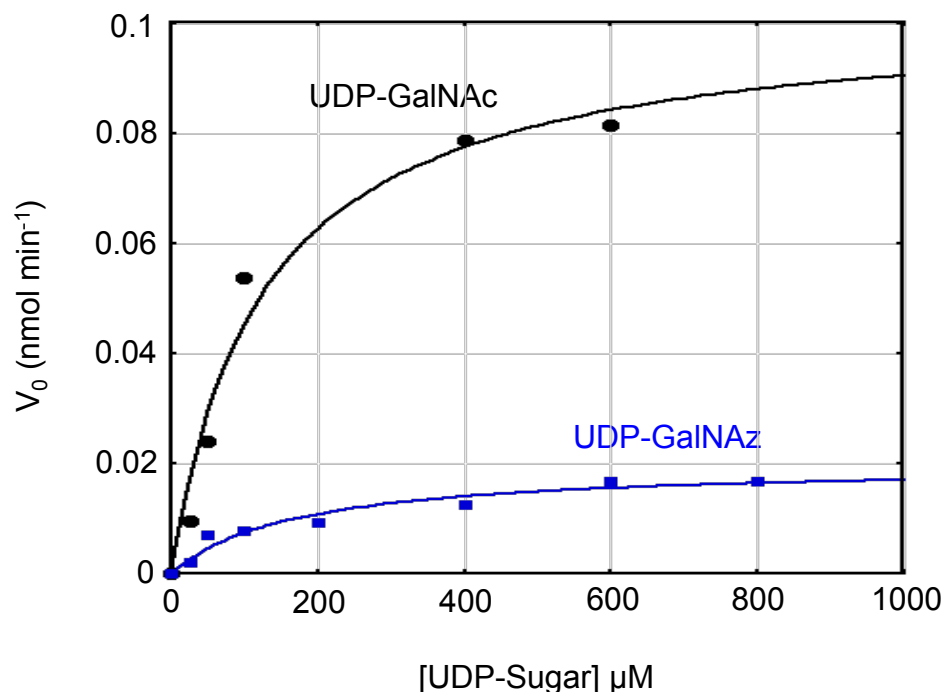


Figure 2.8 Kinetic comparison of the BgtA-catalyzed reaction of **1** with UDP-GalNAc (black) and UDP-GalNAz (blue, **3**). Reactions were performed in duplicate using 100 μM of acceptor **1** and varying concentrations of the donor. Initial rates as a function of substrate concentration were plotted and revealed apparent k_{cat}/K_m values of $5.7 \text{ nM}^{-1}\text{min}^{-1}$ and $40.4 \text{ nM}^{-1}\text{min}^{-1}$, respectively, and apparent K_m values of $127 \pm 36 \mu\text{M}$ and $168 \pm 55 \mu\text{M}$, respectively. The apparent V_{\max} value for UDP-GalNAc ($0.100 \pm 0.010 \text{ nmol}\cdot\text{min}^{-1}$) is approximately 5-fold higher than that of UDP-GalNAz ($0.020 \pm 0.002 \text{ nmol}\cdot\text{min}^{-1}$).

Having demonstrated that BgtA accepts non-natural donor substrates, I next determined the acceptor substrate profile for BgtA using carbohydrate microarrays from the Consortium for Functional Glycomics.²⁶⁻²⁷ These carbohydrate microarrays contain 611 different glycan structures, enabling the characterization of glycans modified by BgtA in a controlled environment. Glycosylation reactions with BgtA and UDP-GalNAz

were performed on the array with 3 different time points (0.5, 2, and 12 h) followed by subsequent reaction with ADIBO-biotin (Figure 2.9). The biotinylated glycans were finally detected using Cy5-conjugated streptavidin.

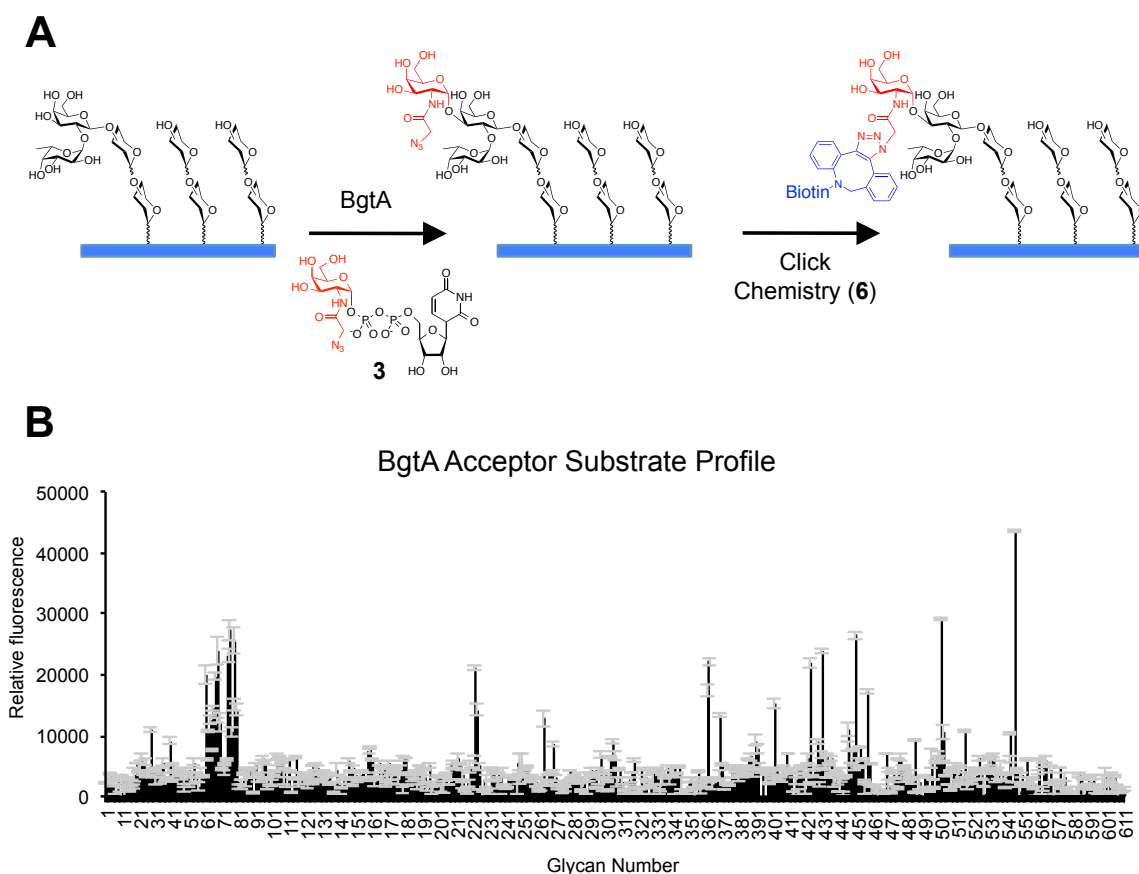


Figure 2.9 Characterization of the the acceptor substrate profile of BgtA. (A) Scheme of the work flow using the glycan array. After treating the slide with BgtA and UDP-GalNAz (**3**), ADIBO-biotin (**6**) was used to install a biotin reporter onto the BgtA modified glycans. Slides were then incubated with a streptavidin conjugated AlexaFluor-488 and slides were scanned with a fluorescent slide reader. (B) Representative data showing the BgtA dependent labeling of different glycan structures.

Strong fluorescence labeling of Fuc α (1-2)Gal structures was observed within 0.5 h and the top 26 glycans labeled contained terminal Fuc α (1-2)Gal structures, highlighting the specificity of the chemoenzymatic approach (Figure 2.10). Moreover, ~91% of the terminal Fuc α (1-2)Gal containing a free C-3 hydroxyl group on Gal were labeled on the array, including the H1 (68, 69) and H2 antigens (76, 77), the ganglioside Fuc-GM1 (65),

and the Globo H antigen (60), a hexasaccharide overexpressed on breast, lung, and prostate tumors and associated with poor prognosis (Figures 2.10 and 2.11).⁸⁻¹² A wide variety of linear (e.g., 501, 75, and 60) and branched structures (e.g., 450, 362, and 457) containing the $\text{Fuca}(1-2)\text{Gal}$ motif were efficiently labeled (Figures 2.10 and 2.12). Modifications of the core disaccharide, such as replacing Gal with GlcNAc, or changing the $\alpha(1-2)$ linkage to an $\alpha(1-3)$, $\alpha(1-4)$ or $\beta(1-3)$ linkage eliminated the enzymatic labeling by BgtA (e.g., 80, 81, and 82; Figure 2.12A).

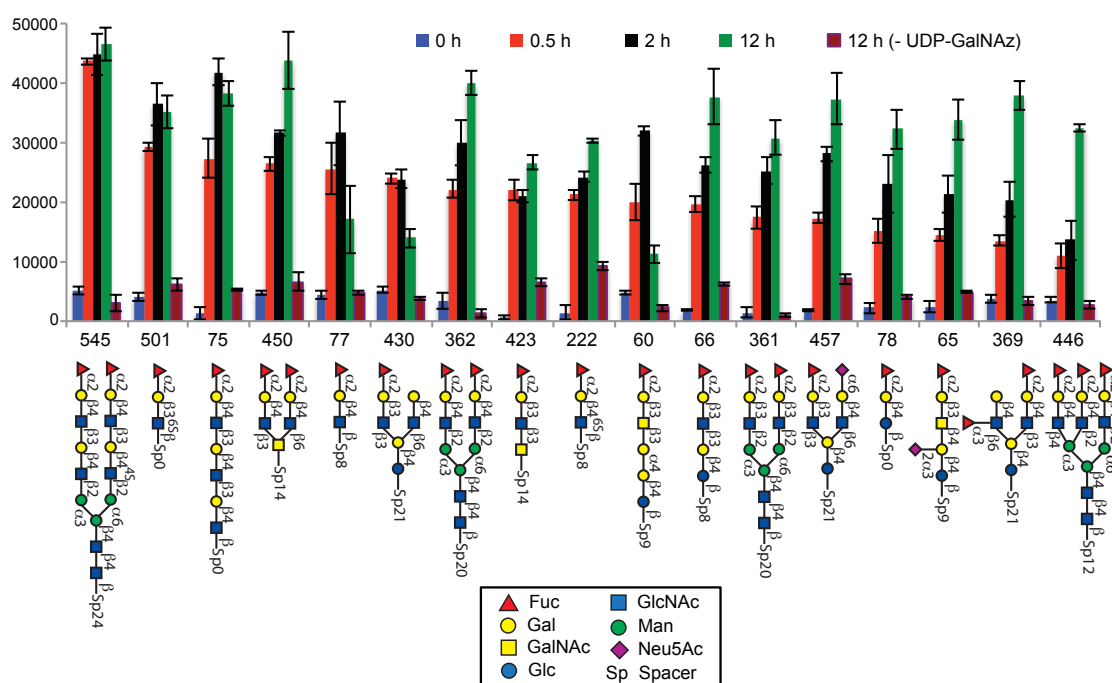


Figure 2.10 Time course analysis using a glycan microarray. Representative structures from the top 26 glycans with the highest relative fluorescence intensity after 0.5 h are plotted, all of which represent terminal $\text{Fuca}(1-2)\text{Gal}$ structures. UDP-GalNAz (**3**) was omitted from some of the reactions as a control (12 h, -UDP-GalNAz).

Consistent with a previous report,²⁵ BgtA exhibited more relaxed specificity toward structures appended to the reducing end of the Gal residue. Specifically, glycans containing a $\beta(1-3)\text{GalNAc}$, $\beta(1-3)\text{GlcNAc}$, $\beta(1-4)\text{GlcNAc}$, or $\beta(1-4)\text{Glc}$ in this position were efficiently labeled (e.g., 62, 66, 74, and 78, respectively; Figure 2.12A).

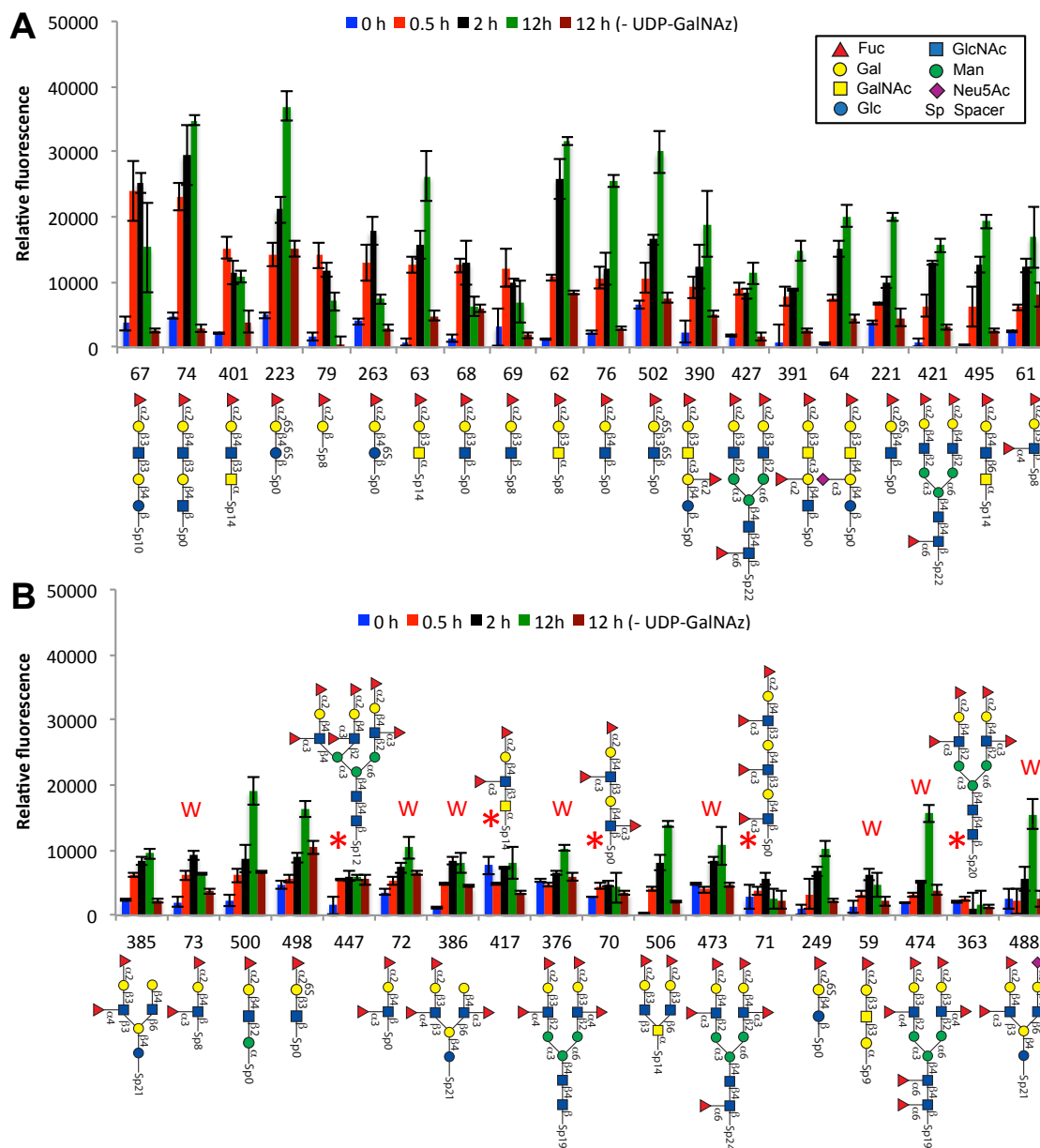


Figure 2.11 Additional Fuc α (1-2)Gal structures on the microarray and their ability to be labeled by BgtA (see also Figure 2 A). Relative fluorescence intensities are plotted as a function of time and represent the mean of 4 values. Error bars represent the standard deviation of the mean. Glycans were considered labeled if they showed a time-dependent increase in fluorescence labeling and their signal at 12 h after subtraction of the background in the absence of UDP-GalNAz (12 h, -UDP-GalNAz) was >1000 relative fluorescence units. The red asterisks indicate structures that were not considered to be labeled. W indicates very weak labeling.

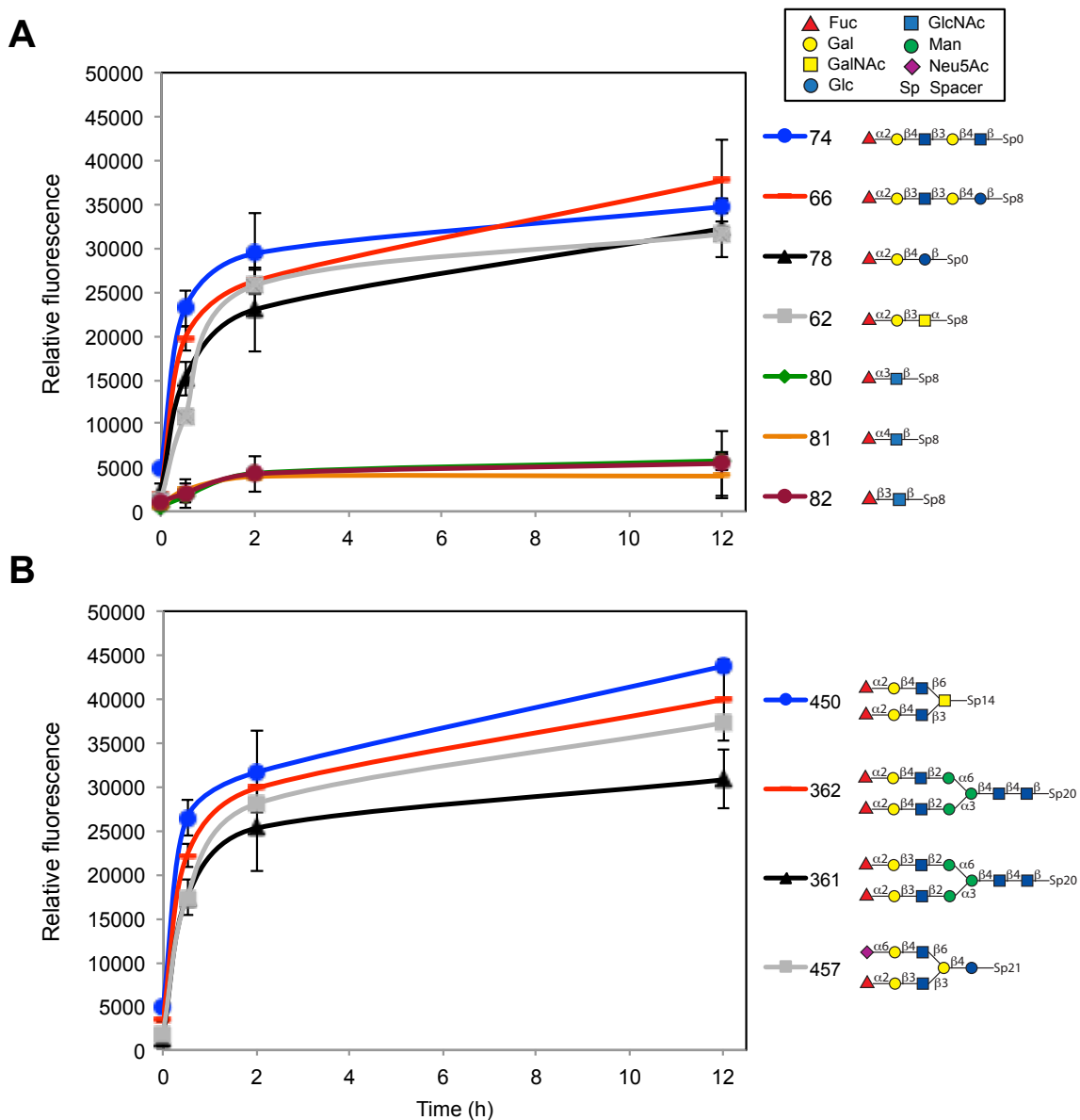


Figure 2.12 The chemoenzymatic approach labels a variety of linear (A) and branched (B) Fuc α (1-2)Gal structures. (A) The third sugar toward the reducing end of the glycan does not significantly affect the labeling reaction (eg., 62, 66, 74, and 78). Acceptor substrate structures that have a GlcNAc, instead of Gal, and change the linkage from α (1-2) to α (1-3), α (1-4), or β (1-3) are not modified by BgtA (eg., 80, 81, and 82). Representative structures from the microarray are shown for comparison. Relative fluorescence intensities are plotted as a function of time to show how subtle changes in the structure affect the kinetics of labeling. Error bars represent the standard deviation of the mean of 4 values after removing the high and low values from $n = 6$ replicates of each glycan printed on the array.

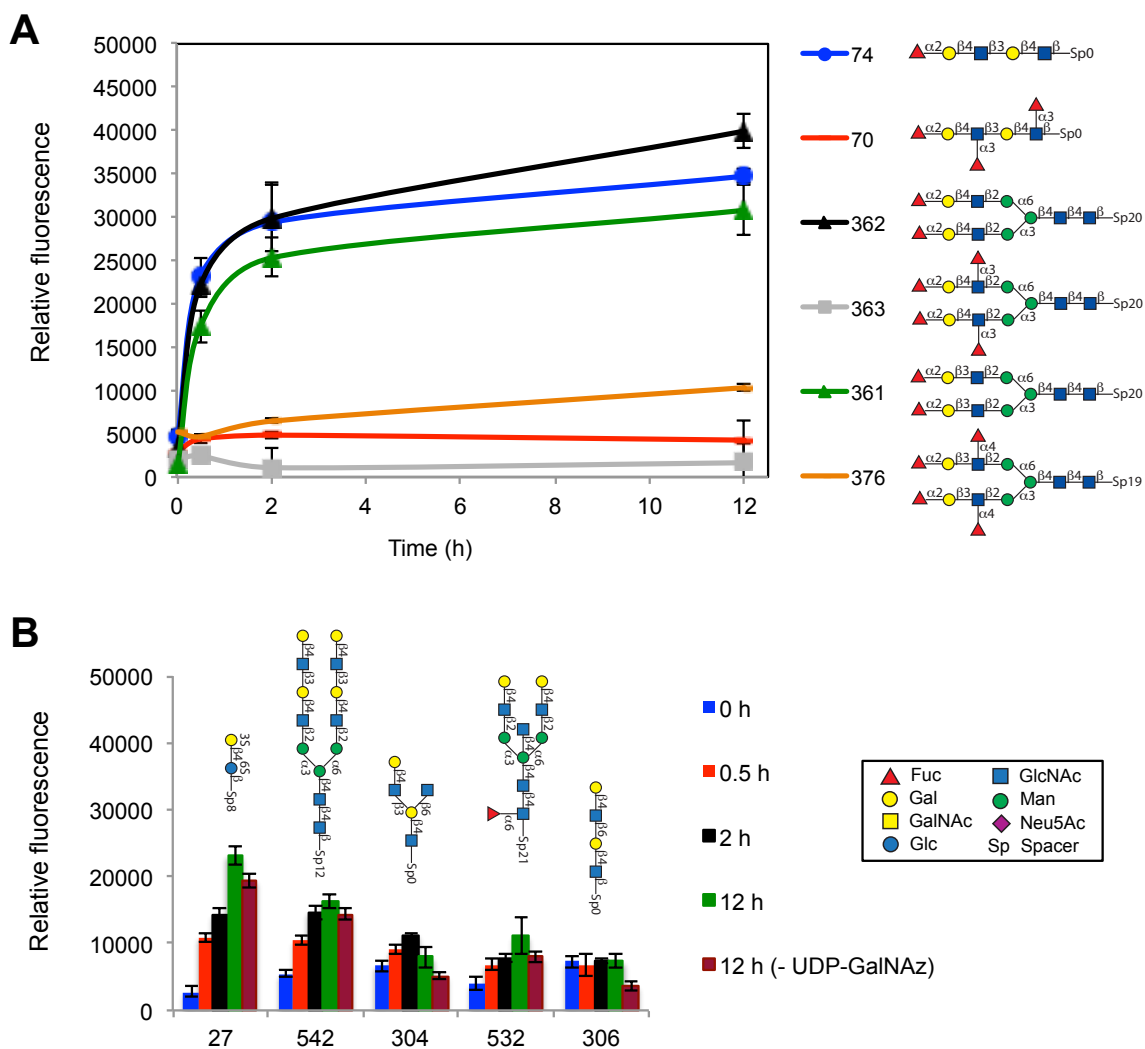


Figure 2.13 The chemoenzymatic approach labels a variety of $\text{Fuca}(1-2)\text{Gal}$ structures. (A) Branching at the third position GlcNAc via $\alpha(1-3)$ or $\alpha(1-4)$ fucosylation severely hindered the labeling efficiency. (B) Weak labeling of $\text{Gal}\beta(1-4)\text{GlcNAc}$ structures was also observed. This labeling was accompanied by high background, as indicated by the 12 h time point in the absence of UDP-GalNAz. No labeling of these structures was observed in solution, suggesting that the labeling was likely due to non-covalent interactions with the microarray. Representative structures are shown for comparison. Relative fluorescence intensities are plotted as a function of time to show how changes in glycan structure affect the labeling reaction. Error bars represent the standard deviation of the mean of 4 values after removing the high and low values from $n = 6$ replicates of each glycan printed on the array.

Although moderate structural substitutions of the GlcNAc were tolerated such as 6-O-sulfation (e.g., 501 and 222; Figure 2.10), branching at this position via $\alpha(1-3)$ or $\alpha(1-4)$ fucosylation of the GlcNAc residue led to weak labeling, as in the case of the

Lewis B (61) and Lewis Y (72, 73) antigens, or no appreciable labeling (e.g., 71, and 363; Figures 2.11 and 2.13A). Interestingly, we also observed weak labeling of Gal β (1-4)GlcNAc structures on the glycan array (Figure 2.13B). However, these structures also exhibited high background signal even in the absence of UDP-GalNAz, and BgtA failed to label *p*-nitrophenyl 2-acetamido-2-deoxy-4-O-(β -D-galactopyranosyl)- β -D-glucopyranoside (Gal β (1-4)GlcNAc-*p*NP) in solution (2 h, 25 °C; data not shown), suggesting that Gal β (1-4)GlcNAc structures are not covalently labeled by BgtA. Together, these studies demonstrate the strong specificity of BgtA for Fuca(1-2)Gal structures and the power of glycan microarrays to rapidly profile the specificities of glycosyltransferases for the development of chemoenzymatic detection strategies.

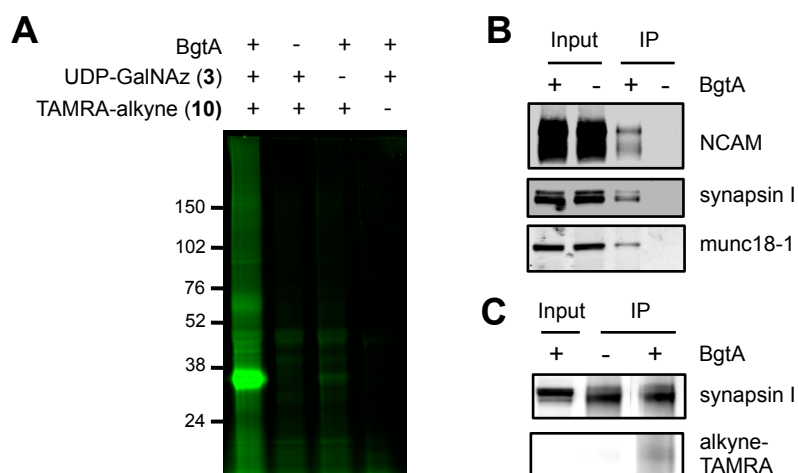


Figure 2.14 Chemoenzymatic labeling of Fuca(1,2)Gal glycoproteins from cells. (A) In-gel fluorescence detection of Fuca(1,2)Gal glycoproteins from olfactory bulb lysates. Low background fluorescence was observed in the absence of BgtA, UDP-GalNAz **3**, or TAMRA-alkyne **10**. The strong band at approximately 35 kDa is likely autoglycosylated BgtA. (B) Specific chemoenzymatic labeling of endogenous Fuca(1,2)Gal glycoproteins from olfactory bulb lysates. Glycosylated NCAM, synapsin I, and munc18-1 were detected after chemoenzymatic labeling with alkyne-biotin, streptavidin pull-down, and immunoblotting for each protein of interest. (C) Specific chemoenzymatic labeling of Flag-tagged synapsin I overexpressed in HeLa cells. Glycosylated synapsin I was detected after chemoenzymatic labeling with alkyne-TAMRA, synapsin pull-down with an anti-Flag antibody, and immunoblotting with an anti-TAMRA antibody. B and C were performed with Chithra Krishnamurthy.

To determine whether the approach could be used to track $\text{Fuca}(1-2)\text{Gal}$ glycoproteins in complex cell lysates, I labeled proteins from rat brain extracts with BgtA and UDP-GalNAz, followed by Cu(I)-catalyzed reaction with the alkyne-functionalized tetramethyl-6-carboxy-rhodamine dye **10** (alkyne-TAMRA; Figure 2.2B). Strong fluorescence labeling of $\text{Fuca}(1-2)\text{Gal}$ glycoproteins was observed, with minimal non-specific labeling in the absence of BgtA, UDP-GalNAz, or alkyne-TAMRA (Figure 2.14A).

Interestingly, a strong band is witnessed at an apparent molecular weight (MW) of 37kDa, the MW of BgtA itself (Figure 2.14A). Considering the fact that the bacterial species that endogenously expresses BgtA contain the $\text{Fuca}(1-2)\text{Gal}$ disaccharide, I suspect that BgtA is a glycoprotein itself and modifies itself to a high degree during the chemoenzymatic labeling. This hypothesis is further supported given that the total concentration of BgtA, relative to other $\text{Fuca}(1-2)\text{Gal}$ proteins, in the labeling reaction is so high that one would expect it would be the brightest band detected. No further studies were conducted to validate this hypothesis; however, no amount of washing the protein pellet could remove this intense band witnessed in every lysate labeling reaction performed.

To confirm further the specificity of the reaction, we labeled the lysates with the alkyne-biotin derivative **11** (Figure 2.2B), captured the biotinylated proteins using streptavidin resin, and immunoblotted for the presence of known $\text{Fuca}(1-2)\text{Gal}$ glycoproteins.^{28,29} Neural cell adhesion molecule (NCAM), synapsin I, and munc18-1 were all chemoenzymatically labeled and detected in the presence, but not in the absence, of BgtA (Figure 2.14B). In contrast, p44 mitogen-associated protein kinase (p44

MAPK), a protein that has not been shown to be fucosylated, was not detected. Glycosylated synapsin I was also readily observed following overexpression of Flag-tagged synapsin I in HeLa cells, chemoenzymatic labeling of the lysates with alkyne-TAMRA, synapsin immunoprecipitation, and visualization using an anti-TAMRA antibody (Figure 2.14C).

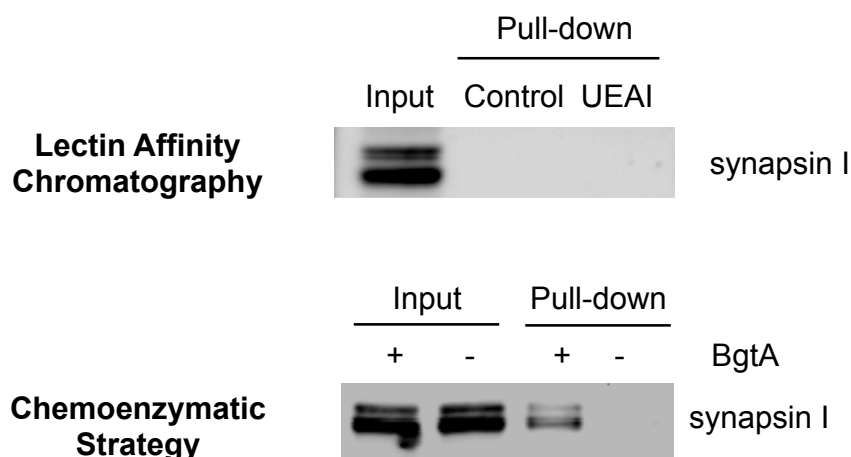


Figure 2.15 Comparison of UEAI lectin affinity chromatography to the chemoenzymatic strategy. Glycosylated synapsin I from olfactory bulb lysate (500 μ g) was subjected to lectin affinity chromatography or chemoenzymatic labeling followed by streptavidin capture. Western blotting for synapsin I indicated that UEAI failed to capture and detect glycosylated synapsin I, whereas the chemoenzymatic strategy allowed for ready detection. Performed by Chithra Krishnamurthy.

Importantly, UEAI lectin affinity chromatography failed to pull-down and detect glycosylated synapsin I when performed on the same scale (Figure 2.15). Moreover, previous studies have reported that the $Fuca(1-2)Gal$ -specific antibody A46-B/B10 does not immunoprecipitate glycosylated synapsin I from the same neuronal lysates.²⁸ Thus, our chemoenzymatic approach enables the highly sensitive detection of glycoproteins and provides a variety of different enrichment strategies and readouts for the $Fuca(1-2)Gal$ motif.

Next, we investigated whether the chemoenzymatic strategy could be used to image $\text{Fuc}\alpha(1-2)\text{Gal}$ glycans in cells. HeLa cells overexpressing Flag-tagged synapsin I were fixed, permeabilized, and chemoenzymatically labeled on coverslip with BgtA and UDP-GalNAz. Cu(I)-catalyzed azide-alkyne cycloaddition (CuAAC) chemistry was then performed using an alkyne-functionalized Alexa Fluor 488 dye (**12**; Figure 2.2) to install a fluorescent reporter onto the $\text{Fuc}\alpha(1-2)\text{Gal}$ glycans. Strong fluorescence labeling was observed in cells transfected with synapsin I, and the labeling showed excellent co-localization with intracellular synapsin I expression (Figure 2.16). No labeling of cells was observed in the absence of BgtA, and only weak labeling of endogenous $\text{Fuc}\alpha(1-2)\text{Gal}$ glycoproteins was seen in the absence of synapsin I overexpression (Figure 2.16), confirming the specificity of the in situ chemoenzymatic reaction.

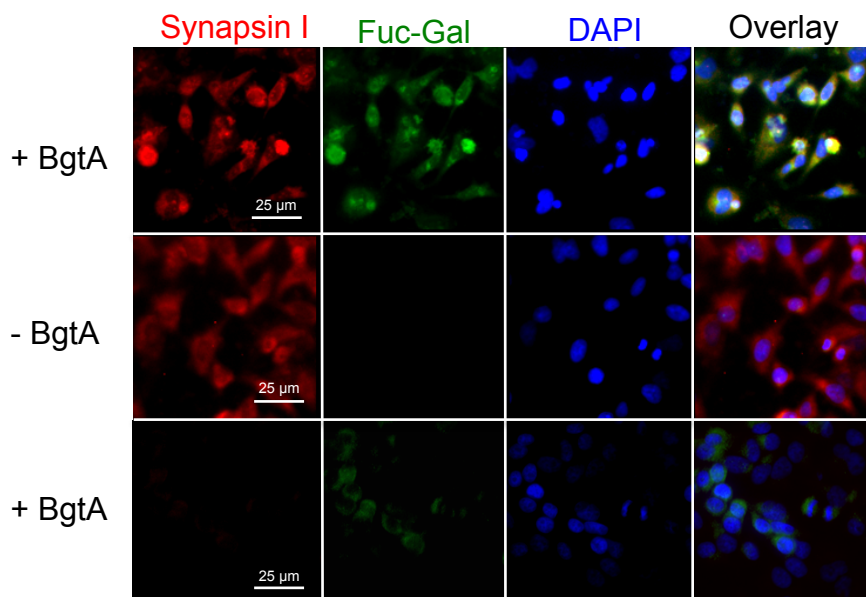


Figure 2.16 Fluorescence detection of $\text{Fuc}\alpha(1,2)\text{Gal}$ glycans (green) in HeLa cells shows significant co-localization (yellow, overlay) with Flag-tagged synapsin I (red). Low levels of fluorescence labeling of endogenous $\text{Fuc}\alpha(1-2)\text{Gal}$ glycoproteins is witnessed in mock-transfected HeLa cells, suggesting low expression levels of endogenous $\text{Fuc}\alpha(1-2)\text{Gal}$ glycoproteins (bottom row). Nuclei were stained with 4',6-diamidino-2-phenylindole (DAPI; blue). Performed by Chithra Krishnamurthy.

As the $\text{Fuca}(1-2)\text{Gal}$ epitope has been reported to be a useful biomarker for cancer progression and prognosis,^{11,12} the ability to detect $\text{Fuca}(1-2)\text{Gal}$ glycan levels on the surface of cancer cells would facilitate investigations into $\text{Fuca}(1-2)\text{Gal}$ as a diagnostic or prognostic marker and a therapeutic target for cancer vaccines. However, antibodies and lectins that bind $\text{Fuca}(1-2)\text{Gal}$ have been shown to cross-react with other sugar epitopes^{14,15} such as β -linked Fuc ,¹⁴ or recognize an incomplete subset of $\text{Fuca}(1-2)\text{Gal}$ glycans,¹⁶ indicating the need for more selective, yet comprehensive, high-affinity detection methods. Therefore we applied the chemoenzymatic approach to the detection of $\text{Fuca}(1-2)\text{Gal}$ glycans on live cancer cells. Cells from the human breast adenocarcinoma cell line MCF-7 were chemoenzymatically labeled with BgtA and UDP-GalNAz for 1 h at 37 °C. After reaction with ADIBO-biotin (1 h, rt), $\text{Fuca}(1-2)\text{Gal}$ glycans were detected using streptavidin conjugated to Alexa Fluor 488 dye. Membrane-associated fluorescence was observed for cells treated with both BgtA and UDP-GalNAz, whereas no labeling was detected for control cells labeled in the absence of BgtA (Figure 2.17).

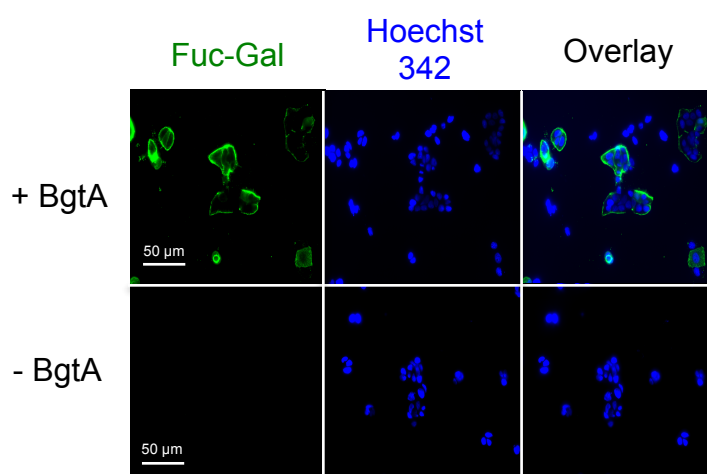


Figure 2.17 Fluorescence detection of $\text{Fuca}(1,2)\text{Gal}$ glycans (green) on live MCF-7 cells. Nuclei were stained with Hoechst 342 (blue). Performed by Chithra Krishnamurthy.

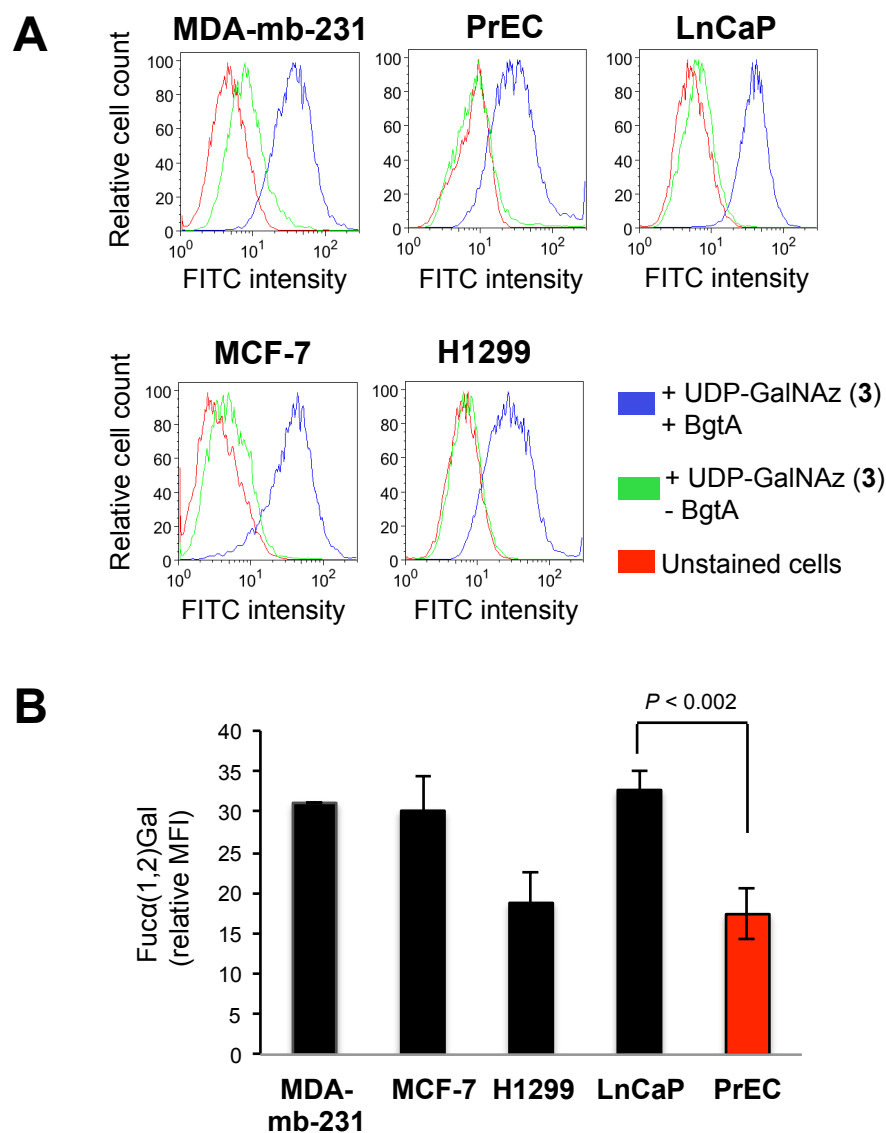


Figure 2.18 (A) Flow cytometry analysis of the relative expression levels of Fuca(1,2)Gal glycans across various cancer cell lines, with comparison to non-cancerous PrEC cells. Cells were untreated (red) or chemoenzymatically labeled in the presence (blue) or absence (green) of BgtA. (B) Quantification of the mean fluorescence intensity (MFI) relative to cells labeled in the absence of. Error bars represent data from duplicate (MCF-7, MDA-mb-231, H1299) or triplicate (LnCaP, PrEC) experiments. Performed by Chithra Krishnamurthy.

Finally, we compared the expression levels of Fuca(1-2)Gal glycans across different cancer and non-cancer cell lines. MCF-7 (breast cancer), MDA-mb-231 (highly invasive breast cancer), H1299 (lung cancer), LnCaP (prostate cancer), and primary prostate epithelial cells (PrEC) cells were chemoenzymatically labeled in suspension

with BgtA and UDP-GalNAz (2 h, 37 °C), reacted with ADIBO-biotin (1 h, rt), and stained with the streptavidin-Alexa Fluor 488 conjugate (20 min, 4 °C). As shown by flow cytometry analysis, LnCaP, MCF-7, and MDA-mb-231 cells displayed the highest levels of fluorescence (Figure 2.18), consistent with reports of high Globo H expression on mammary and prostate tumors.⁸⁻¹⁰ H1299 cells, a model for non-small cell lung carcinoma and also reported to express Globo H,¹³ showed lower Fuc α (1-2)Gal expression. Importantly, flow cytometry analysis revealed a 53% increase in Fuc α (1-2)Gal expression on the surface of LnCAP cells compared to non-cancerous PrEC cells. These results demonstrate that this chemoenzymatic labeling approach can readily discriminate cancerous cells from normal cells, providing a new potential strategy for rapid biomarker detection. The method could be particularly useful for the detection of prostate cancer from tissue biopsies, as the current standard of PSA detection to diagnose prostate cancer has a significant false-positive rate, leading to overtreatment.³⁰ In addition to histological detection, this chemoenzymatic approach could potentially provide a new strategy to distinguish normal PSA from tumorigenic PSA, which is reported to have higher levels of Fuc α (1-2)Gal glycosylation.³¹

CONCLUSION

In this chapter I have described a newly developed chemoenzymatic strategy that detects Fuc α (1-2)Gal glycans with improved efficiency and selectivity over existing methods. This strategy detects a variety of complex Fuc α (1-2)Gal glycans and glycoproteins and permits living cells or complex tissue extracts to be rapidly interrogated. I anticipate that the strategy will accelerate both the discovery of new

Fuca(1-2)Gal glycoproteins and advance an understanding of the biological roles of this important sugar in neurobiology and cancer. Moreover, this study represents a proof-of-concept that chemoenzymatic labeling strategies can be extended to more complex oligosaccharides. Future studies will expand chemoenzymatic detection approaches to a broad range of glycans to provide a powerful new set of tools for glycomics research.

EXPERIMENTAL METHODS

General Methods for Chemical Synthesis. Unless otherwise stated, all starting materials and reagents were purchased from Sigma-Aldrich and used without further purification. All ^1H and ^{13}C NMR spectra were recorded on a Varian Innova 600 spectrometer and referenced to solvent peaks. Data for ^1H NMR spectra are reported as follows: chemical shift (δ ppm), multiplicity (s = singlet, d = doublet, t = triplet, q = quartet, m = multiplet), coupling constant in Hz, and integration. Low-resolution mass spectra were recorded on an 1100 Agilent Liquid Chromatograph Mass Spectrometer with an Agilent SB-C18 reverse-phase column (3.5 μm , 4.6 x 250 mm) with monitoring at 280 and 310 nm. High-resolution mass spectra (HRMS) were obtained using an Agilent 6200 Series Time of Flight Mass Spectrometer with an Agilent G1978A Multimode source using mixed electrospray ionization/atmospheric pressure chemical ionization (MultiMode ESI/APCI).

Synthesis of 1-p-Nitrobenzyl-(2-fucosyl)-lactose (1). A 0.35 M solution of p-nitrobenzylamine in 7:3 (v/v) DMSO/AcOH (50 μL , 18 μmol) was added slowly to 2'-fucosyllactose (1.0 mg, 2.0 μmol) at rt. NaCNBH_3 (50 μL of a 1 M solution in 7:3 (v/v)

DMSO/AcOH, 50 μ mol) was then added slowly at rt, and the solution was stirred at 65 °C for 4 h. The reaction was quenched by adding 10 volumes of MeCN and incubated at -20 °C for 2 h. The precipitated mixture was then centrifuged at 10,000 x g for 5 min at 4 °C, and the supernatant was discarded. Ten additional volumes of MeCN were added to the pellet, and the vortexed mixture was incubated at -20 °C for 2 h and centrifuged as above. This step was repeated two more times to remove the excess p-nitrobenzylamine. The pellet was then resuspended in 5% MeCN and the product purified by semi-preparative HPLC (Agilent 1100) using two preparative reverse-phase columns (Agilent Eclipse XDB-C18; 5 μ m, 9.4 x 250 mm) connected in series and a gradient of 5-20% B over 20 min at 4 mL/min (A, 0.5% aqueous AcOH; B, 100% MeCN). The product eluted at approximately 9.5 min. Lyophilization afforded a fluffy white solid (0.72 mg; 56% yield): ¹H NMR (600 MHz, D₂O) δ 8.33 (d, J = 8.6 Hz, 2H), 7.72 (d, J = 8.7 Hz, 2H), 5.31 (s, 1H), 4.60 (d, J = 7.8 Hz, 1H), 4.33 (q, J = 13.7 Hz, 2H), 4.23 (t, J = 6.3 Hz, 2H), 3.93 (d, J = 3.4 Hz, 1H), 3.91–3.86 (m, 4H), 3.83 (t, J = 4.4 Hz, 4H), 3.79–3.71 (m, 4H), 3.67 (dd, J = 9.5, 7.9 Hz, 1H), 3.32 (d, J = 11.7 Hz, 1H), 3.10 (t, J = 11.1 Hz, 1H), 1.23 (d, J = 6.6 Hz, 3H). ¹³C NMR (151 MHz, D₂O) δ 147.86, 130.43, 124.09, 109.99, 107.14, 100.42, 99.65, 76.94, 76.65, 75.19, 73.42, 71.69, 70.48, 70.19, 69.45, 68.97, 68.51, 68.21, 67.18, 61.93, 60.90, 50.51, 49.52, 23.19, 15.29. HRMS: [M+H]⁺ calculated for C₂₅H₄₀N₂O₁₆ 625.5996, found 625.2451.

Expression and Purification of BgtA. *E. coli* BL21 (DE3) harboring the recombinant plasmid vector pET28a-BtgA-His was kindly provided by Dr. Peng George Wang (Ohio State University). The protein was expressed and purified as described.²⁵ Briefly, the

cells were grown in LB medium (1L) at 37 °C. Isopropyl-1-thio- β -D-galactospyranoside (IPTG, 0.8 mM final concentration; Sigma) was added when the cells reached an OD₆₀₀ of 0.8, and the cells were incubated for an additional 18 h at 16 °C. The pelleted cells were lysed in Cell Lytic B Lysis Reagent (Sigma-Aldrich) supplemented with EDTA-free Complete™ protease inhibitors (Roche), 0.5 M NaCl, and 20 mM imidazole (Sigma-Aldrich) by rotating end-over-end for 20 min at rt. After centrifugation, the clarified lysate was added to prewashed Ni-NTA beads and incubated at 4 °C for 1 h, washed in 20 mM Tris•HCl pH 7.5, 0.5 M NaCl and 50 mM imidazole, and eluted in a step gradient with the elution buffer (20 mM Tris•HCl pH 7.5, 0.5 M NaCl, and 100, 200, or 500 mM imidazole). After SDS–PAGE analysis, the purified protein was concentrated with 10,000 Da molecular weight cut-off (MWCO) spin filters (Millipore) and dialyzed into 20 mM Tris•HCl pH 7.5 containing 10% glycerol and stored at 4 °C.

BgtA Activity Assay and Monitoring of Chemoenzymatic Labeling Reactions by LC-MS/MS. The Fuc α (1-2)Gal substrate **1** (10 μ M) was dissolved in 20 mM Tris•HCl pH 7.5, 50 mM NaCl, and 5 mM MnCl₂. BgtA enzyme and UDP-ketoGal **2**²² or UDP-GalNAz **3** (Invitrogen) were added to final concentrations of 0.16 mg/mL and 50 μ M, respectively, in a final volume of 100 μ L. The reaction was incubated at 4 °C in the dark for 12-16 h, and the reaction progress was monitored by LC-MS/MS. To label with aminoxy-biotin **7**, the reactions were diluted 5-fold with saturated urea, 2.7 M NaOAc pH 3.9 (50 mM final concentration and pH 4.8), and **7** (5 mM final concentration, Dojindo) and incubated for 20–24 h at rt. To label with ADIBO-biotin **6**, 250 μ M of **6** (Click Chemistry Tools) was added, and the reaction was incubated for 3 h at rt.

Following the labeling steps, the azido-labeled samples were filtered through a 3,000 Da MWCO Vivaspin 500 spin filter (GE Lifesciences) and injected on a reverse-phase HPLC column (Phenomenex Gemini; 5 m, 2.0 x 100 mm), fitted with a C8 guard column, using a ThermoScientific Accela 600 HPLC pump interfaced with a ThermoScientific LTQ mass spectrometer. A linear 3-90% gradient of B (A: 0.1% aqueous formic acid, B: 0.1% formic acid in MeCN) over 7 min was used to resolve peaks with a flow rate of 0.21 mL/min. Mass analysis was performed in positive ion mode except in the case of sulfated compound **9**, where the analysis was performed in negative ion mode.

Kinetic Analysis of BgtA with UDP-GalNAz and UDP-GalNAc. Reactions were performed in duplicate with 100 μ M acceptor substrate (**1**), 0.7 μ g BgtA, and varying concentrations of UDP-GalNAz or UDP-GalNAc (50 to 800 μ M) in 20 mM Tris-HCl pH 7.5, 50 mM NaCl, 10 mM MnCl₂ at rt in a total volume of 20 μ L. Product formation was monitored at 280 nm by reverse phase-HPLC (Agilent 1100), and time points were taken over the course of 5 min using a linear, 3-95% gradient of B (A: 0.1% aqueous trifluoroacetic acid B: 0.1% trifluoroacetic acid in MeCN) over 8 min with a flow rate of 1 mL/min. The kinetic parameters, apparent K_m , V_{max} , and k_{cat} , were obtained by linear regression analysis of initial velocity vs. donor substrate concentration using KaleidaGraph (version 4.1.2).

Chemoenzymatic Labeling on the Glycan Array. Glycan Array version 5.0 was provided by the Consortium for Functional Glycomics (CFG). Pre-equilibrated arrays

were treated with BgtA enzyme (0.16 mg/mL) and 500 μ M UDP-GalNAz **3** in 20 mM Tris•HCl pH 7.4, 50 mM NaCl, 2 mM MnCl₂ containing 1% bovine serum albumin (BSA) for various times (0, 0.5, 2, and 12 h) at rt, washed four times with wash buffer (20 mM Tris•HCl pH 7.4, 50 mM NaCl, 0.1% Triton X-100) and then 4 times with rinse buffer (20 mM Tris•HCl pH 7.4, 50 mM NaCl). The arrays were then incubated with ADIBO-biotin **6** (5 μ M) in 20 mM Tris•HCl pH 7.4, 50 mM NaCl for 2 h at rt. After washing as described above, the arrays were washed further with 20% aqueous MeOH and then incubated with streptavidin Cy-5 (0.5 μ g/mL; eBioScience) in 20 mM Tris•HCl pH 7.4, 50 mM NaCl, 0.05% Tween-20, 1% BSA, for 1 h at rt. The arrays were then washed four times with wash buffer (containing 0.05% Tween-20 instead of 0.1% Triton X-100), four times with rinse buffer, four times with water, dried under a low stream of filtered air, and scanned using a PerkinElmer ScanArray Express fluorescence scanner and ImaGene data analysis software (BioDiscovery). Data were analyzed per the guidelines of the CFG.^{26,27,32} The background fluorescence for each spot was determined as the fluorescence signal outside of the area designated as a positive spot on the array. Because background fluorescence can be heterogeneous across the array, each array was divided into areas of 10 by 10 spots, or sub-arrays, and a background fluorescence value was calculated within each sub-array by the software. This value was then subtracted from the fluorescence signal for each glycan spot within the sub-array by the software. Note that each glycan is printed six different times on the array. To calculate the relative fluorescence intensity for a given glycan, the highest and lowest intensities for each glycan were discarded, and the mean and standard deviation of four fluorescence

intensities were calculated. All microarray data will be uploaded on the Consortium of Functional Glycomics website (www.functionalglycomics.org) upon publication.

Chemoenzymatic Labeling of Cell Lysates. The olfactory bulbs of postnatal day 3 rat pups were dissected on ice and lysed in boiling 1% SDS (5 volumes/weight) with sonication until the mixture was homogeneous. Protein was precipitated using methanol/chloroform/water. Briefly, protein was diluted to 200 μ L and precipitated by sequential mixing with 600 μ L of MeOH, 200 μ L of CHCl₃ and 450 μ L H₂O, after which the mixture was centrifuged at 23,000 x g for 15 min. Precipitated protein was washed with 450 μ L of MeOH and centrifuged at 23,000 x g for 10 min. After the protein pellet was allowed to dry briefly, the pellet was re-dissolved at 5 mg/mL in 20 mM HEPES pH 7.9 containing 1% SDS, and diluted 5-fold into a buffer with the following final concentrations: 20 mM HEPES pH 7.9, 50 mM NaCl, 2% NP-40, 5 mM MnCl₂. UDP-GalNAz **3** (25 μ M; Invitrogen) and BgtA (0.16 mg/mL) were added, and the samples were incubated at 4 °C for 16-20 h. The labeled proteins were precipitated as above and resuspended in 50 mM Tris pH 7.4 containing 1% SDS at 4 mg/mL.

The resuspended proteins were subsequently reacted with alkyne-TAMRA **10** (Invitrogen) or alkyne-biotin **11** (Invitrogen) as per the Click-It™ TAMRA and Biotin Glycoprotein Detection Kit (Invitrogen) instructions, except that EDTA-free Complete™ protease inhibitors were added during the reaction. For TAMRA labeling, negative controls were performed under identical conditions except that BgtA, UDP-GalNAz **3**, or alkyne-TAMRA **10** was omitted from the labeling reaction. For biotin labeling, negative controls were performed under identical conditions except that BgtA was omitted from

the labeling reaction. After the labeling reactions, protein was precipitated using chloroform/methanol/water as described above and re-dissolved in boiling 2% SDS. This precipitation and resolubilization was then repeated once more to ensure removal of non-specific interactions. TAMRA-labeled proteins were resolved by SDS-PAGE and visualized in-gel using a Typhoon Scanner (GE Healthcare). Interestingly, BgtA itself was labeled, and attempts to remove the signal by precipitation or heat and detergent denaturation were unsuccessful, suggesting covalent modification of the protein.

Purification of Biotin-Labeled Fuca(1-2)Gal Proteins. Chemoenzymatically labeled samples were precipitated using methanol/chloroform/water as described above and re-dissolved in boiling 1% SDS plus Complete™ protease inhibitors at a concentration of 2 mg/mL. The SDS was quenched with 1 volume of NETFD buffer (100 mM NaCl, 50 mM Tris•HCl pH 7.4, 5 mM EDTA, 6% NP-40) plus protease inhibitors. The samples were incubated with pre-washed streptavidin resin (Pierce; 100 μ L/1 mg protein) for 2 h at 4 °C. The resin was washed twice with 10 column volumes each of low salt buffer (0.1 M Na₂HPO₄ pH 7.5, 0.15 M NaCl, 1% Triton X-100, 0.1% SDS), twice with 10 column volumes each of high salt buffer (0.1 M Na₂HPO₄ pH 7.5, 0.5 M NaCl, 0.2% Triton X-100), and once with 10 column volumes of 50 mM Tris•HCl pH 7.4. Captured protein was eluted in boiling 2X sample buffer (100 mM Tris pH 6.8, 4% SDS, 200 mM DTT, 20% glycerol, 0.1% bromophenol blue; 50 μ L /100 μ L resin) for 5 min.

Western Blotting for Parallel Identification of Fuca(1-2)Gal Glycoproteins. The purified, labeled material from above was resolved on a NuPAGE 4-12% Bis-Tris gel

(Invitrogen) and transferred to a polyvinylidene difluoride (PVDF) membrane (Millipore). The membrane was blocked in 5% milk (BioRad) in TBST (50 mM Tris•HCl, 150 mM NaCl, 0.05% Tween 20, pH 7.4) for 1 h at rt. Primary antibodies in 5% milk in TBST were added overnight at 4 °C at the following concentrations: mouse anti-NCAM monoclonal antibody (Abcam) at 1 µg/mL, mouse anti-synapsin I ascites (Synaptic Systems) at 0.1 µg/ml, mouse anti-munc18-1 (Synaptic Systems) at 0.1 µg/mL, or mouse p44 MAPK monoclonal antibody (Cell Signaling) at 1:2000 dilution. Membranes were washed with TBST, incubated with the appropriate Alexa Fluor 680-conjugated (Invitrogen) or IR800-conjugated (Rockland) secondary antibody, and visualized using a LiCOR Odyssey Imaging System.

Lectin Affinity Chromatography with UEAI. UEAI lectin conjugated to agarose (Vector Laboratories) or control protein A conjugated to agarose (Vector Laboratories) was packed into a minicolumn (50 µL bed volume; Bio-Rad), and the columns were run in parallel. The resin was equilibrated with 10 column volumes of lectin binding buffer (100 mM Tris pH 7.5, 150 mM NaCl, 1 mM CaCl₂, 1 mM MgCl₂, 0.5% NP-40, and 0.2% sodium deoxycholate supplemented with EDTA-free Complete™ protease inhibitors). Olfactory bulb tissue from P3 rat pups was lysed in lectin binding buffer by sonication on ice. The lysate was clarified by centrifugation at 12000 x g for 10 min, and the total protein concentration was determined using the BCA protein assay (Pierce). Lysate (500 µg) was bound batch-wise with gentle end-over-end mixing at rt for 4 h. The agarose was then allowed to settle and the flow-through was passed over the column three additional times. The columns were washed with 40 column volumes of lectin binding

buffer, followed by 10 column volumes of lectin binding buffer lacking detergent. Proteins were eluted in 10 column volumes of lectin binding buffer lacking detergent and supplemented with 200 mM L-fucose and Complete™ protease inhibitors. Protein eluates were concentrated to a volume of 100 μ L using a Vivaspin 500 spin filter (10,000 Da MWCO). Following concentration, samples were boiled in 1X sample buffer (35 μ L of 200 mM Tris pH 6.8, 400 mM DTT, 8% SDS, 0.2% bromophenol blue, and 40% glycerol) and analyzed by SDS-PAGE and western blotting as described above. Synapsin I was detected using mouse anti-synapsin I ascites (Synaptic Systems) at 0.1 μ g/mL.

Cell Culture. HeLa, MCF-7, and MDA-mb-231 cells grown in DMEM medium supplemented with 10% fetal bovine serum (FBS), 100 units/mL penicillin, and 0.1 mg/mL streptomycin (Gibco). LNCaP and H1299 cells were grown in RPMI medium 1640 supplemented with 10% FBS, 100 units/mL penicillin, and 0.1 mg/mL streptomycin (Gibco). The PrEC line was maintained in PrEBM medium (Lonza). All transfections were carried out in antibiotic-free media. In all cases, cells were incubated in a 5% CO₂ humidified chamber at 37 °C. The PrEC line was obtained from Lonza; all other cell lines were obtained from ATCC.

Immunoprecipitation of TAMRA-Labeled Synapsin I from HeLa Cell Lysates.

HeLa cells were transfected with pCMV-FLAG-synapsin Ia²⁸ using Lipofectamine LTX reagent (Invitrogen). The cells were lysed and chemoenzymatically labeled and protein was precipitated as described above. After the protein pellet was allowed to dry briefly,

the pellet was re-dissolved in boiling 1% SDS plus Complete™ protease inhibitors at a concentration of 2 mg/mL. The SDS was quenched with 1 volume of NETFD buffer plus protease inhibitors, and the lysate was incubated with 40 µL of prewashed anti-Flag M2 Affinity Gel (Sigma-Aldrich) for 90 min at 4 °C. The resin was washed once with 4 column volumes of NETFD buffer and three times with 4 column volumes of NETF buffer (100 mM NaCl, 50 mM Tris•HCl pH 7.4, 5 mM EDTA). Captured protein was eluted in boiling 2X sample buffer (50 µL buffer/100 µL resin). Purified, labeled material was resolved by SDS-PAGE and transferred to a polyvinylidene fluoride (PVDF) membrane (Millipore). Western blotting was performed as above except the primary anti-TAMRA rabbit antibody (0.1 µg/µL; Invitrogen) was used.

Detection of Cell-Surface Fuc α (1-2)Gal Glycans on Live MCF-7 Cells by Fluorescence Microscopy. MCF-7 cells (ATCC) were seeded at 2×10^5 cells/coverslip. Twelve hours after plating, the cells were washed twice with 1% FBS, 10 mM HEPES in calcium and magnesium free Hank's Balanced Salt Solution (CMF HBSS, Gibco) and incubated in the chemoenzymatic labeling buffer (2% FBS, 10 mM HEPES pH 7.9 in HBSS) with UDP-GalNAz **3** (500 µM) and BgtA (0.17 mg/mL) in a total volume of 100 µL for 2 h at 37 °C. Mock reactions were performed without the addition of BgtA. After chemoenzymatic labeling, the cells were washed twice with 100% FBS and twice with the chemoenzymatic labeling buffer. Enzymatic addition of GalNAz onto Fuc α (1-2)Gal glycans was detected by incubating the cells with ADIBO-biotin (20 µM in the chemoenzymatic labeling buffer; 500 µL) for 1 h at rt, washing the coverslips as described, and then incubation with streptavidin-Alexa Fluor 488 (1 µg/mL in PBS

containing 3% BSA; Invitrogen) for 30 min at rt. Cells were washed once with PBS, after which nuclei were stained with Hoechst-33342 (1 $\mu\text{g}/\mu\text{L}$; Invitrogen) in PBS for 15 min at rt. Coverslips were washed twice with 100% FBS and mounted in media (on ice), sealed with paraffin, and imaged immediately using a 40x Plan-Achromat objective on a Zeiss Meta510 inverted microscope.

Detection of $\text{Fuca}(1-2)\text{-Gal}$ Glycans on Synapsin I in Fixed HeLa Cells by Fluorescence Microscopy. HeLa cells were plated onto 15 mm coverslips (Carolina Biological) at a density of 75 cells/ mm^2 . After 12 h, cells were transfected with pCMV-Flag-synapsin Ia (0.5 μg DNA/coverslip) using Lipofectamine LTX (4 μL in 200 μL Optimem; Invitrogen). After 24 h, the media was removed, and the cells were rinsed one time with PBS, fixed in 4% paraformaldehyde in PBS, pH 7.5 for 20 min at rt, washed twice with PBS, permeabilized in 0.3% Triton X-100 in PBS for 10 min at rt, and washed twice with the enzymatic labeling buffer (50 mM HEPES, 125 mM NaCl, pH 7.9). Reaction mixtures and negative controls (without BgtA) were prepared by adding 100 μL of 20 mM HEPES pH 7.9, 50 mM NaCl, 2% NP-40, 5 mM MnCl_2 , UDP-GalNAz **3** (25 μM), and BgtA (0.17 mg/mL) at 4 $^\circ\text{C}$ for 24 h (100 μL /coverslip) in a humidified chamber. After chemoenzymatic labeling, the cells were washed twice with the chemoenzymatic labeling buffer. Enzymatic addition of GalNAz onto $\text{Fuca}(1-2)\text{Gal}$ glycans was detected by treating the cells with 5 μM alkyne-functionalized Alexa Fluor 488 (Invitrogen), 0.1 mM triazoleamine ligand (Invitrogen), 2 mM sodium ascorbate (Sigma-Aldrich), and 1 mM CuSO_4 (Sigma-Aldrich) in 2% FBS (Gibco) in PBS at rt for 1 h. Synapsin I was detected by immunostaining with an anti-synapsin I antibody

(Millipore, 1:250 in 3% BSA) for 1 h at rt, followed by an anti-rabbit secondary antibody conjugated to Alexa Fluor 546 (Invitrogen; 1:1000 in 3% BSA) for 1 h at rt. The coverslips were washed with PBS, mounted onto glass slides using Vectashield mounting medium with DAPI (4 μ L; Vector Labs), and sealed with clear nail polish. Cells were imaged using a Nikon Eclipse TE2000-S inverted microscope, and images were captured with Metamorph software using a 20x Plan Fluor objective.

Detection of Cell-Surface Fuca(1-2)Gal Glycans on Live Cancer Cells by Flow Cytometry. All cells were seeded at 4×10^6 cells per 10-cm plate in 10 mL of the appropriate media. On the day of analysis, cells were lifted off the plate with DNase (0.4 mg/mL; Worthington) and 1 mM EDTA and washed with 1% FBS, 10 mM HEPES in CMF HBSS. One million cells were chemoenzymatically labeled with UDP-GalNAz (500 μ M) and BgtA (0.17 μ g/ μ L) in 1% FBS, 10 mM HEPES in CMF HBSS (100 μ L) for 2 h at 37 $^{\circ}$ C. Cells were spun twice through 100% FBS (1 mL) to remove excess reagent (500 x g, 5 min) and resuspended in 1% FBS, 10 mM HEPES in CMF HBSS (100 μ L) containing ADIBO-biotin (20 μ M) and incubated for 1 h at rt. Cells were again spun twice through 100% FBS (1 mL), and washed with 3% BSA in PBS (1 mL). Cells were then resuspended in 3% BSA in PBS (100 μ L) containing streptavidin-Alexa Fluor 488 (1 μ g/mL) and incubated for 20 min at 4 $^{\circ}$ C. Cells were subsequently spun twice through 100% FBS (1 mL) and resuspended in 2% FBS, 10 mM HEPES in CMF HBSS (750 μ L) for flow cytometry analysis. Immediately before analysis, 7-amino-actinomycin D (7-AAD, 5 μ L; eBioscience) was added to measure cell viability. Cells were analyzed for FITC intensity on a Beckman Dickinson FACSCalibur flow cytometer equipped with a

488-nm argon laser. For each experiment, 10,000 live cells were analyzed, and data analysis was performed on FlowJo (Tristar Inc.). Data points for LnCAP and PrEC cells were collected in triplicate, and for all other cells, in duplicate.

REFERENCES

1. Delves, P. J. *Autoimmunity* **1998**, 27, 239.
2. Rexach, J. E.; Clark, P. M.; Hsieh-Wilson, L. C. *Nature Chemical Biology* **2008**, 4, 97.
3. Kim, Y.; Varki, A. *Glycoconjugate Journal* **1997**, 14, 569.
4. McCabe, N. R.; Rose, S. P. *Neurochemistry Research* **1985**, 10, 1083.
5. Pohle, W.; Acosta, L.; Ruthrich, H.; Krug, M.; Matthies, H. R. *Brain Research* **1987**, 410, 245.
6. Tiunova, A.A.; Anokhin, K.V.; Rose, S.P. *Learning and Memory* **1998**, 4, 401.
7. Becker, D. J.; Lowe, J. B. *Glycobiology* **2003**, 13, 41R.
8. Chang, W.-W.; Lee, C. H.; Lee, P.; Lin, J.; Hsu, C.-W.; Hung, J.-T.; Lin, J.-J.; Yu, J.-C.; Shao, L.-e.; Yu, J.; Wong, C.-H.; Yu, A. L. *Proceedings of the National Academy of Sciences USA* **2008**, 105, 11667.
9. Menard, S.; Tagliabue, E.; Canevari, S.; Fossati, G.; Colnaghi, M.I. *Cancer Research* **1983**, 43, 1295.
10. Zhang, S.; Zhang, H.S.; Cordon-Cardo, C.; Ragupathi, G.; Livingston, P.O. *Clinical Cancer Research* **1998**, 4, 2669.
11. Miyake, M.; Taki, T.; Hitomi, S.; Hakomori, S.-i. N. *New England Journal of Medicine* **1992**, 327, 14.
12. Colnaghi, M. I.; Da Dalt, M.G.; Agresti, R.; Cattoretti, G.; Andreola, S.; Di Fronzo, G.; Del Vecchio, M.; Verderio, L.; Cascinelli, N.; Rilke, F. In *Immunological Approaches to the Diagnosis and Therapy of Breast Cancer*; Ceriani, R. L., Ed.; *Plenum Publishing: New York*, **1987**, 21.
13. Lee J.S., R. J. Y., Sahin A.A., Hong, W.K., Brown, B.W., Mountain, C.F., Hittleman, W.N. N. *New England Journal of Medicine* **1991**, 324, 1084.

14. Manimala, J. C.; Roach, T. A.; Li, Z.; Gildersleeve, J. C. *Angewandte Chemie International Edition* **2006**, 45, 3607.
15. Manimala, J. C.; Roach, T. A.; Li, Z.; Gildersleeve, J. C. *Glycobiology* **2007**, 17, 17C.
16. Chang, C.-F.; Pan, J.-F.; Lin, C.-N.; Wu, I.-L.; Wong, C.-H.; Lin, C.-H. *Glycobiology* **2011**, 21, 895.
17. Laughlin, S. T.; Baskin, J. M.; Amacher, S. L.; Bertozzi, C. R. *Science* **2008**, 320, 664.
18. Laughlin, S.T.; Bertozzi, C.R. *Proceedings of the National Academy of Sciences USA* **2009**, 106, 12.
19. Hanson, S. R.; Hsu, T.-L.; Weerapana, E.; Kishikawa, K.; Simon, G. M.; Cravatt, B. F.; Wong, C.-H. *Journal of the American Chemical Society* **2007**, 129, 7266.
20. Tanaka, Y.; Kohler, J. J. *Journal of the American Chemical Society* **2008**, 130, 3278.
21. Zaro, B. W.; Yang, Y.-Y.; Hang, H. C.; Pratt, M. R. *Proceedings of the National Academy of Sciences USA* **2011**, 108, 8146.
22. Khidekel, N.; Arndt, S.; Lamarre-Vincent, N.; Lippert, A.; Poulin-Kerstien, K. G.; Ramakrishnan, B.; Qasba, P. K.; Hsieh-Wilson, L. C. *Journal of the American Chemical Society* **2003**, 125, 16162.
23. Clark, P. M.; Dweck, J. F.; Mason, D. E.; Hart, C. R.; Buck, S. B.; Peters, E. C.; Agnew, B. J.; Hsieh-Wilson, L. C. *Journal of the American Chemical Society* **2008**, 130, 11576.
24. Zheng, T.; Jiang, H.; Gros, M.; Soriano del Amo, D.; Sundaram, S.; Lauvau, G.; Marlow, F.; Liu, Y.; Stanley, P.; Wu, P. *Angewandte Chemie International Edition* **2011**, 50, 4113.
25. Yi, W.; Shen, J.; Zhou, G.; Li, J.; Wang, P. G. *Journal of the American Chemical Society* **2008**, 130, 14420.
26. Blixt, O.; Allin, K.; Bohorov, O.; Liu, X.; Andersson-Sand, H.; Hoffman, J.; Razi, N. *Glycoconjugate Journal* **2008**, 25, 59.
27. Blixt, O.; Head, S.; Mondala, T.; Scanlan, C.; Huflejt, M. E.; Alvarez, R.; Bryan, M. C.; Fazio, F.; Calarese, D.; Stevens, J.; Razi, N.; Stevens, D. J.; Skehel, J. J.; van Die, I.; Burton, D. R.; Wilson, I. A.; Cummings, R.; Bovin, N.; Wong, C.-H.;

- Paulson, J. C. *Proceedings of the National Academy of Sciences USA* **2004**, 101, 17033.
28. Murrey, H. E.; Gama, C. I.; Kalovidouris, S. A.; Luo, W.-I.; Driggers, E. M.; Porton, B.; Hsieh-Wilson, L. C. *Proceedings of the National Academy of Sciences USA* **2006**, 103, 21.
29. Murrey, H. E.; Ficarro, S. B.; Krishnamurthy, C.; Domino, S. E.; Peters, E. C.; Hsieh-Wilson, L. C. *Biochemistry* **2009**, 48, 7261.
30. Schröder, F. H.; Hugosson, J.; Roobol, M. J.; Tammela, T. L. J.; Ciatto, S.; Nelen, V.; Kwiatkowski, M.; Lujan, M.; Lilja, H.; Zappa, M.; Denis, L. J.; Recker, F.; Berenguer, A.; Määttänen, L.; Bangma, C. H.; Aus, G.; Villers, A.; Rebillard, X.; van der Kwast, T.; Blijenberg, B. G.; Moss, S. M.; de Koning, H. J.; Auvinen, A. *New England Journal of Medicine* **2009**, 360, 1320.
31. Peracaula, R.; Tabarés, G.; Royle, L.; Harvey, D. J.; Dwek, R. A.; Rudd, P. M.; de Llorens, R. *Glycobiology* **2003**, 13, 457.
32. Smith, D. S.; Song, X.; Cummings, R.D. *Methods in Enzymology* **2010**, 480, 417.

Chapter 3

Chemoenzymatic Detection of the Cancer-Relevant Core Fucose Biomarker

ABSTRACT

Core fucosylation is an abundant post-translational modification that regulates many important physiological functions, including cell signaling, long-term potentiation, and antibody-dependent cellular cytotoxicity, and is unregulated in various cancers. However, the tools currently used to detect core fucose suffer from poor specificity, exhibiting cross reactivity with all types of fucosylation. In this chapter, I report the development of a new chemoenzymatic strategy for the rapid and selective detection of core fucosylated glycoproteins. I demonstrate that the approach exhibits superior specificity towards core fucose on a variety of complex *N*-glycans. Further, the approach is amenable to detection of core fucosylated glycans from complex cell lysates and the cell surface of live cells, and can be integrated into a diagnostic platform for the profiling of protein specific core fucosylation levels. This chemoenzymatic labeling approach offers a new strategy for the identification of disease biomarkers and enables researchers to further characterize the fundamental role that this carbohydrate plays in normal and disease physiology.

INTRODUCTION

Protein glycosylation is an abundant post-translational modification that regulates a variety of physiological functions such as development, cell signaling, mediating host-pathogen interactions, and disease pathogenesis.¹ With aberrant glycosylation being a hallmark of many human disease states, a major focus in the field has been elucidating the functional role that these carbohydrates play. Core fucose, a FUT8 catalyzed α -1,6-fucose attached to the reducing end *N*-Acetylglucosamine (GlcNAc) of *N*-glycans, is an abundant post-translational modification that regulates many important physiological functions such as cell signaling,^{2,3} cell adhesion,^{4,5} long-term potentiation,⁶ and antibody-dependent cellular cytotoxicity⁷ and is upregulated in various cancers.⁸⁻¹⁴ Specifically, increased core fucosylation of serum glycoproteins has been discovered in breast cancer,⁸ prostate cancer,⁹ and pancreatic cancer,¹⁰ but perhaps has been best studied in the case of Hepatocellular Carcinoma (HCC), where increased core fucosylation of α -fetoprotein (AFP), among other proteins, has been shown to directly correlate with HCC pathogenesis.¹¹⁻¹⁴

Currently, antibodies and/or lectins are commonly used to detect carbohydrate structures; however, these methods suffer from both weak binding and/or cross reactivity towards similar glycan structures.¹⁵⁻¹⁷ Alternatively, metabolic labeling of cells and model organisms with non-natural monosaccharides has become a valued strategy towards the detection and study of glycoconjugates.^{18,19} However, by hijacking the cells salvage and biosynthetic pathways for metabolic incorporation of these non-natural monosaccharides, the sugar of choice is incorporated non-specifically anywhere the monosaccharide is endogenously found. Additionally, competition with the natural

substrate in the cell leads to low incorporation efficiency. Consequently, unique carbohydrate structures, such as of defined monosaccharide connectivity, α -1,2-fucose vs. α -1,6-fucose, and higher order glycans, such as unique disaccharide or trisaccharide motifs, cannot be specifically detected. Given these specificity constraints imposed by current glycan detection strategies and the diversity of cellular glycans, there is an urgent need for new technologies to be developed to enable the detailed study of specific glycan structures.

More recently, chemoenzymatic labeling approaches have been developed to detect specific and complex glycan structures such as *O*-linked- β -*N*-acetylglucosamine (*O*-GlcNAc),^{20,21} *N*-Acetyllactosamine (LacNAc),²² and fucose- α -1,2-galactose (Fuca(1,2)Gal).²³ This approach exploits the acceptor substrate specificity of a glycosyltransferase to install a non-natural sugar analogue, bearing a chemical handle, onto the specific glycan structure of interest. Then, a reporter tag is installed using bioorthogonal chemistry, such as click chemistry, for detection. Because the enzymatic reaction proceeds in a quantitative yield and directs the specificity of labeling, the chemoenzymatic approach affords both superior specificity and sensitivity over antibody, lectin, and metabolic labeling approaches. Herein, I report the first strategy for the selective detection of core fucosylated glycans, enabling the investigation of a broad range of physiologically important glycoproteins and cancer biomarkers (Figure 3.1).

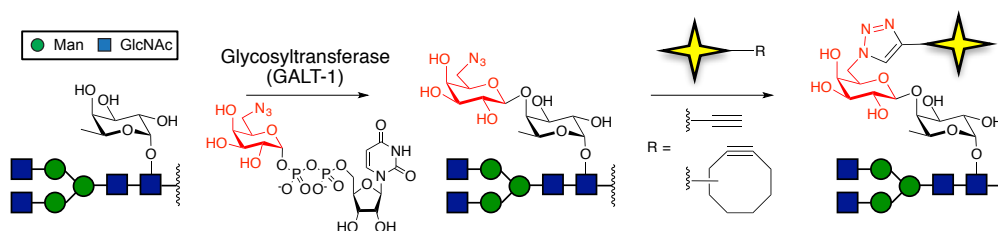


Figure 3.1 The chemoenzymatic labeling approach for the detection of core fucosylated glycoproteins.

RESULTS AND DISCUSSION

To develop such an approach, I exploited the *C. elegans* β -1,4-galactosyltransferase (GALT-1), which transfers galactose (Gal) from UDP-Gal onto the 4 position of an α 1,6-fucose (core fucose), generating a Gal- β -1,4-fucose structure.²⁴ We reasoned that GALT-1 may tolerate substitution on the C-6 position of Gal,²⁵ allowing for the selective tagging of core fucosylated glycans with azido functionality and enabling subsequent click chemistry detection of target glycoproteins (Figure 3.2A).

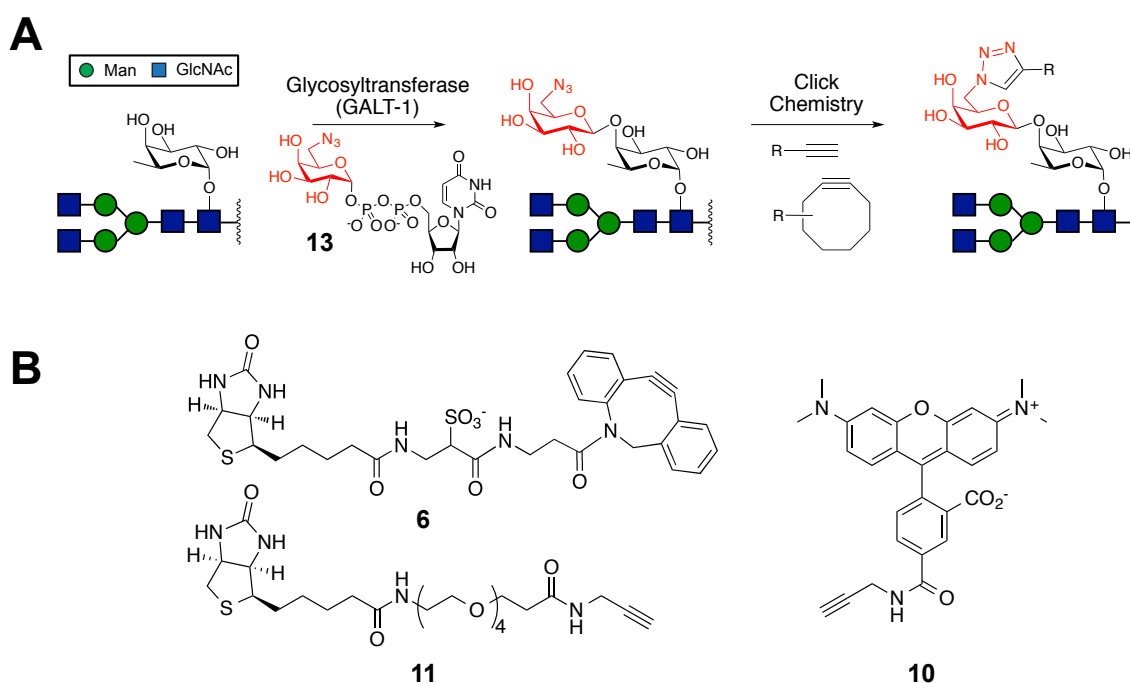


Figure 3.2 (A) Chemoenzymatic labeling strategy for the detection of core fucosylated glycoproteins. Glycoproteins are treated with **13** and GALT-1, followed by subsequent click chemistry reaction with alkyne containing, readout-specific reagents (immunohistochemistry, FACS, WB, affinity enrichment,...). **13**, UDP-6-deoxy-6-azido-D-galactose (UDP-Gal-6-N₃) (B) Chemical reagents used for click chemistry (**6**, **10**, and **11**).; **6**, Azadibenzocyclooctyne-sulfo-biotin (ADIBO-biotin); **10**, 5-Carboxytetramethylrhodamine-alkyne (TAMRA-alkyne); **11**, biotin-alkyne.

To test the approach, GALT-1 was cloned into a pet28a vector containing an N-terminal 6-his tag followed by a SUMO solubilization tag, yielding a His-SUMO-GALT-1 pet28a construct. This construct was transformed into BL21 (DE3) cells and protein

expression was induced with IPTG. Cobalt-NTA resin purified GALT-1 was incubated with either UDP-galactose or the UDP-gal analogue, UDP-6-deoxy-6-azido-galactose (UDP-Gal-6-N₃, **13**) and a dabsylated-core fucosylated glycopeptide (**14**) for 2 hours at room temperature (Figure 3.3). Indeed, complete conversion of **14** to the desired products **15** and **16**, respectively, was witnessed, as determined by matrix-assisted laser desorption/ionization – time of flight mass spectrometry (MALDI-TOF MS; Figure 3.3).

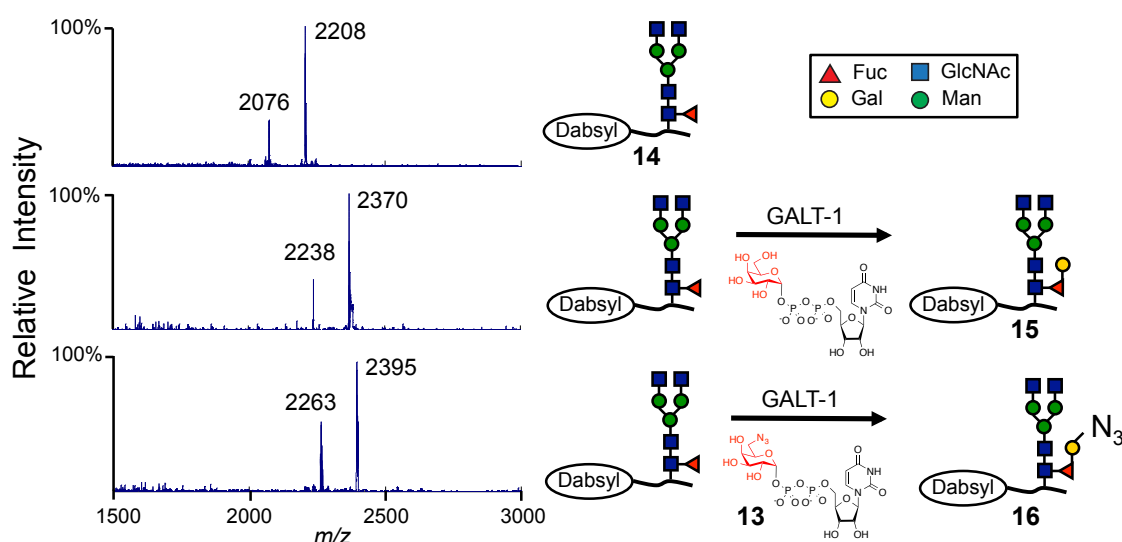


Figure 3.3 GALT-1 accepts the non-natural UDP-galactose analogue UDP-6-deoxy-6-azido-galactose (**13**). MALDI-TOF-MS analysis of GALT-1 donor substrate specificity using a dabsylated glycopeptide acceptor substrate (**14**, m/z 2208 and 2076, upper). GALT-1 utilizes the natural donor substrate UDP-galactose to give the predicted product (**15**, m/z 2370 and 2238, middle). GALT-1 also utilizes the non-natural donor substrate **13** to give the azido-functionalized product (**16**, m/z 2095 and 2263). In each spectrum, the smaller peak (-136 Da) is due to loss of the dabsyl group from the N-terminus of the peptide.

Kinetic analysis for GALT-1 substrates revealed an apparent k_{cat}/K_m of 0.994 nM⁻¹ min⁻¹ for UDP-Gal-6-N₃, approximately 3 fold lower than the value of 3.195 nM⁻¹ min⁻¹ for the natural substrate, UDP-Gal (Figures 3.4A and B). Furthermore, GALT-1 exhibited an apparent k_{cat}/K_m of 0.650 nM⁻¹ min⁻¹ for the core fucosylated acceptor substrate, N6000 (Figures 3.4A and C). Additional kinetic parameters for all substrates, such as K_m , V_{max} , and k_{cat} , are noted in figure 3.4A. Taken together, the results from the glycopeptide

analysis above and the determination of these kinetic parameters demonstrate that GALT-1 can efficiently utilize the non-natural UDP-Gal analogue, UDP-Gal-6-N₃ (**13**), without engineering of the glycosyltransferase.

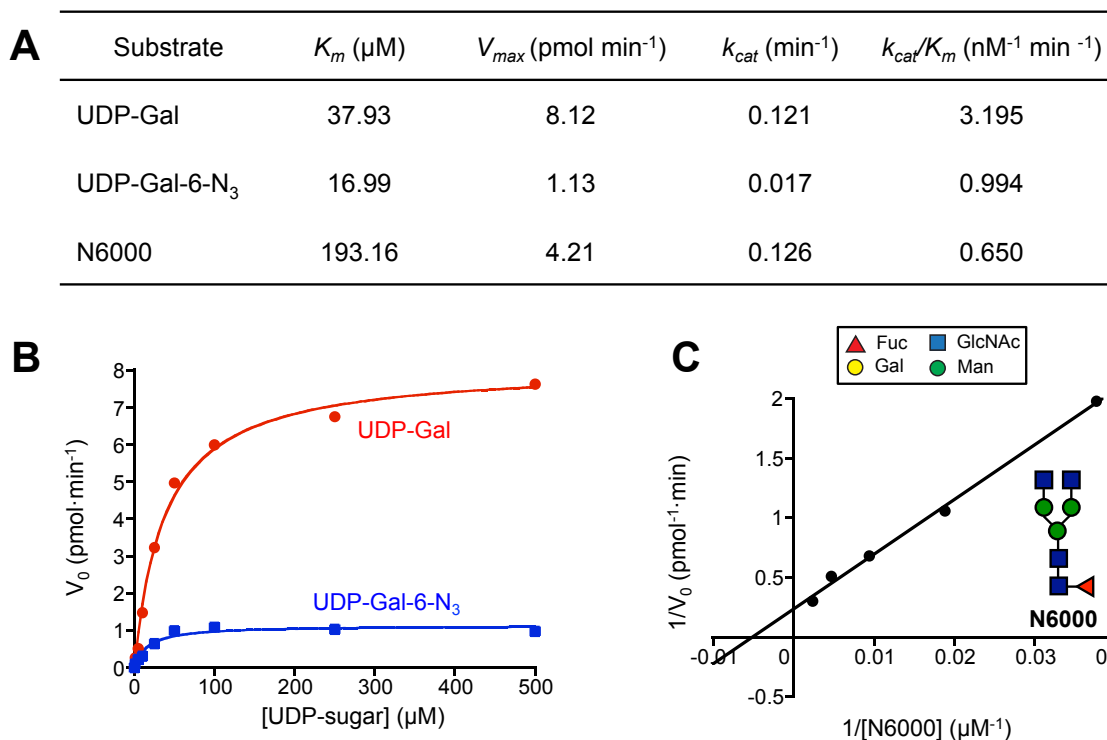


Figure 3.4. Determination of the kinetic parameters of GALT-1 towards its substrates. (A) N6000 was used as substrate to study the kinetic parameters towards donor substrates, and UDP-Gal was used as a substrate to study the kinetic parameters towards acceptor substrate N6000. (B) Kinetic comparison of the GALT-1-catalyzed reaction of N6000 with UDP-Gal (red) and UDP-Gal-6-N₃ (blue; **13**) using a UDP-dependent turn-on fluorescent sensor specific for UDP (see chapter 5). Reactions were preformed in duplicate using 50 μM acceptor substrate, N6000, and varying concentrations of the donor substrates. (C) Determination of GALT-1's kinetic parameters towards core fucosylated N-glycan structure N6000, inserted in graph. Reactions were preformed in duplicate using 50 μM donor substrate, UDP-Gal, and varying concentrations of the acceptor substrate N6000.

With GALT-1's ability to efficiently utilize the non-natural UDP-Gal-6-N₃, I next sought to investigate the acceptor substrate specificity of GALT-1 using a collection of synthetically prepared, homogenous N-glycans provided by the Peng George Wang lab (Figures 3.5 and 3.6).²⁶ With biologically relevant core fucosylated N-glycans being heterogeneous in nature, it would be difficult to determine the acceptor substrate

specificity of GALT-1 without such purified compounds. To determine the preference of GALT-1 towards different acceptor substrates, I incubated GALT-1 and UDP-Gal-6-N₃ with *N*-glycans varying in antenna length (N6000, N6001, N6002), fucose connectivity (N224), and presence of core fucose (N000). These reactions were then analyzed by MALDI-TOF MS in positive mode (Figure 3.5). GALT-1 efficiently installed UDP-Gal-6-N₃ onto N6000, N6001, and N6002, suggesting that GALT-1 can label core fucosylated *N*-glycans whose antenna vary in length and terminate in GlcNAc, Gal, or sialic acid, respectively (Figures 3.5 A, C, and E). This suggests that these features still allowed GALT-1 to access the core fucose residue for modification. However, it is noted that while these three *N*-glycans are all substrates for GALT-1, they are not all modified with the same efficiency (Figure 3.6). In fact, progressive elongation of the *N*-glycan antenna, seem to perturb the addition of Gal-6-N₃ on these different substrates. This phenomenon is important to keep in mind when using this method in cell or protein labeling experiments.

To address non-specific addition of UDP-Gal-6-N₃ onto other fucose residues of *N*-glycans, I tested structure N224, containing no core fucose, but an outer-arm α 1,3 fucosylation on one antenna. No GALT-1 dependent addition of UDP-Gal-6-N₃ was witnessed on N224 (Figure 3.5B). As a final control, *N*-glycan structure N000, containing no fucose, was tested and did not result in addition of UDP-Gal-6-N₃ (Figure 3.5D). These results demonstrate the strong specificity of GALT-1 for core fucose on various complex *N*-glycan structures (Figures 3.5 and 3.6).

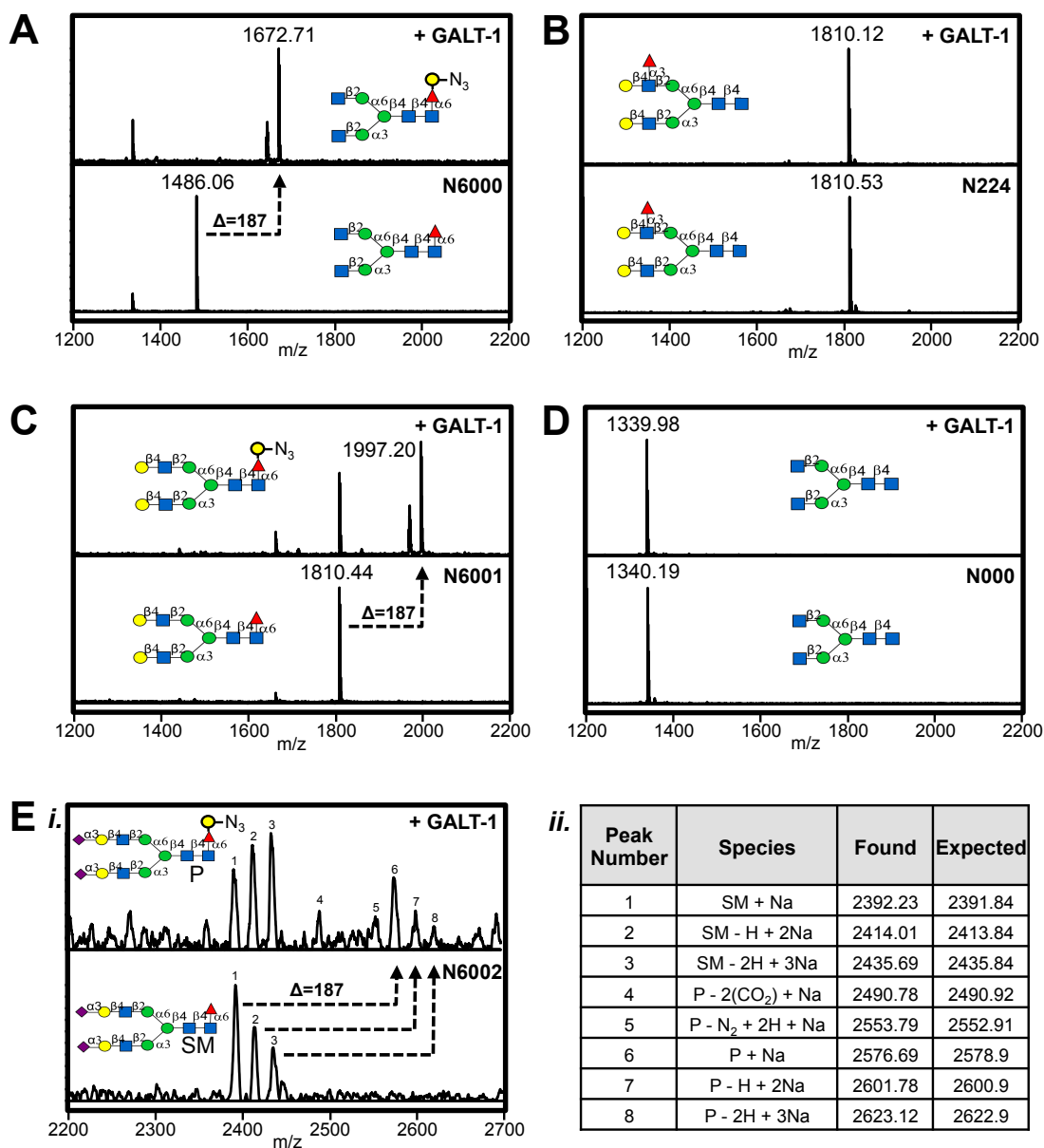


Figure 3.5 GALT-1 acceptor substrate specificity. GALT-1 was incubated with UDP-Gal-6-N₃ (**13**) and different acceptor substrates (A-E) followed by MALDI-TOF MS analysis after two hours. A shift of 187 m/z resulted from the GALT-1 dependent addition of **13** onto the acceptor substrates (A) N6000, (C) N6001, and (E) N6002. No shift was witnessed for substrate (B) N224 and control substrate (D) N000. (E) *i.*) Acceptor substrate N6002, due to various Na⁺ adducts and fragmentation. *ii.*) This table notes the peaks identified from *i* and the predicted molecular species are noted. All spectra were collected in positive mode.

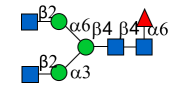
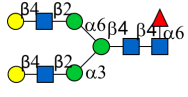
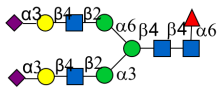
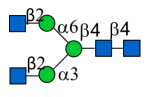
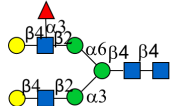
Acceptor Substrate	% Conversion
N6000 	> 98%
N6001 	~ 70%
N6002 	~ 35%
N000 	0%
N224 	0%

Figure 3.6 GALT-1 acceptor substrate specificity continued. Approximate conversion percentages for the GALT-1 reaction with each acceptor substrate at the two hour time point (spectra from Figure 3.5). Percentages were calculated from the starting material and product peak intensity areas of the MALDI-TOF MS analysis.

To determine whether a chemoenzymatic approach could be used to detect core fucosylated glycoproteins, a known core fucosylated glycoprotein, bovine thyroglobulin,²⁷ was incubated with GALT-1 and UDP-Gal-6-N₃. Samples taken at various time points were subjected to the copper(I)-catalyzed alkyne-azide cycloaddition (CuAAC) with TAMRA-alkyne (Figure 3.2B; **10**) for 1 hour at room temperature. Strong TAMRA specific signal was detected in a time dependent manner, illustrating the ability of the approach to label core fucosylated glycoproteins (Figure 3.7A). Core fucose was also robustly detected on secreted proteins secreted from liver cancer cells grown in culture, HepG2, with minimal non-specific signal witnessed when removing GALT-1, UDP-Gal-6-N₃, or biotin-alkyne **11** (Figure 3.7B). To further investigate the specificity of our approach, protein lysates were chemoenzymatically labeled with biotin-alkyne **11**, incubated with streptavidin resin to enrich biotinylated proteins, and immunoblotted for

known core fucosylated glycoproteins. Core fucosylated epidermal growth factor receptor (EGFR) from MDA-MB-231 cells, α -fetoprotein (AFP) from HepG2 cells, and E-Cadherin from MCF-7 cells, all established core fucosylated glycoproteins,^{2,28,29} were detected in a GALT-1 specific manner (Figure 3.7C). Taken together, these results highlight the ability of the approach to specifically detect core fucosylated glycoproteins in a complex protein sample.

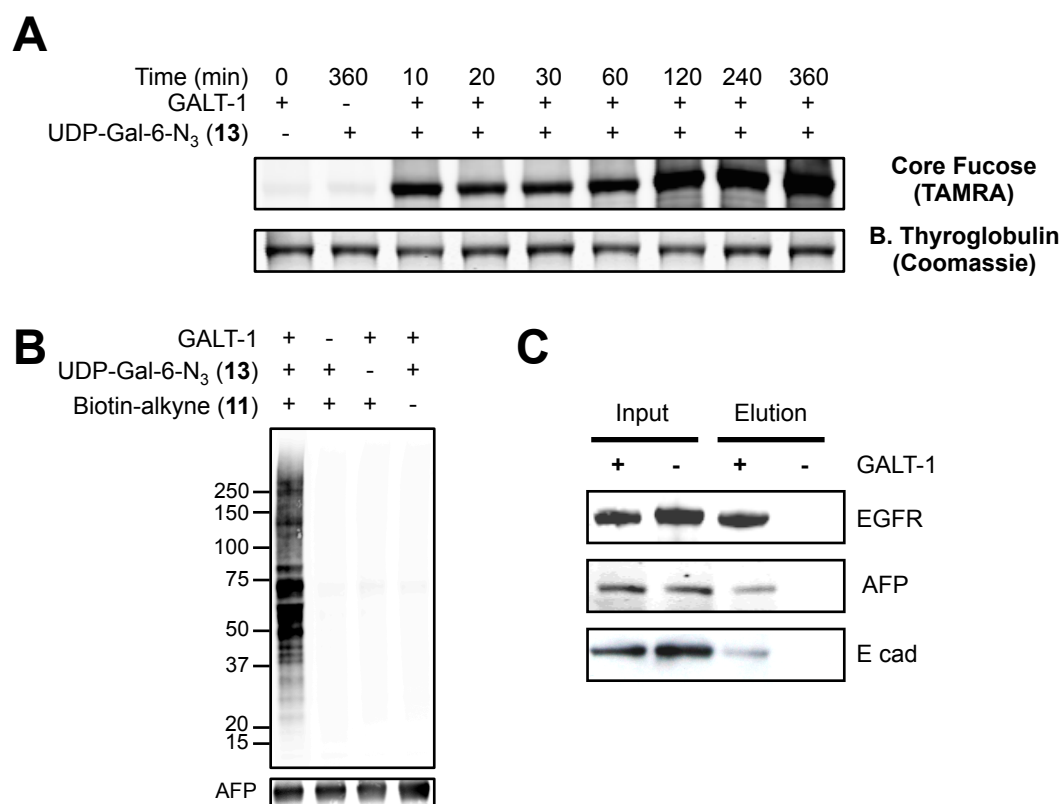


Figure 3.7 GALT-1 efficiently labels core fucosylated glycoproteins. (A) Time course of the GALT-1 reaction using purified bovine thyroglobulin as acceptor substrate. Labeling was detected by copper(I)-catalyzed azide-alkyne cycloaddition (CuAAC) with TAMRA-alkyne (10). (B) Chemoenzymatic detection of HepG2 secreted core fucose glycoproteins. Western blot detection was performed using streptavidin-conjugated Alexa Fluor 680 with subsequent detection of α -fetoprotein (AFP) for loading control. (C) Chemoenzymatic labeling of cell lysates with TAMRA-alkyne (10) followed by a immunoprecipitation of TAMRA labeled material and western blot detection of known core fucosylated glycoproteins from human MDA-MB-231 breast cancer cell lines (EGF receptor; EFGR), human HepG2 liver cancer cell lines (AFP), and human MCF-7 breast cancer (E cadherin; E cad) cell lines. C performed by Lan Ban.

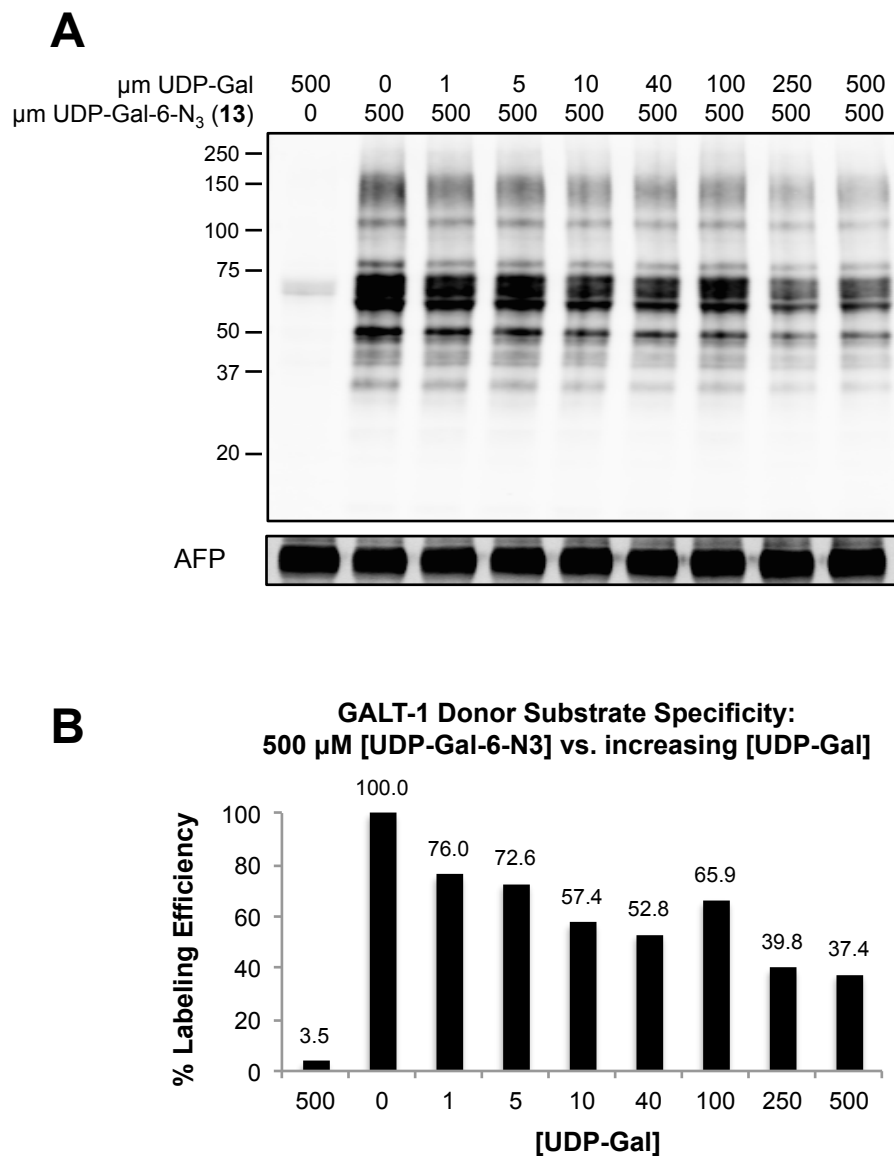


Figure 3.8 GALT-1 enzymatic efficiency comparing natural and non-natural donor substrates. (A) Chemoenzymatically labeled HepG2 proteins were treated with 500 μM UDP-Gal-6-N₃ (**13**) and increasing amounts of the natural donor substrate UDP-Gal for 4 hours at room temperature. Samples were then subjected to CuAAC using TAMRA-alkyne (**10**) and western blot analysis for detection of TAMRA (top) and AFP (bottom). (B) Quantification of the percent labeling efficiency of **13** by GALT-1 with increasing the competing amounts of UDP-Gal. The reaction without UDP-Gal was set to 100%.

Importantly, when performing the chemoenzymatic labeling approach, the naturally occurring UDP-Gal molecule could be present in the sample. The procedure generally calls for a protein precipitation step prior to the enzymatic labeling step in order to remove these types of metabolites from the sample. It has been witnessed in the lab

that subjecting a protein lysate directly to enzymatic labeling, with no prior precipitation step, does not enable efficient enzymatic labeling. It is suspected that metabolites, likely the natural UDP-Gal substrate, among others, cause competition of the reaction, reducing the sensitivity of detection. To determine the level of competition between the natural UDP-Gal and non-natural UDP-Gal-6-N₃ (**13**), protein samples from HepG2 cells were subjected to the GALT-1 reaction with 500 μM UDP-Gal-6-N₃ and increasing amounts of UDP-Gal, followed by the CuAAC reaction with TAMRA-alkyne **10** (Figure 3.8). Low levels of UDP-Gal, 1 μM, decreased the TAMRA signal by 25% and when these substrates were present at equal concentrations (500 μM) the signal decreased by over 60%, suggesting that GALT-1 demonstrates a preference for the natural UDP-Gal substrate over the non-natural UDP-Gal-6-N₃ (**13**). While these findings are not surprising, they highlight the importance of complete removal of endogenous metabolites to maximize the efficiency of enzymatic labeling.

To confirm the specificity for GALT-1 dependent chemoenzymatic labeling of core fucosylated glycoproteins, *Fut8* knock-out (*Fut8*^{-/-}) and wild type (*Fut8*^{+/+}) brain lysates were treated with or without PNGaseF, followed by chemoenzymatic labeling and western blot detection (Figure 3.9). Only *Fut8*^{+/+} samples treated with GALT-1, and without PNGaseF (lane 2), show labeling over background, suggesting that α1-6 fucose of *N*-glycans is the only substrate modified by GALT-1. The *Fut8*^{-/-} samples treated with GALT-1, without PNGaseF (lane 4), did not show labeling over background, demonstrating that the approach presents excellent specificity towards core fucose (Figure 3.9B). L1CAM, a heavily *N*-glycosylated glycoprotein, was used as a positive control for the PNGaseF reaction.³⁰

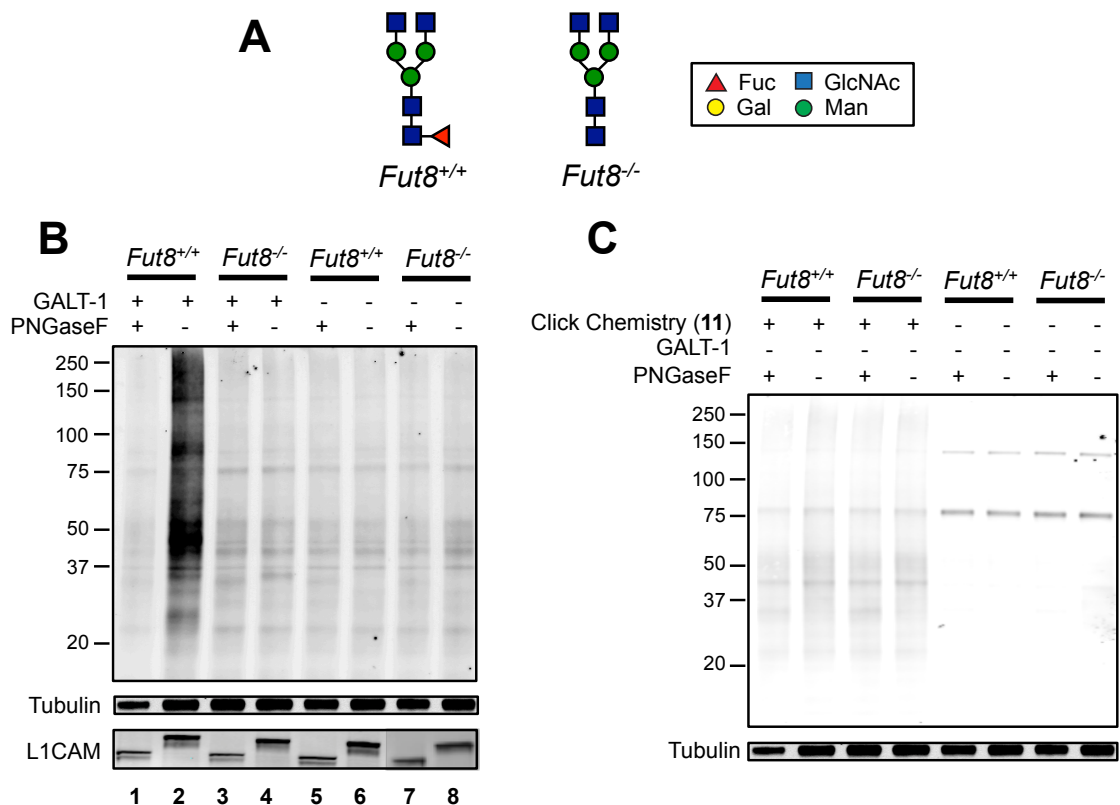


Figure 3.9 GALT-1 specifically labels core fucosylated glycoproteins. (A) Cartoon representation of the *N*-glycans produced by *Fut8* wild type (*Fut8*^{+/+}), and knock-out (*Fut8*^{-/-}) mice. FUT8 is the glycosyltransferase responsible for core fucosylation (red triangle). (B) Brain lysates from *Fut8*^{-/-} and *Fut8*^{+/+} mice were chemoenzymatically labeled after PNGaseF digestion, or a mock control reaction without PNGaseF. Western blot detection of biotinylated proteins using streptavidin-conjugated Alexa Fluor 680 demonstrates that GALT-1 is specific to core fucose. Tubulin was detected as a loading control and L1CAM was detected to ensure completion of the PNGaseF reaction. (C) Click chemistry on mouse brain samples with biotin-alkyne (**11**) causes non-specific background. These samples also contain proteins that are endogenously biotinylated.

Based on these findings, PNGaseF treatment eliminates the substrate for GALT-1 and, most importantly, no *Fut8*^{-/-} samples exhibit GALT-1 specific signal, further supporting the conclusion that GALT-1 is highly specific towards core fucose. We attribute the background labeling witnessed in all lanes (Figure 3.9B) to the CuAAC reaction with biotin-alkyne (**11**) and endogenously biotinylated proteins (Figures 3.9C and 3.10). This high specificity towards core fucose is significant, given that many lectins commonly used to detect core fucose, such as Lens Culinaris Agglutinin (LCA),

Aleuria Aurantia Lectin (AAL), and Aspergillus Oryzae Lectin (AOL), exhibit cross reactivity with other fucosylated motifs.¹⁵⁻¹⁷

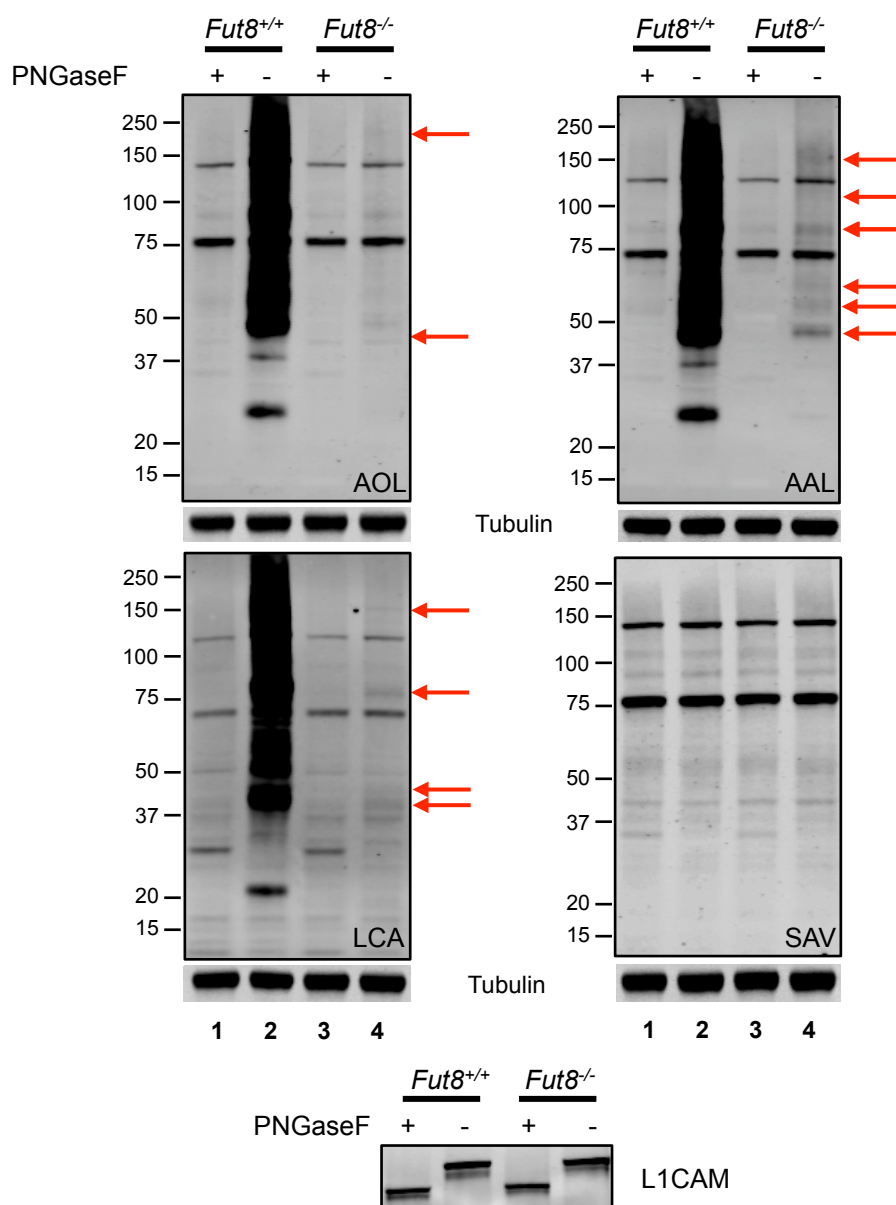


Figure 3.10 Lectin blot analysis of *Fut8*^{-/-} and *Fut8*^{+/+} mouse brain lysates treated with or without PNGaseF. Membranes were treated with the fucose specific biotinylated lectins Aspergillus Oryzae Lectin (AOL), Aleuria Aurantia Lectin (AAL), and Culinaris Agglutinin Lectin (LCA) followed by streptavidin conjugated Alexa Fluor 680 (SAV). A control western blot was performed to determine the background signal resulting from SAV, presumably due to endogenously biotinylated proteins. Western blot analysis was performed against the known glycoprotein L1CAM, to ensure the complete digestion of *N*-glycans. The fucose specific lectins AOL, AAL, and LCA detected non-core fucosylated *N*-glycan containing glycoproteins, highlighted by the red arrows.

Additionally, the samples used above (Figure 3.9B) were subjected to lectin blot analysis, prior to chemoenzymatic labeling, to highlight the superior specificity of GALT-1 towards core fucose when compared to the biotinylated lectins LCA, AAL, and AOL (Figure 3.10; lane 4). These lectins all detected proteins in the *Fut8*^{-/-} samples that were mock treated with PNGaseF treatment, further demonstrating their cross reactivity with other non-core fucose epitopes found on *N*-glycans.

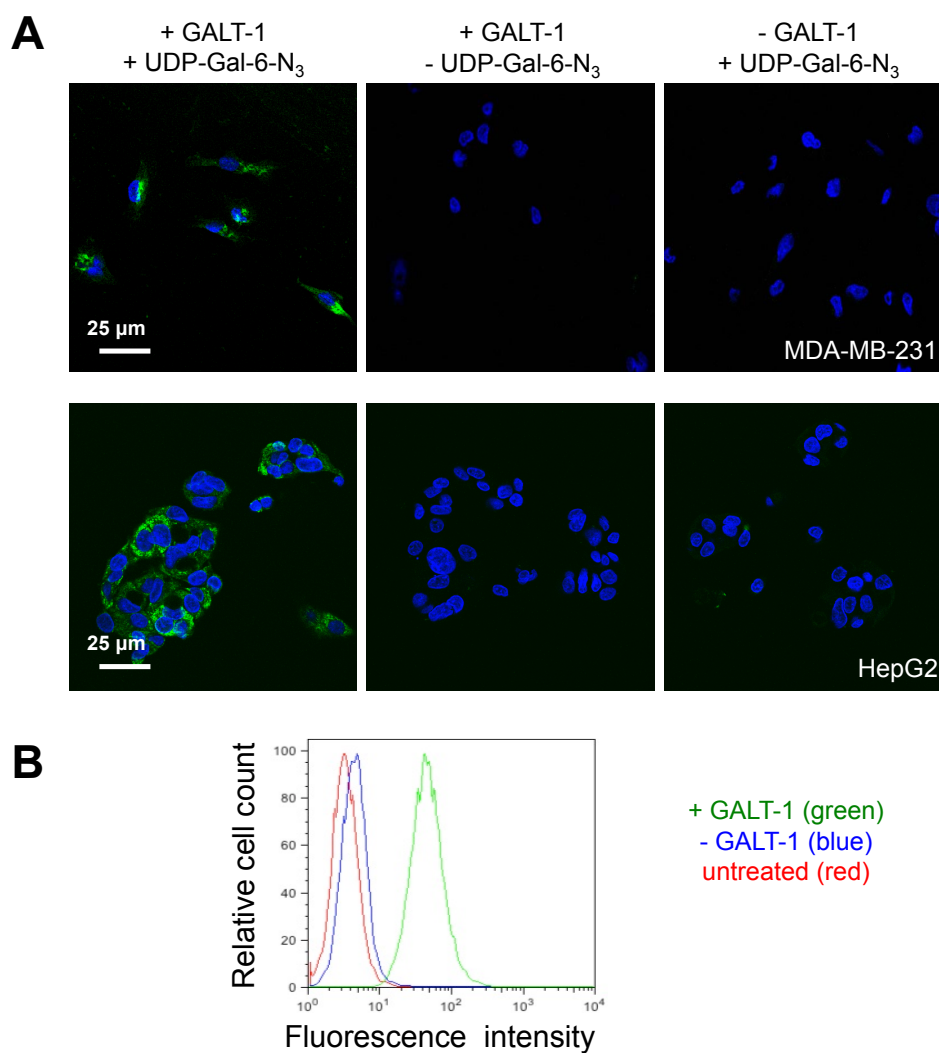


Figure 3.11 Chemoenzymatic labeling of cell surface core fucose. (A) Fluorescence detection of core fucosylated glycans (green) on fixed MDA-MB-231 cells (upper) and HepG2 cells (lower). No labeling was observed in the absence of either GALT-1 or UDP-Gal-6-N₃. Nuclei were stained with DAPI, blue. (B) Flow cytometry analysis detected the existence of core fucosylated glycans (green) on live breast cancer MDA-MB-231 cancer cell lines. No labeling was observed from untreated cells (red) or in the absence of GALT-1 (blue). Performed by Lan Ban.

Having established the superior specificity of the approach for core fucose, we next investigated whether the chemoenzymatic strategy could image cell surface core fucosylated glycans. First, MDA-MB-231 and HepG2 cells were fixed, permeabilized, and chemoenzymatically labeled on coverslips with GALT-1 and UDP-Gal-6-N₃. The CuAAC reaction was then performed using alkyne-biotin (**11**), followed by incubation with streptavidin-conjugated Alexa Fluor 488 to install a fluorescent reporter onto the core fucosylated glycans (green pseudo color; Figure 3.11A). Cell nuclei were detected with DAPI stain (blue pseudo color). In both cell lines, membrane-associated fluorescence was observed for cells treated with both GALT-1 and UDP-Gal-6-N₃, whereas no labeling was detected for control cells labeled in the absence of GALT-1 or UDP-Gal-6-N₃ (Figure 3.11A). Additionally, no nuclear labeling was observed, confirming the specificity of the chemoenzymatic strategy, as core fucose is only found on the cell surface (Figure 3.11A).

Next, we determined whether the approach could be used to track core fucose on live cells (Figure 3.11B). MDA-MB-231 cells were chemoenzymatically labeled, reacted with the strain-promoted alkyne-azide cycloaddition (SPAAC) reagent, ADIBO-biotin (**6**), and treated with a streptavidin-conjugated Alexa Fluor 488 dye. Flow cytometry analysis revealed strong fluorescence intensity of cells treated with GALT-1 and minimal background signal observed in both the absence of GALT-1 and untreated cells (Figure 3.11B). These results highlight the flexibility of the chemoenzymatic approach, enabling the tracking of core fucose on both fixed and live cells.

With increasing reports suggesting that increased core fucosylation of serum glycoproteins is correlated with HCC pathogenesis,¹¹⁻¹⁴ I sought to explore the diagnostic

potential for this method. To first determine if varying levels of core fucose could be detected from similar protein samples, HepG2 glycoproteins were subjected to PNGaseF treatment, and serially diluted into mock PNGaseF control samples, generating protein samples with decreasing core fucose levels with constant protein concentration levels. These samples were then chemoenzymatically labeled and subjected to western blot analysis (Figure 3.12).

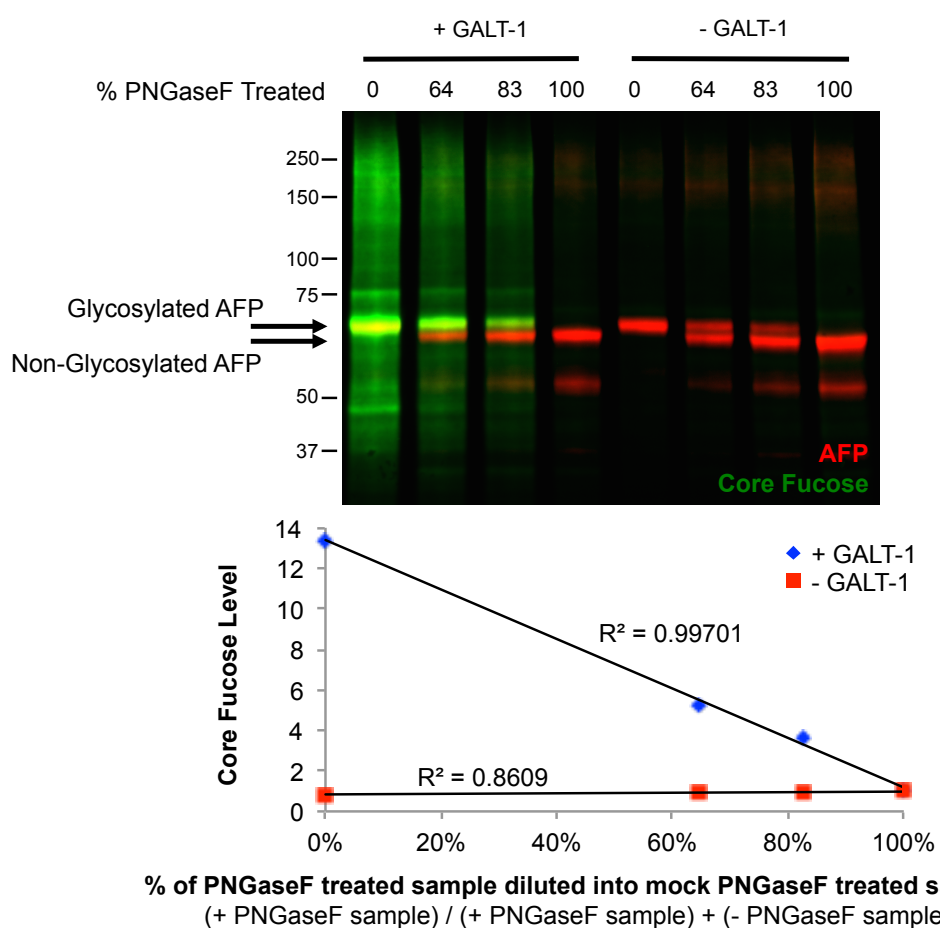


Figure 3.12 GALT-1 efficiently labels samples of comparable protein concentration with differing levels of core fucosylation. HepG2 proteins were treated with or without PNGaseF followed by serial dilution of the PNGaseF treated samples into the mock PNGaseF treated samples. These samples were then treated with or without GALT-1 and subjected to western blot analysis with streptavidin-conjugated Alexa Fluor 680 (green) and AFP (red). Intensity was quantified and plotted. The trendline of the GALT-1 treated samples has R^2 values consistent with a linear response to levels of core fucose.

The signal witness from these samples exhibited a linear response in intensity when comparing the expected decreased levels of GALT-1 dependent signal and percentage of PNGaseF diluted sample (Figure 3.12). This suggests that the approach could be used to confidently compare core fucose levels across different protein samples.

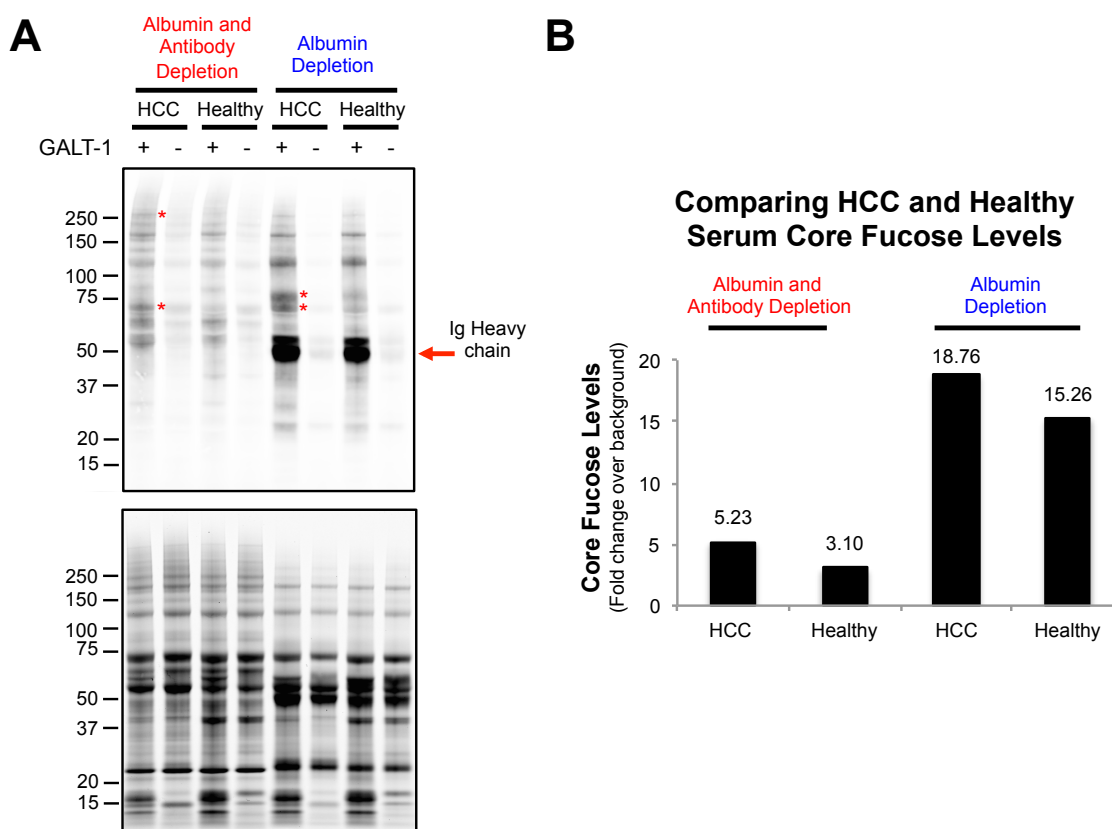


Figure 3.13 Chemoenzymatic labeling of serum from a healthy donor and an HCC patient. (A) Serum samples were depleted of either (i.) serum albumin and antibodies (red) or (ii.) only serum albumin (blue), chemoenzymatically labeled, and subjected to SDS-PAGE for western blot analysis with streptavidin-conjugated Alexa Fluor 680 (top) and coomassie stain for loading control (bottom). Red asterisks denote proteins with potentially increased core fucose levels. Red arrow denotes the suspected immunoglobulin heavy chain based on apparent molecular weight. (B) Core fucose signal was quantified and normalized over background from the minus GALT-1 samples.

Next, serum from an HCC patient and a healthy individual were depleted of (i) serum albumin and antibodies or (ii) only serum albumin. Depleted serum samples were then chemoenzymatically labeled and subjected to western blot analysis (Figure 3.13). Robust labeling of core fucosylated serum glycoproteins was witnessed in both depletion

cases. As expected in the serum albumin depleted samples, due to the high levels of core fucosylation of antibodies, strong signal was witnessed at ~50kda, where the immunoglobulin heavy chain is expected to appear. Additionally, stronger core fucose signal was witnessed on specific protein bands (~65 and 250 kda, red asterisk), and more generally overall, from HCC samples when compared to healthy controls (Figure 3.13). These findings agree with the reported increased levels of core fucose on serum glycoproteins from HCC patients when compared to healthy control.¹¹⁻¹⁴ While I have only interrogated these two serum samples, I have demonstrated a proof-of-principle that serum glycoproteins can be detected with the approach. The efficient labeling of core fucosylated serum glycoproteins opens the door for researchers to exploit our approach for the identification of new diagnostic cancer biomarkers.

In order to identify new cancer biomarkers, a proteomic workflow was developed that leverages a cleavable tag that installs a mass tag onto the site of glycosylation, enabling simultaneous protein identification and glycosylation site mapping (Figure 3.14A). Since core fucose is only found on *N*-glycans, PNGaseF can be used to selectively cleave the core fucosylated proteins from the affinity resin. This PNGaseF reaction also converts the asparagine, *N*-glycans are exclusively found on asparagine residues in mammals, to an aspartate. This reaction installs a one Dalton mass tag onto the site of glycosylation. If the reaction is performed in ¹⁸O labeled H₂O, a shift of three Daltons is witnessed. To test this approach, protein samples were subjected to chemoenzymatic labeling with biotin-alkyne **11** and enriched with streptavidin-conjugated agarose resin. Following extensive washing, the resin was incubated with PNGaseF and the eluted proteins were subjected to SDS-PAGE followed by silver

staining (Figure 3.14B). Many proteins were eluted during this procedure with no visible proteins eluted in the control sample (Figure 3.14B). Here, I have developed and demonstrated a simple and efficient proteomic workflow with commercially available reagents that can be used to identify new cancer biomarkers.

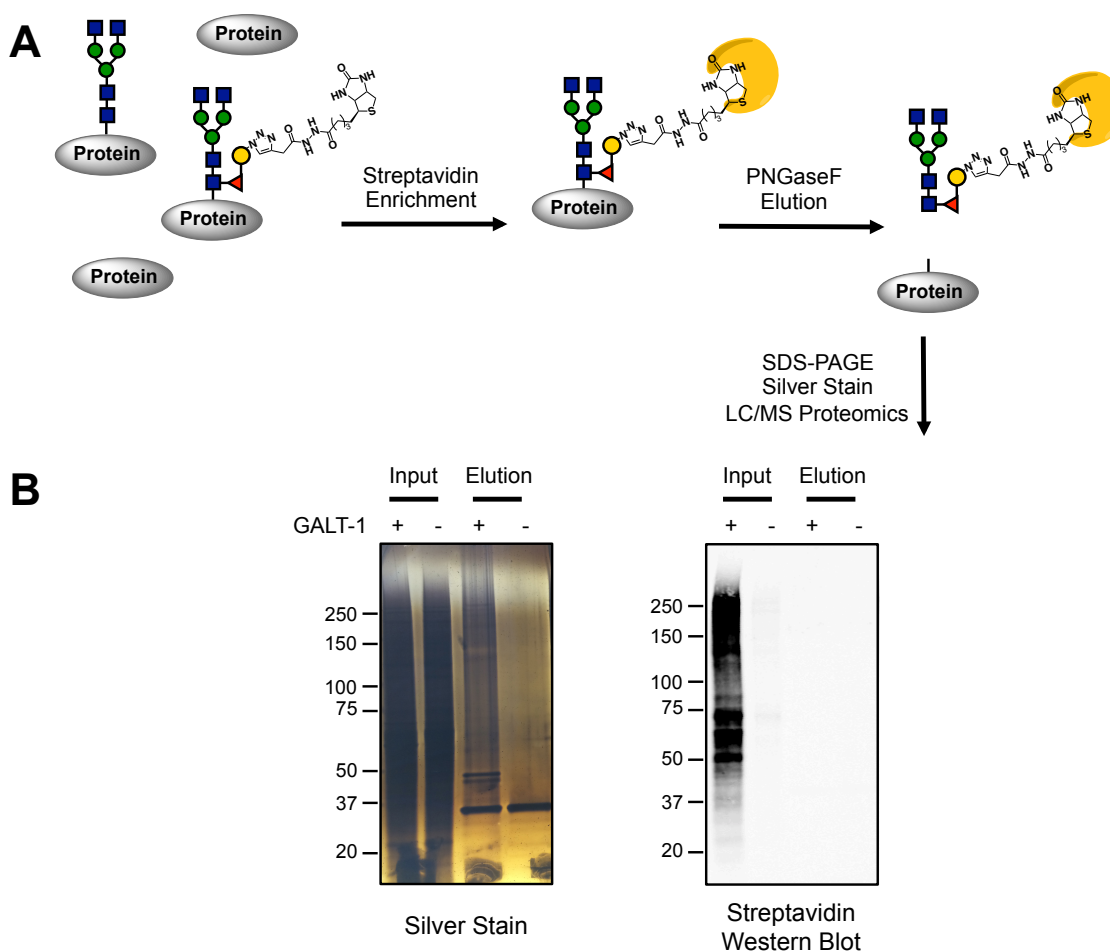


Figure 3.14 The chemoenzymatic approach can easily be incorporated into a proteomic workflow with the *N*-glycan acting as a cleavable linker. (A) Following chemoenzymatic labeling with biotin alkyne (**11**), biotinylated core fucose glycoproteins are enriched with streptavidin resin. The glycoproteins are then cleaved using PNGaseF, which normally cleaves *N*-glycans from the glycoprotein. Eluted proteins are then resolved by SDS-PAGE, silver stained, and bands can be excised for proteomic identification. (B) Silver stain (left) and western blot (streptavidin blot; right) demonstrate the feasibility of this workflow.

To integrate this chemoenzymatic approach into a common diagnostic platform, an ELISA was developed for the detection of core fucosylated AFP, a known biomarker for HCC.³¹⁻³³ Following chemoenzymatic labeling, capture of total AFP in an ELISA

well with subsequent detection of biotinylated core fucose, using a streptavidin-conjugated HRP, would enable quantification of core fucosylated AFP (Figure 3.16A). Alternatively, biotinylated AFP could be captured in a streptavidin coated ELISA well and AFP could be detected with an anti-AFP-conjugated HRP antibody (Figure 3.17A). While other methods used for detection of core fucosylated AFP rely on lectins and/or expensive machinery, this approach could be used as a more specific and cheaper alternative.^{34,35}

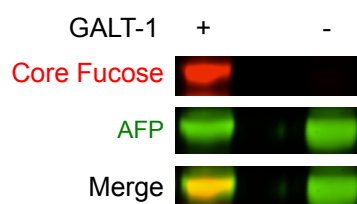


Figure 3.15 The chemoenzymatic approach can label the Hepatocellular Carcinoma (HCC) biomarker, core fucosylated α -fetoprotein (AFP). AFP was purified chemoenzymatically labeled followed by western blot detection using streptavidin-conjugated Alexa Fluor 680 (core fucose, red) and anti-AFP (green).

To test this system, AFP was first purified from the media of HepG2 cells, using IMAC resin charged with Cu(II), and then enzymatically labeled to confirm that AFP from HepG2 media was indeed core fucosylated (Figure 3.15). Next, proteins secreted from HepG2 cells were labeled, serially diluted, and added to the ELISA plate. Each sample was added to additional wells for the quantification of total AFP using an anti-AFP-conjugated HRP antibody and all samples were run in duplicate. Core fucosylated AFP could be robustly detected over a large dynamic range, from 1 ng/mL to 500 ng/mL, exhibiting sufficient sensitivity (Figure 3.16B). These experiments were repeated using the streptavidin coated ELISA plates and core fucosylated AFP was detected with the anti-AFP-conjugated HRP antibody (Figure 3.17B). Using the streptavidin-coated plates, core fucosylated AFP could be robustly detected in a linear dynamic range from 1 ng/mL

to 800 ng/mL, also exhibiting sufficient sensitivity. Together, these experiments highlight the ability of this approach to detect core fucosylated AFP in a complex protein sample. These results also constitute the first demonstration of a chemoenzymatic approach to be integrated into an ELISA format, enabling researchers to rapidly interrogate core fucose levels of specific proteins on a large sample population for biomarker verification tests.

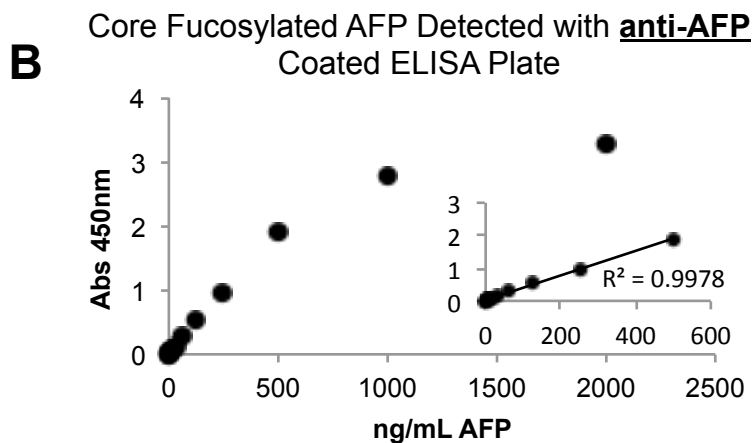
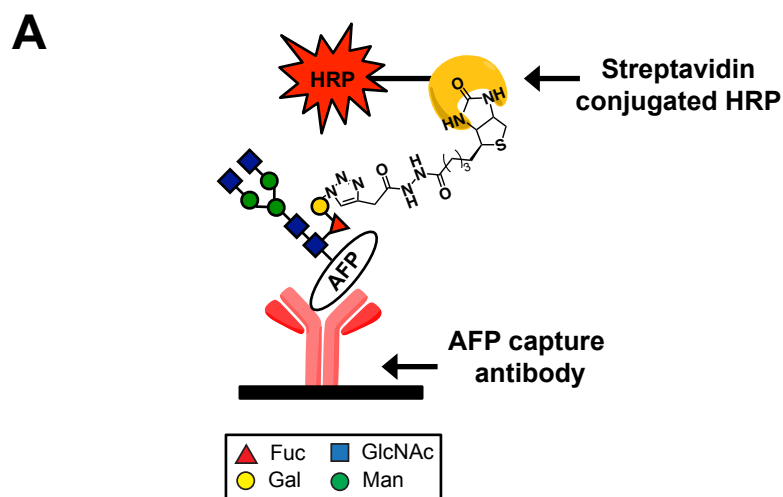


Figure 3.16 (A) Following chemoenzymatic labeling, AFP is captured in an ELISA well and biotinylated core fucose is detected with a streptavidin-conjugated horse radish peroxidase (HRP). (B) Proteins secreted from HepG2 cells were chemoenzymatically labeled, serially diluted, and applied to the ELISA wells for detection of core fucosylated AFP. Total AFP was also quantified and the total AFP levels were plotted against core fucose signal (Abs 450nm). The core fucosylated AFP ELISA demonstrated a linear detection range from 1-500 ng/mL of total AFP (insert) and was able to detect core fucose levels on samples containing AFP concentrations as low as 1 ng/mL.

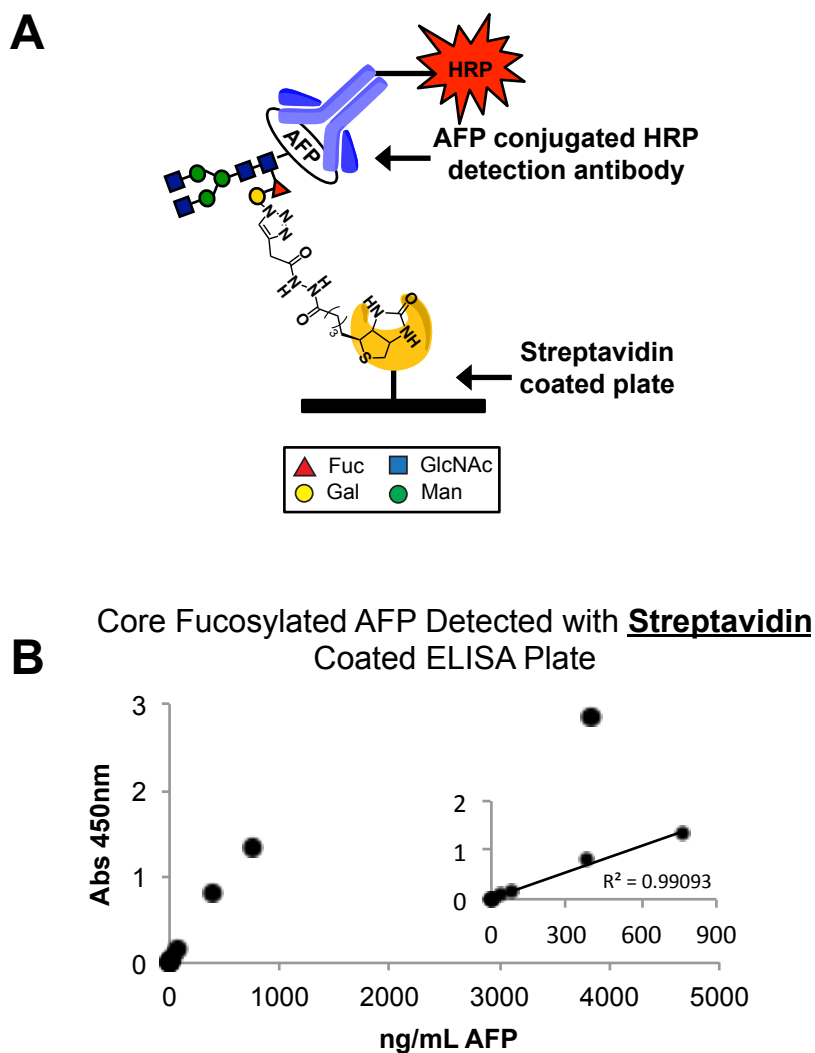


Figure 3.17 Integration of chemoenzymatic labeling approach into an ELISA format for quantification of core fucosylated AFP. (A) Following chemoenzymatic labeling, biotin labeled material is captured in an ELISA well and biotinylated core fucosylated AFP is detected with an anti-AFP-conjugated horse radish peroxidase (HRP). (B) Proteins secreted from HepG2 cells were chemoenzymatically labeled, serially diluted, and applied to the ELISA wells for detection of core fucosylated AFP. Total AFP was also quantified using an AFP ELISA and the total AFP levels were plotted against core fucose signal (Abs 450nm). The core fucosylated AFP ELISA demonstrated a linear detection range from 1-800 ng/mL of total AFP (insert) and was able to detect core fucose levels on samples containing AFP concentrations as low as 1 ng/mL.

CONCLUSION

In conclusion, I have developed a new chemoenzymatic labeling approach for the detection of core fucosylated glycans with superior specificity over existing methods. This strategy can detect a variety of core fucosylated *N*-glycans from complex cell

lysates, human serum, and on both live and fixed cells. Additionally, this method can be integrated into an ELISA platform for tracking core fucose changes on specific proteins. I anticipate that this tool will be used to advance our understanding of the physiological functions of core fucose but also to identify new disease biomarkers. Future studies will apply this powerful strategy in systematic studies of core fucosylated proteins and will possibly identify a new set of effective glycoprotein biomarkers for the diagnosis of a variety of human diseases.

EXPERIMENTAL METHODS

General Reagents and Methods. Unless otherwise noted, reagents were purchased from the commercial suppliers Fisher (Fairlawn, NJ) or Sigma-Aldrich (St. Louis, MO). All the primers were purchased from Integrated DNA Technologies (IDT). Bovine thyroglobulin was purchased from Sigma-Aldrich. Protease inhibitor cocktails (PIC) were purchased from Roche Applied Sciences (Indianapolis, IN). HisPure Cobalt Resin and agarose-conjugated protein A/G was from Pierce (Rockford, IL) and Immobilon-FL PDVF membrane was from Millipore (Billerica, MA). Dulbecco's modified Eagle media (DMEM), fetal bovine serum (FBS), and penicillin/streptomycin were from Gibco (Carlsbad, CA). The mouse anti-AFP for western blot is from Abcam. Rabbit Anti-EGFR is from Santa Cruz Biotechnology. Rabbit anti-E cadherin is from Cell signaling technology. Click-It™ Biotin Glycoprotein Detection Kit, anti-TAMRA antibody, 4-12% NuPAGE® Bis-Tris Mini gels, streptavidin-IR680, streptavidin-Alexa488, anti-mouse IR680 and goat anti-rabbit IR680, goat anti-mouse Alexa488 conjugates, normal goat serum were from Invitrogen (Carlsbad, CA). The click chemistry ligand, Tris(3-

hydroxypropyltriazolylmethyl)amine (THTPA), was purchased from Sigma-Aldrich (St. Louis, MO). TAMRA-alkyne and Biotin-alkyne were purchased from clickchemistrytools.com (Scottsdale, AZ). (Peptide N-glycosidase F (PNGaseF) was purchased from New England Biolabs (Beverly, MA). Biotinylated Aleuria Aurantia Lectin (AAL) and Biotinylated Lens Culinaris Agglutinin Lectin (LCA) were purchased from Vector laboratories (Burlingame, CA). Aspergillus Oryzae Lectin (AOL) was purchased from TCI America (Boston, MA). The secondary goat anti-rabbit and goat anti-mouse antibody conjugated to IRDye800 was from Rockland Immunochemicals (Gilbertsville, PA). Western blots were visualized and quantified using an Odyssey infrared imaging system (LI-COR Biosciences).

Cloning, Expression and Purification of GALT-1. The *Galt-1* cDNA was amplified from sf9 cell harboring the bacmid pFastBac1-GALT-1, generously provided by Markus Aebi,²⁴ by PCR using Expand High fidelity PCR system (Roche). After unsuccessful attempts at bacterial expression of active N- or C- terminal His tagged GALT-1, I designed a construct consisting of an N-terminal His tag, followed by a SUMO (small ubiquitin-related modifier) domain and GALT-1 for increased solubilization of recombinant GALT-1. The pet28a vector containing a N-terminal His tagged SUMO domain directly upstream of the multiple cloning site was provided by the Andre Holtz lab (California Institute of Technology, Pasadena CA). The construct of N-His-SUMO-GALT-1 was generated by PCR amplification of cDNA using the forward and reverse primers overlapping the BamH1 and Not1 restriction sites, respectively (forward: GAGGCTCACAGAGAACAGATTGGTGGCCCGCGTATTACCGCTTCC; reverse:

GTGGTGCTCGAGTGCGGCCCTTACAGGTCCAGCAGGCCGA). The resulting PCR fragments were cloned into the pet28a-N-term-His-SUMO vector, cut with BamHI and NotI, by Gibson Assembly. The resulting plasmids were transformed into DH5 α (subcloning efficiency, Invitrogen) and grown at 37 °C overnight on Agar plates supplemented with kanamycin (50 μ g/mL). Resulting colonies were used to inoculate 5 mL 2xYT media and grown overnight at 37 °C and 225 rpm. Plasmids were extracted by miniprep kit (Qiagen) and the resulting clones, with the correct sequence and frame, were transformed into *E. coli* BL21 (DE3) cells. The colonies were inoculated into 5 mL 2xYT media supplemented with kanamycin (50 μ g/mL) and grew for 18 hours at 37 °C. The resulting culture is supplemented with glycerol (15% final concentration) and stored in -80 °C for long storage.

The proteins were expressed and purified as described in the following. *E. coli* BL21 (DE3) harboring the pet28a-N-term-His-SUMO plasmid were grown in 2xTY medium (1L) at 37 °C and 250 rpm. Isopropyl-1-thio- β -D-galactospyranoside (IPTG, 0.5 mM final concentration; Sigma) was added when the cells reached an OD600 of 0.6-0.8, and the cells were incubated for an additional 15 h at 18 °C. The pelleted cells were lysed in 2% Triton X-100 (vol%) in TBS buffer (50 mM Tris-HCl pH 8, 0.5 M NaCl) supplemented with EDTA-free Complete™ protease inhibitors (Roche). Lysozyme (1 mg per liter culture) and DNase (50 μ g per liter culture) were added to the lysis buffer and the cells were homogenized under sonication. After centrifugation at 17,000 x g for 20 minutes, the clarified lysate was added to prewashed Cobalt affinity beads (2 mL for 1 L culture, Pierce) and incubated at 4 °C for 1 h, end-over-end, in a batch format followed by washing with 20 volumes of wash buffer (50 mM Tris-HCl pH 8, 0.5 M NaCl, and 10

mM imidazole). Resin was transferred to a column, washed with wash buffer until no protein was removed from the resin, checked by monitoring absorbance at 280 nm, and eluted with a gradient of increasing elution buffer (50 mM Tris-HCl pH 8, 0.5 M NaCl, and 150 mM imidazole) at 1 mL/minute. After SDS-PAGE and WB analysis (anti-His antibody, GE Lifesciences), the purified protein was concentrated with 30,000 Da molecular weight cut-off (MWCO) spin filters (Millipore) and exchanged to the storage buffer (50mM Tris-HCl pH 8, 0.5 M NaCl, 5% glycerol), flash frozen, and stored at -80 °C for longer term storage, up to 6 months, 4 °C up to 1 month.

Synthesis of UDP-6-deoxy-6-azido-galactose (UDP-Gal-6-N₃; **13).** The synthesis of UDP-Gal-6-N₃ was performed following literature report without modifications.²⁵ The purification of the final product was done on a Biogel P2 column using water as the mobile phase instead of HPLC purification. ESI-MS and ¹H, ³¹P NMR confirmed the identity of the final product.

Chemoenzymatic Labeling of Core Fucosylated Glycopeptide. The core fucosylated glycopeptide was generously provided by Iain Wilson (Universität für Bodenkultur, Vienna, Austria).²⁴ The reaction cocktail contained GALT-1 (0.4 mg/mL), 500 μM UDP-Gal-6-N₃ (**13**) or UDP-Gal, 50 mM Tris-HCl pH 7.5, 5 mM MnCl₂, 0.1% Triton X-100. After 2 hours incubation at RT, 2 μL solution from each reaction was transferred into 5 μL α-Cyano-4-hydroxycinnamic acid (CHCA, 4 mg/mL) dissolved in 50% acetonitrile in water supplemented with 0.1% trifluoroacetic acid (TFA). 4 μL resulting

solution from each sample was transferred onto MALDI-TOF MS source and dried. The acquisition was done on reflector (2500) and positive mode.

Kinetic Analysis of GALT-1 with UDP-Gal, UDP-Gal-6-N₃ and N6000. Kinetic parameters were determined using the turn-on fluorescent sensor, 17-2Zn(II) (Chapter 5, Figure 5.1A), which detects UDP but not UDP-Gal.³⁶ Reactions were set up in duplicate as follows: 50 mM HEPES pH 7.4, 10 mM NaCl, 0.1 mM MgCl₂, 0.2 mM MnCl₂, 0.3 mM ZnCl₂, 2.5 μM 17-2Zn(II) Sensor, 50 μM N6000, 1-500 μM UDP-Sugar, 0.2 mg/mL GALT-1. For determining GALT-1 kinetic parameters towards N6000, the reactions were set up identical to above except N6000 was varied from 25-500 μM and UDP-Gal was fixed to 50 μM. Background was determined with the same reaction conditions without N6000. Fluorescence was detected with excitation and emission wavelengths of 500 nm and 534 nm respectively, with a 530 nm cutoff, using the Flexstation 3 (Molecular Devices). Initial rates were calculated and plotted as a function of UDP-Sugar concentration. Km's were determined by fitting initial rates to a Michaelis-Menten model or Lineweaver-Burk plot using Kaleidagraph 4.0.

GALT-1 Acceptor Substrate Specificity Characterization with Small Molecule N-glycans and MALDI-TOF Analysis. Purified *N*-glycans, N6000, N6001, N6002, N000, and N224, provided by Peng George Wang (Georgia State University, Georgia),³⁷ were dissolved into 5 mM HEPES pH 7.4, 1 mM MnCl₂, 500 μM UDP-Gal-6-N₃ (**13**), 0.2 mg/mL GALT-1 at room temperature. 2 μL aliquots were taken at various time points and mixed 1:1 into 60 mg/mL Super DHB (Sigma-Aldrich) matrix in MeOH. 0.1 μL was

plated onto MALDI-TOF MS source, dried, and analyzed using the Voyager D-Pro MS using 1500 Reflector mode. 10 spectra were accumulated per spot, with two spots analyzed per sample. Spectra were baseline corrected and noise filtered by smoothing. The area of intensities was used to quantify the approximate reaction completion percentage.

Chemoenzymatic Labeling of Bovine Thyroglobulin. The bovine thyroglobulin was dissolved in water as 10 mg/mL stock solution. For a typical galactosylation reaction, the cocktail contained GALT-1 (0.2 mg/mL), 500 μ M UDP-Gal-6-N₃ (**13**), 50 mM HEPES pH 7.5, 5mM MnCl₂, 1% Triton X-100, 1x PIC at room temperature. Negative controls were performed under identical conditions, except GALT-1 or UDP-Gal-6-N₃ were left out of the reactions. Aliquots of the reaction were quenched over 6 hours by adding 5 volumes of ice cold acetone and storing at -20 °C overnight. Pellets were collected by centrifugation, resuspended in 1% SDS buffer in Tris-HCl 50 mM, pH 8.0, and brought to 0.05 mM TAMRA-alkyne, 0.1 mM THPTA ligand, 0.2 mM CuSO₄, and 2 mM sodium ascorbate for 1 hour at room temperature. Samples were then acetone precipitated for 2 hours at -20 °C, and then resuspended into 2x protein loading buffer, minus a reducing reagent, to resolve discrete bands by western blot detection. Bovine thyroglobulin has many disulfide bonds connecting separate polypeptides, many of which are glycosylated.

Western Blot Detection of Core Fucosylated Glycoproteins. Labeled protein samples were resolved on 1.5 mm, 10-well NuPAGE 4-12% Bis-Tris gels and transferred to PDVF. The membrane was blocked with 5% nonfat milk in 50 mM Tris-HCl pH 7.4, 150

mM NaCl containing 0.1% Tween-20 (TBST) for 1 h at RT. For TAMRA labeled proteins, the membrane was incubated with rabbit anti-TAMRA antibody in blocking buffer (1:1000) for 1 h at RT or 4 °C overnight, followed by incubation in anti-rabbit antibody conjugated to an IR680 dye (1:10,000). A fraction of the samples were analyzed separately by SDS-PAGE and coomassie staining (Bio-Rad) for total protein normalization.

Chemoenzymatic Labeling of Cell Lysates and Serum Samples. All the cell lines were obtained from ATCC. HepG2, MCF-7, and MDA-MB-231 cells grown in DMEM medium supplemented with 10% fetal bovine serum (FBS), 100 units/mL penicillin, and 0.1 mg/mL streptomycin (Gibco). Cells were incubated in a 5% CO₂ humidified chamber at 37 °C. One 150 mm culture dish of MDA-MB-231 breast cancer cell line, MCF-7 breast cancer cell line, HepG2 liver cancer cell line were lysed directly in dish by adding 2 mL of hot 1% SDS in Tris-HCl 50 mM (pH 8.0). HepG2 cells were grown to 80% confluency and washed in serum and phenol red free RPMI 1640 media twice then grown for three days in the same media. The secreted proteins were collected from this media by concentration in 30,000 MWCO spin filters and stored at -80 °C. The serum of a Hepatocellular Carcinoma (HCC) patient and a healthy donor were obtained from City of Hope (Duarte, CA). Serum was depleted using either Pierce™ Top 2 Abundant Protein Depletion Spin Columns (ThermoFisher Scientific) for removal of serum albumin and antibodies or Pierce™ Albumin Depletion Kit (ThermoFisher Scientific) to remove albumin only. Following cell lysis or depletion, protein samples were precipitated using methanol/chloroform/water. Briefly, protein was diluted to 200 µL and precipitated by

sequential mixing with 600 μL of MeOH, 150 μL of CHCl_3 and 450 μL H_2O , after which the mixture was centrifuged at 15,000 rpm for 15 minutes. The supernatant was removed, 450 μL of MeOH was added to the protein pellet and CHCl_3 that remained, and the sample was centrifuged at 15,000 x g for 10 minutes. After removal of the supernatant, the protein pellet was allowed to dry, ~10-15 minutes until translucent. The protein pellet was then resuspended into 1% SDS, 50mM Tris HCl pH 7.5 and BCA assayed for protein concentration.

The protein pellet was re-dissolved at 5 mg/mL by boiling in 1% SDS with 50 mM HEPES pH 7.5 for 5 minutes. The sample was then brought to 1 mg/mL in 5 mM MnCl_2 , 1x protease inhibitor complex, 0.5 mM UDP-Gal-6- N_3 (**13**), 0.2 mg/mL GALT-1 and incubated at RT for 4 h. The labeled proteins were precipitated as above and resuspended in 50 mM Tris-HCl, pH 8 containing 1% SDS at 1 mg/mL. The resuspended proteins were subsequently reacted 0.1 mM biotin-alkyne (**11**), 3 mM THTPA (ligand), 1 mM CuSO_4 , and 2 mM sodium ascorbate for 1 hour at room temperature. For TAMRA-alkyne labeling, conditions were followed as above. Negative controls were performed under identical conditions except that GALT-1, UDP-Gal-6- N_3 (**13**), or TAMRA-/biotin-alkyne were omitted from the labeling reaction. After the labeling reactions, protein was precipitated using chloroform/methanol/water as described above and re-dissolved in 1% SDS. This precipitation and resolubilization was then repeated once more to ensure removal of non-specific interactions. TAMRA-labeled proteins were resolved by SDS-PAGE and visualized by western blot analysis as above. Biotin labeled proteins were resolved identically except that the blocking buffer used was 3% BSA (ThermoFisher

Scientific) in TBST and membranes were probed with streptavidin-conjugated IR680 (Invitrogen) at 0.5 µg/mL for 30 minutes at RT in blocking buffer.

Immunoprecipitation and Identification of TAMRA-Labeled Core Fucosylated Glycoproteins. The TAMRA labeled protein pellets of MDA-MB-231, MCF-7 and HepG2 cells from above were allowed to dry briefly. The pellets were re-dissolved in boiling 1% SDS plus Complete™ protease inhibitors at a concentration of 4 mg/mL. The SDS was then quenched with 1 volume of NETFD buffer (100 mM NaCl, 50 mM Tris-HCl pH 7.4, 5 mM EDTA, 6% NP-40) plus protease inhibitors, and the lysate was pre-cleared against washed protein A/G sepharose beads (1 mL/ 2 mg of protein) at 4 °C for 1 hour. After centrifugation, the supernatant was collected and incubated with an anti-TAMRA antibody (100 µg/ 2 mg of protein) at 4 °C for 4 hours. The samples were then added to pre-washed protein A/G sepharose beads (1 mL/ 2 mg of protein) at 4 °C for 1.5 hours. Following centrifugation, the beads were washed once with 4 column volumes of NETFD buffer and three times with 4 column volumes of NETF buffer (100 mM NaCl, 50 mM Tris-HCl pH 7.4, 5 mM EDTA). After washing, the beads were boiled in elution buffer (200 mM Tris pH 6.8, 400 mM DTT, 8% SDS, 50 µL buffer/ 100 µL beads). The supernatant was collected after centrifugation and precipitated by adding 5 volumes of ice-cold acetone and incubating at -20 °C overnight.

The protein pellet was then dissolved in 2x SDS protein loading buffer and was resolved by western blotting as above except, primary antibodies in TBST were added overnight at 4 °C at the following concentrations: mouse anti-AFP monoclonal antibody (Cell Signaling Technologies) at 1 µg/mL, rabbit anti-E cadherin (Cell

Signaling Technologies) at 2 $\mu\text{g}/\text{mL}$, rabbit anti-EGF receptor (Santa Cruz Biotechnology) at 0.2 $\mu\text{g}/\text{mL}$. Membranes were washed with TBST, and incubated with the appropriate Alexa Fluor 680-conjugated secondary antibody (Invitrogen, 1:10,000 dilution in blocking buffer) for detection.

Comparing GALT-1 Donor Substrate Preference by Completion: UDP-Galactose vs. UDP-Gal-6-N₃. Proteins secreted from HepG2 cells were chemoenzymatically labeled as above except that each reaction had increasing concentrations of UDP-Gal (0 – 500 μM). A control sample did not include any UDP-Gal-6-N₃ (**13**), but 500 μM UDP-Gal. The samples were treated with TAMRA-alkyne (**10**) as above and subjected to western blot analysis as above.

Determination of GALT-1 Specificity using *Fut8* knock-out and wild type Mouse Brain Lysates with PNGaseF Treatment. The brains of *Fut8*^{-/-} and *Fut8*^{+/+} mice, generously provided by Jianguo Gu (Tohoku Pharmaceutical University, Japan), were lysed in 1% SDS (5 volumes/weight) by sonication and boiled until the mixture was homogeneous. Protein was precipitated using methanol/chloroform/water as above. Samples were then subjected to PNGaseF treatment as recommended (NEB). Briefly, samples were resuspended into 1x Glycoprotein Denaturing Buffer at 2 mg/mL followed by boiling for 10 minutes. After allowing samples to cool to room temperature, samples were brought to 1 mg/ml, 1x Glycobuffer 2 and 1% NP-40. Samples were then split to prepare a PNGaseF treated and a mock treated sample. PNGaseF was added at 12.5 U/ μg protein and samples were incubated at 37 °C for 1 hour followed by precipitation with

methanol/chloroform/water as above. Samples were then subjected to chemoenzymatic labeling as above, using biotin-alkyne **11**, and visualized using SDS-PAGE and western blotting as above. To determine background labeling, *Fut8*^{-/-} and *Fut8*^{+/+} brain lysates from above were subjected to only the CuAAC reaction with biotin-alkyne **11** and subjected to SDS-PAGE and western blot analysis. All samples were also subjected to western blot analysis for L1CAM, an internal control for the PNGaseF reaction containing 21 putative N-glycan sites.^{38,39} Western blot analysis was carried out as noted above except using anti-L1CAM antibody (ab24345) diluted 1:1000 into blocking buffer and incubated overnight at 4 °C.

Lectin Blot Analysis of *Fut8* knock-out and wild type Mouse Brain Lysates with PNGaseF Treatment. PNGaseF brain lysate samples, generated above, were subjected to SDS-PAGE and lectin blot analysis prior to chemoenzymatic labeling. Protein samples were resolved on 1.5 mm, 10-well NuPAGE 4-12% Bis-Tris gels and transferred to PDVF. The membrane was blocked with 3% BSA in TBST for 1 hour at room temperature. Membranes were subsequently incubated with the biotinylated lectins AAL (2 µg/mL), LCA (5 µg/mL), AOL (5 µg/mL), and a mock incubation (a biotin negative control) in blocking buffer. After overnight incubated at 4 °C, membranes were incubated with a streptavidin-conjugated IR680 dye (0.5 µg/mL), washed, and imaged.

Biotinylation of AOL Lectin. 1 mL AOL (5mg/mL in PBS from TCI America) was added with 15 µL EZ-Link™ NHS-PEG4-Biotin (ThermoFisher Scientific) in DMF and incubated for 2 hours at RT. The pH of the solution was adjusted to pH 5 by adding 1 M

HCl, and loaded to two 0.5 mL filter tubes (MWCO 10,000) at 4 °C and concentrated to around 100 µL. The solution was exchanged to 1X PBS using the same filter tubes. LC-MS analysis of the flow through for each run was used to confirm that biotin-PEG4-NHS or its byproduct (biotin-PEG4-COOH) no longer exists in the lectin solution. The biotinylated AOL lectin was stored in a PBS solution 4 °C.

Detection of Core Fucosylated Glycans in Fixed Cells by Fluorescence Microscopy.

MDA-MB-231 and HepG2 cells were plated onto 15 mm coverslips (Carolina Biologics) at a density of 100 cells/mm². After 12 hours, the media was removed, and the cells were rinsed with PBS, fixed in 3.7% formaldehyde in PBS, pH 7.2 for 8 minutes at room temperature, washed twice with PBS, permeabilized in 0.3% Triton X-100 in PBS for 10 minutes at room temperature, and washed twice with the enzymatic labeling buffer (50 mM Tris-HCl, pH 7.5, 0.1% Triton X-100, 5 mM MnCl₂, 150 mM NaCl). Reaction mixtures and negative controls (without GALT-1 or without UDP-Gal-6-N₃) were prepared by adding GALT-1 (0.2 mg/mL) and UDP-Gal-6-N₃ (**13**; 0.5 mM) to the enzymatic-labeling buffer. The reaction cocktail was added to the coverslip (100 µL/coverslip) and incubated for 2 hours at room temperature in a humidified chamber. After chemoenzymatic labeling, the cells were washed twice with the chemoenzymatic-labeling buffer. Enzymatic addition of Gal-6-N₃ onto core fucose was detected by treating the cells with Click-It™ Biotin Glycoprotein Detection Kit, followed by incubating the slides with 0.1 µg/mL streptavidin-Alexa Fluor488 (Invitrogen) for 30 minutes at room temperature. The coverslips were washed with PBS, mounted onto glass slides using Vectashield mounting medium with DAPI stain (4 µL; Vector Labs), and sealed with

clear nail polish. Cells were imaged using a Nikon Eclipse TE2000-S inverted microscope, and images were captured with a Zeiss LSM 510 Meta NLO confocal microscope using 40x Plain Fluor objective and were processed in Image J.

Detection of Cell-Surface Core Fucosylated Glycans on Live Cancer Cells by Flow

Cytometry. MDA-MB-231 cells were seeded at 10^7 cells per 150 mm plate in 25 mL of DMEM with 10% FBS and 1% penicillin/streptomycin. On the day of analysis, cells were lifted off the plate with 2 mM EDTA and 1 mM EGTA, and washed with 1% FBS, 10 mM HEPES in 1X HBSS. One million cells were chemoenzymatically labeled with UDP-Gal-6-N₃ (**13**; 500 μ M) and GALT-1 (0.2 μ g/ μ L) in 1% BSA, 10 mM HEPES in HBSS (100 μ L) for 1 hour at room temperature. Cells were spun twice through 100% FBS (1 mL) to remove excess reagent (500 x g, 5 minutes) and resuspended in 1% FBS, 10 mM HEPES in CMF HBSS (100 μ L) containing ADIBO-biotin, **6**, (20 μ M) and incubated for 1 hour at room temperature. Negative controls were performed with identical conditions, except for that GALT-1 or all reagents (untreated) were omitted. Cells were again spun twice through 100% FBS (1 mL), and washed with 3% BSA in PBS (1 mL). Cells were then resuspended in 3% BSA in PBS (100 μ L) containing streptavidin-Alexa Fluor 488 (1 μ g/mL) and incubated for 30 minutes at 4 °C. Cells were subsequently spun twice through 100% FBS (1 mL) and resuspended in BSA (1 mg/mL), 20 mM MgCl₂, 0.5 μ g/mL DNase, 10 mM HEPES in HBSS (600 μ L) for flow cytometry analysis. Immediately before analysis, 7-amino-actinomycin D (7-AAD, 5 μ L; eBioscience) was added to measure cell viability. Cells were analyzed for FITC intensity on a Beckman Dickenson FACSCalibur flow cytometer equipped with a 488-nm argon

laser. For each experiment, 10,000 live cells were analyzed, and data analysis was performed on FlowJo (Tristar Inc.).

PNGaseF Treatment of HepG2 Secreted Proteins for Chemoenzymatic Detection of Protein Samples with Different Core Fucose Levels. Proteins secreted into the culture media from HepG2 cells were treated with PNGaseF as above, including a PNGaseF mock control. Mock control samples were serially diluted into PNGaseF treated samples, generating multiple samples with differing levels of core fucosylated glycoproteins. Samples were then chemoenzymatically labeled as above and imaged by western blotting for biotin as above. The exact percentage of PNGaseF treated sample was calculated from the signal of glycosylated AFP band (from mock PNGaseF treated sample, top band; Figure 3.12) and non-glycosylated AFP band (from PNGaseF treated sample, bottom band; Figure 3.12). Quantification of both AFP intensities and biotin (core fucose) intensities were calculated using Image Studio software (LI-COR).

Proteomic Work Flow with PNGaseF Release for Cleavable Linker. Chemoenzymatically labeled protein, biotinylated, was incubated with magnetic streptavidin resin, (1mL per 100 μ g protein; Peirce) for 1 hour at room temperature. Resin was washed 2x with PBS, 2x with PBS and 1% SDS, and then 2x with PBS again. Each wash was done rotating end-over-end for 5 minutes. Resin was resuspended into 500 μ L of PBS with 5000U PNGaseF and rotated end-over-end for 5 hours at room temperature. Supernatant was collected and acetone precipitated overnight at -20 $^{\circ}$ C. Sample was resuspended into 2x SDS protein loading buffer, boiled for 5 minutes, and

subjected to SDS-PAGE and silver stain (BioRad). A fraction of the sample was used for western blot analysis with streptavidin-conjugated Alexa Fluor 680 as above.

Preparation of AFP. Literature report has been followed to prepare partially pure AFP from HepG2 cell lines.⁴⁰ Briefly, HepG2 cells were cultured on a 150 mm culture dish with DMEM (10 % FBS) until there were 80% confluent. The cells were then washed with phenol free 1640 media three times (ThermoFisher Scientific). The same media (25 mL), supplemented with 5% penicillin/streptomycin, was added to the dish and incubated for 72 hours. The media was transferred to a tube and insoluble precipitates were spun down at 2000 rpm for 2 minutes. The supernatant was concentrated with 10,000 Da molecular weight cut-off (MWCO) spin filters (Millipore) to a volume of about 1 mL from 100 mL media. The media was loaded to a 1 mL IMAC FF column (GE Healthcare) pre-charged with CuSO₄. The column was washed with 10 column volumes of binding buffer (20 mM Na₂HPO₄, pH 7.2, 1 M NaCl). The protein was eluted by adding 5 column volumes of elution buffer (20 mM Na₂HPO₄, pH 7.2, 1M NH₄Cl) with 0.5 mL for each fraction. After SDS-PAGE and coomassie staining analysis, the purified protein was concentrated with 30,000 Da molecular weight cut-off (MWCO) spin filters and dissolved into 50 mM Tris-HCl pH 7.5 containing 0.015 M NaCl and stored at -20 °C.

ELISA for Detection of Core Fucosylated α -Fetoprotein (AFP). HepG2 protein samples were chemoenzymatically labeled with biotin as above. Samples were then serially diluted into Calibrator Diluent RD5-24, applied to the ELISA wells, and the procedure was carried out following the protocol for the Quantikine® ELISA Human α -

Fetoprotein Immunoassay (R&D systems) with exception to the detection of core fucose. Briefly, each sample was applied to four wells and incubated for two hours. Wells were then washed four times with wash buffer, and the anti-AFP conjugated HRP detection antibody was added to two duplicate wells and a streptavidin-conjugated HRP (R&D systems) was added to the other two duplicate wells. After two hours, wells were washed and incubated with substrate solution for 15-30 minutes to allow adequate reaction time. Samples were quenched with a stop solution and quantified on the Flexstation 3 (Molecular Devices) by measuring absorbance at 450 nm. Both total AFP levels, determined against a standard curve of provided pure AFP, and core fucosylated AFP, after background subtracting the samples treated without GALT-1, were determined.

Detecting core fucosylated AFP using the Pierce™ Streptavidin Coated High Capacity Plates (ThermoFisher Scientific) was performed as above except that the biotinylated (core fucosylated) AFP was applied to the streptavidin coated plate and detected with the anti-AFP-conjugated HRP from the R&D kit above.

REFERENCES

1. Varki, A.; Cummings, R.D.; Esko, J.D.; H Freeze, H.H.; Stanley, P.; Bertozzi, C.R.; Hart, G.W.; Etzler, M.E. *Essential of Glycobiology, 2nd Edition*; Cold Spring Harbor Laboratory Press: Cold Spring Harbor, New York, **2009**.
2. Wang, X.; Gu, J.; Ihara, H.; Miyoshi, E.; Honke, K.; Taniguchi, N. *Journal of Biological Chemistry* **2006**, *281*, 2572.
3. Shen, N.; Lin, H.; Wu, T.; Wang, D.; Wang, W.; Xie, H.; Zhang, J.; Feng, Z. *Kidney International* **2013**, *84*, 64.
4. Zhao, Y.; Itoh, S.; Wang, X.; Isaji, T.; Miyoshi, E.; Kariya, Y.; Miyazaki, K.; Kawasaki, N.; Taniguchi, N.; Gu, J. *Journal of Biological Chemistry* **2006**, *281*, 38343.

5. Li, W.; Ishihara, K.; Yokota, T.; Nakagawa, T.; Koyama, N.; Jin, J.; Mizuno-Horikawa, Y.; Wang, X.; Miyoshi, E.; Taniguchi, N. *Glycobiology* **2008**, *18*, 114.
6. Gu, W.; Fukuda, T.; Isaji, T.; Hang, Q.; Lee, H.-h.; Sakai, S.; Morise, J.; Mitoma, J.; Higashi, H.; Taniguchi, N. *Journal of Biological Chemistry* **2015**, *290*, 17566.
7. Shields, R. L.; Lai, J.; Keck, R.; O'Connell, L. Y.; Hong, K.; Meng, Y. G.; Weikert, S. H.; Presta, L. G. *Journal of Biological Chemistry* **2002**, *277*, 26733.
8. Kyselova, Z.; Mechref, Y.; Kang, P.; Goetz, J. A.; Dobrolecki, L. E.; Sledge, G. W.; Schnaper, L.; Hickey, R. J.; Malkas, L. H.; Novotny, M. V. *Clinical Chemistry* **2008**, *54*, 1166.
9. Saldova, R.; Fan, Y.; Fitzpatrick, J. M.; Watson, R. W. G.; Rudd, P. M. *Glycobiology* **2011**, *21*, 195.
10. Lin, Z.; Simeone, D. M.; Anderson, M. A.; Brand, R. E.; Xie, X.; Shedden, K. A.; Ruffin, M. T.; Lubman, D. M. *Journal of Proteome Research* **2011**, *10*, 2602.
11. Yuen, M.-F.; Lai, C.-L. *Best Practice & Research Clinical Gastroenterology* **2005**, *19*, 91.
12. Chen, D.-S.; Sung, J.; Sheu, J.; Lai, M.-Y.; How, S.; Hsu, H.; Lee, C.-S.; Wei, T. *Gastroenterology* **1984**, *86*, 9.
13. Buamah, P. K.; Gibb, I.; Bates, G.; Ward, A. M. *Clinica chimica acta* **1984**, *139*, 313.
14. Comunale, M. A.; Rodemich-Betesh, L.; Hafner, J.; Wang, M.; Norton, P.; Di Bisceglie, A. M.; Block, T.; Mehta, A. *PloS One* **2010**, *5*, e12419.
15. Manimala, J. C.; Roach, T. A.; Li, Z.; Gildersleeve, J. C. *Glycobiology* **2007**, *17*, 17C.
16. Manimala, J. C.; Roach, T. A.; Li, Z.; Gildersleeve, J. C. *Angewandte Chemie* **2006**, *118*, 3689.
17. Chang, C.-F.; Pan, J.-F.; Lin, C.-N.; Wu, I.-L.; Wong, C.-H.; Lin, C.-H. *Glycobiology* **2011**, *21*, 895.
18. Laughlin, S. T.; Bertozzi, C. R. *ACS Chemical Biology* **2009**, *4*, 1068.
19. Al-Shareffi, E.; Chaubard, J.-L.; Leonhard-Melief, C.; Wang, S.-K.; Wong, C.-H.; Haltiwanger, R. S. *Glycobiology* **2013**, *23*, 188.

20. Khidekel, N.; Arndt, S.; Lamarre-Vincent, N.; Lippert, A.; Poulin-Kerstien, K. G.; Ramakrishnan, B.; Qasba, P. K.; Hsieh-Wilson, L. C. *Journal of the American Chemical Society* **2003**, *125*, 16162.
21. Clark, P. M.; Dweck, J. F.; Mason, D. E.; Hart, C. R.; Buck, S. B.; Peters, E. C.; Agnew, B. J.; Hsieh-Wilson, L. C. *Journal of the American Chemical Society* **2008**, *130*, 11576.
22. Zheng, T.; Jiang, H.; Gros, M.; Soriano del Amo, D.; Sundaram, S.; Lauvau, G.; Marlow, F.; Liu, Y.; Stanley, P.; Wu, P. *Angewandte Chemie International Edition* **2011**, *50*, 4113.
23. Chaubard, J.-L.; Krishnamurthy, C.; Yi, W.; Smith, D. F.; Hsieh-Wilson, L. C. *Journal of the American Chemical Society* **2012**, *134*, 4489.
24. Titz, A.; Butschi, A.; Henrissat, B.; Fan, Y.-Y.; Hennet, T.; Razzazi-Fazeli, E.; Hengartner, M. O.; Wilson, I. B.; Künzler, M.; Aebi, M. *Journal of Biological Chemistry* **2009**, *284*, 36223.
25. Bosco, M.; Le Gall, S.; Rihouey, C.; Couve-Bonnaire, S.; Bardor, M.; Lerouge, P.; Pannecoucke, X. *Tetrahedron Letters* **2008**, *49*, 2294.
26. Li, L.; Liu, Y.; Ma, C.; Qu, J.; Calderon, A. D.; Wu, B.; Wei, N.; Wang, X.; Guo, Y.; Xiao, Z. *Chemical Science* **2015**, *6*, 5652.
27. Zhao, Y.; Jia, W.; Wang, J.; Ying, W.; Zhang, Y.; Qian, X. *Analytical Chemistry* **2011**, *83*, 8802.
28. Nakagawa, T.; Moriwaki, K.; Terao, N.; Nakagawa, T.; Miyamoto, Y.; Kamada, Y.; Miyoshi, E. *Journal of Proteome Research* **2012**, *11*, 2798.
29. Fei, G.; Shi, B. Z.; Yuan, Y. F.; WU, X. Z. *Cell Research* **2004**, *14*, 423.
30. Wolff, J.; Frank, R.; Mujoo, K.; Spiro, R.; Reisfeld, R.; Rathjen, F. *Journal of Biological Chemistry* **1988**, *263*, 11943.
31. Behne, T.; Copur, M. S. *International Journal of Hepatology* **2012**, 2012.
32. Sato, Y.; Nakata, K.; Kato, Y.; Shima, M.; Ishii, N.; Koji, T.; Taketa, K.; Endo, Y.; Nagataki, S. *New England Journal of Medicine* **1993**, *328*, 1802.
33. Kumada, T.; Toyoda, H.; Tada, T.; Kiriya, S.; Tanikawa, M.; Hisanaga, Y.; Kanamori, A.; Tanaka, J.; Kagebayashi, C.; Satomura, S. *Journal of Gastroenterology* **2014**, *49*, 555.

34. Korekane, H.; Hasegawa, T.; Matsumoto, A.; Kinoshita, N.; Miyoshi, E.; Taniguchi, N. *Biochimica et Biophysica Acta (BBA)-General Subjects* **2012**, *1820*, 1405.
35. Kagebayashi, C.; Yamaguchi, I.; Akinaga, A.; Kitano, H.; Yokoyama, K.; Satomura, M.; Kurosawa, T.; Watanabe, M.; Kawabata, T.; Chang, W. *Analytical Biochemistry* **2009**, *388*, 306.
36. Akio Ojida, Ippei Takashima, Takahiro Kohira, Hiroshi Nonaka, Itaru Hamachi. *Journal of the American Chemical Society*, **2008**, *130*, 12095.
37. Lei Li, Yunpeng Liu, Cheng Ma, Jingyao Qu, Angie D. Calderon, Baolin Wu, Na Wei, Xuan Wang, Yuxi Guo, Zhongying Xiao, Jing Song, Go Sugiarto, Yanhong Li, Hai Yu, Xi Chen, Peng George Wang. *Chemical Science*, **2015**, *6*, 5652.
38. J. Michael Wolffs, Rainer Frank, Kalpana Mujool, Robert C. Spiroll, Ralph A. Reisfeldll, Fritz G. Rathjen. *Journal of Biological Chemistry*, **1988**, *263* (24), 11943-11947.
39. Bernd Wollscheid, Damaris Bausch-Fluck, Christine Henderson, Robert O'Brien, Miriam Bibel, Ralph Schiess, Ruedi Aebersold, Julian D Watts. *Nature Biotechnology*, **2009**, *27* (4), 378.
40. Patrizia Carlini, Pasquale Ferranti, Francesca Polizio, Maria R. Ciriolo, Giuseppe Rotilio. *Biometals*, **2007**, *20*, 869.

Chapter 4

Antibody-Conjugation using the Core Fucose Chemoenzymatic Approach

ABSTRACT

Antibody-drug conjugates (ADCs) have become a coveted method for targeted drug delivery. With only a few examples of ADCs passing FDA regulations, many companies are actively pursuing ADC leads. However, the conjugation methods currently used vary greatly, from exploiting reactive and non-natural amino acid chains to enzymatic manipulations and antibody engineering. More recently, newer conjugation methods have been focused on exploiting the single *N*-glycan site of the heavy chain at Asn-297. In this chapter, I describe the development of an antibody conjugation method that exploits the chemoenzymatic labeling approach used for the detection of core fucose glycoproteins (Chapter 3). Enzymatic installation of azide functionality followed by conjugation to biotin, through the strain-promoted azide alkyne cycloaddition (SPAAC), enables antibodies to be labeled with biotin. MS analysis confirms that the azide is indeed directly added to core fucose. The proof-of-principle experiments described in this chapter demonstrate that the chemoenzymatic approach can be utilized for antibody-conjugation.

INTRODUCTION

Antibody-drug conjugates (ADC) have become a popular method for targeted drug delivery. Many strategies have been used to install drugs onto antibodies. These include utilizing amino acid side chain reactivity (lysine and cysteine), primary sequence engineering, non-natural amino acid incorporation, and enzymatic transformations.¹ Additionally, many attempts have been made to glycoengineer the *N*-glycan present on antibodies, enabling the site-specific conjugation of 2-4 drugs per antibody (drug-antibody ratio, DAR).¹ Oxidation of core fucose, enzymatic remodeling of the glycans with non-natural sugars and bioorthogonal chemistry have all been employed for this approach, with only a handful of these ADCs currently in clinical trials.¹

In this chapter, I will describe a workflow that repurposes the chemoenzymatic labeling approach described in chapter 3 (chemoenzymatic detection of core fucose) to selectively install chemical functionality onto two different antibodies (Figure 4.1). Core fucose is present on almost all antibodies and exists with over 90% stoichiometry.²⁻⁴ Additionally, each antibody contains two *N*-glycans, one on each heavy chain Asn-297. Using the chemoenzymatic labeling method to install azide functionality onto the core fucose of antibodies, followed by the strain-promoted azide-alkyne cycloaddition (SPAAC) reaction, will enable site-specific conjugation of cyclooctyne derivatized drugs with a theoretical DAR of 1.8 (Figure 4.1). This workflow will enable a new strategy for antibody conjugation and highlight the versatility of the chemoenzymatic approach.

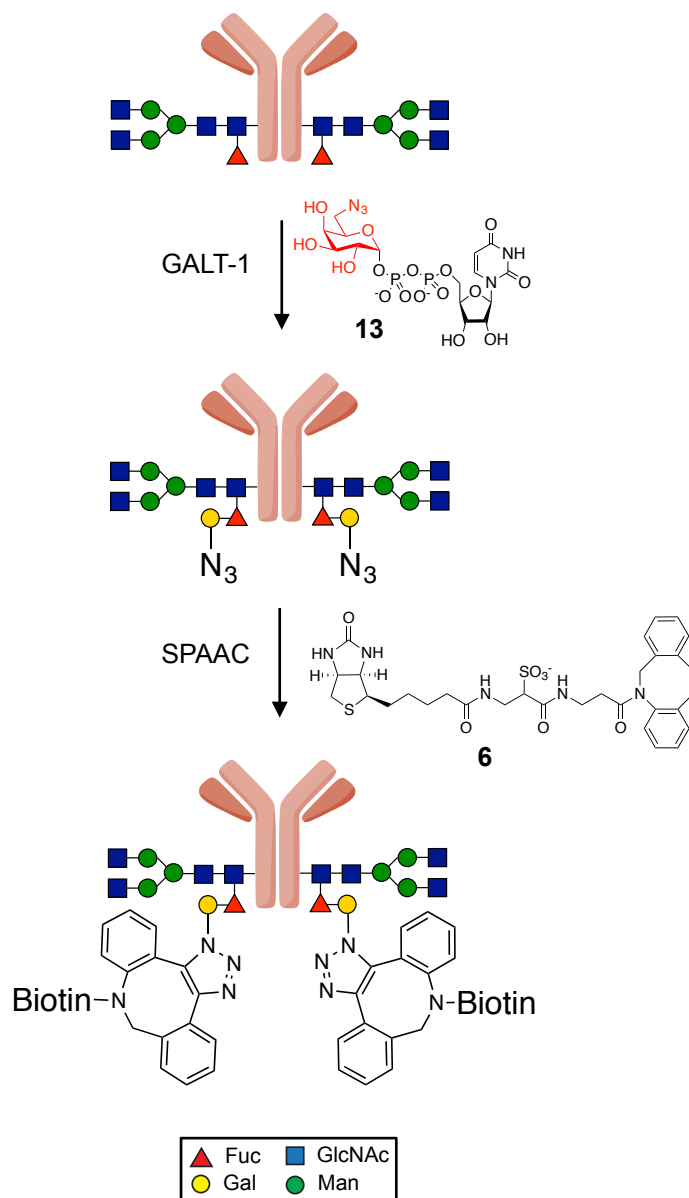


Figure 4.1 Schematic demonstrating proof-of-concept that the chemoenzymatic labeling strategy for core fucose detection can also be utilized as an antibody conjugation method. Antibodies are treated with GALT-1 and UDP-Gal-6-N₃ (**13**) followed by the SPAAC with ADIBO-biotin (**6**).

RESULTS AND DISCUSSION

To determine if the chemoenzymatic approach developed in chapter 3 could be utilized as an antibody-conjugation method, the commercially available anti-TAMRA polyclonal antibody was used as an initial model antibody. The antibody was treated with

GALT-1 and UDP-Gal-6-N₃ (**13**) and then split into four separate samples. Each of these samples were treated with either, increasing amounts of ADIBO-Biotin (**6**; 5, 50, 500 μ M), reacting with the azide through the SPAAC, or with biotin-alkyne (**11**) using the CuAAC as described in chapter 3 (Figure 4.2). These samples were subjected to western blot analysis for detection of both biotin and heavy chain IgG, as well as a coomassie stain for detection of total protein (Figure 4.2A).

As expected this approach could be used to label the antibody heavy chain. Each click chemistry reaction tested demonstrated significant signal over background (Figure 4.2). Interestingly, the CuAAC provided the lowest signal-to-noise, about a seven-fold increase in signal over background (Figure 4.2B). The SPAAC reaction provided lower background when compared to the CuAAC. The 50 μ M SPAAC condition exhibited the best signal-to-noise ratio of ~ 21 (Figure 4.2B). The 500 μ M SPAAC condition exhibited a higher signal than the 50 μ M condition; however, the background witnessed was also higher than desired. Background labeling exhibited by the SPAAC is suspected to be a result of the cysteine side chain thiol nucleophilic attack of the strained cyclooctyne,⁵ as antibodies contain many cysteine residues that participate in disulfide bonds.¹ Based on this exploratory and optimization experiment, the chemoenzymatic labeling approach developed to detect core fucose can also be utilized to conjugate molecules to antibodies and 50 μ M of ADIBO-molecule would be the ideal concentration moving forward.

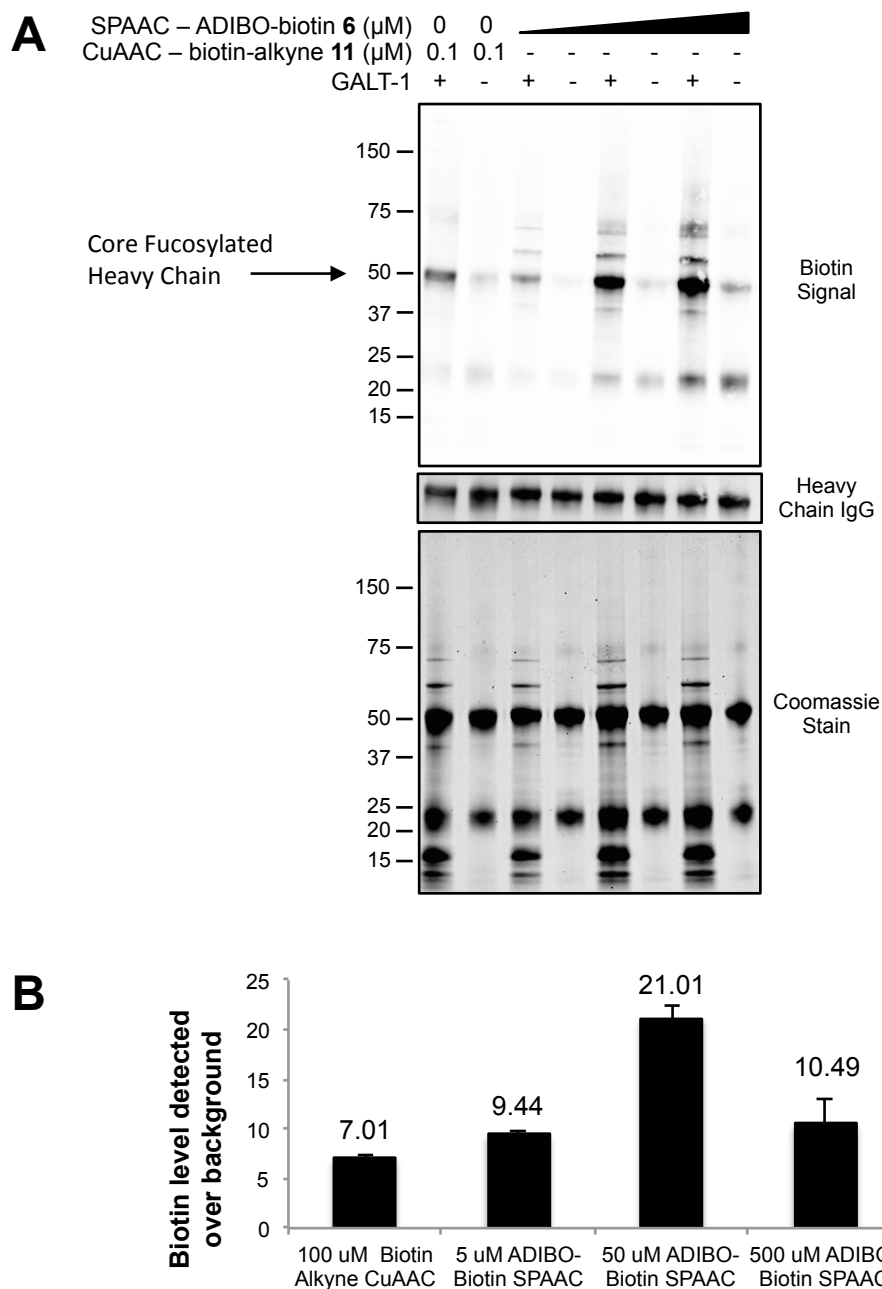


Figure 4.2 (A) Optimization of ADIBO-biotin (**6**) concentration for antibody conjugation using the chemoenzymatic labeling approach. Anti-TAMRA antibody was treated with GALT-1 and UDP-Gal-6-N₃ (**13**) followed by treatment with increasing concentrations of ADIBO-biotin (concentrations used were 5, 50, 500 μM). SDS-PAGE and western blot detection using streptavidin-conjugated Alexa Fluor 680 (top), anti-rabbit antibody (middle), and coomassie stain (bottom). (B) Quantification of signal over background for different concentrations of ADIBO-biotin and comparison to the CuAAC with biotin-alkyne (**11**).

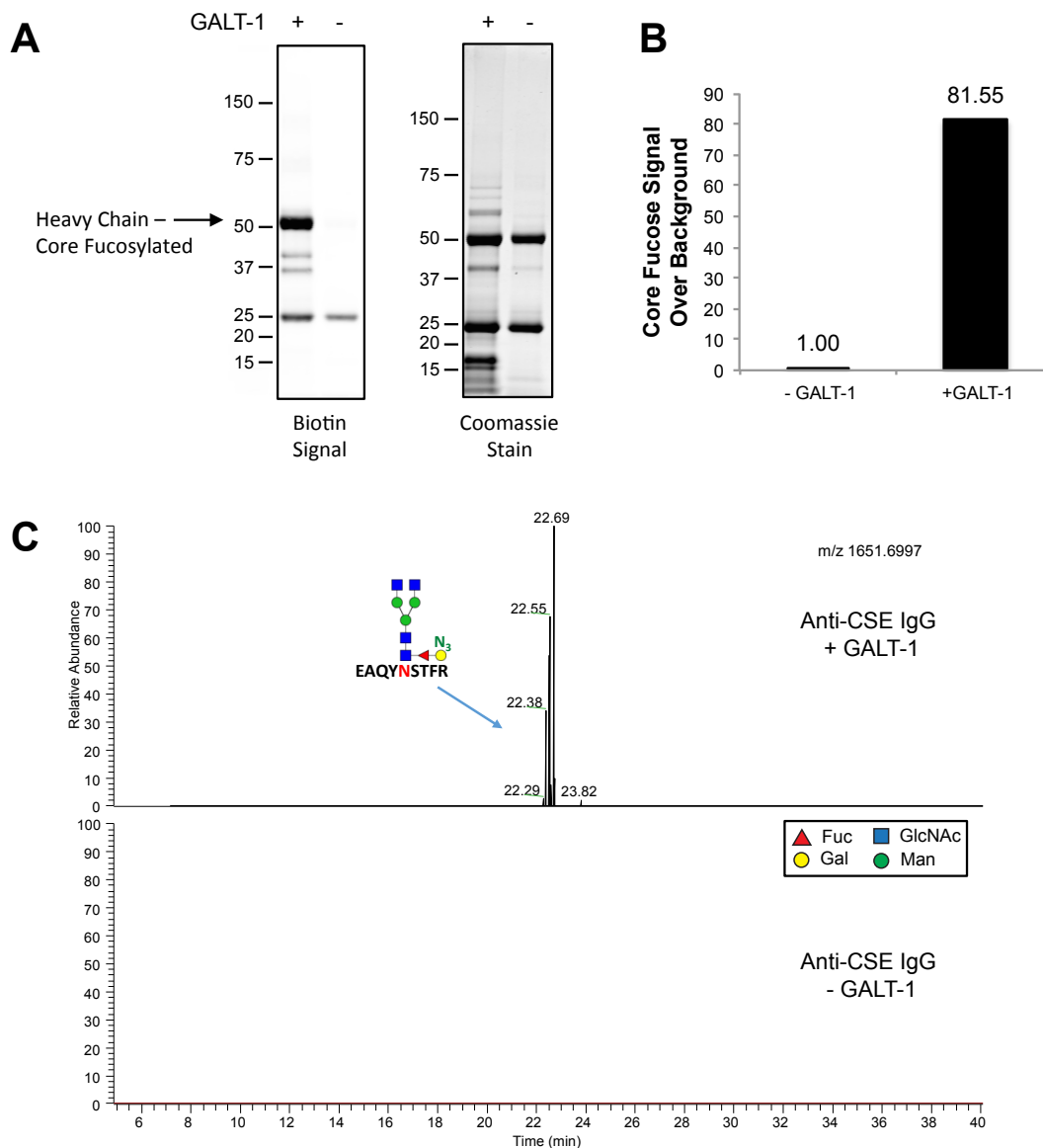


Figure 4.3 Antibody conjugation study using the core fucose chemoenzymatic approach with the anti-CSE antibody. (A) SDS-PAGE and western blot detection of chemoenzymatic labeling-dependent biotin conjugation using streptavidin-conjugated Alexa Fluor 680 (left) and coomassie stain (right). (B) Heavy chain labeling is quantified over the background biotin signal. (C) Extracted ion chromatogram of the glycopeptide, EAQYN*STFR resulting from the tryptic digest of anti-CSE antibody treated with (top) and without (bottom) GALT-1 in the presence of UDP-Gal-6-N₃ (**13**).

With this antibody-conjugation procedure beginning to take form, I decided to test the versatility of this approach on another antibody. I selected the monoclonal anti-Chondroitin Sulfate E (CSE) antibody because our lab has a good deal of this antibody on hand and its binding parameters have been characterized in house. While I did not

conduct binding studies of pre- and post- conjugated antibodies, the Hsieh-Wilson lab is well equipped to conduct these studies in the future. To determine if the anti-CSE antibody could be conjugated to ADIBO-biotin using this method, the antibody was chemoenzymatically labeled as above with the optimized conditions (Figure 4.3). The anti-CSE heavy chain was efficiently labeled, as determined by western blot analysis using streptavidin conjugated Alexa Fluor 680. This labeled demonstrated greater than an 80-fold increase in signal over background (Figure 4.3B). When comparing the signal-to-noise ratios of anti-TAMRA and anti-CSE labeling, anti-CSE appears to be labeled at over a four fold greater efficiency than anti-TAMRA (Figures 4.2B and 4.3B). Based on the specificity and preference for GALT-1 acceptor substrates determined in chapter 3 (Figure 3.5), I suspect the difference in labeling efficiency witnessed is a result of the origin of these antibodies. They were produced in different species and, as a result, will have different *N*-glycan structures. This difference in glycan structure will require that the enzymatic labeling step will need to be optimized for each antibody used.

In order to further characterize this method, a mass spectrometry (MS) approach was utilized to better understand the labeling efficiency, identify the *N*-glycan structures modified by GALT-1, and to definitively demonstrate that Gal-6-N₃ is directly added to core fucose. To achieve these goals, I set up a collaboration with a glycomics core facility run by Parastoo Azadi at the complex carbohydrate research center (CCRC) at the University of Georgia at Athens. The anti-CSE antibody was labeled with and without GALT-1, in the presence of UDP-Gal-6-N₃ (**13**). The antibody was then reduced, alkylated, and digested with trypsin. Since antibodies contain only one *N*-glycan site at Asn-297 of the heavy chain, the glycopeptide EAQYN*STFR could easily be identified

using an extracted ion chromatogram. MS analysis demonstrated that, in the presence of GALT-1, this core fucosylated glycopeptide was indeed labeled with Gal-6-N₃ (Figure 4.3C).

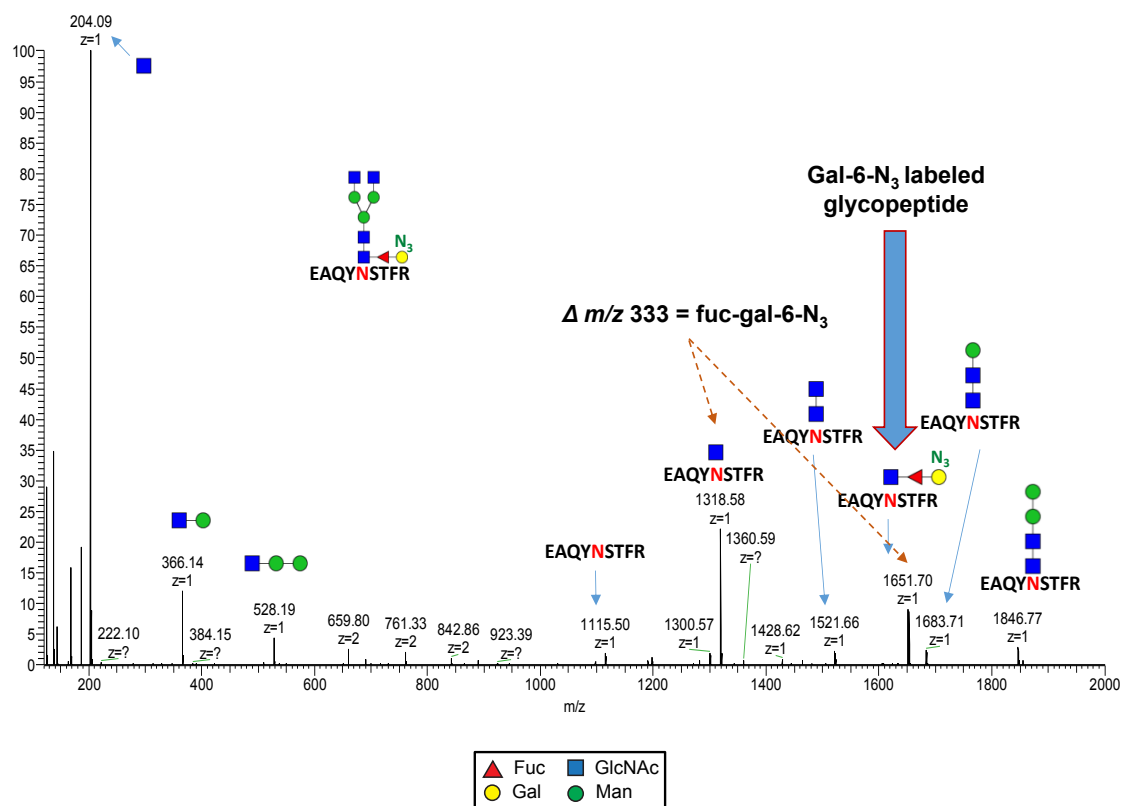


Figure 4.4 Antibody conjugation study using the core fucose chemoenzymatic approach with the anti-CSE antibody. Shown is the HCD MS² spectra of the glycopeptide, EAQYN*STFR, resulting from the tryptic digest of anti-CSE treated with GALT-1 and UDP-Gal-6-N₃ (13).

To further confirm that Gal-6-N₃ was directly added onto core fucose, the glycopeptide sample was subjected to a tandem MS analysis using higher-energy collisional disassociation (HCD). Fragments consistent with the loss of fuc-gal-6-N₃ (m/z 333) were identified, confirming that, in fact, the Gal-6-N₃ was added directly onto core fucose (Figure 4.4). This data directly demonstrates that the chemoenzymatic labeling approach developed for the detection of core fucose directly adds Gal-6-N₃ onto

glycoproteins. Additionally, this method can be used to install a chemical handle onto antibodies for the development of ADCs.

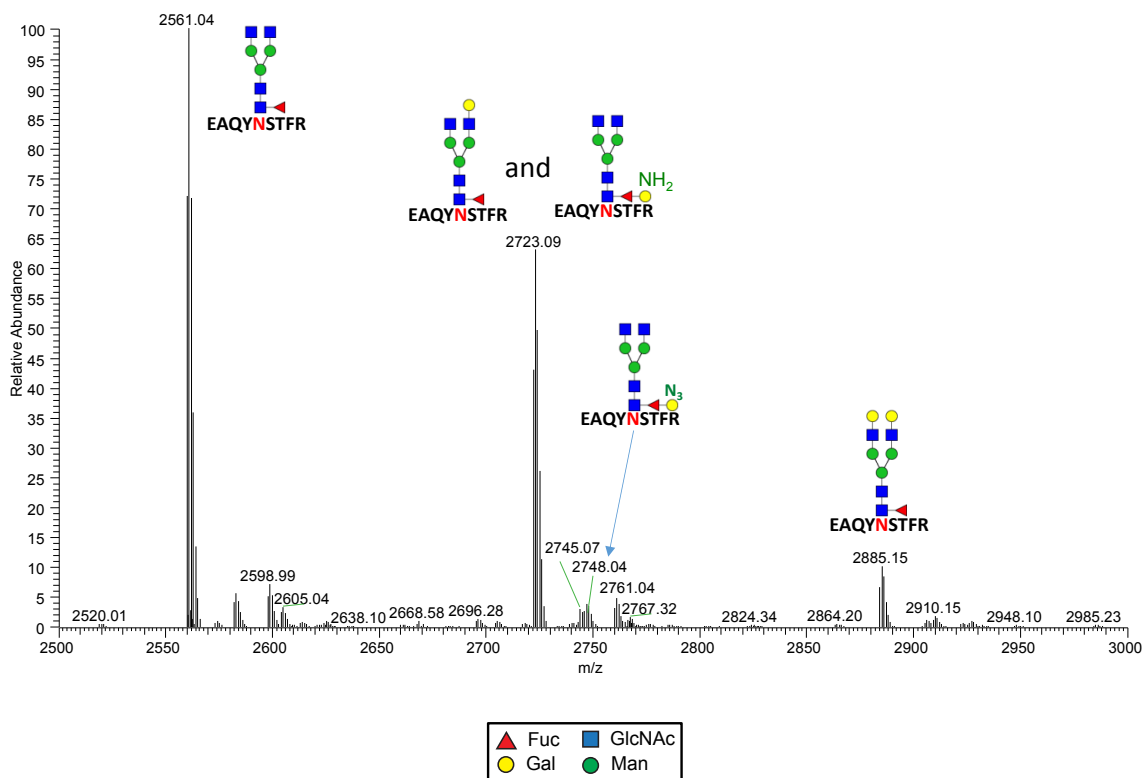


Figure 4.5 Antibody conjugation study using the core fucose chemoenzymatic approach with the anti-CSE antibody. Above is the full MS spectra of the glycopeptide, EAQYN*STFR, resulting from the tryptic digest of anti-CSE treated with GALT-1 and UDP-Gal-6-N₃ (**13**). This glycopeptide is present at low abundances compared to the unmodified glycopeptide suggesting incomplete enzymatic labeling.

Finally, to determine if Gal-6-N₃ is added to other types of *N*-glycan structures on the anti-CSE antibody, a full scan MS analysis was conducted of the glycopeptides generated above (Figure 4.5). While addition of Gal-6-N₃ onto core fucosylated glycopeptide is witnessed, the current strategy used seems to display poor labeling efficiency, despite the western blot analysis on the same sample (Figures 4.5 and 4.3A). This data suggests that only one form of *N*-glycan is labeled, while elongation of the antenna with galactose hinders the reaction (Figure 4.5). This finding is not surprising and

is supported by the MALDI-TOF analysis of GALT-1 specificity presented in chapter 3 (Figure 3.5) However, it is possible that during the reduction and alkylation process, much of the azide is reduced to an amine, a difference of only one dalton from a hydroxyl group. When considering that the natural abundance of isotopes found in these glycopeptides produce multiple peaks during MS analysis, it is possible that when the Gal-6-N₃ is reduced to Gal-6-NH₂, Gal-6-N₃ could ultimately be mistaken for galactose. Since it is established that *N*-glycan antenna are elongated by galactose, it is possible that the signal produced in the MS analysis could be misleading and perhaps the labeling efficacy is not as low as initially thought. Further studies will need to be conducted that do not utilize reduction and alkylation, use higher sensitivity instrumentation, and use more rounds of tandem MS to confirm this hypothesis. Additionally, reaction of the azide with a strained cyclooctyne, prior to reduction and alkylation, could provide a unique mass signature that could help elucidate this hypothesis.

CONCLUSION

In this chapter, I have described an antibody-conjugation method that exploits the core fucose chemoenzymatic labeling approach developed in chapter 3. Two different antibodies were labeled, demonstrating the versatility of the approach; however, each were labeled with different efficiencies. This is likely due to different types of *N*-glycans present on each of the antibodies, resulting from the species in which the antibodies were produced. Using an MS analysis of the glycopeptides produced from the anti-CSE antibody, direct evidence was generated supporting previous findings that GALT-1 directly adds Gal-6-N₃ onto the core fucose of *N*-glycans. Further optimization of this

antibody-conjugation method is required to make this process more efficient and if this technology will ever be commercialized. Additional studies are also needed that determine how ADCs produced using this technology effect the binding of this antibody to its target antigen and Fc receptors. Despite the requirement for further optimization and characterization of this strategy, I have provided proof-of-principle studies demonstrating that this approach presents a novel method for generating antibody-drug conjugates.

EXPERIMENTAL METHODS

General Reagents and Methods. Unless otherwise noted, reagents were purchased from the commercial suppliers Fisher (Fairlawn, NJ) or Sigma-Aldrich (St. Louis, MO). Protease inhibitor cocktails (PIC) were purchased from Roche Applied Sciences (Indianapolis, IN). Immobilon-FL PDVF membrane was from Millipore (Billerica, MA). The anti-TAMRA antibody, 4-12% NuPAGE® Bis-Tris Mini gels, streptavidin-conjugated Alexa Flour 680 were from Invitrogen (Carlsbad, CA). The click chemistry ligand, Tris(3-hydroxypropyltriazolylmethyl)amine (THTPA) was purchased from Sigma-Aldrich (St. Louis, MO). Biotin-alkyne was purchased from clickchemistrytools.com (Scottsdale, AZ). Western blots were visualized and quantified using an Odyssey infrared imaging system (LI-COR Biosciences). The anti-CSE antibody was purified in house.

Chemoenzymatic Labeling of anti-TAMRA and anti-CSE Antibodies. Antibodies were precipitated using chloroform/methanol/water as described in the experimental procedures section in chapters 2 and 3. The antibody pellet was re-dissolved at 5 mg/mL

by boiling in 1% SDS with 50 mM HEPES pH 7.5 for 5 minutes. The sample was then brought to 1 mg/mL in 5 mM MnCl₂, 1x protease inhibitor complex, 0.5 mM UDP-Gal-6-N₃ (**13**), 0.2 mg/mL GALT-1 and incubated at RT for 4 h. The labeled antibody was precipitated as above and resuspended in 50 mM Tris-HCl, pH 8 containing 1% SDS at 1 mg/mL. The resuspended antibody was subsequently reacted 0.1 mM biotin-alkyne (**11**), 3 mM THPTA (ligand), 1 mM CuSO₄, and 2 mM sodium ascorbate for 1 hour at room temperature or incubated with 5, 50, or 500 μM ADIBO-biotin (**6**) for 2 hours. Negative controls were performed under identical conditions except that GALT-1 was omitted from the labeling reaction. After the labeling reactions, antibody was precipitated using chloroform/methanol/water as described and re-dissolved in 1% SDS. This precipitation and resolubilization was then repeated once more to ensure removal of non-specific interactions.

Western Blot Detection of Core Fucosylated Glycoproteins. Labeled antibodies were resolved on 1.5 mm, 10-well NuPAGE 4-12% Bis-Tris gels and transferred to PDVF. The membrane was blocked with 3% BSA (ThermoFisher Scientific) in 50 mM Tris-HCl pH 7.4, 150 mM NaCl containing 0.1% Tween-20 (TBST) for 1 h at RT and then the membranes were probed with streptavidin-conjugated IR680 (Invitrogen) at 0.5 μg/mL for 30 minutes at RT in blocking buffer. A fraction of the samples were analyzed separately by SDS-PAGE and coomassie staining (Bio-Rad) for total protein normalization.

Detection of Antibody N-glycans by MS Analysis. Anti-CSE antibody was enzymatically labeled as above and precipitated as described. The protein pellet was washed two times in 80% MeOH. The antibody pellet was then frozen and shipped to the CCRC as noted. The protein was resuspended, reduced with TCEP and alkylated with iodoacetamide, and digested with trypsin. Samples were desalted and subjected to LC-MS analysis. Tandem MS was conducted using higher-energy collisional disassociation (HCD). Additional details can be found by contacting Parastoo Azadi at the complex carbohydrate research center (CCRC) at the University of Georgia at Athens.

REFERENCES

1. Paresh, A.; Bertozzi, C.R. *Bioconjugate Chemistry* **2015**, 26, 176.
2. Natsume, A.; Niwa, R.; Satoh M. *Drug Design, Development, Therapy* **2009**, 3 7.
3. Iida, S; Misaka, H; Inoue, M; et al. *Clinical Cancer Research* **2006**, 12, 2879.
4. Kanda, Y.; Yamada, T.; Mori, K.; et al. *Glycobiology* **2007**, 17, 104.
5. van Geel, R.; Pruijn, G.J.; van Delft, F.L.; Boelens, W.C. *Bioconjugate Chemistry* **2012**, 23, 392.

Chapter 5

Glycosyltransferase Assay Development

ABSTRACT

During the development of chemoenzymatic labeling approaches, multiple tools are relied upon to monitor glycosyltransferase activity. In this chapter, I describe the development of LC-MS, HPLC, and fluorescence-based assays that were used to monitor glycosyltransferase reactions. These assays were developed for GalT, the enzyme used for chemoenzymatic labeling of *O*-GlcNAc. GalT was also used as a model enzyme to optimize a fluorescence-based assay that utilizes a xanthene-based Zn (II) complex chemosensor **17-2Zn(II)**, which exhibits turn-on fluorescence in the presence of nucleotide diphosphate (NDP). This fluorescence-based assay was also used to describe the kinetic parameters of GALT-1, used for chemoenzymatic labeling of core fucose (Chapter 3), towards its substrates. Finally, the **17-2Zn(II)** sensor was used to monitor GalT labeling of the *O*-GlcNAcylated protein, alpha-crystallin. The ability of the **17-2Zn(II)** sensor to monitor glycosyltransferase reactions with protein acceptor substrates is a novel finding and provides the groundwork for new methods of *O*-GlcNAc detection.

INTRODUCTION

When characterizing glycosyltransferase activity during the development of chemoenzymatic labeling methods, tools to monitor glycosyltransferase reactions are imperative. Traditionally, the field has used radiolabeled nucleotide sugars and a scintillation counter.¹ Additionally, acceptor substrate derivatization has been utilized for capillary electrophoresis (CE), high performance liquid chromatography (HPLC), or mass spectrometry (MS) analysis.² More recently, reactions have been monitored using glycan array technologies with MS or fluorescent readouts.^{3,4} Finally, in solution fluorescent based assays have proven to be effective and simple readouts for glycosyltransferase activity.

Due to the nature of glycosyltransferase donor substrates being almost exclusively nucleotide diphosphate-sugars (NDP-sugar), colorimetric assays rely on the enzymatic release of the NDP for detection of the reaction progress. A commercially available kit from R&D Systems relies on a phosphatase-coupled assay which converts the NDP to a monophosphate, which can be detected by malachite green.⁵ Recently, a turn-on fluorescence sensor was developed that directly detects free NDPs but not NDP-sugars.^{6,7} This xanthene-based Zn (II) complex chemosensor **17-2Zn(II)** fluoresces in the presence of NDPs but not NDP-sugars (Figure 5.1A).

This type of sensor is extremely valuable when characterizing glycosyltransferases that have complex acceptor substrates, as in the case of GALT-1 discussed in chapter 3. This type of chemosensor is also a valuable tool for development of a high-throughput assay that should enable the discovery of candidate glycosyltransferases amenable to chemoenzymatic labeling (Figure 5.2). This could lead

to the development of a suite of chemoenzymatic labeling approach in a high-throughput fashion.

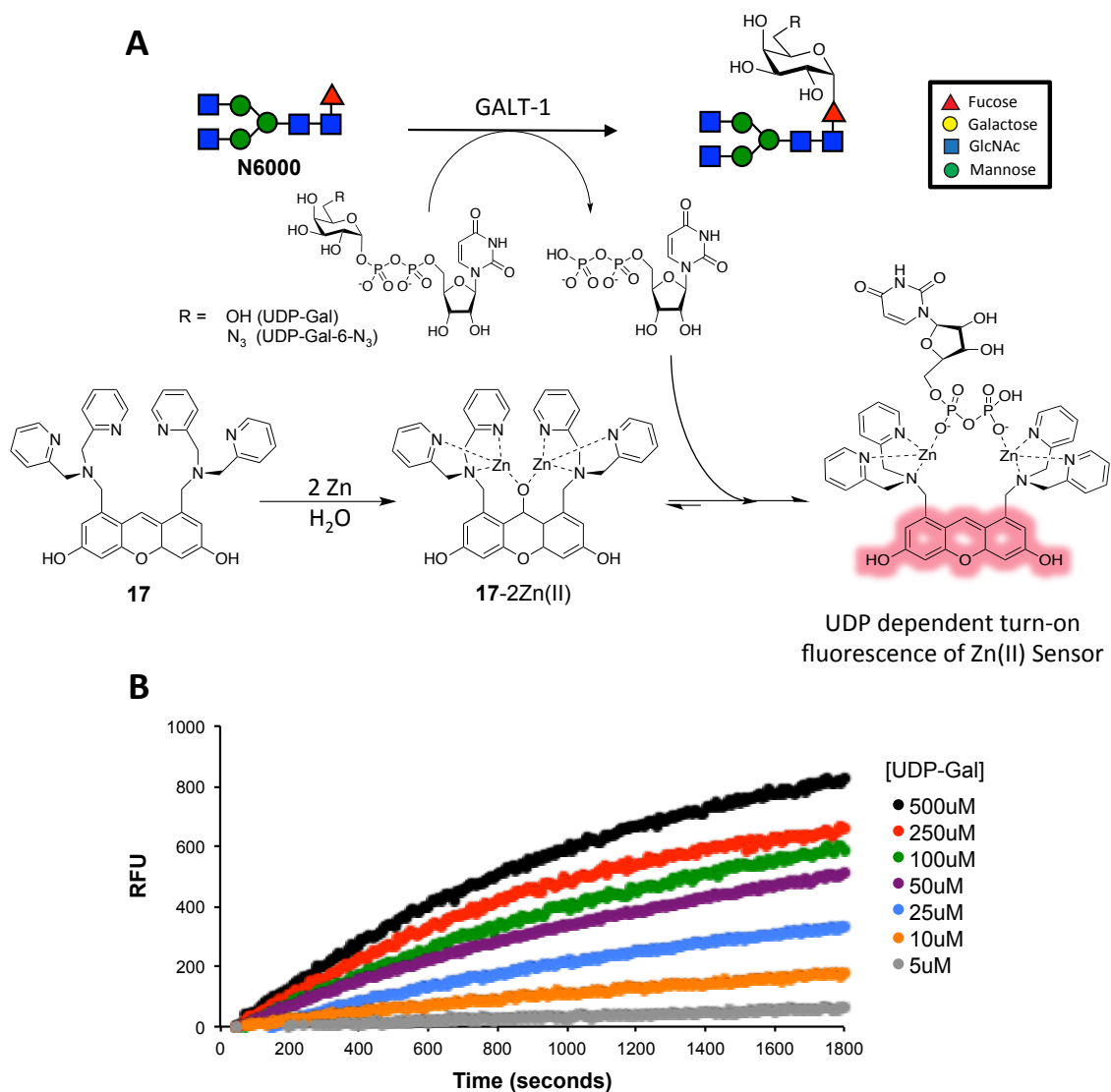


Figure 5.1 Turn-on fluorescence xanthene-based Zn (II) complex chemosensor (**17-2Zn(II)**) for the monitoring of glycosyltransferase reactions. (A) Scheme of fluorescent glycosyltransferase assay used to compared the kinetic parameters of GALT-1 towards UDP-Gal and UDP-Gal-6-N₃. (Full kinetic data noted in Figure 3.4). The sensor (**17**) is non-fluorescent in the presence of Zn. Following Zn binding, the sensor (**17-2Zn(II)**) binds UDP, generated during the glycosyltransferase reaction, and turns on the fluorescence of the sensor. (B) Representative time course data of kinetic assay with increasing concentration of UDP-Gal. Initial rates were determined using the first five minutes of this time course assay.

In this chapter I will describe the development and optimization of this sensor, as well as HPLC and MS based glycosyltransferase assays for the monitoring of

glycosyltransferase activity of GALT-1 (labeling of core fucose) and GalT (labeling of *O*-GlcNAc). I will also explore the ability of this sensor to be utilized for detecting *O*-GlcNAc on purified glycoproteins.

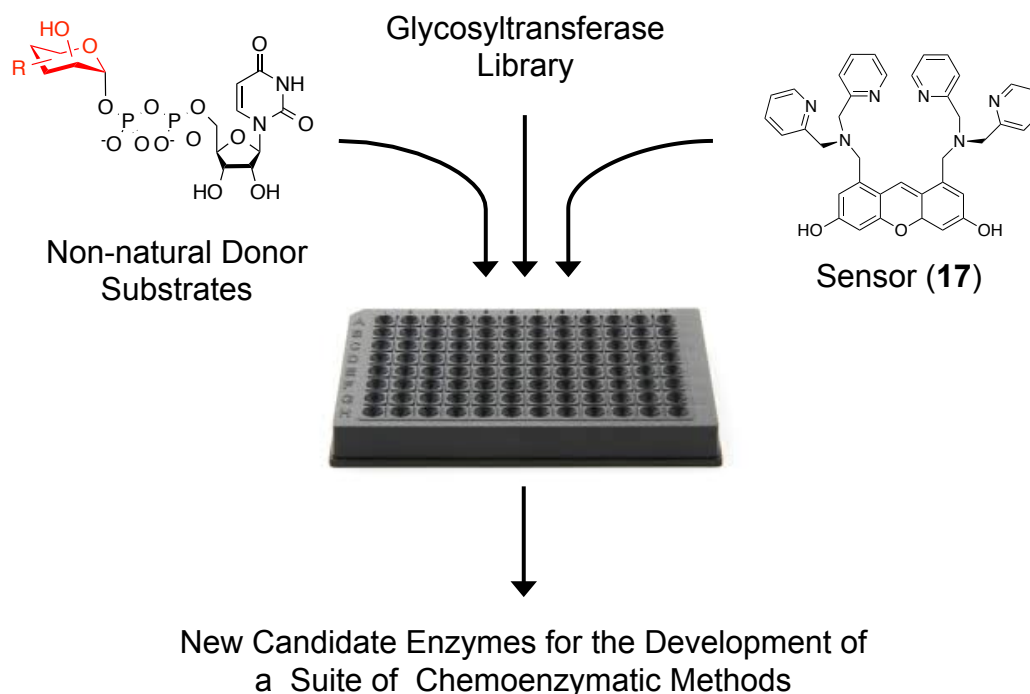


Figure 5.2 Use of the fluorescent sensor (**17**-2Zn(II)) for development a high throughput discovery platform that will enable the identification of novel chemoenzymatic labeling enzymes and rapid characterization of donor substrate specificities. This platform can also be utilized for the high-throughput engineering of mutant glycosyltransferases with enhanced specificity and activity.

RESULTS AND DISCUSSION

Briefly mentioned in chapter 3, was the use of the xanthene-based Zn (II) complex chemosensor **17**-2Zn(II) for the kinetic characterization of GALT-1. The ability to characterize GALT-1's kinetic parameters towards its various substrates was challenging due to the complexity of even its most basic acceptor substrates, N6000 (Figure 5.1A). Through the collaboration with the Wang lab, previously motioned in chapter 3, I was able to obtain the small molecule acceptor substrate, N6000, which could

be used to compare kinetic parameters with the natural and non-natural donor substrates of GALT-1 (Figure 3.4).

To describe the function of this sensor **17-2Zn(II)** I have highlighted the time course data resulting from GALT-1 was incubation with N6000, **17-2Zn(II)**, and increasing concentrations of UDP-Gal (Figure 5.1B). During the reaction, GALT-1 transferred Gal from UDP-Gal to N6000, liberating UDP. With Zn present in the reaction, **17-2Zn(II)** was then able to bind UDP and fluorescence was turned on (Figure 5.1A). It is important to note that **17-2Zn(II)** does bind UDP-sugars to a small degree so background fluorescence control reactions are run in the absence of acceptor substrate. After background subtraction and normalizing the first time point to zero, a time course analysis plot was generated (Figure 5.1B).

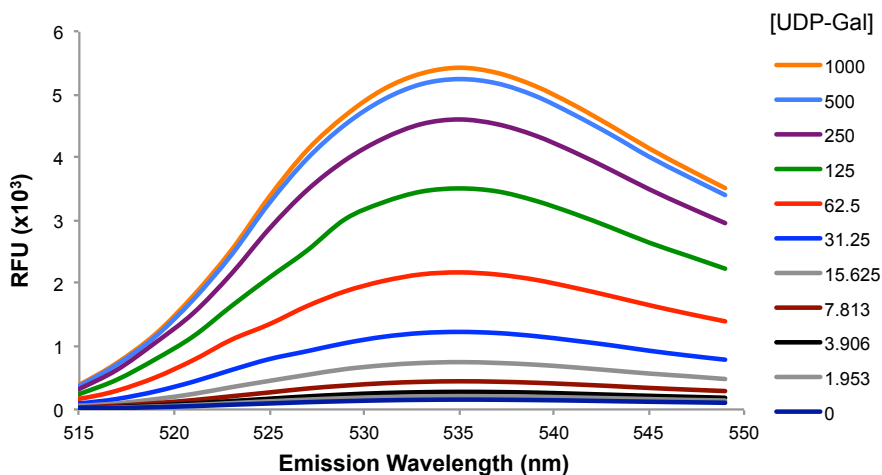


Figure 5.3 Emission profile optimization for the sensor (**17-2Zn(II)**) in presence of UDP. Excitation wavelength set to 490 nm and filter cut-off set to 530 nm. UDP was serially diluted ten times from 1 mM (orange) to 0 mM (dark blue). 534 nm determined to be the λ_{max} .

However, before these kinetic assays could be performed, much optimization was required. While the excitation and emission profiles of the sensor were previously characterized in different groups, I validated these numbers in our system. By setting up mock reactions with increasing concentrations of UDP, I was able to determine that the

optimal excitation wavelength was 500 nm, previously determined to be 488 nm, and the optimal emission wavelength was 534 nm, previously determined to be 523 nm (Figure 5.3). With a 530 nm filter cutoff, I was able to generate robust signals over background (Figure 5.3).

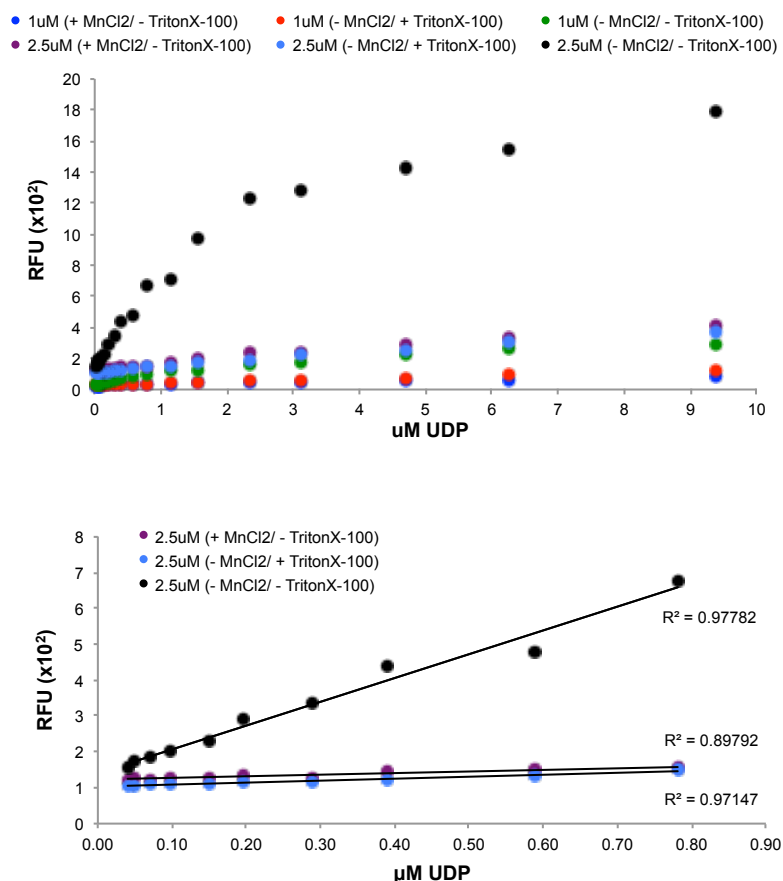


Figure 5.4 Investigating the effects of sensor (**17-2Zn(II)**) concentration and efficacy in the presence of 5 mM MnCl₂ and 1% Triton X-100. These additives are used for glycosyltransferase reactions of interest. Sensor concentrations tested were 1 and 2.5 μM. UDP standards were added in increasing concentrations to determine linear range of detection.

With these parameters in hand, I next set out to determine the effects different reagents, required for GALT-1 activity, would have on sensor performance. GALT-1 had been optimized with 5 mM MnCl₂. In previous reports, **17-2Zn(II)** was utilized in the presence of 0.2 mM MnCl₂; however, it was not determined if higher MnCl₂ concentrations would affect the sensor's performance.⁶ To determine if **17-2Zn(II)** would

maintain its turn-on fluorescent properties in the presence of 5 mM MnCl_2 , I incubated **17-2Zn(II)** in mock reaction buffer with and without 5 mM MnCl_2 and increasing concentrations of UDP (Figure 5.4). The addition of 5 mM MnCl_2 was detrimental to the performance of the sensor **17-2Zn(II)**, indicating that this amount of MnCl_2 could be not be tolerated for proper sensor function.

Next, I tested the performance of the sensor **17-2Zn(II)** in the presence of 1% Triton X-100. Before obtaining **17**, GALT-1 activity assays were performed on purified protein acceptor substrates in the presence of 1% Triton X-100 (Figure 3.7A). If these initial activity assay conditions were going to be used in the fluorescence assay, **17-2Zn(II)** would need to perform in the presence of this detergent. To test this, mock reactions were set up with and without 1% Triton X-100 and showed that the presence of this detergent killed the fluorescent properties of **17-2Zn(II)** (Figure 5.4). Thus, modifications to the initial GALT-1 activity assay were required when using **17-2Zn(II)** to monitor the GALT-1 reaction. It was later determined that 1% Triton X-100 was not required for the activity of GALT-1, data not shown.

Finally, I set out to determine if the effects of MnCl_2 and 1% Triton X-100 could be mitigated by increasing the concentration of **17-2Zn(II)**. The studies mentioned above were conducted following the previous reports of using 1 μM **17-2Zn(II)**. I repeated the above experiments in 2.5 μM **17-2Zn(II)** and determined that, (i) the linear dynamic range and sensitivity were both increased at this concentration for the UDP concentrations desired, and (ii) MnCl_2 and 1% Triton X-100 still killed the activity of the **17-2Zn(II)** despite the higher concentrations (Figure 5.4). Taken together, these key

optimization steps shaped the assays used to determine the kinetic parameters for GALT-1 (Figure 3.4).

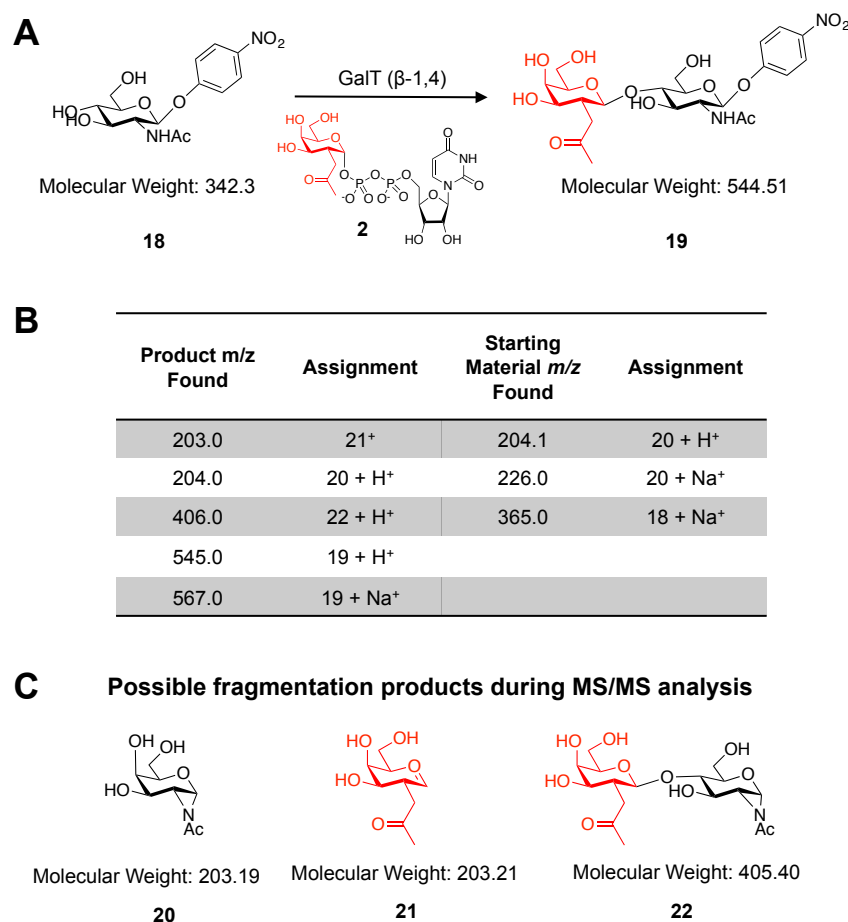


Figure 5.5 Development of MS based glycosyltransferase assay for GalT, the enzyme used for the chemoenzymatic labeling of *O*-GlcNAc. (A) Reaction scheme for the MS analysis confirming that *p*-nitrophenol-GlcNAc (**18**) acts as a substrate for GalT. UDP-ketoGal (**2**; Figure 2.2) was used as a donor substrate and *p*-nitrophenol-GlcNAc (**18**) was used as an acceptor substrate. LC-MS analysis revealed the product **19**, suggesting that GalT does utilize *p*-nitrophenol-GlcNAc (**18**) as an acceptor substrate. (B) Starting material and product peaks identified during the LC-MS analysis. (C) Fragmentation products identified during MS/MS analysis.

With this fluorescent glycosyltransferase assay in hand, I wanted to see if other this chemoenzymatic labeling methods developed in the lab could utilize this assay. The Hsieh-Wilson lab has developed a chemoenzymatic approach for the detection of *O*-GlcNAc; however, the activity assay currently used for GalT, the enzyme for this approach, requires multiple steps and utilizes an expensive commercially available *O*-

GlcNAc glycopeptide with a MALDI-TOF readout after overnight incubation.^{8,9} For these reasons I developed several additional activity assays for GalT that are cheaper, faster, and technically simple.

First, I utilized a cheap and commercially available acceptor substrate, *p*-nitrophenol-GlcNAc (**18**, pnp-GlcNAc). The nitrobenzyl group acts as a UV tag for HPLC and allows the molecule have a significant retention time using any reverse phase column, compared to free GlcNAc. Additionally, this *p*-nitrophenol group helps with ionization for MS analysis. However, *p*-nitrophenol groups have also been shown to inhibit some glycosyltransferases.¹⁰ To address this concern, pnp-GlcNAc **18** was incubated with GalT and UDP-ketoGal (**2**) overnight (Figure 5.5A). LC-MS analysis discovered the expected ketoGal-GlcNAc-pnp product **19**, demonstrating that pnp-GlcNAc **18** could act as an acceptor substrate for GalT (Figure 5.5). Both Na⁺ and H⁺ forms of pnp-GlcNAc, in the control and the product, were discovered (Figure 5.5B). Tandem MS analysis of the product confirmed its identity by identifying the expected fragmentation ions (Figures 5.5 B and C). This data demonstrates that pnp-GlcNAc **18** acts as a suitable substrate for GalT and that this LC-MS method could be used to monitor GalT activity.

Next, an HPLC based assay was developed to establish a quick and easy way to determine the activity of new GalT preparations. The UV active *p*-nitrophenol group enables both a visualization tag and adds hydrophobic character to the GlcNAc substrate for adequate retention on a reverse phase column. To test this assay, GalT was incubated with pnp-GlcNAc **18** and UDP-ketoGal **2**, as above (Figure 5.6A). The reaction was started, by addition of GalT, directly before the autosampler needle could draw the first

time point. Time points were taken every 14 minutes and the reaction was monitored at 280 nm. Within the first time point (14 minutes), the reaction was over 60% complete and the reaction reached completion between 84 and 98 minutes (Figures 5.6 B and C).

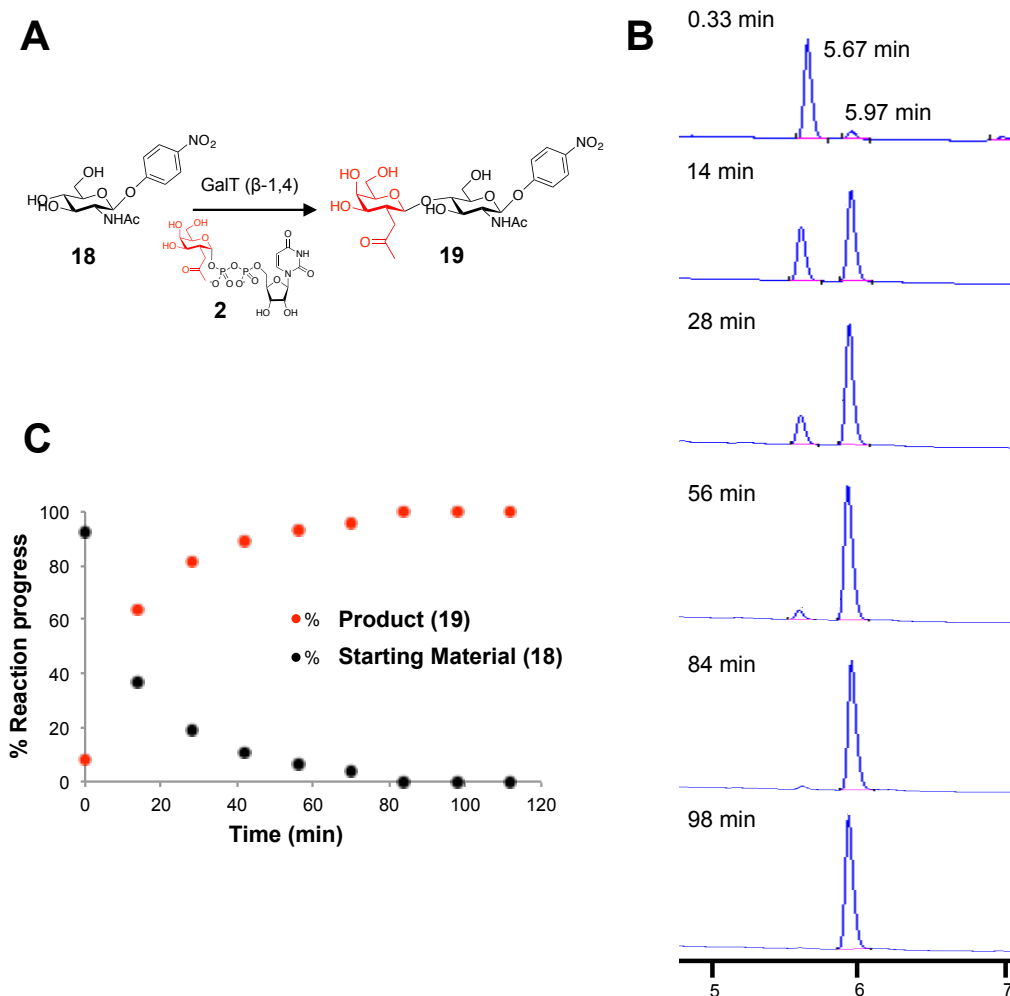


Figure 5.6 Development of HPLC based glycosyltransferase assay for GalT. (A) Reaction scheme using *p*-nitrophenol-GlcNAc (**18**) as acceptor substrate and UDP-KetoGal (**2**) as the donor substrate. (B) HPLC spectra of selected time points demonstrating the reaction progress over time. The detection of the *p*-nitrophenol group was achieved by monitoring at 280 nm. (C) Quantification of starting material (**18**) and product (**19**) percentages using the area under the curve for the respective chromatogram peaks.

This reaction was very easy to set up and monitor, as the autosampler could be set up to monitor time points of the the reaction. This method offers the lab a quick and easy activity assay for GalT. This also shed light onto the speed of this reaction with the

concentration used (500 μM UDP-ketoGal **2**, 100 μM pnp-GlcNAc **18**). This information on reaction rate was considered during the development of the fluorescence-based assay.

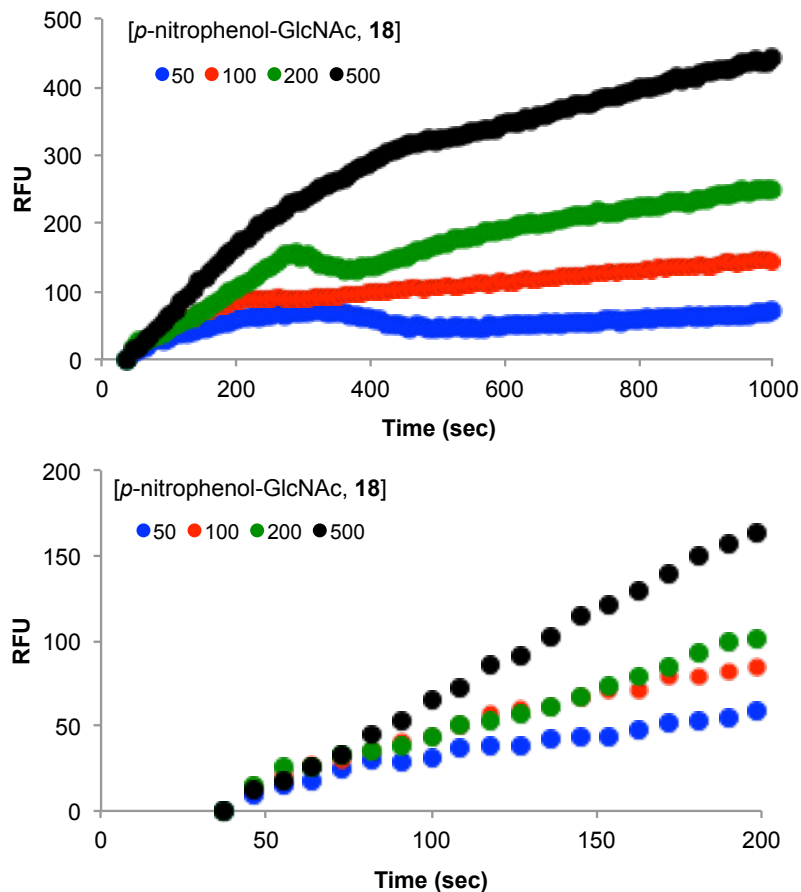


Figure 5.7 Development of fluorescence based glycosyltransferase assay for GalT, the enzyme used for the chemoenzymatic labeling of *O*-GlcNAc. Fluorescent sensor **17-2Zn(II)** monitoring of the glycosyltransferase reaction over 1000 seconds (top) was conducted using 20 μM UDP-KetoGal and increasing concentrations of *p*-nitrophenol-GlcNAc (**18**). The first 200 seconds of the reaction are highlighted (bottom).

With the LC-MS assay confirming that pnp-GlcNAc could act as a substrate for GalT and the HPLC based assay informing the speed of the reaction, I tested if this reaction could be monitored with the fluorescence-based assay described above. GalT was incubated with UDP-ketoGal **2** and increasing concentrations of pnp-GlcNAc **18** in the presence of the fluorescent sensor **17-2Zn(II)** (Figure 5.7). A time dependent increase in signal was witnessed for each pnp-GlcNAc concentration used and increased

concentrations of pnp-GlcNAc correlated to increased reaction rates (Figure 5.7). This data shows that GalT activity can also be monitored using this fluorescence-based assay. Further engineering of GalT or optimization of its reaction conditions could now be conducted in a high-throughput format with the new assay developed above.

Given the versatility of the chemoenzymatic approach, I hypothesized that the fluorescent sensor **17-2Zn(II)** might be able to act as a readout for changes in levels of protein *O*-GlcNAcylation. To test this hypothesis, I repeated the above fluorescent assay with alpha-crystallin as an acceptor substrate because this protein is an established *O*-GlcNAcylated protein detected by this chemoenzymatic approach.⁸ A time dependent increase in signal was witnessed; however, increasing alpha-crystallin concentrations seemed to perturb the fluorescence change (Figure 5.8). When alpha-crystallin was present at 0.5 mg/mL, a robust time depend increase in fluorescence was clear (Figure 5.8). Increasing the protein concentration seemed to be negatively correlated with reaction progress. When alpha-crystallin was present at 2 mg/mL, very low levels of fluorescence change was witnessed over 30 minutes (Figure 5.8). Present at 1 mg/mL, alpha-crystallin showed an intermediate signal over background over this time scale (Figure 5.8). It is not clear whether the decrease in protein concentration allows the GalT reaction to proceed faster or if the increased protein concentration inhibits the capacity or fluorescent properties of the sensor. It is possible that the protein itself chelates metal away from **17-2Zn(II)** or binds the sensor directly, inhibiting the accessibility for UDP to bind **17-2Zn(II)**. More studies are needed to elucidate these issues; however, this data suggests that it is possible to utilize this sensor to detect *O*-GlcNAc on glycoproteins and utilize glycoproteins as acceptor substrates.

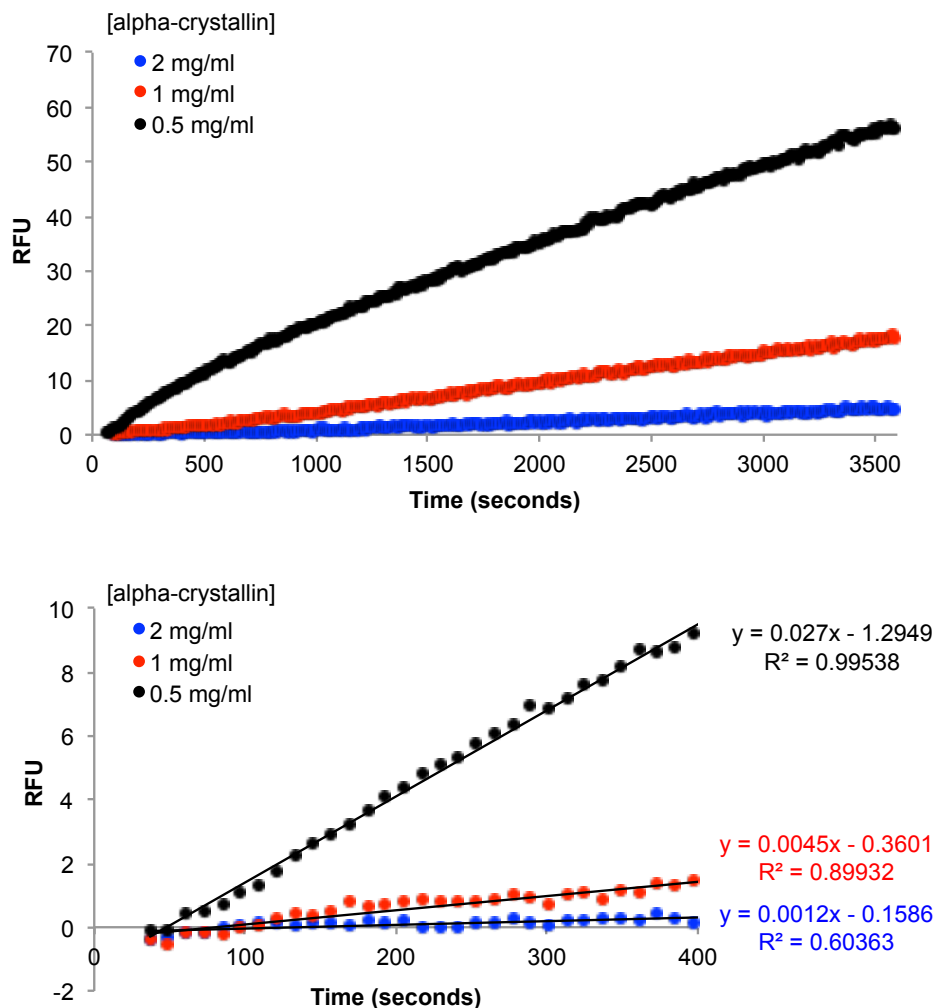


Figure 5.8 Using fluorescent glycosyltransferase assay sensor **17-2Zn(II)** to monitor reaction progress during chemoenzymatic labeling of alpha-crystallin. Readings were taken over one hour (top) and the first five minutes of the reaction are highlighted (bottom). Increasing the protein acceptor substrate concentration causes a decreased response in fluorescence.

This assay could be used to determine kinetic parameters that describe how a glycosyltransferase adds sugars onto specific glycoprotein substrates. One could envision an ELISA-type assay where proteins are immunoprecipitated in a well and changes in *O*-GlcNAcylation on these proteins can be detected using **17-2Zn(II)** based on rates of reaction. Taken together, this data demonstrates that this fluorescent assay can be used to monitor glycosyltransferase activity when utilizing glycoprotein acceptor substrates, opening the door for multiple possible applications for the glycobiology field.

CONCLUSION

In this chapter I have described the development of multiple glycosyltransferase assays that can be utilized in house to decrease cost and time used for monitoring glycosyltransferase activity of our chemoenzymatic labeling enzymes, GalT (*O*-GlcNAc) and GALT-1 (core fucose). These assays rely on LC-MS, HPLC, and fluorescence-based readouts. Optimization of the fluorescent sensor **17-2Zn(II)**, used to determine the kinetic parameters of GALT-1 towards its substrates, was also discussed. The **17-2Zn(II)** sensor was finally used to monitor the GalT reaction to detect *O*-GlcNAc on a protein acceptor substrate, alpha-crystallin. This sensor also affords the ability to monitor glycosyltransferase reactions in a high-throughput fashion, enabling studies to identify a suite of glycosyltransferases amenable to chemoenzymatic labeling.

EXPERIMENTAL METHODS

General Reagents and Methods. Unless otherwise noted, reagents were purchased from the commercial suppliers Fisher (Fairlawn, NJ) or Sigma-Aldrich (St. Louis, MO). Alpha-crystallin, UDP and *p*-nitrophenol-GlcNAc were from ThermoFisher Scientific (Carlsbad, CA). Fluorescent assay were detected using the Flexstation 3 (Molecular Devices). HPLC analysis was performed on an Agilent 1100 HPLC with C-18 reverse phase column (150 mm x 4.6 mm with 3.5 μ m pore size).

GALT-1 Activity Assay Monitoring with Fluorescent Sensor. The turn-on fluorescent sensor, **17-2Zn(II)**, detects UDP but not UDP-Gal.^{6,7} 50 μ L reactions were set up in

duplicate in a 96 well plate format as follows: 50 mM HEPES pH 7.4, 10 mM NaCl, 0.1 mM MgCl₂, 0.2 mM MnCl₂, 0.3 mM ZnCl₂, 2.5 μM **17-2Zn(II)** sensor, 50 μM N6000, 1-500 μM UDP-Gal, 0.2 mg/mL GALT-1. Background was determined with the same reaction conditions without N6000. Fluorescence was detected with excitation and emission wavelengths of 500 nm and 534 nm, respectively, with a 530 nm cutoff.

Sensor Emission Profile Optimization. Mock Reactions were set up as above except UDP-Gal, N6000, and GALT-1 were omitted and a starting UDP concentration was set to 1 mM. Serial dilutions were made into the same mock reaction buffer without UDP. One condition contained no UDP. Fluorescence was detected with an excitation wavelength set to 500 nm, previously determined, and emission profiles were determined by sweeping an emission range of 515 – 549 nm with a 530 nm cutoff. The λ_{max} was determined to be 534nm. Raw data was worked up and plotted in excel.

Determining the Effects of MnCl₂ and 1% Triton X-100 on Sensor Performance.

Mock reactions were set up as above, in the optimization experiments, except that either 5 mM MnCl₂ or 1% Triton X-100 were added to the solution. Increasing concentrations of UDP were added and fluorescence was determined as above. Raw data was plotted in EXCEL.

LC-MS Analysis of GalT Reaction with *p*-nitrophenol-GlcNAc (18**) and UDP-ketoGal (**2**).** The *O*-GlcNAc substrate **18** (100 μM) was dissolved in 10 mM HEPES pH 7.5 and 5 mM MnCl₂. GalT enzyme and UDP-ketoGal (**2**) were added to final

concentrations of 0.1 mg/mL and 500 μ M, respectively. The reaction was incubated at room temperature in the dark for 12-16 h, and the reaction progress was monitored by LC-MS. The samples were injected on a reverse-phase HPLC column (Phenomenex Gemini; 5 m, 2.0 x 100 mm), fitted with a C8 guard column, using a ThermoScientific Accela 600 HPLC pump interfaced with a ThermoScientific LTQ mass spectrometer. A linear 3-90% gradient of B (A: 0.1% aqueous formic acid, B: 0.1% formic acid in MeCN) over 7 min was used to resolve peaks with a flow rate of 0.21 mL/min. Mass analysis was performed in positive ion mode.

HPLC Monitoring of GalT Reaction with *p*-nitrophenol-GlcNAc (18) and UDP-ketoGal (2). The reactions were set up as described above except that the total volume was 200 μ L and reactions were added to LC/MS vials. Product formation was monitored at 280 nm by reverse phase-HPLC (Agilent 1100), and 10 μ L time points were taken every 14 minutes over the course of 126 min using a linear, 3-95% gradient of B (A: 0.1% aqueous trifluoroacetic acid B: 0.1% trifluoroacetic acid in MeCN) over 8 min with a flow rate of 1 mL/min. Starting material and product formation percentages were quantified using area under the curve from the corresponding chromatograms.

Fluorescent Sensor Monitoring of GalT Reaction with *p*-nitrophenol-GlcNAc and UDP-ketogal. Reactions were set up as for GALT-1 and UDP-Gal above, except that GalT (0.1 mg/mL) and UDP-ketoGal (20 μ M) were used and *p*-nitrophenol-GlcNAc (**X**) was used at 0.05, 0.1, 0.2, and 0.5 mM. All reactions were performed in duplicate. Fluorescence was monitored as above.

Fluorescent Sensor Monitoring of GalT Reaction with alpha-crystallin Acceptor Substrate. Reactions were set up as above except that alpha-crystallin was substituted for *p*-nitrophenol-GlcNAc at 0, 0.5, 1, and 2 mg/mL. The 0 mg/mL acted as the negative control.

REFERENCES

1. Palcic, M.M.; Pierce, M.; Hindsgaul, O. *Methods Enzymology* **1994**, 247, 215.
2. Lamari, F.N.; Kuhn, R.; and Karamanos, N.K. *Journal of Chromatography B*, **2003**, 793, 15.
3. Park, S.; Gildersleeve, J.C.; Blixt, O.; and Shin, I. *Chemical Society Reviews* **2013**, 42, 4310.
4. Ban, L.; Pettit, N.; Li, L.; Stuparu, A.D.; Cai, L.; Chen, W.; Guan, W.; Han, W.; Wang, P.G.; Mrksich, M. *Nature Chemical Biology* **2012**, 8, 769.
5. Wu, Z.L.; Ethen, C.M.; Prather, B.; Machacek, M.; Jiang, W. *Glycobiology* **2010**, 21 727.
6. Ojida, A.; Takashima, I.; Kohira, T.; Nonaka, H.; Hamachi, I. *Journal of the American Chemical Society* **2008**, 130, 12095.
7. Lee, H.S.; Thorson, J.S. *Analytical Biochemistry* **2011**, 418, 85.
8. Khidekel, N.; Arndt, S.; Lamarre-Vincent, N.; Lippert, A.; Poulin-Kerstien, K. G.; Ramakrishnan, B.; Qasba, P. K.; Hsieh-Wilson, L. C. *Journal of the American Chemical Society* **2003**, 125, 16162.
9. Clark, P. M.; Dweck, J. F.; Mason, D. E.; Hart, C. R.; Buck, S. B.; Peters, E. C.; Agnew, B. J.; Hsieh-Wilson, L. C. *Journal of the American Chemical Society* **2008**, 130, 11576.
10. Toki, D.; Granovsky, M.A.; Reck, F.; Kuhns, W.; Baker, M.A.; Matta, K.L. and Brockhausen, I. *Biochemical and Biophysical Research Communications* **1994** 198, 417.

Appendix 1

Glycan Array Data Profiling the Acceptor Substrate Specificity of BgtA (see Chapter 2)

This data is organized with the highest signal for the 0.5 hr time point. All the data numbers, RFU, below for 0 – 12 hour time points are divided by 1000 from the raw data to simplify the viewing of this data. The chart # is in reference to the glycan number on the CFG glycan array, version 5.0. The fuc-gal # represents on of the Fuca(1-2)-Gal structures on the array. When reading the structure, a = alpha, b = beta, and sp = spacer number.

Chart #	Fuc-gal #	Structure	0 hr	0.5 hr	2 hr	12 hr	- 12 hr
545	55	Fuca1-2Galb1-4GlcNAcb1-3Galb1-4GlcNAcb1-2Mana1-6(Fuca1-2Galb1-4GlcNAcb1-3Galb1-4GlcNAcb1-2Mana1-3)Manb1-4GlcNAcb1-4GlcNAcb-Sp24	5.2	43.6	44.8	46.4	3.0
501	52	Fuca1-2Galb1-3(6S)GlcNAcb-Sp0	4.0	29.2	36.5	35.1	6.1
75	17	Fuca1-2Galb1-4GlcNAcb1-3Galb1-4GlcNAcb-Sp0	1.4	27.3	41.7	38.3	5.3
450	44	Fuca1-2Galb1-4GlcNAcb1-6(Fuca1-2Galb1-4GlcNAcb1-3)GalNAc-Sp14	4.8	26.5	31.7	43.7	6.6
77	19	Fuca1-2Galb1-4GlcNAcb-Sp8	4.4	25.6	31.6	17.1	4.7
430	41	Galb1-4GlcNAcb1-6(Fuca1-2Galb1-3GlcNAcb1-3)Galb1-4Glc-Sp21	5.3	24.0	23.9	13.9	3.8
67	9	Fuca1-2Galb1-3GlcNAcb1-3Galb1-4Glc-Sp10	3.7	23.9	25.2	15.3	2.5
74	16	Fuca1-2Galb1-4GlcNAcb1-3Galb1-4GlcNAcb-Sp0	4.8	23.1	29.4	34.7	3.0
362	28	Fuca1-2Galb1-4GlcNAcb1-2Mana1-6(Fuca1-2Galb1-4GlcNAcb1-2Mana1-3)Manb1-4GlcNAcb1-4GlcNAcb-Sp20	3.4	22.2	29.8	39.9	1.3
423	39	Fuca1-2Galb1-3GlcNAcb1-3GalNAc-Sp14	0.7	22.0	20.9	26.7	6.6
222	23	Fuca1-2Galb1-4(6S)GlcNAcb-Sp8	1.5	21.2	24.2	30.2	9.2
60	2	Fuca1-2Galb1-3GalNAcb1-3Gala1-4Galb1-4Glc-Sp9	4.8	20.1	31.9	11.2	2.2
66	8	Fuca1-2Galb1-3GlcNAcb1-3Galb1-4Glc-Sp8	1.9	19.7	26.3	37.7	6.3
361	27	Fuca1-2Galb1-3GlcNAcb1-2Mana1-6(Fuca1-2Galb1-3GlcNAcb1-2Mana1-3)Manb1-4GlcNAcb1-4GlcNAcb-Sp20	1.4	17.4	25.3	30.8	1.1
457	45	Neu5Aca2-6Galb1-4GlcNAcb1-6(Fuca1-2Galb1-3GlcNAcb1-3)Galb1-4Glc-Sp21	1.8	17.4	28.1	37.3	7.0
401	36	Fuca1-2Galb1-4GlcNAcb1-3GalNAc-Sp14	2.2	15.3	11.5	10.8	3.9
78	20	Fuca1-2Galb1-4Glc-Sp0	2.2	15.1	23.0	32.2	4.1
65	7	Fuca1-2Galb1-3GalNAcb1-4(Neu5Aca2-3)Galb1-4Glc-Sp9	2.4	14.5	21.2	33.8	4.9
223	24	Fuca1-2(6S)Galb1-4(6S)Glc-Sp0	5.0	14.2	21.1	37.0	15.1
79	21	Fuca1-2Galb-Sp8	1.6	14.2	11.9	7.0	0.3
369	30	Galb1-4(Fuca1-3)GlcNAcb1-6(Fuca1-2Galb1-4GlcNAcb1-3)Galb1-4Glc-Sp21	3.7	13.5	20.4	37.8	3.4

263	26	Fuca1-2Galb1-4(6S)GlcB-Sp0	4.0	12.9	17.9	7.3	2.9
63	5	Fuca1-2Galb1-3GalNAca-Sp14	0.8	12.6	15.6	26.2	4.8
68	10	Fuca1-2Galb1-3GlcNAcb-Sp0	1.4	12.5	12.9	6.2	5.9
69	11	Fuca1-2Galb1-3GlcNAcb-Sp8	3.1	12.1	10.0	7.0	1.8
446	42	Fuca1-2Galb1-4 GlcNAcb1-2Mana1-6(Fuca1-2Galb1-4GlcNAcb1-2(Fuca1-2Galb1-4GlcNAcb1-4)Mana1-3)Manb1-4GlcNAcb1-4GlcNAcb-Sp12	3.5	11.0	13.6	32.5	2.8
27		(3S)Galb1-4(6S)GlcB-Sp8	2.8	11.0	14.2	23.1	19.3
515		GalNAcb1-4(6S)GlcNAc-Sp8	4.7	10.8	16.4	13.3	5.3
62	4	Fuca1-2Galb1-3GalNAca-Sp8	1.3	10.8	25.8	31.6	8.5
76	18	Fuca1-2Galb1-4GlcNAcb-Sp0	2.4	10.7	11.9	25.5	3.0
502	53	Fuca1-2(6S)Galb1-3(6S)GlcNAcb-Sp0	6.5	10.6	16.5	30.0	7.6
542		Galb1-4GlcNAcb1-3Galb1-4GlcNAcb1-2Mana1-6(Galb1-4GlcNAcb1-3Galb1-4GlcNAcb1-2Mana1-3)Manb1-4GlcNAcb1-4GlcNAcb-Sp12	5.4	10.5	14.6	16.3	14.4
486		Galb1-4GlcNAcb1-6(Galb1-4GlcNAcb1-2)Mana1-6(Galb1-4GlcNAcb1-2Mana1-3)Manb1-4GlcNAcb1-4(Fuca1-6)GlcNAcb-Sp24	4.8	9.3	9.9	22.9	4.6
390	34	Fuca1-2Galb1-3GalNAca1-3(Fuca1-2)Galb1-4GlcB-Sp0	2.3	9.2	12.4	18.9	5.1
39		(6S)(4S)Galb1-4GlcNAcb-Sp0	2.7	9.1	14.1	22.2	12.0
304		GlcNAcb1-6(Galb1-4GlcNAcb1-3)Galb1-4GlcNAc-Sp0	6.7	9.0	11.2	8.0	5.2
427	40	Fuca1-2Galb1-3GlcNAcb1-2Mana1-6(Fuca1-2Galb1-3GlcNAcb1-2Mana1-3)Manb1-4GlcNAcb1-4(Fuca1-6)GlcNAcb-Sp22	1.8	9.0	8.3	11.3	1.6
268		Neu5Aca2-6Galb1-4(6S)GlcNAcb-Sp8	4.6	8.7	12.6	25.7	18.6
445		(6S)Galb1-3(6S)GlcNAc-Sp0	3.7	8.4	17.7	27.7	16.7
452		GalNAca1-3(Fuca1-2)Galb1-4GlcNAcb1-6(GalNAca1-3(Fuca1-2)Galb1-4GlcNAcb1-3)GalNAc-Sp14	4.7	8.2	11.1	20.4	3.9
159		Galb1-4GalNAcb1-3(Fuca1-2)Galb1-4GlcNAcb-Sp8	2.3	7.9	14.4	10.8	8.0
391	35	Fuca1-2Galb1-3GalNAca1-3(Fuca1-2)Galb1-4GlcNAcb-Sp0	0.8	7.8	8.8	14.8	2.5
448		Galb1-4(Fuca1-3)GlcNAcb1-6GalNAc-Sp14	5.7	7.5	10.1	21.8	10.2
64	6	Fuca1-2Galb1-3GalNAcb1-4(Neu5Aca2-3)Galb1-4GlcB-Sp0	0.5	7.5	15.1	20.1	4.4
158		Galb1-4GalNAca1-3(Fuca1-2)Galb1-4GlcNAcb-Sp8	4.2	7.4	8.8	9.0	3.3
409		GalNAcb1-3Gala1-6Galb1-4GlcB-Sp8	3.4	7.1	10.6	10.9	4.7
468		Gala1-3(Fuca1-2)Galb1-3GalNAca-Sp8	7.5	7.0	9.8	18.8	12.0
429		Galb1-3GlcNAcb1-6(Galb1-3GlcNAcb1-2)Mana1-6(Galb1-3GlcNAcb1-2Mana1-3)Manb1-4GlcNAcb1-4GlcNAcb-Sp19	4.6	7.0	7.0	9.9	2.6

433		GlcNAcb1-2Mana1-6(GlcNAcb1-4)(GlcNAcb1-4(GlcNAcb1-2)Mana1-3)Manb1-4GlcNAcb1-4GlcNAc-Sp21	2.8	6.9	10.5	10.0	4.5
297		4S(3S)Galb1-4GlcNAcb-Sp0	3.4	6.9	9.1	11.9	7.2
532		Galb1-4GlcNAcb1-2 Mana1-6(GlcNAcb1-4)(Galb1-4GlcNAcb1-2Mana1-3)Manb1-4GlcNAcb1-4(Fuca1-6)GlcNAc-Sp21	4.0	6.8	7.9	11.1	7.9
306		Galb1-4GlcNAcb1-6Galb1-4GlcNAcb-Sp0	7.3	6.8	7.4	7.3	3.7
499		Gala1-3(Fuca1-2)Galb1-4GlcNAcb1-6GalNAca-Sp14	2.0	6.8	12.1	33.9	13.0
221	22	Fuca1-2(6S)Galb1-4GlcNAcb-Sp0	3.8	6.7	10.0	20.0	4.6
103		Gala1-3(Fuca1-2)Galb1-3GlcNAcb-Sp8	5.0	6.6	12.3	14.0	11.1
387		Galb1-3GlcNAcb1-3Galb1-4(Fuca1-3)GlcNAcb1-6(Galb1-3GlcNAcb1-3)Galb1-4Glc-Sp21	4.0	6.5	6.2	14.5	4.9
303		Galb1-4GlcNAcb1-6(Galb1-4GlcNAcb1-3)Galb1-4GlcNAc-Sp0	2.6	6.5	8.2	14.1	3.6
22		6S(3S)Galb1-4(6S)GlcNAcb-Sp0	4.7	6.4	6.3	12.2	8.9
180		GlcNAcb1-3GalNAca-Sp8	3.5	6.4	7.6	16.7	7.6
477		Galb1-3GlcNAcb1-2Mana1-6(GlcNAcb1-4)(Galb1-3GlcNAcb1-2Mana1-3)Manb1-4GlcNAcb1-4GlcNAcb-Sp21	4.9	6.4	9.2	12.0	4.9
114		Gala1-3Galb1-4(Fuca1-3)GlcNAcb-Sp8	3.9	6.4	5.8	7.4	9.1
105		Gala1-3(Fuca1-2)Galb1-4(Fuca1-3)GlcNAcb-Sp8	7.1	6.4	12.4	8.5	6.1
94		GalNAca1-4(Fuca1-2)Galb1-4GlcNAcb-Sp8	4.8	6.3	6.9	4.4	6.9
529		GalNAcb1-4GlcNAcb1-2Mana-Sp0	1.5	6.3	8.4	16.9	4.1
421	38	Fuca1-2Galb1-4GlcNAcb1-2Mana1-6(Fuca1-2Galb1-4GlcNAcb1-2Mana1-3)Manb1-4GlcNAcb1-4(Fuca1-6)GlcNAcb-Sp22	0.7	6.3	12.9	15.6	3.1
476		GlcNAcb1-6(GlcNAcb1-2)Mana1-6(GlcNAcb1-2Mana1-3)Manb1-4GlcNAcb1-4(Fuca1-6)GlcNAcb-Sp24	6.2	6.2	5.6	9.8	5.3
543		Galb1-4GlcNAcb1-3Galb1-4GlcNAcb1-2Mana1-6(Galb1-4GlcNAcb1-3Galb1-4GlcNAcb1-2Mana1-3)Manb1-4GlcNAcb1-4GlcNAcb-Sp24	4.6	6.2	12.0	16.2	3.1
524		GalNAca1-3(Fuca1-2)Galb1-4 GlcNAcb1-2Mana-Sp0	7.9	6.2	6.7	10.9	2.9
110		Gala1-4(Gala1-3)Galb1-4GlcNAcb-Sp8	4.7	6.2	9.4	19.4	6.9
495	49	Fuca1-2Galb1-4GlcNAcb1-6GalNAca-Sp14	0.3	6.2	12.7	19.3	2.6
212		Mana1-2Mana1-6(Mana1-3)Mana1-6(Mana1-2Mana1-2Mana1-3)Manb1-4GlcNAcb1-4GlcNAcb-Sp12	4.5	6.2	6.5	10.4	4.3
179		GlcNAcb1-6(GlcNAcb1-3)Galb1-4GlcNAcb-Sp8	5.3	6.2	8.1	12.4	6.2
61	3	Fuca1-2Galb1-3(Fuca1-4)GlcNAcb-Sp8	2.5	6.2	12.5	16.9	8.1
385	32	Galb1-4GlcNAcb1-6(Fuca1-4(Fuca1-2Galb1-3)GlcNAcb1-3)Galb1-4Glc-Sp21	2.3	6.2	8.3	9.4	2.3

435		GlcNAcb1-6(GlcNAcb1-2)Mana1-6(GlcNAcb1-4)(GlcNAcb1-4(GlcNAcb1-2)Mana1-3)Manb1-4GlcNAcb1-4GlcNAc-Sp21	4.5	6.2	8.5	12.4	7.8
73	15	Fuca1-2Galb1-4(Fuca1-3)GlcNAcb-Sp8	2.0	6.1	9.2	6.3	3.7
500	51	Fuca1-2Galb1-4GlcNAcb1-2Mana-Sp0	2.3	6.1	8.7	19.1	6.6
560		Galb1-4GlcNAcb1-3Galb1-4GlcNAcb1-6(Galb1-4GlcNAcb1-3Galb1-4GlcNAcb1-2)Mana1-6(Galb1-4GlcNAcb1-3Galb1-4GlcNAcb1-2Mana1-3)Mana1-4GlcNAcb1-4GlcNAc-Sp24	3.7	6.1	5.8	12.2	2.4
454		GalNAcb1-4Galb1-4Glc-Sp0	2.2	6.1	7.5	13.0	5.1
564		GalNAcb1-4GlcNAcb1-3GalNAcb1-4GlcNAcb-Sp0	4.6	6.1	10.6	10.5	4.0
160		Galb1-4GlcNAcb1-3GalNAca-Sp8	4.6	6.0	6.6	13.1	7.2
552		Galb1-3GlcNAcb1-3Galb1-4GlcNAcb1-2Mana1-6(Galb1-3GlcNAcb1-3Galb1-4GlcNAcb1-2Mana1-3)Manb1-4GlcNAcb1-4GlcNAc-Sp25	1.7	6.0	10.6	19.8	2.0
317		Mana1-2Mana1-6(Mana1-2Mana1-3)Mana1-6(Mana1-2Mana1-2Mana1-3)Mana-Sp9	3.4	5.9	4.5	5.8	10.3
531		GlcNAcb1-2 Mana1-6(GlcNAcb1-4)(GlcNAcb1-2Mana1-3)Manb1-4GlcNAcb1-4(Fuca1-6)GlcNAc-Sp21	6.4	5.9	5.5	10.3	5.4
146		Galb1-3GalNAcb1-4Galb1-4Glc-Sp8	3.4	5.8	8.1	11.3	6.2
106		Gala1-3(Fuca1-2)Galb1-4GlcNAc-Sp0	7.4	5.7	7.9	14.3	5.3
24		(3S)Galb1-4(Fuca1-3)(6S)Glc-Sp0	5.0	5.7	8.9	11.5	8.8
53		GlcNAcb1-2Mana1-6(GlcNAcb1-2Mana1-3)Manb1-4GlcNAcb1-4GlcNAcb-Sp13	3.7	5.6	7.8	6.5	6.9
498	50	Fuca1-2(6S)Galb1-3GlcNAcb-Sp0	4.7	5.6	8.8	16.2	10.4
503		Neu5Aca2-6GalNAcb1-4(6S)GlcNAcb-Sp8	3.4	5.6	9.9	20.1	4.3
104		Gala1-3(Fuca1-2)Galb1-4(Fuca1-3)GlcNAcb-Sp0	5.0	5.6	6.4	14.0	4.3
35		(3S)Galb1-4(6S)GlcNAcb-Sp8	3.1	5.6	8.0	9.3	4.9
208		Mana1-2Mana1-2Mana1-3Mana-Sp9	2.5	5.6	9.3	8.4	4.1
96		GalNAcb1-3(Fuca1-2)Galb-Sp8	3.6	5.6	7.3	12.3	6.4
19		Galb1-4GlcNAcb1-6(Galb1-4GlcNAcb1-3)GalNAca-Sp8	7.6	5.6	8.1	11.9	2.7
451		Gala1-3Fuca1-2Galb1-4GlcNAcb1-6(Gala1-3Fuca1-2Galb1-4GlcNAcb1-3)GalNAc-Sp14	4.6	5.5	7.5	12.9	4.3
170		Galb1-4GlcNAcb-Sp8	1.0	5.5	7.5	5.9	5.5
447	43	Fuca1-2Galb1-4(Fuca1-3)GlcNAcb1-2Mana1-6(Fuca1-2Galb1-4(Fuca1-3)GlcNAcb1-4(Fuca1-2Galb1-4(Fuca1-3)GlcNAcb1-2)Mana1-3)Manb1-4GlcNAcb1-4GlcNAcb-Sp12	1.5	5.5	6.0	5.9	5.5
213		Mana1-2Mana1-6(Mana1-2Mana1-3)Mana1-6(Mana1-2Mana1-2Mana1-3)Manb1-4GlcNAcb1-4GlcNAcb-Sp12	4.6	5.5	8.5	12.5	2.9

164		Galb1-4GlcNAcb1-3Galb1-4GlcNAcb-Sp0	4.5	5.4	7.3	10.5	1.2
459		Galb1-4GlcNAcb1-6(Galb1-4GlcNAcb1-2)Mana1-6(Galb1-4GlcNAcb1-2Mana1-3)Manb1-4GlcNAcb1-4GlcNAcb-Sp19	3.2	5.4	6.9	14.9	4.4
248		Neu5Aca2-3Galb1-3GlcNAcb1-3Galb1-4GlcNAcb-Sp0	4.3	5.3	3.8	6.6	2.9
72	14	Fuca1-2Galb1-4(Fuca1-3)GlcNAcb-Sp0	3.6	5.3	7.3	10.4	6.5
370		Galb1-4GlcNAcb1-2Mana1-6(Galb1-4GlcNAcb1-4(Galb1-4GlcNAcb1-2)Mana1-3)Manb1-4GlcNAcb1-4GlcNAcb-Sp21	4.2	5.3	8.9	10.4	2.2
41		(6P)Mana-Sp8	2.2	5.2	11.1	31.9	6.6
434		GlcNAcb1-6(GlcNAcb1-2)Mana1-6(GlcNAcb1-4)(GlcNAcb1-2Mana1-3)Manb1-4GlcNAcb1-4GlcNAcb-Sp21	1.0	5.2	7.4	7.3	4.9
510		Galb1-3GlcNAca1-3Galb1-4GlcNAcb-Sp8	2.1	5.2	15.2	14.9	7.4
563		GalNAcb1-3GlcNAcb-Sp0	4.2	5.2	8.5	8.2	1.4
195		GlcNAcb1-6Galb1-4GlcNAcb-Sp8	3.8	5.1	5.7	7.8	5.6
124		Gala1-4GlcNAcb-Sp8	3.5	5.1	7.5	9.7	4.7
250		Neu5Aca2-3Galb1-3GlcNAcb-Sp0	4.3	5.1	5.3	3.9	3.4
90		GalNAca1-3(Fuca1-2)Galb-Sp8	3.0	5.1	3.9	8.3	8.8
378		Neu5Aca2-6Galb1-4GlcNAcb1-3GalNAcb-Sp14	3.6	5.1	7.4	8.3	2.8
188		GlcNAcb1-6(GlcNAcb1-4)GalNAca-Sp8	3.9	5.1	2.2	0.0	5.2
530		Neu5Aca2-3Galb1-3GlcNAcb1-4Galb1-4Glc-Sp0	1.2	5.0	10.5	25.4	11.7
34		(3S)Galb1-4(6S)GlcNAcb-Sp0	3.0	5.0	8.0	11.0	3.9
224		Neu5Aca2-3Galb1-3GalNAca-Sp8	1.6	5.0	5.4	10.3	4.1
479		Neu5Aca2-3Galb1-4GlcNAcb1-2Mana-Sp0	4.0	5.0	9.6	17.9	5.4
253		Neu5Aca2-3Galb1-4(Fuca1-3)(6S)GlcNAcb-Sp8	3.3	4.9	7.6	19.1	6.7
426		Gala1-3Galb1-3GlcNAcb1-3GalNAcb-Sp14	4.1	4.9	6.6	13.8	6.0
174		GlcNAca1-3Galb1-4GlcNAcb-Sp8	2.4	4.9	5.5	3.8	4.4
377		Neu5Aca2-3Galb1-4GlcNAcb1-3GalNAcb-Sp14	1.9	4.9	5.5	7.6	3.7
386	33	Galb1-4(Fuca1-3)GlcNAcb1-6(Fuca1-4(Fuca1-2Galb1-3)GlcNAcb1-3)Galb1-4Glc-Sp21	1.1	4.9	8.4	8.0	4.4
417	37	Fuca1-2Galb1-4(Fuca1-3)GlcNAcb1-3GalNAca-Sp14	7.6	4.9	7.3	8.1	3.5
453		Neu5Aca2-8Neu5Aca2-3Galb1-3GalNAcb1-4(Neu5Aca2-8Neu5Aca2-3)Galb1-4Glc-Sp0	6.0	4.8	5.6	9.8	3.0
219		Neu5Aca2-3Galb1-4GlcNAcb1-3Galb1-4(Fuca1-3)GlcNAcb-Sp0	1.9	4.8	5.5	5.0	2.7
126		Galb1-2Galb-Sp8	3.0	4.8	9.5	16.4	10.5
344		GlcNAca1-4Galb1-4GlcNAcb1-3Galb1-4GlcNAcb-Sp0	3.6	4.8	5.6	4.6	5.0

20		Galb1-4GlcNAcb1-6(Galb1-4GlcNAcb1-3)GalNAc-Sp14	2.9	4.8	6.9	8.4	3.4
167		Galb1-4GlcNAcb1-6(Galb1-3)GalNAca-Sp8	6.8	4.8	7.8	9.3	6.4
388		Galb1-4GlcNAcb1-6(Galb1-4GlcNAcb1-2)Mana1-6(Galb1-4GlcNAcb1-4(Galb1-4GlcNAcb1-2)Mana1-3)Manb1-4GlcNAcb1-4GlcNAcb-Sp21	2.5	4.8	8.2	8.6	5.3
220		(3S)Galb1-4(Fuca1-3)(6S)GlcNAcb-Sp8	3.3	4.8	14.3	26.4	13.9
342		GlcNAca1-4Galb1-4GlcNAcb1-3Galb1-4Glc-Sp0	3.3	4.7	3.2	3.6	4.0
536		GlcNAcb1-3Galb1-4GlcNAcb1-6(GlcNAcb1-3)Galb1-4GlcNAc-Sp0	2.9	4.7	4.8	6.4	3.4
231		Neu5Aca2-3(6S)Galb1-4(Fuca1-3)GlcNAcb-Sp8	1.7	4.7	10.6	20.5	10.9
573		Galb1-3GlcNAcb1-3Galb1-4GlcNAcb1-6(Galb1-3GlcNAcb1-3Galb1-4GlcNAcb1-2)Mana1-6(Galb1-3GlcNAcb1-3Galb1-4GlcNAcb1-2Mana1-3)Manb1-4GlcNAcb1-4(Fuca1-6)GlcNAcb-Sp24	4.6	4.7	9.5	30.0	3.1
478		Neu5Aca2-6Galb1-4GlcNAcb1-6(Galb1-3GlcNAcb1-3)Galb1-4Glc-Sp21	3.3	4.7	7.5	14.7	3.6
449		Galb1-4GlcNAcb1-2Mana-Sp0	2.3	4.7	5.9	10.0	6.8
210		Mana1-2Mana1-3Mana-Sp9	2.9	4.7	4.7	4.7	3.8
328		Galb1-4(Fuca1-3)GlcNAcb1-2Mana1-6(Galb1-4(Fuca1-3)GlcNAcb1-2Mana1-3)Manb1-4GlcNAcb1-4GlcNAcb-Sp20	4.0	4.7	8.4	19.9	5.2
209		Mana1-2Mana1-6(Mana1-2Mana1-3)Mana-Sp9	1.2	4.7	9.1	7.7	7.4
392		Galb1-3GlcNAcb1-3GalNAca-Sp14	4.2	4.7	5.3	9.1	2.8
407		Galb1-3GlcNAcb1-6Galb1-4GlcNAcb-Sp0	11.7	4.7	4.5	6.8	1.7
337		GalNAca1-3(Fuca1-2)Galb1-4GlcNAcb1-3Galb1-4GlcNAcb1-3Galb1-4GlcNAcb-Sp0	3.5	4.6	6.4	9.2	4.5
376	31	Fuca1-4(Fuca1-2Galb1-3)GlcNAcb1-2Mana1-3(Fuca1-4(Fuca1-2Galb1-3)GlcNAcb1-2Mana1-3)Manb1-4GlcNAcb1-4GlcNAcb-Sp19	5.3	4.6	6.4	10.3	5.9
128		Galb1-3GlcNAcb1-3Galb1-4(Fuca1-3)GlcNAcb-Sp0	5.5	4.6	8.4	10.4	7.1
403		GalNAca1-3GalNAcb1-3Gala1-4Galb1-4GlcNAcb-Sp0	3.0	4.6	6.8	7.6	3.1
149		Galb1-3GlcNAcb1-3Galb1-4Glc-Sp10	0.8	4.6	5.6	7.9	5.2
95		GalNAcb1-3GalNAca-Sp8	2.0	4.6	5.2	2.5	3.8
87		GalNAca1-3(Fuca1-2)Galb1-4GlcNAcb-Sp8	3.0	4.6	4.8	8.1	3.9
431		Fuca1-3GlcNAcb1-6(Galb1-4GlcNAcb1-3)Galb1-4Glc-Sp21	7.5	4.6	6.7	8.5	2.7
416		GalNAca1-3GalNAcb1-3Gala1-4Galb1-4Glc-Sp0	3.0	4.6	5.0	6.6	3.9
252		Neu5Aca2-3Galb1-4(6S)GlcNAcb-Sp8	3.3	4.5	10.7	23.9	7.8
85		(3S)Galb1-4(Fuca1-3)Glc-Sp0	1.9	4.5	8.3	13.9	9.4

45		(6S)Galb1-4(6S)GlcB-Sp8	2.7	4.5	8.9	9.8	3.9
139		Neu5Aca2-6(Galb1-3)GlcNAcb1-4Galb1-4GlcB-Sp10	2.5	4.5	6.1	11.3	5.0
513		(6S)GalNAcb1-4GlcNAc-Sp8	3.7	4.5	9.0	15.7	4.3
29		(3S)Galb1-3GalNAca-Sp8	1.5	4.5	5.7	5.7	5.8
381		Galb1-3GalNAca1-3(Fuca1-2)Galb1-4Glc-Sp0	4.2	4.5	3.8	6.9	1.9
322		Neu5Aca2-8Neu5AcB-Sp17	4.2	4.4	11.8	13.3	6.2
165		Galb1-4GlcNAcb1-3Galb1-4GlcB-Sp0	3.4	4.4	6.3	8.6	3.4
567		GlcNAb1-3Galb1-3GalNAc-Sp14	0.3	4.4	2.7	6.1	2.5
402		Galb1-4(Fuca1-3)GlcNAcb1-3GalNAca-Sp14	5.3	4.4	6.1	12.4	2.8
528		Gala1-3Galb1-3GlcNAcb1-2Mana-Sp0	3.6	4.4	7.5	14.4	5.8
177		GlcNAcb1-6(GlcNAcb1-3)GalNAca-Sp8	6.8	4.4	4.8	7.2	2.6
546		GlcNAcb1-3Galb1-4GlcNAcb1-3Galb1-4GlcNAcb1-2Mana1-6(GlcNAcb1-3Galb1-4GlcNAcb1-3Galb1-4GlcNAcb1-2Mana1-3)Manb1-4GlcNAcb1-4GlcNAcb-Sp12	7.4	4.4	6.5	8.2	2.7
51		Mana1-6(Mana1-3)Manb1-4GlcNAcb1-4GlcNAcb-Sp13	1.1	4.4	7.3	5.7	6.0
70	12	Fuca1-2Galb1-4(Fuca1-3)GlcNAcb1-3Galb1-4(Fuca1-3)GlcNAcb-Sp0	2.9	4.4	4.8	4.3	3.5
308		GlcAb1-3GlcNAcb-Sp8	4.5	4.4	5.3	7.1	1.4
331		Neu5Aca2-6Galb1-4GlcNAcb1-3Galb1-3GlcNAcb-Sp0	3.5	4.4	5.5	8.1	2.3
394		GalNAca1-3(Fuca1-2)Galb1-3GalNAca1-3(Fuca1-2)Galb1-4GlcNAcb-Sp0	3.8	4.4	4.9	9.5	4.4
523		Gala1-3(Fuca1-2)Galb1-4GlcNAcb1-2Mana-Sp0	3.7	4.3	3.9	6.6	4.4
518		Galb1-4(6P)GlcNAcb-Sp0	1.4	4.3	5.4	25.4	6.5
425		GalNAca1-3(Fuca1-2)Galb1-3GlcNAcb1-3GalNAc-Sp14	4.1	4.3	6.3	7.7	6.4
469		Gala1-3(Fuca1-2)Galb1-3GalNAcb-Sp8	8.6	4.3	5.4	3.9	3.5
86		GalNAca1-3(Fuca1-2)Galb1-4GlcNAcb-Sp0	1.1	4.3	8.5	6.7	6.0
295		Neu5Aca2-3Galb1-3GlcNAcb1-3Galb1-3GlcNAcb-Sp0	4.0	4.3	6.2	6.6	3.1
438		Galb1-4GlcNAcb1-6(Galb1-4GlcNAcb1-2)Mana1-6(GlcNAcb1-4)(Galb1-4GlcNAcb1-2Mana1-3)Manb1-4GlcNAcb1-4GlcNAc-Sp21	2.5	4.3	3.6	4.2	4.7
305		Galb1-4GlcNAca1-6Galb1-4GlcNAcb-Sp0	7.0	4.3	7.6	12.7	3.6
291		Galb1-4(Fuca1-3)(6S)GlcNAcb-Sp0	3.5	4.3	7.3	10.3	5.9
508		GlcNAcb1-6(GlcNAcb1-2)Mana1-6(GlcNAcb1-4)(GlcNAcb1-4(GlcNAcb1-2)Mana1-3)Manb1-4GlcNAcb1-4(Fuca1-6)GlcNAc-Sp21	1.2	4.3	9.7	8.7	5.9
279		Neu5AcB2-6GalNAca-Sp8	2.2	4.3	7.5	14.4	9.9
30		(3S)Galb1-3GlcNAcb-Sp0	2.9	4.3	7.0	7.5	6.0
111		Gala1-3GalNAca-Sp8	1.0	4.2	6.5	9.7	6.8

379		Neu5Aca2-3Galb1-4(Fuca1-3)GlcNAcb1-3GalNAca-Sp14	5.3	4.2	5.9	6.9	2.1
28		(3S)Galb1-3(Fuca1-4)GlcNAcb-Sp8	3.7	4.2	6.3	8.1	6.4
147		Galb1-3Galb-Sp8	0.8	4.2	4.9	5.0	3.4
408		Galb1-3GlcNAca1-6Galb1-4GlcNAcb-Sp0	11.0	4.2	5.5	4.4	3.0
32		(3S)Galb1-4(Fuca1-3)GlcNAc-Sp0	3.1	4.1	7.6	10.2	4.6
102		Gala1-3(Fuca1-2)Galb1-3GlcNAcb-Sp0	3.4	4.1	8.3	12.2	7.0
21		GlcNAcb1-6(GlcNAcb1-4)(GlcNAcb1-3)GlcNAc-Sp8	4.9	4.1	5.3	8.7	2.1
533		Galb1-4GlcNAcb1-2 Mana1-6(Galb1-4GlcNAcb1-4)(Galb1-4GlcNAcb1-2Mana1-3)Manb1-4GlcNAcb1-4(Fuca1-6)GlcNAc-Sp21	6.5	4.1	6.0	8.7	2.7
356		(6S)GlcNAcb1-3Galb1-4GlcNAcb-Sp0	5.1	4.1	6.2	7.7	2.6
42		(6S)Galb1-4Glc-Sp0	1.0	4.1	7.7	28.0	13.4
506	54	Fuca1-2Galb1-3GlcNAcb1-6(Fuca1-2Galb1-3GlcNAcb1-3)GalNAca-Sp14	0.1	4.1	8.1	14.0	2.1
154		Galb1-4(Fuca1-3)GlcNAcb1-3Galb1-4(Fuca1-3)GlcNAcb-Sp0	4.6	4.1	4.4	7.7	0.8
397		Neu5Aca2-3Galb1-3GlcNAcb1-2Mana1-6(Neu5Aca2-3Galb1-3GlcNAcb1-2Mana1-3)Manb1-4GlcNAcb1-4GlcNAc-Sp19	1.4	4.1	9.7	15.8	14.2
410		Gala1-3(Fuca1-2)Galb1-4(Fuca1-3)Glc-Sp21	1.0	4.1	7.9	10.2	6.4
547		GlcNAcb1-3Galb1-4GlcNAcb1-3Galb1-4GlcNAcb1-2Mana1-6(GlcNAcb1-3Galb1-4GlcNAcb1-3Galb1-4GlcNAcb1-2Mana1-3)Manb1-4GlcNAcb1-4GlcNAcb-Sp25	6.3	4.1	5.1	9.5	2.0
522		Gala1-3Galb1-4GlcNAcb1-2Mana-Sp0	5.5	4.0	6.4	10.3	6.5
233		GalNAcb1-4(Neu5Aca2-3)Galb1-4GlcNAcb-Sp8	1.9	4.0	5.8	10.4	6.8
559		GlcNAcb1-3Galb1-4GlcNAcb1-6(GlcNAcb1-3Galb1-4GlcNAcb1-2)Mana1-6(GlcNAcb1-3Galb1-4GlcNAcb1-2Man a1-3)Manb1-4GlcNAcb1-4GlcNAc-Sp24	4.1	4.0	1.0	-0.9	3.4
173		Galb1-4Glc-Sp8	2.1	4.0	9.7	19.9	11.8
269		Neu5Aca2-6Galb1-4GlcNAcb-Sp0	3.7	4.0	5.2	8.9	4.9
330		Neu5,9Ac2a2-3Galb1-3GlcNAcb-Sp0	2.5	4.0	6.6	11.3	2.9
399		Galb1-4GlcNAcb1-2Mana1-6(GlcNAcb1-2Mana1-3)Manb1-4GlcNAcb1-4GlcNAc-Sp12	1.0	4.0	5.1	6.4	4.9
419		GalNAca1-3(Fuca1-2)Galb1-4(Fuca1-3)GlcNAcb1-3GalNAc-Sp14	6.3	4.0	7.1	11.7	2.4
267		Neu5Aca2-6GalNAcb1-4GlcNAcb-Sp0	3.0	4.0	6.5	9.1	2.0
473	46	Fuca1-2Galb1-4(Fuca1-3)GlcNAcb1-2Mana1-6(Fuca1-2Galb1-4(Fuca1-3)GlcNAcb1-2Mana1-3)Manb1-4GlcNAcb1-4(Fuca1-6)GlcNAcb-Sp24	4.8	4.0	8.5	10.7	4.7

155		Galb1-4(Fuca1-3)GlcNAcb1-3Galb1-4(Fuca1-3)GlcNAcb1-3Galb1-4(Fuca1-3)GlcNAcb-Sp0	4.8	4.0	6.7	6.4	2.6
166		Galb1-4GlcNAcb1-3Galb1-4Glc-Sp8	5.0	4.0	6.1	5.8	2.3
300		Neu5Aca2-3Galb1-4(Fuca1-3)GlcNAcb1-6(Galb1-3)GalNAca-Sp14	2.9	3.9	4.7	6.5	2.6
108		Gala1-3(Fuca1-2)Galb-Sp8	4.8	3.9	5.3	10.1	1.0
316		Mana1-2Mana1-6(Mana1-3)Mana1-6(Mana1-2Mana1-2Mana1-3)Mana-Sp9	4.6	3.9	6.3	12.4	3.8
119		Gala1-3Galb-Sp8	1.1	3.9	4.1	5.9	4.6
134		GlcNAcb1-6(Galb1-3)GalNAca-Sp8	1.8	3.9	6.3	9.4	4.7
535		Neu5Aca2-3Galb1-4(Fuca1-3)GlcNAcb1-2Mana-Sp0	1.9	3.9	4.6	10.7	2.3
57		Neu5Aca2-6Galb1-4GlcNAcb1-2Mana1-6(Neu5Aca2-6Galb1-4GlcNAcb1-2Man-a1-3)Manb1-4GlcNAcb1-4GlcNAcb-Sp21	1.6	3.9	5.1	7.1	2.4
411		Galb1-4GlcNAcb1-6(Neu5Aca2-6Galb1-3GlcNAcb1-3)Galb1-4Glc-Sp21	2.4	3.9	4.0	8.5	3.0
541		GlcNAcb1-3Galb1-4GlcNAcb1-2Mana1-6(GlcNAcb1-3Galb1-4GlcNAcb1-2Mana1-3)Manb1-4GlcNAcb1-4GlcNAcb-Sp25	0.9	3.8	4.1	6.6	2.5
132		Galb1-4GlcNAcb1-6GalNAca-Sp8	4.4	3.8	6.3	5.4	3.3
236		Neu5Aca2-6(Neu5Aca2-3)GalNAca-Sp8	1.8	3.8	5.8	10.2	2.7
538		Gala1-3(Fuca1-2)Galb1-3GalNAcb1-3Gala1-4Galb1-4Glc-Sp21	5.6	3.8	5.9	10.0	3.2
189		GlcNAcb1-4Galb1-4GlcNAcb-Sp8	4.5	3.8	3.7	6.4	0.8
293		Galb1-4(Fuca1-3)GlcNAcb1-3Galb1-3(Fuca1-4)GlcNAcb-Sp0	4.1	3.8	6.7	10.8	3.7
131		Fuca1-4(Galb1-3)GlcNAcb-Sp8	4.9	3.8	5.6	11.4	0.9
83		GalNAca1-3(Fuca1-2)Galb1-3GlcNAcb-Sp0	3.0	3.8	5.9	3.1	2.1
343		GlcNAca1-4Galb1-4GlcNAcb1-3Galb1-4(Fuca1-3)GlcNAcb1-3Galb1-4(Fuca1-3)GlcNAcb-Sp0	1.7	3.8	5.4	6.5	6.9
71	13	Fuca1-2Galb1-4(Fuca1-3)GlcNAcb1-3Galb1-4(Fuca1-3)GlcNAcb1-3Galb1-4(Fuca1-3)GlcNAcb-Sp0	2.7	3.8	5.7	2.5	2.3
23		6S(3S)Galb1-4GlcNAcb-Sp0	3.6	3.8	9.8	13.6	3.6
184		GlcNAcb1-3Galb1-4GlcNAcb-Sp8	1.2	3.8	5.7	1.7	6.5
238		Neu5Aca2-3GalNAcb1-4GlcNAcb-Sp0	3.4	3.8	6.4	7.7	3.8
389		GlcNAcb1-2Mana1-6(GlcNAcb1-4(GlcNAcb1-2)Mana1-3)Manb1-4GlcNAcb1-4GlcNAc-Sp21	5.9	3.8	6.3	8.9	3.1
584		GlcNAcb1-3Galb1-4GlcNAcb1-3Galb1-4GlcNAcb1-6(GlcNAcb1-3Galb1-4GlcNAcb1-3Galb1-4GlcNAcb1-2)Mana1-6(GlcNAcb1-3Galb1-4GlcNAcb1-3Galb1-4GlcNAcb1-2Mana1-3)Manb1-4GlcNAcb1-4(Fuca1-6)GlcNAcb-Sp24	4.5	3.7	3.3	1.5	2.0
368		Neu5Aca2-6GlcNAcb1-4GlcNAcb1-4GlcNAc-Sp21	3.8	3.7	5.6	4.2	3.1

418		Gala1-3(Fuca1-2)Galb1-4(Fuca1-3)GlcNAcb1-3GalNAc-Sp14	3.0	3.7	5.0	5.4	3.7
127		Galb1-3(Fuca1-4)GlcNAcb1-3Galb1-4(Fuca1-3)GlcNAcb-Sp0	4.1	3.7	5.9	9.6	5.3
183		GlcNAcb1-3Galb1-4GlcNAcb-Sp0	2.1	3.7	4.4	7.9	4.8
43		(6S)Galb1-4Glc-Sp8	1.1	3.7	6.5	10.8	3.4
384		Galb1-4(Fuca1-3)GlcNAcb1-6(Galb1-3GlcNAcb1-3)Galb1-4Glc-Sp21	6.6	3.7	3.7	4.8	1.2
382		Galb1-3GalNAca1-3(Fuca1-2)Galb1-4GlcNAc-Sp0	5.4	3.7	5.0	9.2	2.0
186		GlcNAcb1-3Galb1-4Glc-Sp0	2.2	3.7	4.4	9.9	9.8
182		GlcNAcb1-3Galb-Sp8	0.7	3.7	8.6	12.5	10.2
18		GlcN(Gc)b-Sp8	3.1	3.7	4.5	20.4	7.3
335		GalNAcb1-3Gala1-4Galb1-4GlcNAcb1-3Galb1-4Glc-Sp0	5.7	3.7	8.1	4.9	3.0
511		Galb1-3(6S)GlcNAcb-Sp8	3.2	3.6	7.4	19.7	4.8
436		Galb1-4GlcNAcb1-2Mana1-6(GlcNAcb1-4)(Galb1-4GlcNAcb1-2Mana1-3)Manb1-4GlcNAcb1-4GlcNAc-Sp21	1.4	3.6	5.5	11.3	7.0
175		GlcNAca1-6Galb1-4GlcNAcb-Sp8	5.8	3.6	7.5	8.1	4.1
3		Mana-Sp8	1.4	3.6	8.4	13.5	14.8
153		Galb1-4(Fuca1-3)GlcNAcb-Sp8	3.5	3.6	4.7	2.0	2.0
54		Galb1-4GlcNAcb1-2Mana1-6(Galb1-4GlcNAcb1-2Mana1-3)Manb1-4GlcNAcb1-4GlcNAcb-Sp12	2.9	3.6	4.3	9.0	5.7
441		Galb1-6Galb-Sp10	1.1	3.6	7.4	11.3	4.2
161		Galb1-4GlcNAcb1-3GalNAc-Sp14	0.3	3.6	4.4	14.4	5.3
483		Neu5Aca2-6Galb1-4GlcNAcb1-2Mana1-6(Neu5Aca2-6Galb1-4GlcNAcb1-2Mana1-3)Manb1-4GlcNAcb1-4(Fuca1-6)GlcNAcb-Sp24	1.3	3.6	2.5	4.0	1.7
44		(6S)Galb1-4GlcNAcb-Sp8	1.8	3.6	6.2	7.7	5.7
266		Neu5Aca2-6GalNAca-Sp8	2.9	3.5	5.3	7.5	2.9
140		Galb1-3GalNAca-Sp8	2.2	3.5	4.9	6.7	8.4
150		Galb1-3GlcNAcb-Sp0	3.2	3.5	6.3	9.5	6.0
215		Mana1-2Mana1-2Mana1-6(Mana1-3)Mana-Sp9	6.8	3.5	7.6	10.1	2.4
383		Galb1-3GlcNAcb1-3Galb1-4GlcNAcb1-6(Galb1-3GlcNAcb1-3)Galb1-4Glc-Sp0	5.0	3.5	4.7	5.6	1.4
251		Neu5Aca2-3Galb1-3GlcNAcb-Sp8	4.3	3.5	6.6	6.1	4.3
130		Galb1-3(Fuca1-4)GlcNAc-Sp8	6.6	3.5	5.2	5.9	3.9
26		(3S)Galb1-4(6S)Glc-Sp0	3.4	3.5	15.5	26.1	10.8
200		Glc-Sp8	2.1	3.5	5.9	16.9	10.5
256		Neu5Aca2-3Galb1-4(Fuca1-3)GlcNAcb-Sp8	2.5	3.4	4.8	6.5	4.8
549		Galb1-4GlcNAcb1-3Galb1-4GlcNAcb1-3Galb1-4GlcNAcb1-2Mana1-6(Galb1-4GlcNAcb1-3Galb1-4GlcNAcb1-3Galb1-4GlcNAcb1-2Mana1-3)Manb1-4GlcNAcb1-4GlcNAcb-Sp24	4.8	3.4	4.1	7.2	0.2
491		Galb1-3(Fuca1-4)GlcNAcb1-6GalNAca-Sp14	3.0	3.4	3.9	9.6	1.5

340		GlcNAc1-4Galb1-4GlcNAcb-Sp0	2.2	3.4	5.0	9.6	8.9
504		GalNAcb1-4(Fuca1-3)(6S)GlcNAcb-Sp8	3.0	3.4	7.6	9.5	3.5
120		Gala1-4(Fuca1-2)Galb1-4GlcNAcb-Sp8	8.3	3.4	4.4	4.3	1.9
605		GlcNAcb1-6(Neu5Aca2-3Galb1-3)GalNAca-Sp14	3.5	3.4	1.7	5.7	2.4
242		Neu5Aca2-3Galb1-4(Neu5Aca2-3Galb1-3)GlcNAcb-Sp8	2.4	3.4	6.7	8.6	4.0
204		GlcAb1-3Galb-Sp8	1.4	3.4	4.1	14.4	6.0
338		Neu5Aca2-3Galb1-4(Fuca1-3)GlcNAcb1-6(Neu5Aca2-3Galb1-3)GalNAc-Sp14	2.1	3.4	4.7	7.0	1.2
525		Galb1-3GlcNAcb1-2Mana-Sp0	4.5	3.4	4.9	4.6	0.9
244		Neu5Aca2-6(Neu5Aca2-3Galb1-3)GalNAca-Sp8	2.5	3.4	6.9	14.7	3.1
521		Neu5Aca2-6Galb1-4GlcNAcb1-2Man-Sp0	1.0	3.4	6.2	11.1	11.5
101		Gala1-2Galb-Sp8	1.9	3.4	5.8	11.6	3.8
424		Gala1-3(Fuca1-2)Galb1-3GlcNAcb1-3GalNAc-Sp14	3.2	3.4	6.5	12.6	7.8
534		Fuca1-4(Galb1-3)GlcNAcb1-2 Mana-Sp0	2.3	3.3	5.4	13.4	5.6
190		GlcNAcb1-4GlcNAcb1-4GlcNAcb1-4GlcNAcb1-4GlcNAcb1-Sp8	2.2	3.3	6.0	10.5	2.4
49		Neu5,9Ac2a2-6Galb1-4GlcNAcb-Sp8	1.3	3.3	6.5	3.6	2.5
92		GalNAca1-3GalNAcb-Sp8	2.3	3.3	3.6	2.1	4.1
590		Galb1-4GlcNAcb1-3Galb1-4GlcNAcb1-3GalNAca-Sp14	4.9	3.3	2.0	6.3	1.7
444		(6S)Galb1-3GlcNAcb-Sp0	1.7	3.3	5.4	12.6	8.5
324		Neu5Gcb2-6Galb1-4GlcNAc-Sp8	4.8	3.3	6.2	5.5	3.0
405		Gala1-4Galb1-4GlcNAcb1-2Mana1-6(Gala1-4Galb1-4GlcNAcb1-2Mana1-3)Manb1-4GlcNAcb1-4GlcNAcb-Sp24	6.3	3.3	0.9	1.7	0.1
599		GlcNAcb1-3Galb1-4GlcNAcb1-3Galb1-4GlcNAcb1-3GalNAca-Sp14	3.2	3.3	4.2	9.6	3.5
55		Neu5Aca2-6Galb1-4GlcNAcb1-2Mana1-6(Neu5Aca2-6Galb1-4GlcNAcb1-2Mana1-3)Manb1-4GlcNAcb1-4GlcNAcb-Sp12	2.2	3.3	5.7	7.3	1.6
249	25	Fuca1-2(6S)Galb1-4Glc-Sp0	0.9	3.2	6.8	10.2	2.3
25		(3S)Galb1-4Glc-Sp8	0.7	3.2	6.9	8.3	7.0
292		Galb1-4(Fuca1-3)(6S)Glc-Sp0	1.5	3.2	4.9	8.3	2.9
107		Gala1-3(Fuca1-2)Galb1-4Glc-Sp0	4.0	3.2	5.5	8.1	4.4
432		GlcNAcb1-2Mana1-6(GlcNAcb1-4)(GlcNAcb1-2Mana1-3)Manb1-4GlcNAcb1-4GlcNAc-Sp21	6.9	3.2	5.5	9.0	2.5
554		Neu5Aca2-8Neu5Gca2-3Galb1-4GlcNAc-Sp0	1.3	3.2	6.4	8.6	5.4
88		GalNAca1-3(Fuca1-2)Galb1-4Glc-Sp0	0.9	3.2	5.0	6.4	7.9
59	1	Fuca1-2Galb1-3GalNAcb1-3Gala-Sp9	1.2	3.2	6.2	4.6	2.2
36		(3S)Galb1-4GlcNAcb-Sp0	3.3	3.2	6.6	5.5	2.9
575		GlcNAcb1-3Galb1-4GlcNAcb1-2Mana1-6(GlcNAcb1-3Galb1-4GlcNAcb1-2Mana1-3)Manb1-4GlcNAcb1-4(Fuca1-6)GlcNAcb-Sp24	5.1	3.2	3.8	5.3	0.9

205		GlcAb1-6Galb-Sp8	2.9	3.2	13.7	21.4	7.8
192		GlcNAcb1-4GlcNAcb1-4GlcNAcb-Sp8	4.4	3.2	5.6	8.2	1.9
84		GalNAca1-3(Fuca1-2)Galb1-4(Fuca1-3)GlcNAcb-Sp0	3.2	3.2	5.6	6.3	2.1
493		(3S)Galb1-3(Fuca1-4)GlcNAcb-Sp0	4.3	3.2	5.3	6.9	3.2
593		Neu5Aca2-3Galb1-4GlcNAcb1-3Galb1-4GlcNAcb1-3GalNAca-Sp14	4.3	3.2	6.1	9.7	3.9
115		Gala1-3Galb1-3GlcNAcb-Sp0	0.8	3.2	6.2	7.8	9.3
270		Neu5Aca2-6Galb1-4GlcNAcb-Sp8	3.4	3.2	3.3	3.7	2.0
243		Neu5Aca2-3Galb1-3(6S)GalNAca-Sp8	2.7	3.2	9.6	21.3	8.5
282		Neu5Gca2-3Galb1-3GlcNAcb-Sp0	3.4	3.2	6.2	9.1	3.7
480		Neu5Aca2-3Galb1-4GlcNAcb1-6GalNAca-Sp14	1.8	3.1	8.6	18.5	3.6
202		GlcAa-Sp8	0.9	3.1	7.2	8.1	5.6
375		Gala1-3(Fuca1-2)Galb1-3GlcNAcb1-2Mana1-6(Gala1-3(Fuca1-2)Galb1-3GlcNAcb1-2Mana1-3)Manb1-4GlcNAcb1-4GlcNAcb-Sp20	1.0	3.1	3.8	1.9	3.4
539		Galb1-3GalNAcb1-3Gal-Sp21	0.9	3.1	5.7	11.1	4.1
91		GalNAca1-3(Fuca1-2)Galb-Sp18	2.9	3.1	4.8	5.6	2.7
172		Galb1-4Glc-Sp0	0.7	3.1	4.9	8.4	8.9
284		Neu5Gca2-3Galb1-4GlcNAcb-Sp0	2.8	3.1	6.0	9.9	1.9
46		Neu5Aca2-3(6S)Galb1-4GlcNAcb-Sp8	1.8	3.1	5.6	10.0	6.1
404		Gala1-4Galb1-3GlcNAcb1-2Mana1-6(Gala1-4Galb1-3GlcNAcb1-2Mana1-3)Manb1-4GlcNAcb1-4GlcNAcb-Sp19	5.1	3.1	2.6	5.7	1.2
156		Galb1-4(6S)Glc-Sp0	1.6	3.1	5.4	18.0	5.9
603		Neu5Aca2-6Galb1-4GlcNAcb1-6(Galb1-3)GalNAca-Sp14	0.9	3.1	2.1	5.8	1.9
257		Neu5Aca2-3Galb1-4(Fuca1-3)GlcNAcb1-3Galb-Sp8	1.1	3.1	5.3	5.7	5.9
474	47	Fuca1-2Galb1-3(Fuca1-4)GlcNAcb1-2Mana1-6(Fuca1-2Galb1-3(Fuca1-4)GlcNAcb1-2Mana1-3)Manb1-4GlcNAcb1-4(Fuca1-6)GlcNAcb1-4(Fuca1-6)GlcNAcb-Sp19	1.9	3.1	5.2	15.6	3.8
481		Neu5Aca2-6Galb1-4GlcNAcb1-6GalNAca-Sp14	4.2	3.1	8.4	18.5	6.5
336		GalNAca1-3(Fuca1-2)Galb1-4GlcNAcb1-3Galb1-4GlcNAcb-Sp0	6.3	3.0	4.2	6.1	2.7
97		GalNAcb1-3Gala1-4Galb1-4GlcNAcb-Sp0	4.6	3.0	6.3	5.6	2.1
280		Neu5Acb2-6Galb1-4GlcNAcb-Sp8	0.9	3.0	8.1	5.0	5.5
519		(6P)Galb1-4GlcNAcb-Sp0	1.1	3.0	7.1	10.8	15.8
281		Neu5Gca2-3Galb1-3(Fuca1-4)GlcNAcb-Sp0	3.0	3.0	5.8	3.7	4.6
152		Galb1-4(Fuca1-3)GlcNAcb-Sp0	4.8	3.0	6.6	7.8	3.7
380		GalNAcb1-4GlcNAcb1-2Mana1-6(GalNAcb1-4GlcNAcb1-2Mana1-3)Manb1-4GlcNAcb1-4GlcNAcb-Sp12	1.0	3.0	0.4	5.7	0.0
113		Gala1-3GalNAcb-Sp8	0.7	3.0	10.4	12.7	7.9

406		Gala1-3Galb1-4GlcNAcb1-3GalNAca-Sp14	4.0	3.0	4.0	4.8	2.2
442		Neu5Aca2-3Galb1-4GlcNAcb1-3Galb-Sp8	2.8	3.0	3.4	8.3	4.5
47		(6S)GlcNAcb-Sp8	4.0	3.0	7.5	10.5	4.1
298		(6S)Galb1-4(6S)GlcNAcb-Sp0	2.7	3.0	9.2	9.4	12.0
37		(3S)Galb1-4GlcNAcb-Sp8	1.3	2.9	4.6	8.2	3.3
439		Galb1-4GlcNAcb1-6(Galb1-4GlcNAcb1-2)Mana1-6(GlcNAcb1-4)(Galb1-4GlcNAcb1-4(Galb1-4GlcNAcb1-2)Mana1-3)Manb1-4GlcNAcb1-4GlcNAc-Sp21	5.3	2.9	6.0	10.4	1.5
245		Neu5Aca2-6(Neu5Aca2-3Galb1-3)GalNAca-Sp14	2.4	2.9	3.5	4.1	5.6
117		Gala1-3Galb1-4Glc-Sp0	2.4	2.9	11.8	10.2	9.7
482		Neu5Aca2-6Galb1-4 GlcNAcb1-6(Neu5Aca2-6Galb1-4GlcNAcb1-3)GalNAca-Sp14	2.0	2.9	2.2	7.6	2.8
191		GlcNAcb1-4GlcNAcb1-4GlcNAcb1-4GlcNAcb1-4GlcNAcb1-Sp8	3.8	2.9	7.0	4.1	2.1
246		Neu5Aca2-3Galb-Sp8	2.4	2.9	4.3	9.5	5.1
122		Gala1-4Galb1-4GlcNAcb-Sp8	4.3	2.9	5.0	7.3	3.9
400		Neu5Aca2-3Galb1-3GlcNAcb1-3GalNAca-Sp14	2.3	2.9	4.0	5.6	5.0
4		GalNAca-Sp8	1.5	2.9	4.9	10.7	8.1
163		Galb1-4GlcNAcb1-3Galb1-4GlcNAcb1-3Galb1-4GlcNAcb-Sp0	2.7	2.9	5.4	8.2	4.7
185		GlcNAcb1-3Galb1-4GlcNAcb1-3Galb1-4GlcNAcb-Sp0	3.5	2.9	5.6	9.2	3.8
38		(3S)Galb-Sp8	0.5	2.9	8.9	18.3	14.1
287		Neu5Gca2-6Galb1-4GlcNAcb-Sp0	4.7	2.9	1.2	2.0	1.7
496		Gala1-3Galb1-4GlcNAcb1-6GalNAca-Sp14	2.9	2.9	5.7	6.9	2.6
145		Galb1-3GalNAcb1-4(Neu5Aca2-3)Galb1-4Glc-Sp0	3.1	2.9	5.4	7.0	4.1
11		Neu5Acb-Sp8	1.3	2.9	5.2	7.6	2.1
586		GlcNAcb1-3Galb1-4GlcNAcb1-3Galb1-4GlcNAcb1-3Galb1-4GlcNAcb1-6(GlcNAcb1-3Galb1-4GlcNAcb1-3Galb1-4GlcNAcb1-3Galb1-4GlcNAcb1-2)Mana1-6(GlcNAcb1-3Galb1-4GlcNAcb1-3Galb1-4GlcNAcb1-3Galb1-4GlcNAcb1-2Mana1-3)Manb1-4GlcNAcb1-4(Fuca1-6)GlcNAcb-Sp24	3.6	2.9	3.1	2.6	1.4
290		Galb1-3GlcNAcb1-3Galb1-3GlcNAcb-Sp0	2.0	2.8	6.4	7.1	3.0
334		Gala1-4Galb1-4GlcNAcb1-3Galb1-4Glc-Sp0	5.4	2.8	4.2	3.9	1.6
365		Galb1-4GlcNAcb1-2Mana1-6(Mana1-3)Manb1-4GlcNAcb1-4GlcNAcb-Sp12	1.9	2.8	1.9	5.1	1.2
116		Gala1-3Galb1-4GlcNAcb-Sp8	3.9	2.8	5.1	12.6	4.2
13		Glc-Sp8	1.4	2.8	10.0	22.6	9.6
199		Glc-Sp8	0.4	2.8	6.5	10.5	11.5

207		KDNa2-3Galb1-4GlcNAcb-Sp0	2.0	2.8	4.9	6.4	0.8
157		Galb1-4(6S)Glc-Sp8	2.3	2.8	5.2	16.1	4.8
516		(3S)GalNAcb1-4GlcNAc-Sp8	3.2	2.8	6.7	7.5	4.2
93		GalNAca1-3Galb-Sp8	2.4	2.8	2.5	3.3	3.3
537		GalNAca1-3(Fuca1-2)Galb1-3GalNAcb1-3Gala1-4Galb1-4Glc-Sp21	5.9	2.8	8.5	7.1	4.6
176		GlcNAcb1-2Galb1-3GalNAca-Sp8	3.3	2.8	4.5	2.9	2.4
351		Galb1-4GlcNAcb1-2Mana1-6Manb1-4GlcNAcb1-4GlcNAc-Sp12	3.0	2.7	5.4	9.0	5.1
358		KDNa2-6Galb1-4GlcNAc-Sp0	5.1	2.7	4.4	6.9	2.3
143		Galb1-3GalNAcb-Sp8	7.2	2.7	3.5	5.3	2.1
315		Mana1-6(Mana1-3)Mana1-6(Mana1-3)Manb-Sp10	0.9	2.7	5.6	7.5	3.8
367		Neu5Aca2-6GlcNAcb1-4GlcNAc-Sp21	2.9	2.7	3.4	3.2	2.5
255		Neu5Aca2-3Galb1-4(Fuca1-3)GlcNAcb-Sp0	0.6	2.7	7.5	6.8	3.7
211		Mana1-6(Mana1-2Mana1-3)Mana1-6(Mana1-2Mana1-3)Manb1-4GlcNAcb1-4GlcNAcb-Sp12	0.6	2.7	4.1	7.6	6.1
329		Neu5,9Ac2a2-3Galb1-4GlcNAcb-Sp0	1.9	2.7	5.0	7.5	3.0
144		Galb1-3GalNAcb1-3Gala1-4Galb1-4Glc-Sp0	2.8	2.7	5.9	6.0	2.4
33		(3S)Galb1-4(Fuca1-3)GlcNAc-Sp8	3.0	2.7	4.5	4.9	0.8
8		Rhaa-Sp8	1.5	2.7	3.0	5.0	0.1
228		Neu5Aca2-8Neu5Aca2-8Neu5Aca2-3Galb1-4Glc-Sp0	2.0	2.6	4.2	4.6	1.2
414		Gala1-3(Fuca1-2)Galb1-4GlcNAcb1-3GalNAca-Sp14	2.4	2.6	4.2	5.9	3.9
234		GalNAcb1-4(Neu5Aca2-3)Galb1-4Glc-Sp0	0.9	2.6	4.9	8.7	9.5
133		Galb1-4GlcNAcb1-6GalNAc-Sp14	1.9	2.6	11.6	24.8	7.3
339		GlcNAca1-4Galb1-4GlcNAcb1-3Galb1-4GlcNAcb1-3Galb1-4GlcNAcb-Sp0	3.3	2.6	4.6	8.3	2.8
283		Neu5Gca2-3Galb1-4(Fuca1-3)GlcNAcb-Sp0	2.9	2.6	5.5	6.4	2.1
514		(3S)GalNAcb1-4(3S)GlcNAc-Sp8	2.6	2.6	3.9	9.0	4.2
129		Galb1-3(Fuca1-4)GlcNAc-Sp0	4.2	2.6	5.8	7.1	3.7
232		GalNAcb1-4(Neu5Aca2-3)Galb1-4GlcNAcb-Sp0	0.8	2.6	6.3	4.4	4.4
52		GlcNAcb1-2Mana1-6(GlcNAcb1-2Mana1-3)Manb1-4GlcNAcb1-4GlcNAcb-Sp12	2.4	2.6	3.3	5.0	3.5
555		Neu5Gca2-8Neu5Aca2-3Galb1-4GlcNAc-Sp0	1.4	2.6	4.1	7.9	5.0
121		Gala1-4Galb1-4GlcNAcb-Sp0	2.8	2.5	5.4	5.0	1.9
301		Galb1-3Galb1-4GlcNAcb-Sp8	2.3	2.5	5.3	5.7	2.9
310		GlcNAcb1-3Man-Sp10	2.1	2.5	3.4	1.2	1.7

572		Galb1-3GlcNAcb1-3Galb1-4GlcNAcb1-3Galb1-4GlcNAcb1-6(Galb1-3GlcNAcb1-3Galb1-4GlcNAcb1-3Galb1-4GlcNAcb1-2)Mana1-6(Galb1-3GlcNAcb1-3Galb1-4GlcNAcb1-3Galb1-4GlcNAcb1-2Mana1-3)Manb1-4GlcNAcb1-4(Fuca1-6)GlcNAcb-Sp24	0.5	2.5	8.9	15.2	3.6
40		(4S)Galb1-4GlcNAcb-Sp8	1.0	2.5	5.1	16.1	13.7
31		(3S)Galb1-3GlcNAcb-Sp8	2.6	2.5	5.9	5.6	2.8
118		Gala1-3Galb1-4Glc-Sp10	3.1	2.5	6.0	6.2	2.1
171		Galb1-4GlcNAcb-Sp23	1.3	2.5	6.1	7.6	3.3
151		Galb1-3GlcNAcb-Sp8	1.9	2.5	6.8	2.6	3.4
10		Neu5Aca-Sp11	1.5	2.5	6.5	10.7	3.8
278		Galb1-3(Fuca1-4)GlcNAcb1-3Galb1-3(Fuca1-4)GlcNAcb-Sp0	0.5	2.5	6.7	6.2	2.9
520		GalNAca1-3(Fuca1-2)Galb1-4GlcNAcb1-6GalNAc-Sp14	2.2	2.5	4.7	7.3	2.1
363	29	Fuca1-2Galb1-4(Fuca1-3)GlcNAcb1-2Mana1-6(Fuca1-2Galb1-4(Fuca1-3)GlcNAcb1-2Mana1-3)Manb1-4GlcNAcb1-4GlcNAcb-Sp20	2.0	2.5	1.1	1.7	1.4
325		Galb1-3GlcNAcb1-2Mana1-6(Galb1-3GlcNAcb1-2Mana1-3)Manb1-4GlcNAcb1-4GlcNAcb-Sp19	1.9	2.5	5.2	14.6	0.7
254		Neu5Aca2-3Galb1-4(Fuca1-3)GlcNAcb1-3Galb1-4(Fuca1-3)GlcNAcb1-3Galb1-4(Fuca1-3)GlcNAcb-Sp0	1.0	2.5	3.6	3.2	2.3
138		Neu5Acb2-6(Galb1-3)GalNAca-Sp8	0.6	2.4	7.8	6.3	5.6
265		Neu5Aca2-3Galb1-4Glc-Sp8	1.8	2.4	4.6	5.1	3.3
455		GalNAca1-3(Fuca1-2)Galb1-4GlcNAcb1-2Mana1-6(GalNAca1-3(Fuca1-2)Galb1-4GlcNAcb1-2Mana1-3)Manb1-4GlcNAcb1-4(Fuca1-6)GlcNAcb-Sp22	5.2	2.4	6.3	7.2	4.4
81		Fuca1-4GlcNAcb-Sp8	0.5	2.4	4.0	4.0	1.3
544		Neu5Gca2-3Galb1-4GlcNAcb1-3Galb1-4GlcNAcb1-2Mana1-6(Neu5Gca2-3Galb1-4GlcNAcb1-3Galb1-4GlcNAcb1-2Mana1-3)Manb1-4GlcNAcb1-4GlcNAcb-Sp24	2.6	2.4	2.3	2.9	2.7
277		Neu5Aca2-8Neu5Aca2-3Galb1-4Glc-Sp0	0.5	2.4	5.6	15.8	5.7
484		Neu5Aca2-3Galb1-4GlcNAcb1-2Mana1-6(Neu5Aca2-3Galb1-4GlcNAcb1-2Mana1-3)Manb1-4GlcNAcb1-4(Fuca1-6)GlcNAcb-Sp24	1.3	2.4	3.4	6.8	3.3
162		Galb1-4GlcNAcb1-3Galb1-4(Fuca1-3)GlcNAcb1-3Galb1-4(Fuca1-3)GlcNAcb-Sp0	4.1	2.4	5.8	11.9	2.4
16		GlcNAcb-Sp0	0.1	2.4	3.4	11.7	8.4
136		Neu5Aca2-6(Galb1-3)GalNAca-Sp8	0.6	2.4	7.6	7.8	4.3

373		Gala1-3Galb1-4(Fuca1-3)GlcNAcb1-2Mana1-6(Gala1-3Galb1-4(Fuca1-3)GlcNAcb1-2Mana1-3)Manb1-4GlcNAcb1-4GlcNAcb-Sp20	1.1	2.4	4.1	3.0	1.5
350		Galb1-4GlcNAcb1-2Mana1-3Manb1-4GlcNAcb1-4GlcNAc-Sp12	3.0	2.4	5.1	6.9	2.6
169		Galb1-4GlcNAcb-Sp0	1.6	2.3	3.8	4.5	3.5
553		Neu5Gca2-8Neu5Gca2-3Galb1-4GlcNAc-Sp0	0.2	2.3	3.9	12.2	4.2
307		GalNAcb1-3Galb-Sp8	3.2	2.3	5.3	7.9	0.1
571		(3S)GlcAb1-3Galb1-4GlcNAcb1-2Mana-Sp0	2.8	2.3	2.8	15.7	6.7
437		Galb1-4GlcNAcb1-2Mana1-6(GlcNAcb1-4)(Galb1-4GlcNAcb1-4(Galb1-4GlcNAcb1-2)Mana1-3)Manb1-4GlcNAcb1-4GlcNAc-Sp21	4.2	2.3	6.0	11.6	2.9
100		GalNAcb1-4GlcNAcb-Sp8	2.1	2.3	6.6	9.1	4.1
398		GlcNAcb1-2Mana1-6(Galb1-4GlcNAcb1-2Mana1-3)Manb1-4GlcNAcb1-4GlcNAc-Sp12	1.9	2.3	5.0	8.4	2.1
1		Gala-Sp8	1.0	2.3	7.5	8.5	9.4
259		Neu5Aca2-3Galb1-4GlcNAcb1-3Galb1-4GlcNAcb1-3Galb1-4GlcNAcb-Sp0	4.1	2.3	3.1	1.8	1.0
123		Gala1-4Galb1-4Glc-Sp0	1.1	2.3	5.1	5.9	3.2
602		Neu5Aca2-6Galb1-4GlcNAcb1-3Galb1-4GlcNAcb1-6(Galb1-3)GalNAca-Sp14	1.4	2.3	3.1	10.2	2.6
352		Mana1-6(Galb1-4GlcNAcb1-2Mana1-3)Manb1-4GlcNAcb1-4GlcNAcb-Sp12	3.6	2.3	4.8	6.4	1.1
235		Neu5Aca2-3Galb1-3GalNAcb1-4(Neu5Aca2-3)Galb1-4Glc-Sp0	2.7	2.3	3.6	4.4	1.2
600		Galb1-4GlcNAcb1-3Galb1-3GalNAca-Sp14	0.3	2.3	7.6	11.0	2.1
258		Neu5Aca2-3Galb1-4(Fuca1-3)GlcNAcb1-3Galb1-4GlcNAcb-Sp8	4.7	2.2	1.7	2.5	-0.8
2		Glc-Sp8	2.9	2.2	12.4	23.8	9.7
512		(6S)(4S)GalNAcb1-4GlcNAc-Sp8	2.6	2.2	5.3	6.0	5.2
526		Gala1-3(Fuca1-2)Galb1-3GlcNAcb1-6GalNAc-Sp14	4.2	2.2	1.8	9.9	1.8
218		Manb1-4GlcNAcb-Sp0	1.6	2.2	4.0	4.0	2.0
488	48	Neu5Aca2-6Galb1-4GlcNAcb1-6(Fuca1-2Galb1-4(Fuca1-3)GlcNAcb1-3)Galb1-4Glc-Sp21	2.4	2.2	5.6	15.5	2.5
591		Galb1-4GlcNAcb1-3Galb1-4GlcNAcb1-6(Galb1-3)GalNAca-Sp14	3.3	2.2	2.5	11.0	1.1
566		Galb1-4GlcNAcb1-3Galb1-4GlcNAcb1-3Galb1-4GlcNAcb1-3Galb1-4GlcNAcb1-2Mana1-6(Galb1-4GlcNAcb1-3Galb1-4GlcNAcb1-3Galb1-4GlcNAcb1-3Galb1-4GlcNAcb1-2Mana1-3)Manb1-4GlcNAcb1-4GlcNAcb-Sp25	0.5	2.2	3.7	4.1	1.8
345		GlcNAca1-4Galb1-3GalNAc-Sp14	-1.5	2.2	4.3	4.0	5.9

135		GlcNAcb1-6(Galb1-3)GalNAca-Sp14	0.3	2.0	3.0	4.8	2.8
14		Manb-Sp8	0.4	2.0	12.9	26.7	14.2
214		Mana1-6(Mana1-3)Mana-Sp9	7.2	2.0	3.1	3.2	0.5
472		Neu5Aca2-3Galb1-4GlcNAcb1-6(Neu5Aca2-3Galb1-4GlcNAcb1-3)GalNAca-Sp14	0.5	1.9	2.8	3.6	1.7
372		Gala1-3(Fuca1-2)Galb1-4GlcNAcb1-2Mana1-6(Gala1-3(Fuca1-2)Galb1-4GlcNAcb1-2Mana1-3)Manb1-4GlcNAcb1-4GlcNAcb-Sp20	1.1	1.9	3.2	4.5	0.5
374		GalNAca1-3(Fuca1-2)Galb1-3GlcNAcb1-2Mana1-6(GalNAca1-3(Fuca1-2)Galb1-3GlcNAcb1-2Mana1-3)Manb1-4GlcNAcb1-4GlcNAcb-Sp20	0.9	1.9	3.8	3.2	1.5
458		GalNAca1-3(Fuca1-2)Galb1-3GlcNAcb1-2Mana1-6(GalNAca1-3(Fuca1-2)Galb1-3GlcNAcb1-2Mana1-3)Manb1-4GlcNAcb1-4(Fuca1-6)GlcNAcb-Sp22	0.2	1.9	3.3	5.8	2.1
203		GlcAb-Sp8	3.3	1.9	6.4	7.2	6.8
275		Neu5Aca2-6Galb-Sp8	1.6	1.9	4.7	6.7	3.8
206		KDNa2-3Galb1-3GlcNAcb-Sp0	2.0	1.9	3.2	7.8	2.1
198		Glca1-6Glca1-6Glc-Sp8	1.3	1.9	7.6	13.8	7.0
181		GlcNAcb1-3GalNAca-Sp14	0.7	1.9	4.2	11.1	4.3
327		Neu5Aca2-3Galb1-4GlcNAcb1-2Mana1-6(Neu5Aca2-6Galb1-4GlcNAcb1-2Mana1-3)Manb1-4GlcNAcb1-4GlcNAcb-Sp12	2.1	1.9	1.6	1.4	0.9
148		Galb1-3GlcNAcb1-3Galb1-4GlcNAcb-Sp0	0.8	1.9	4.3	7.7	1.4
99		GalNAcb1-4GlcNAcb-Sp0	1.9	1.9	5.2	8.3	2.2
271		Neu5Aca2-6Galb1-4GlcNAcb1-3Galb1-4(Fuca1-3)GlcNAcb1-3Galb1-4(Fuca1-3)GlcNAcb-Sp0	2.2	1.8	2.5	-0.5	1.8
239		Neu5Aca2-3Galb1-3(6S)GlcNAc-Sp8	1.7	1.8	6.5	6.8	2.3
264		Neu5Aca2-3Galb1-4Glc-Sp0	2.2	1.8	4.6	5.9	3.2
261		Neu5Aca2-3Galb1-4GlcNAcb-Sp8	3.9	1.8	4.1	6.5	1.4
247		Neu5Aca2-3Galb1-3GalNAcb1-3Gala1-4Galb1-4Glc-Sp0	1.2	1.8	1.3	2.3	0.4
470		Glca1-6Glca1-6Glca1-6Glc-Sp10	2.0	1.8	6.0	8.1	2.7
606		Neu5Aca2-6Galb1-4GlcNAcb1-3Galb1-4GlcNAcb1-6(Neu5Aca2-6Galb1-4GlcNAcb1-3Galb1-4GlcNAcb1-3)GalNAca-Sp14	4.5	1.8	-0.1	1.9	1.0
56		Neu5Aca2-6Galb1-4GlcNAcb1-2Mana1-6(Neu5Aca2-6Galb1-4GlcNAcb1-2Mana1-3)Manb1-4GlcNAcb1-4GlcNAcb-Sp13	3.1	1.8	4.6	4.9	1.3
509		Galb1-4GlcNAcb1-6(Galb1-4GlcNAcb1-2)Mana1-6(GlcNAcb1-4)Galb1-4GlcNAcb1-4(Gal b1-4GlcNAcb1-2)Mana1-3)Manb1-4GlcNAcb1-4(Fuca1-6)GlcNAc-Sp21	1.6	1.7	3.9	10.0	4.0
17		GlcNAcb-Sp8	0.1	1.7	7.1	15.7	5.0

551		Galb1-4GlcNAcb1-3Galb1-4GlcNAcb1-3Galb1-4GlcNAcb1-3Galb1-4GlcNAcb1-2Mana1-6(Galb1-4GlcNAcb1-3Galb1-4GlcNAcb1-3Galb1-4GlcNAcb1-3Galb1-4GlcNAcb1-2Mana1-3)Manb1-4GlcNAcb1-4GlcNAcb-Sp25	0.1	1.7	3.5	5.4	1.5
314		Mana1-6Manb-Sp10	1.6	1.7	5.0	7.2	4.1
588		GlcNAcb1-3Galb1-4GlcNAcb1-3Galb1-4GlcNAcb1-3Galb1-4GlcNAcb1-6(GlcNAcb1-3Galb1-4GlcNAcb1-3Galb1-4GlcNAcb1-3Galb1-4GlcNAcb1-2)Mana1-6(GlcNAcb1-3Galb1-4GlcNAcb1-3Galb1-4GlcNAcb1-3Galb1-4GlcNAcb1-2Mana1-3)Manb	3.8	1.7	2.0	3.3	1.1
187		GlcNAcb1-4-MDPLys	-0.1	1.7	3.2	4.7	1.8
80		Fuca1-3GlcNAcb-Sp8	0.6	1.7	4.3	5.8	1.4
597		Neu5Aca2-3Galb1-4GlcNAcb1-3Galb1-4GlcNAcb1-6(Neu5Aca2-3Galb1-4GlcNAcb1-3Galb1-4GlcNAcb1-3)GalNAca-Sp14	0.4	1.6	2.5	3.1	0.9
109		Gala1-3(Fuca1-2)Galb-Sp18	2.6	1.6	6.9	5.1	4.0
318		Neu5Aca2-3Galb1-4GlcNAcb1-6(Neu5Aca2-3Galb1-3)GalNAca-Sp14	2.9	1.6	6.0	9.4	2.8
50		Mana1-6(Mana1-3)Manb1-4GlcNAcb1-4GlcNAcb-Sp12	1.6	1.6	3.5	4.3	1.0
240		Neu5Aca2-3Galb1-3(Fuca1-4)GlcNAcb-Sp8	3.7	1.6	6.3	5.8	3.3
492		Neu5Aca2-3Galb1-3GlcNAcb1-6GalNAca-Sp14	3.0	1.6	4.8	4.3	2.4
272		Neu5Aca2-6Galb1-4GlcNAcb1-3Galb1-4GlcNAcb-Sp0	1.0	1.5	3.9	2.3	2.0
497		Galb1-4(Fuca1-3)GlcNAcb1-2Mana-Sp0	0.8	1.5	6.4	20.1	9.2
570		(3S)GlcAb1-3Galb1-4GlcNAcb1-3Galb1-4Glc-Sp0	2.2	1.5	7.6	13.3	7.3
517		(4S)GalNAcb-Sp10	0.4	1.5	4.8	9.8	5.1
286		Neu5Gca2-6GalNAca-Sp0	1.7	1.5	6.2	2.0	2.1
142		Galb1-3GalNAca-Sp16	0.9	1.5	3.4	4.8	2.4
574		Neu5Aca2-8Neu5Aca2-3Galb1-3GalNAcb1-4(Neu5Aca2-3)Galb1-4Glc-Sp21	0.4	1.5	3.1	5.9	1.7
333		Neu5Aca2-6Galb1-4GlcNAcb1-3Galb1-4GlcNAcb1-3Galb1-4GlcNAcb-Sp0	4.9	1.5	4.0	0.0	0.7
464		Neu5Aca2-6Galb1-4GlcNAcb1-2Mana1-6(GlcNAcb1-4)(Neu5Aca2-6Galb1-4GlcNAcb1-2Mana1-3)Manb1-4GlcNAcb1-4GlcNAcb-Sp21	2.0	1.5	3.3	7.1	0.9
323		Neu5Aca2-8Neu5Aca2-8Neu5Acb-Sp8	1.3	1.5	1.9	3.2	1.9
540		GlcNAcb1-3Galb1-4GlcNAcb1-2Mana1-6(GlcNAcb1-3Galb1-4GlcNAcb1-2Mana1-3)Manb1-4GlcNAcb1-4GlcNAcb-Sp12	0.4	1.5	2.2	1.7	1.7

241		Neu5Aca2-3Galb1-3(Fuca1-4)GlcNAcb1-3Galb1-4(Fuca1-3)GlcNAcb-Sp0	2.1	1.5	4.4	4.1	2.2
294		Galb1-4GlcNAcb1-3Galb1-3GlcNAcb-Sp0	0.5	1.5	3.2	5.5	4.4
583		Galb1-4GlcNAcb1-3Galb1-4GlcNAcb1-6(Galb1-4GlcNAcb1-3Galb1-4GlcNAcb1-2)Mana1-6(Galb1-4GlcNAcb1-3Galb1-4GlcNAcb1-2Mana1-3)Manb1-4GlcNAcb1-4(Fuca1-6)GlcNAcb-Sp24	-0.7	1.4	1.0	1.0	1.6
321		GlcNAcb1-2Mana1-6(Neu5Aca2-6Galb1-4GlcNAcb1-2Mana1-3)Manb1-4GlcNAcb1-4GlcNAcb-Sp12	1.7	1.4	2.1	3.9	0.8
611		Galb1-3GalNAcb1-4(Neu5Aca2-8Neu5Aca2-8Neu5Aca2-3)Galb1-4Glc-Sp21	0.2	1.4	3.1	3.9	1.7
201		G-ol-Sp8	0.8	1.4	3.7	5.9	3.8
475		Neu5Aca2-3Galb1-3GlcNAcb1-6(Neu5Aca2-3Galb1-4GlcNAcb1-2)Mana1-6(Neu5Aca2-3Galb1-3GlcNAcb1-2Mana1-3)Manb1-4GlcNAcb1-4GlcNAcb-Sp19	2.4	1.3	1.1	1.1	2.5
456		Gala1-3(Fuca1-2)Galb1-3GlcNAcb1-2Mana1-6(Gala1-3(Fuca1-2)Galb1-3GlcNAcb1-2Mana1-3)Manb1-4GlcNAcb1-4(Fuca1-6)GlcNAcb-Sp22	4.7	1.3	5.5	6.8	1.7
420		Galb1-4(Fuca1-3)GlcNAcb1-2Mana1-6(Galb1-4(Fuca1-3)GlcNAcb1-2Mana1-3)Manb1-4GlcNAcb1-4(Fuca1-6)GlcNAcb-Sp22	-0.4	1.3	3.0	5.3	1.6
562		GlcNAcb1-3Galb1-4GlcNAcb1-6(GlcNAcb1-3Galb1-3)GalNAca-Sp14	3.2	1.3	1.2	7.3	1.3
276		Neu5Aca2-8Neu5Aca-Sp8	0.0	1.3	3.1	3.7	1.6
193		GlcNAcb1-6GalNAca-Sp8	5.8	1.3	4.0	-0.9	0.7
225		Neu5Aca2-3Galb1-3GalNAca-Sp14	1.3	1.2	3.3	4.5	1.1
357		KDNa2-3Galb1-4(Fuca1-3)GlcNAc-Sp0	1.4	1.2	5.2	8.2	1.3
371		GalNAca1-3(Fuca1-2)Galb1-4GlcNAcb1-2Mana1-6(GalNAca1-3(Fuca1-2)Galb1-4GlcNAcb1-2Mana1-3)Manb1-4GlcNAcb1-4GlcNAcb-Sp20	2.1	1.2	1.9	4.0	0.9
48		Neu5,9Ac ₂ a-Sp8	2.0	1.2	3.4	4.0	2.6
592		Galb1-4GlcNAcb1-3Galb1-4GlcNAcb1-6(Galb1-4GlcNAcb1-3Galb1-4GlcNAcb1-3)GalNAca-Sp14	4.1	1.2	3.0	3.6	1.6
604		Neu5Aca2-3Galb1-4GlcNAcb1-3Galb1-4GlcNAcb1-2Mana1-6(Neu5Aca2-3Galb1-4GlcNAcb1-3Galb1-4GlcNAcb1-2Mana1-3)Manb1-4GlcNAcb1-4GlcNAcb-Sp12	2.9	1.2	1.4	3.3	0.0
460		Neu5Aca2-3Galb1-4GlcNAcb1-2Mana1-6(GlcNAcb1-4)(Neu5Aca2-3Galb1-4GlcNAcb1-2Mana1-3)Manb1-4GlcNAcb1-4GlcNAcb-Sp21	1.1	1.2	1.8	6.4	2.5

507		GalNAca1-3(Fuca1-2)Galb1-3GlcNAcb1-6GalNAca-Sp14	0.2	1.2	4.5	9.9	4.3
178		GlcNAcb1-6(GlcNAcb1-3)GalNAca-Sp14	1.0	1.1	4.1	4.1	1.9
302		Neu5Aca2-6Galb1-4GlcNAcb1-2Mana1-6(Galb1-4GlcNAcb1-2Mana1-3)Manb1-4GlcNAcb1-4GlcNAcb-Sp12	1.6	1.1	1.7	2.6	0.3
12		Galb-Sp8	1.7	1.0	3.8	7.3	2.1
577		GlcNAcb1-3Galb1-4GlcNAcb1-3Galb1-4GlcNAcb1-2Mana1-6(GlcNAcb1-3Galb1-4GlcNAcb1-3Galb1-4GlcNAcb1-2Mana1-3)Manb1-4GlcNAcb1-4(Fuca1-6)GlcNAcb-Sp24	6.0	1.0	-0.5	2.2	0.8
229		GalNAcb1-4(Neu5Aca2-8Neu5Aca2-3)Galb1-4Glc-Sp0	1.9	1.0	1.9	3.9	0.9
349		Neu5Aca2-6Galb1-4GlcNAcb1-2Mana1-3Manb1-4GlcNAcb1-4GlcNAc-Sp12	0.6	1.0	2.1	2.4	0.5
576		Galb1-4GlcNAcb1-3Galb1-4GlcNAcb1-2Mana1-6(Galb1-4GlcNAcb1-3Galb1-4GlcNAcb1-2Mana1-3)Manb1-4GlcNAcb1-4(Fuca1-6)GlcNAcb-Sp24	4.2	1.0	5.1	12.8	2.6
216		Mana1-6(Mana1-3)Mana1-6(Mana1-2Mana1-3)Manb1-4GlcNAcb1-4GlcNAcb-Sp12	5.1	1.0	3.5	7.4	3.7
217		Mana1-6(Mana1-3)Mana1-6(Mana1-3)Manb1-4GlcNAcb1-4GlcNAcb-Sp12	2.0	1.0	6.4	6.8	1.1
285		Neu5Gca2-3Galb1-4Glc-Sp0	2.2	0.9	4.4	2.5	0.9
274		Neu5Aca2-6Galb1-4Glc-Sp8	2.0	0.9	5.2	4.1	2.3
15		GalNAcb-Sp8	0.1	0.9	3.1	7.2	3.1
312		GlcNAcb1-4GlcNAcb-Sp12	1.6	0.9	5.6	5.0	3.4
594		GlcNAcb1-3Galb1-4GlcNAcb1-3GalNAca-Sp14	3.6	0.9	3.8	4.7	2.2
260		Neu5Aca2-3Galb1-4GlcNAcb-Sp0	3.2	0.9	3.3	4.0	1.0
608		Neu5Aca2-3Galb1-4GlcNAcb1-3Galb1-4GlcNAcb1-3Galb1-4GlcNAcb1-2Mana1-6(Neu5Aca2-3Galb1-4GlcNAcb1-3Galb1-4GlcNAcb1-3Galb1-4GlcNAcb1-2Mana1-3)Manb1-4GlcNAcb1-4GlcNAcb-Sp12	5.7	0.9	5.1	8.5	3.6
548		Galb1-4GlcNAcb1-3Galb1-4GlcNAcb1-3Galb1-4GlcNAcb1-2Mana1-6(Galb1-4GlcNAcb1-3Galb1-4GlcNAcb1-3Galb1-4GlcNAcb1-2Mana1-3)Manb1-4GlcNAcb1-4GlcNAcb-Sp12	0.0	0.8	9.0	17.0	4.8
494		Galb1-4(Fuca1-3)GlcNAcb1-6(Neu5Aca2-6(Neu5Aca2-3Galb1-3)GlcNAcb1-3)Galb1-4Glc-Sp21	0.7	0.8	3.5	4.9	1.7
558		Neu5Aca2-8Neu5Aca2-3Galb1-4GlcNAc-Sp0	-1.0	0.8	2.3	8.8	1.6
196		Glc1-4Glc-Sp8	0.6	0.8	3.7	5.0	3.2
610		GlcNAcb1-3Fuca-Sp21	0.7	0.8	4.1	6.5	2.3
227		GalNAcb1-4(Neu5Aca2-8Neu5Aca2-8Neu5Aca2-3)Galb1-4Glc-Sp0	1.0	0.8	1.1	3.1	1.1

466	Neu5Aca2-6Galb1-4GlcNAcb1-6(Neu5Aca2-6Galb1-4GlcNAcb1-2)Mana1-6(GlcNAcb1-4)(Neu5Aca2-6Galb1-4GlcNAcb1-2Mana1-3)Manb1-4GlcNAcb1-4GlcNAcb-Sp21	1.7	0.8	2.1	5.2	1.3
332	Neu5Aca2-3Galb1-3(Fuca1-4)GlcNAcb1-3Galb1-3(Fuca1-4)GlcNAcb-Sp0	3.0	0.8	4.6	7.7	1.4
440	Galb1-4Galb-Sp10	0.4	0.8	4.9	9.2	4.4
596	GlcNAcb1-3Galb1-4GlcNAcb1-6(GlcNAcb1-3Galb1-4GlcNAcb1-3)GalNAca-Sp14	0.6	0.8	3.7	5.6	1.9
112	Gala1-3GalNAca-Sp16	0.0	0.7	1.8	6.2	3.1
485	Mana1-6(Mana1-3)Manb1-4GlcNAcb1-4(Fuca1-6)GlcNAcb-Sp19	0.1	0.7	4.8	4.0	1.7
137	Neu5Aca2-6(Galb1-3)GalNAca-Sp14	-0.1	0.7	5.2	8.3	5.0
89	GlcNAcb1-3Galb1-3GalNAca-Sp8	1.8	0.7	3.8	8.8	1.4
471	Glca1-4Glca1-4Glca1-4Glc-Sp10	0.9	0.7	4.2	9.7	3.5
461	Neu5Aca2-3Galb1-4GlcNAcb1-4Mana1-6(GlcNAcb1-4)(Neu5Aca2-3Galb1-4GlcNAcb1-4(Neu5Aca2-3Galb1-4GlcNAcb1-2)Mana1-3)Manb1-4GlcNAcb1-4GlcNAcb-Sp21	0.0	0.7	6.4	10.4	2.3
415	GalNAca1-3(Fuca1-2)Galb1-4GlcNAcb1-3GalNAca-Sp14	1.7	0.6	4.1	9.9	2.1
527	Neu5Aca2-3Galb1-3GlcNAcb1-2Mana-Sp0	0.9	0.6	7.4	14.0	5.1
319	Neu5Aca2-6Galb1-4GlcNAcb1-2Mana1-6(Neu5Aca2-3Galb1-4GlcNAcb1-2Mana1-3)Manb1-4GlcNAcb1-4GlcNAcb-Sp12	0.8	0.6	3.9	2.7	0.5
346	Neu5Aca2-6Galb1-4GlcNAcb1-2Mana1-6(Mana1-3)Manb1-4GlcNAcb1-4GlcNAcb-Sp12	1.8	0.6	1.4	1.7	0.4
412	Galb1-3GalNAcb1-4(Neu5Aca2-8Neu5Aca2-3)Galb1-4Glc-Sp0	0.1	0.5	3.9	9.6	6.7
582	Galb1-4GlcNAcb1-3Galb1-4GlcNAcb1-3Galb1-4GlcNAcb1-3Galb1-4GlcNAcb1-2Mana1-6(Galb1-4GlcNAcb1-3Galb1-4GlcNAcb1-3Galb1-4GlcNAcb1-3Galb1-4GlcNAcb1-3Galb1-4GlcNAcb1-2Mana1-3)Manb1-4GlcNAcb1-4(Fuca1-6)GlcNAcb-Sp19	0.1	0.5	1.4	3.7	1.1
443	GalNAcb1-6GalNAcb-Sp8	0.6	0.5	6.8	9.4	1.4
578	Galb1-4GlcNAcb1-3Galb1-4GlcNAcb1-3Galb1-4GlcNAcb1-2Mana1-6(Galb1-4GlcNAcb1-3Galb1-4GlcNAcb1-3Galb1-4GlcNAcb1-2Mana1-3)Manb1-4GlcNAcb1-4(Fuca1-6)GlcNAcb-Sp24	-0.6	0.5	0.9	0.9	-1.0
320	Galb1-4GlcNAcb1-2Mana1-6(Neu5Aca2-6Galb1-4GlcNAcb1-2Mana1-3)Manb1-4GlcNAcb1-4GlcNAcb-Sp12	-0.8	0.4	3.4	1.6	1.4
230	Neu5Aca2-8Neu5Aca2-8Neu5Aca-Sp8	1.4	0.4	2.1	3.7	0.9

487	Neu5Aca2-3Galb1-3GlcNAcb1-2Mana1-6(GlcNAcb1-4)(Neu5Aca2-3Galb1-3GlcNAcb1-2Mana1-3)Manb1-4GlcNAcb1-4GlcNAc-Sp21	-0.1	0.4	6.0	9.0	1.7
348	Neu5Aca2-6Galb1-4GlcNAcb1-2Mana1-6Manb1-4GlcNAcb1-4GlcNAc-Sp12	1.3	0.4	1.8	2.1	0.2
347	Mana1-6(Neu5Aca2-6Galb1-4GlcNAcb1-2Mana1-3)Manb1-4GlcNAcb1-4GlcNAc-Sp12	1.2	0.4	2.0	1.5	0.6
237	Neu5Aca2-3GalNAca-Sp8	1.9	0.4	2.3	3.2	1.1
354	Galb1-4GlcNAcb1-2Mana1-6(Galb1-4GlcNAcb1-2Mana1-3)Manb1-4GlcNAcb1-4(Fuca1-6)GlcNAcb-Sp22	2.4	0.4	-0.2	-0.2	-0.3
587	Galb1-4GlcNAcb1-3Galb1-4GlcNAcb1-3Galb1-4GlcNAcb1-3Galb1-4GlcNAcb1-6(Galb1-4GlcNAcb1-3Galb1-4GlcNAcb1-3Galb1-4GlcNAcb1-3Galb1-4GlcNAcb1-2)Mana1-6(Galb1-4GlcNAcb1-3Galb1-4GlcNAcb1-3Galb1-4GlcNAcb1-3Galb1-4GlcNAcb1-2Mana1-3)Manb1-4GlcNAcb1-4(Fuca1-6)GlcNAcb-	-1.0	0.4	3.9	5.5	0.7
311	GlcNAcb1-4GlcNAcb-Sp10	0.6	0.3	5.6	2.3	1.2
326	Neu5Aca2-3Galb1-4GlcNAcb1-2Mana1-6(Neu5Aca2-3Galb1-4GlcNAcb1-2Mana1-3)Manb1-4GlcNAcb1-4GlcNAcb-Sp12	0.3	0.3	1.1	-0.7	0.2
579	GlcNAcb1-3Galb1-4GlcNAcb1-3Galb1-4GlcNAcb1-3Galb1-4GlcNAcb1-2Mana1-6(GlcNAcb1-3Galb1-4GlcNAcb1-3Galb1-4GlcNAcb1-3Galb1-4GlcNAcb1-2Mana1-3)Manb1-4GlcNAcb1-4(Fuca1-6)GlcNAcb-Sp24	5.0	0.3	0.0	-0.2	1.0
413	Neu5Aca2-3Galb1-3GalNAcb1-4(Neu5Aca2-8Neu5Aca2-3)Galb1-4Glc-Sp0	-0.5	0.3	4.1	8.4	3.7
601	Neu5Aca2-3Galb1-4GlcNAcb1-3Galb1-4GlcNAcb1-6(Galb1-3)GalNAca-Sp14	0.6	0.3	7.2	7.2	3.2
595	GlcNAcb1-3Galb1-4GlcNAcb1-6(Galb1-3)GalNAca-Sp14	2.4	0.3	4.5	7.5	2.2
313	MurNAcb1-4GlcNAcb-Sp10	0.8	0.2	3.2	5.1	1.9
289	Neu5Aca2-3Galb1-4GlcNAcb1-6(Galb1-3)GalNAca-Sp14	2.5	0.2	5.0	3.3	0.9
6	Fuca-Sp8	0.3	0.2	3.8	0.2	2.0
467	Neu5Aca2-6Galb1-4GlcNAcb1-6(Neu5Aca2-6Galb1-4GlcNAcb1-2)Mana1-6(GlcNAcb1-4)(Neu5Aca2-6Galb1-4GlcNAcb1-4)(Neu5Aca2-6Galb1-4GlcNAcb1-2)Mana1-3)Manb1-4GlcNAcb1-4GlcNAcb-Sp21	0.0	0.2	2.2	10.5	1.5

581	GlcNAcb1-3Galb1-4GlcNAcb1-3Galb1-4GlcNAcb1-3Galb1-4GlcNAcb1-3Galb1-4GlcNAcb1-2Mana1-6(GlcNAcb1-3Galb1-4GlcNAcb1-3Galb1-4GlcNAcb1-3Galb1-4GlcNAcb1-2Mana1-3)Manb1-4GlcNAcb1-4(Fuca1-6)GlcNAcb-Sp19	0.3	0.1	1.1	-0.3	0.8
561	Gala1-3Galb1-4GlcNAcb1-2Mana1-6(Gala1-3Galb1-4GlcNAcb1-2Mana1-3)Manb1-4GlcNAcb1-4GlcNAc-Sp24	5.6	0.0	0.7	3.5	3.6
490	Gala1-3Galb1-3GlcNAcb1-6GalNAca-Sp14	1.8	0.0	5.8	13.0	3.3
568	Galb1-3GlcNAcb1-6(Galb1-3)GalNAc-Sp14	0.0	0.0	1.0	10.0	2.1
366	Fuca1-4(Galb1-3)GlcNAcb1-2Mana1-6(Fuca1-4(Galb1-3)GlcNAcb1-2Mana1-3)Manb1-4GlcNAcb1-4(Fuca1-6)GlcNAcb-Sp22	-0.3	-0.1	1.2	-1.1	0.9
580	Galb1-4GlcNAcb1-3Galb1-4GlcNAcb1-3Galb1-4GlcNAcb1-3Galb1-4GlcNAcb1-2Mana1-6(Galb1-4GlcNAcb1-3Galb1-4GlcNAcb1-3Galb1-4GlcNAcb1-3Galb1-4GlcNAcb1-2Mana1-3)Manb1-4GlcNAcb1-4(Fuca1-6)GlcNAcb-Sp24	0.2	-0.1	-0.8	0.5	-0.5
309	Neu5Aca2-6Galb1-4GlcNAcb1-2Mana1-6(GlcNAcb1-2Mana1-3)Manb1-4GlcNAcb1-4GlcNAcb-Sp12	1.6	-0.1	5.9	5.9	0.7
194	GlcNAcb1-6GalNAca-Sp14	0.6	-0.1	3.5	6.3	1.4
462	Neu5Aca2-3Galb1-4GlcNAcb1-6(Neu5Aca2-3Galb1-4GlcNAcb1-2)Mana1-6(GlcNAcb1-4)(Neu5Aca2-3Galb1-4GlcNAcb1-2Mana1-3)Manb1-4GlcNAcb1-4GlcNAcb-Sp21	1.4	-0.1	2.2	1.6	1.5
141	Galb1-3GalNAca-Sp14	0.6	-0.2	5.2	8.1	4.1
288	Neu5Gca-Sp8	1.1	-0.2	5.8	3.7	1.8
341	GlcNAca1-4Galb1-3GlcNAcb-Sp0	-0.1	-0.2	5.6	2.4	2.0
9	Neu5Aca-Sp8	1.0	-0.3	4.2	4.0	1.7
489	Galb1-3GlcNAcb1-6GalNAca-Sp14	0.3	-0.3	4.3	4.5	1.8
226	GalNAcb1-4(Neu5Aca2-8Neu5Aca2-8Neu5Aca2-8Neu5Aca2-3)Galb1-4Glc-Sp0	3.6	-0.3	5.4	6.9	3.6
353	GlcNAcb1-2Mana1-6(GlcNAcb1-2Mana1-3)Manb1-4GlcNAcb1-4(Fuca1-6)GlcNAcb-Sp22	-0.7	-0.4	-0.3	-0.1	-0.4
463	Neu5Aca2-3Galb1-4GlcNAcb1-6(Neu5Aca2-3Galb1-4GlcNAcb1-2)Mana1-6(GlcNAcb1-4)(Neu5Aca2-3Galb1-4GlcNAcb1-4)(Neu5Aca2-3Galb1-4GlcNAcb1-2)Mana1-3)Manb1-4GlcNAcb1-4GlcNAcb-Sp21	-0.5	-0.4	5.5	7.5	0.7
393	GalNAcb1-4(Neu5Aca2-3)Galb1-4GlcNAcb1-3GalNAca-Sp14	2.4	-0.6	3.0	6.7	1.1

396		Gala1-3Galb1-3(Fuca1-4)GlcNAcb1-2Mana1-6(Gala1-3Galb1-3(Fuca1-4)GlcNAcb1-2Mana1-3)Manb1-4GlcNAcb1-4GlcNAc-Sp19	-1.0	-0.6	2.4	4.6	1.1
585		Galb1-4GlcNAcb1-3Galb1-4GlcNAcb1-3Galb1-4GlcNAcb1-6(Galb1-4GlcNAcb1-3Galb1-4GlcNAcb1-3Galb1-4GlcNAcb1-2)Mana1-6(Galb1-4GlcNAcb1-3Galb1-4GlcNAcb1-3Galb1-4GlcNAcb1-2Mana1-3)Manb1-4GlcNAcb1-4(Fuca1-6)GlcNAcb-Sp24	-0.1	-0.6	3.1	7.3	2.3
609		Neu5Aca2-6Galb1-4GlcNAcb1-3Galb1-4GlcNAcb1-2Mana1-6(Neu5Aca2-6Galb1-4GlcNAcb1-3Galb1-4GlcNAcb1-2Mana1-3)Manb1-4GlcNAcb1-4GlcNAcb-Sp12	0.8	-0.6	0.0	2.3	-0.4
465		Neu5Aca2-6Galb1-4GlcNAcb1-4Mana1-6(GlcNAcb1-4)(Neu5Aca2-6Galb1-4GlcNAcb1-4(Neu5Aca2-6Galb1-4GlcNAcb1-2)Mana1-3)Manb1-4GlcNAcb1-4GlcNAcb-Sp21	-0.5	-0.8	0.3	5.2	2.1
395		Gala1-3Galb1-3GlcNAcb1-2Mana1-6(Gala1-3Galb1-3GlcNAcb1-2Mana1-3)Manb1-4GlcNAcb1-4GlcNAc-Sp19	0.1	-0.9	1.1	2.4	-0.1
7		Fuca-Sp9	0.3	-1.0	1.3	0.5	-0.1
607		Neu5Aca2-6Galb1-4GlcNAcb1-3Galb1-4GlcNAcb1-3Galb1-4GlcNAcb1-2Mana1-6(Neu5Aca2-6Galb1-4GlcNAcb1-3Galb1-4GlcNAcb1-3Galb1-4GlcNAcb1-2Mana1-3)Manb1-4GlcNAcb1-4GlcNAcb-Sp12	3.4	-1.0	-0.1	0.8	0.2
565		GlcNAcb1-3Galb1-4GlcNAcb1-3Galb1-4GlcNAcb1-3Galb1-4GlcNAcb1-2Mana1-6(GlcNAcb1-3Galb1-4GlcNAcb1-3Galb1-4GlcNAcb1-3Galb1-4GlcNAcb1-2Mana1-3)Manb1-4GlcNAcb1-4GlcNAcb-Sp25	0.0	-1.1	-0.8	-1.5	-0.3
355		Galb1-3GlcNAcb1-2Mana1-6(Galb1-3GlcNAcb1-2Mana1-3)Manb1-4GlcNAcb1-4(Fuca1-6)GlcNAcb-Sp22	-0.9	-1.2	-0.5	-0.3	-0.5
58		Neu5Aca2-6Galb1-4GlcNAcb1-2Mana1-6(Neu5Aca2-6Galb1-4GlcNAcb1-2Mana1-3)Manb1-4GlcNAcb1-4GlcNAcb-Sp24	1.9	-2.0	1.2	2.2	0.2